



Universidad de Sevilla

Departamento de Ingeniería de Sistemas y Automática

Memoria de Tesis Doctoral

**Modelado y control hídrico del continuo
suelo-planta-atmósfera en cultivos leñosos**

**Hydraulic modelling and control of the soil-
plant-atmosphere continuum in woody crops**

Rafael Romero Vicente

Directores:

José Enrique Fernández Luque

Instituto de Recursos Naturales y Agrobiología (IRNAS-CSIC)

José Luis Muriel Fernández

IFAPA, Centro Las Torres-Tomejil

David Muñoz de la Peña Sequedo

Dpto. Ingeniería de Sistemas y Automática. Universidad de Sevilla

A Cris y Héctor...

Agradecimientos

La senda que culmina en este trabajo de tesis representa mucho más que un hito profesional en mi carrera investigadora. Estos años de dedicación a esta profesión que tanto amo me ha permitido atesorar grandes, más que compañeros, amigos que me han demostrado que su valor humano supera incluso su talento profesional. Sin ellos mi trabajo no solo hubiera sido infinitamente más difícil, sino también mucho más aburrido y menos enriquecedor. Es por esto que me gustaría dedicar a todos ellos las primeras palabras de esta tesis expresando mi profundo y eterno agradecimiento:

A mis compañeros y profesores de la Universidad de Sevilla donde inicié mi formación en Ingeniería en un ya lejano 1993; y en particular a Ismael Alcalá con el que compartí innumerables horas domando al viejo robot RM10, a los Manolos, Fernando Castaño, Dani Jiménez y tantos otros compañeros de laboratorio que siempre están dispuestos a ayudar a los recién llegados. Gracias a mis profesores Carlos Bordons, Javier Aracil, Eduardo Fernández y Miguel Ángel Ridao por inspirarme y mostrarme el camino de mi vocación. A Francisco Rodríguez por su paciencia y apoyo durante el desarrollo de mi proyecto de fin de carrera, y por ser mi mentor en la universidad durante tantos años...y los que están por venir. Y finalmente a mis compis Rubén, Javi, Virginia, Antonio y, cómo no, a mi querido José Luis, *Jere*. ¡Qué grande es! Nos presentaron durante nuestro primer día en la universidad y, desde entonces, ya nunca volvimos a separarnos.

A los compañeros del Instituto de Recursos Naturales y Agrobiología de Sevilla (IRNAS). A Juan Carlos Montañó por valorarme tanto y creer siempre en mí y a Fran Moreno por ofrecerme su ayuda constante y regalarme tantas conversaciones en los laboratorios de electrónica. A Antonio por nuestros largos y fructíferos diálogos telefónicos, y porque siempre encuentra un hueco a pesar de estar tan ocupado; ojalá pronto acabemos trabajando juntos. Gracias A Vicky, Vanesa, José Manuel, Luisa Candau, Maria José, a las recepcionistas y limpiadoras y todos los demás compañeros, por recibirme siempre con una sonrisa y hacerme sentir como en casa.

A los compañeros del Instituto de Investigación y Formación Agraria y Pesquera de Andalucía (IFAPA); empezando por Fernando Romero, que siempre me ha aportado

buenos consejos y tratado como a un hijo. A Joaquín y Jorge, siempre generosos en ayudarme, especialmente cuando algo se torcía, y a las recepcionistas y limpiadoras que derrochan amabilidad con todos. En compañeros como ellos se cimienta sin duda el alma de la institución. Gracias también a Antonio Daza, Paco Perea, Arturo, Dulce, Pedro Cermeño, Berta, Jorge Andrada, José Luis Campos, Paco Fuentes, Víctor, Marcelino, Fernando Morillo, José Rodríguez, Miguel Ángel... y tantos otros que no podría nombrar, no por falta de merecimiento sino de espacio y tiempo.

Y muy especialmente a mis queridos amigos y compañeros de departamento. A Juan Antonio, que se hace querer tanto que vaya donde vaya todo el mundo le conoce. A Jorge, Miguel Ángel y Manolo, que siempre están dispuestos a ayudar en los trabajos más difíciles y cuyo esfuerzo ha sido imprescindible para conseguir los resultados presentados en esta tesis. A los Antonios, Sara, Ainhoa, y todos cuanto pasaron en algún momento por allí y nunca olvidaremos. A Iván, con el que he compartido y aprendido lecciones de trabajo y de vida. El mundo sería un lugar más humano y justo con más personas como él. Gracias a María Antonia y Natalia, que siempre han sabido escuchar mis problemas con cariño y ayudarme. A Gonzalo, el mejor compañero de despacho que se pueda tener y a Víctor Hugo, con el que no tuve oportunidad de compartir tantos momentos como hubiera deseado. A Karl, por tener tiempo siempre para iluminarme senderos de conocimiento.

Thanks to Alan Zinober for teaching me mathematics, control theory, English jokes, delicious foods and great landscapes when I was living in England. And to my dear fellow Zhivko Stoyanov, who is as good person as he is tall (2 m!). I will never forget the moments we shared when his first son was born. And thanks to Alex and Iman, my Mexican and Iranian brothers, and to all the friends that I met in Sheffield. They helped me to enjoy such a wonderful city.

Thanks to my kiwi family: my father Brent, my mother Penny and my grumpy uncle Steve. I learned a lot of science knowledge during my stay in New Zealand but, above all, they showed me the meaning of hospitality and how to be a better man. I don't need to say that I will never forget them, because hopefully they will be forever in my life. Thanks again to all those wonderful people I met in that magical country: Rosa, Stephanie, Jenny, Kim, Sam, Malin, Edward, Ian, Alistair, Carlo, Markus, Siva, and all the staff in Plant and Food.

A David. Nos conocimos hace mucho siendo aun estudiantes, quien me iba a decir que acabaría teniendo el honor de tenerle como director de tesis. Espero y deseo que todo el tiempo dedicado en este trabajo sea solo el comienzo de muchas y fructíferas colaboraciones. No imagino mejor compañero que un amigo como él. Este agradecimiento es poco para compensar el tiempo que me ha dedicado a costa de su familia. Gracias a ellos por extensión.

A José Enrique. No sé si se puedo llamar trabajo a dedicarme a algo que me gusta tanto y además con amigos y maestros como Enrique, que lo hacen todo aún más fácil. Me ha enseñado mucho, y no solo en mi carrera investigadora, sino también en deliciosas lecciones de vida durante tantos viajes y jornadas de trabajo. Es para mí una fuente de inspiración inagotable. Gracias a sus hijos, por prestarme a su papi en tantas (demasiadas) ocasiones.

A José Luís, por su eterno apoyo y dedicación. Cuando nació él ya estabas allí, muy cerquita. ¿Imaginaría entonces que algún día dirigiría mi tesis doctoral? Siempre he sentido a sus hijos como mis hermanos, así que eso le convierte en un segundo padre para mí, y sin duda lo ha sido en estos años de dedicación profesional. Gracias por creer en mí, gracias por enseñarme tanto, y gracias por darme la oportunidad de dedicarme a la profesión que adoro.

Gracias a mi otra familia. Dicen que los amigos son la familia que se elige. Si esto es así, no podría haber elegido mejor, aunque no dejo de reconocer la enorme y hermosa fortuna que he debido tener para haberlos encontrado. Gracias a los Caimanes y Caimanas por entender mis ausencias en los momentos más exigentes de trabajo, y por regalarme tantos instantes de diversión, risas y emociones.

Gracias a mis abuelos, que siempre me demostraron mucho más amor del que nunca merecí. A mis tíos y primos del Sur y del Norte, a los que adoro y espero no dejar nunca de ver. A mis suegros y cuñada por permitirme secuestrar de Almería su bien máspreciado y estar siempre ahí cuando les hemos necesitado.

Gracias a mis padres, que siempre antepusieron la felicidad de sus hijos a la suya propia. Todo lo que soy o pueda llegar a ser algún día se lo debo a ellos. Lucharé toda mi vida por honrarles, buscando cada día ser un poco mejor persona. Ahora que yo también soy padre, no imagino mejor forma de devolverles parte de lo que me han

regalado todos estos años que revelándoles lo que espero ya sepan, que soy un hijo muy feliz y se lo debo a ellos. Gracias también a ellos por regalarme a mis hermanos, que son además mis mejores amigos, los que nunca me fallan, a los que nunca fallaré. Y gracias a mis cuñados, por su colaboración en la bendita tarea de hacerme tío dentro de unos meses.

Y por supuesto, a mi alma gemela, mi hermosa flor de adversidad, a mi amada esposa Cris. Tú completas mi vida y me motivas a querer superarme. Atraes las sonrisas de mis días y ahuyentas la soledad de mis noches, haces que me sienta pleno y feliz. No hay noche que no recuerde la inmensa suerte que he tenido de haberte conocido. Y si todo esto fuera poco me regalaste al ser más hermoso que la tierra haya visto jamás: a nuestro hijo Héctor. Algún día, no demasiado lejano, cuando aprenda a leer, espero que encuentre en estas líneas un atisbo del inmenso amor que sentimos por él. Para ti Cris, y para ti hijo mío, va dedicada esta tesis y mi vida entera.

Table of contents

Figures	7
Tables.....	15
Symbols and abbreviations	17
Abstract.....	21
Resumen.....	23
<i>Chapter 1. Introduction.....</i>	<i>25</i>
1.1. The need for better water management.....	25
1.2. Background.....	27
1.3. Hypothesis and objectives	30
1.4. Outline	32
1.5. Publications by the author.....	33
1.6. References.....	35
<i>Chapter 2. Impact of sustained deficit irrigation on yield, water productivity and fruit quality in a commercial citrus orchard, cv. Salustiana.....</i>	<i>39</i>
2.1. Introduction.....	40
2.2. Material and methods.....	42
2.2.1. Experimental site.....	42
2.2.2. Irrigation treatments and experimental design	43
2.2.3. Plant measurements.....	44

2.2.4. Statistical analysis	45
2.3. Results.....	46
2.3.1. Water relations.....	46
2.3.2. Plant-water measurements.....	46
2.3.3. Effects of irrigation treatments on yield, fruit quality, and water productivity	50
2.3.4. Temporal variability of data and the overall analysis.....	53
2.4. Discussion.....	55
2.5. Conclusions.....	58
2.6. References.....	58
<i>Chapter 3. Impact of regulated deficit irrigation on yield, water productivity and fruit quality in a commercial citrus orchard, cv. Navelina</i>	<i>64</i>
3.1. Introduction.....	65
3.2. Material and methods.....	66
3.2.1. Experimental site.....	66
3.2.2. Irrigation treatments and experimental design	67
3.2.3. Plant measurements.....	69
3.2.4. Statistical analysis	70
3.3. Results.....	70
3.3.1. Water conditions.....	70
3.3.2. Plant water status and gas exchange.....	74
3.3.3. Yield, fruit quality and water productivity	75
3.3.4. Plant water status and gas exchange versus yield and fruit quality	79
3.4. Discussion.....	90
3.5. Conclusions.....	92

3.6. References.....	93
<i>Chapter 4. Impact of sustained and low frequency deficit irrigation on the physiological response, water productivity and fruit yield of citrus trees cv. Navelina.....</i>	<i>99</i>
4.1. Introduction.....	100
4.2. Material and methods.....	101
4.2.1. Experimental site.....	101
4.2.2. Irrigation treatments and experimental design	102
4.2.3. Measurements.....	103
4.3. Results.....	104
4.3.1. Water supplies	104
4.3.2. Plant-based measurements.....	107
4.3.3. Yield and fruit quality response.....	111
4.4. Discussion.....	112
4.5. Conclusions.....	116
4.6. References.....	116
<i>Chapter 5. An automatic irrigation controller for fruit tree orchards, based on sap flow measurements</i>	<i>123</i>
5.1. Introduction.....	124
5.2. Materials and methods	126
5.2.1. Irrigation controller	126
5.2.2. Field trial	129
5.3. Results and discussion	131
5.3.1. CRP reliability	131

5.3.2. CRP performance	134
5.4. Conclusions.....	140
5.5. References.....	141
Appendix 5.....	149
<i>Chapter 6. An automatic controller for high frequency irrigation based on soil water content measurements combined with the crop coefficient approach</i>	<i>151</i>
6.1. Introduction.....	152
6.2. Materials and methods	153
6.2.1. Orchard characteristics	153
6.2.2. Evaluation of the AIC.....	154
6.2.3. Fundamentals of the AIC.....	156
6.3. Results and discussion	157
6.4. Conclusions.....	160
6.5. References.....	161
<i>Chapter 7. Improving methods to measure sap flow.....</i>	<i>165</i>
7.1. Introduction.....	166
7.2. Materials and methods	167
7.2.1. Two new heat-pulse methods	167
7.2.2. Experimental site	169
7.3. Results and discussion	170
7.4. Conclusions.....	172
7.5. Acknowledgements.....	173
7.6. References.....	173

<i>Chapter 8. Modeling and control of the soil water content in an almond orchard</i>	177
8.1. Introduction.....	178
8.2. Materials and methods	179
8.2.1. Experimental site	179
8.2.2. SPA dynamic model	180
8.2.3. CROPSYST	187
8.2.4. Model identification	187
8.2.5. PID control	189
8.2.6. Model predictive control	191
8.2.7. Hybrid MPC	192
8.2.8. Model predictive control applied to crop fields.....	193
8.3. Results.....	197
8.3.1. Cropsyst validation results.....	197
8.3.2. Identified values of the parameters.....	197
8.3.3. Controllers simulations.....	204
8.3.4. Application to real field of the PID controller.....	213
8.4. Discussion	215
8.5. Conclusions.....	218
8.6. References.....	219
Appendix 8.....	226
<i>Chapter 9. Concluding remarks</i>	231
9.1. Deficit irrigation	231
9.2. Automatic irrigation controllers.....	232

9.3. New sap flow methods.....	233
9.4. Modeling and control of SPA systems	234

Figures

- Fig. 1.1.** World (A), national (B) and regional (C) water demand distributions by sectors. 26
- Fig. 2.1.** Effective precipitation (P_e), crop (ET_c) and potential (ET_o) evapotranspiration, and irrigation amounts (IA) for each treatment during the tree experimental years. DOY = day of year. 48
- Fig. 2.2.** Seasonal patterns of midday stem water potential (Ψ_{stem}) for each irrigation treatment and experimental year. Each point represents the average of 20 readings. Vertical bars represent the standard deviation. DOY = day of year. 49
- Fig. 2.3.** Linear correlation between relative ratio of water stress integral (S_{RI}) and irrigation amounts (IA) in stressed treatments during the irrigation period normalized at 130 days (days of year 164-292). IN = irrigation needs. 51
- Fig. 2.4.** Classification tree for all studied treatments (SDI53, SDI67, SDI77 and control) and parameters: water stress integral (S_ψ , MPa); total soluble solids (TSS, °Brix); titratable acidity (TA, g l⁻¹); weight (g); yield (kg tree⁻¹); equatorial diameter (ED, mm); peel thickness (PT, mm). 54
- Fig. 2.5.** Loadings of the studied variables (yield, fruit weight and water stress integral, S_ψ) to the first three principal components (PC1, PC2 and PC3). 56
- Fig. 3.1.** Effective precipitation (P_e), crop (ET_c) and potential (ET_o) evapotranspiration during the experimental years. DOY = day of year. 72
- Fig. 3.2.** Irrigation amounts (IA) in mm and as percentage of the irrigation needs (IN) during the irrigation periods on 2007 and 2008. 73
- Fig. 3.3.** Irrigation amounts (IA) for each treatment during the experimental years. DOY = day of year. 77

- Fig. 3.4.** Soil water content in the root zone for each treatment at the end of the fruit growth period of 2007 and 2008. The line inside the box shows the median and the letters after each box-whiskler plot show statistical differences at $P < 0.05$ level..... 78
- Fig. 3.5.** Evolution of midday stem water potential (Ψ_{stem}) in each treatment during the fruit growth and fruit maturation periods of the experimental years. Vertical bars indicate the standard deviation in each treatment (ten repetitions per treatment). DOY = day of year. 80
- Fig. 3.6.** Evolution of stomatal conductance (g_s) in each treatment during the fruit growth and fruit maturation periods of the experimental years. Vertical bars indicate the standard deviation in each treatment (ten repetitions per treatment). DOY = day of year. 81
- Fig. 3.7.** Box and whisker plots for water stress integral (S_Ψ) and stomatal conductance integral (S_g) during the studied years. Vertical lines indicate the standard deviation for each treatment..... 82
- Fig. 3.8.** Linear relationships among irrigation amounts (IAs) and water stress integral (S_Ψ) and stomatal conductance integral (S_g) in control and RDI treatments during the irrigation period. 83
- Fig. 3.9.** Yield vs. annual irrigation amounts (IAs). Yield was normalized to take into account the temporal variability of the results due to changing weather conditions during the studied years. 83
- Fig. 3.10.** Box and whisker plot for yield (years 2007 and 2008). The line inside the box shows the median and the letters after each box-whiskler plot show statistical differences at $P < 0.05$ level. 84
- Fig. 3.11.** Box and whisker plot for water productivity (years 2007 and 2008). The line inside the box shows the median and the letters after each box and whiskler plot show statistical differences at $P < 0.05$ level. 87
- Fig. 3.12.** Relationships among water stress integral (S_Ψ , MPa) and yield and fruit quality parameters (years 2007 and 2008). PT, peel thickness; TSS, total soluble solids; MI maturity index; TA, titratable acidity; ED and PD equatorial and polar diameter respectively..... 88

Fig. 3.13. Relationships among stomatal conductance integral (S_g , $\text{mmol s}^{-1} \text{m}^{-2}$) and yield and fruit quality parameters (years 2007 and 2008). PT, peel thickness; TSS, total soluble solids; MI maturity index; TA, titratable acidity; ED and PD equatorial and polar diameter respectively..... 89

Fig. 4.1. Effective precipitation (P_e), crop (ET_c) and potential (ET_o) evapotranspiration (A), and irrigation amounts (IA) for each treatment (B) during the irrigation season. DOY = day of year. 105

Fig. 4.2. Dynamics of soil water content (SWC) in each treatment at 30 and 60 cm depth. SDI: Sustainable deficit irrigation; LFDI: Low frequency deficit irrigation. DOY = day of year. 106

Fig. 4.3. Dynamics for stem water potential (A), stomatal conductance (B) and maximum daily shrinkage (C) in each treatment during the irrigation period. DOY = day of year. 108

Fig. 4.4. Temporal evolution of the daily maximum stem diameter (MXSD) in each treatment during the studied period. SDI: Sustainable deficit irrigation; LFDI: Low frequency deficit irrigation. DOY = day of year. 110

Fig. 5.1. Flow diagram showing the tasks of the three main physical components of the CRP: the measuring unit (MU), the control unit (CU), and the pump & electrovalve controller (PEC). See text for details..... 128

Fig. 5.2. Output voltage (U) from the outer pair of thermocouples of one of the probe sets monitored by the measurement unit 1, before (A) and after (B) being amplified and filtered by the CRP. Amplified sections of the graphs correspond to the calculated t_z values, indicated by the dashed lines. The X-axis shows the time (t) after the firing of the heat pulse. 133

Fig. 5.3. Daily transpiration (E_p) values calculated by the CRP from the sap flow records in two OI trees — those for which the highest (Δ) and the lowest (∇) transpiration rates were estimated (A). Fig. B is the same but for the NI trees. Also shown are the potential evapotranspiration (ET_o) values estimated from the FAO56

Penman-Monteith equation and the data recorded by the weather station next to the orchard (●). DOY = day of year. 134

Fig. 5.4. Daily values of the transpiration ratio between the normally irrigated and overirrigated trees (E_{pNI}/E_{pOI}) determined by the CRP during the field trial (B), and the derived irrigation doses, ID (C). Irrigation began on day-of-year (DOY) 128. Water supply on DOY 199 corresponds to a recovery irrigation (see text for details). Also shown are the values of stem water potential measured at midday (Ψ_{stem}) in the instrumented trees ($n = 6$) (A) and the relative extractable water (REW) calculated from the soil water profiles measured in the rootzone of the instrumented trees ($n = 7$ for the NI trees and $n = 3$ for the OI trees) (D). Vertical bars represent \pm the standard error. The crop evapotranspiration values (ET_c), calculated as explained in the Materials and Methods section, are represented in panel C. 135

Fig. 6.1. Location of the treatments in the IFAPA experimental farm (1 = 100% IN; 2 = 75% IN; 3 = Treatment normally carried out in the orchard, ca 70% IN)..... 154

Fig. 6.2. Spatial variability of the soil electrical conductivity determined with an EM38-DD electromagnetic induction sensor in the area of orchard where the water treatments were imposed (marked area in Fig 1). Also shown are the representative locations for the 100% IN treatment (a1) and the 75% IN treatment (a2). 155

Fig. 6.3. Cumulated values of the water supplies made by the AIC in each treatment, as recorded by the flow meters. The irrigation needs calculated by the AIC with Eq. 1 (see text for details), are also shown. 158

Fig. 6.4. Root distribution observed by the trench method in October 18th. The trench was dug in the vertical of the irrigation pipe. There was as a dripper at $x = 50$ cm and another at $x = 150$ cm. 159

Fig. 6.5. Seasonal dynamics of the volumetric soil water content measured in both treatments at the maximum root depth (0.8 m) and at 1.5 m depth. See text for details on the treatments and on the measurements. Dashed lines represent the water contents at field capacity (-0.03 MPa) and wilting point (-1.5 MPa). 159

Fig. 6.6. Seasonal dynamics of the average volumetric soil water content in the top 0.5 m of soil of each treatment. See text for details on the treatments and on the measurements. Dashed lines as in Fig. 6.5..... 161

Fig. 7.1. Analysis scheme for two new heat-pulse methods. The left panel represents the Symmetrical Gradient method (HPSG) whereby the temperature difference signal is averaged over the first 60 s (ΔT). The right panel shows the Symmetrical Derivative method (HPSD) where we register the maximum value of the derivative of the temperature difference signal. 168

Fig. 7.2. Computer simulations of the performance of two new heat-pulse methods. The left panel shows the Symmetrical Gradient method (HPSG) and the right panel shows the Symmetrical Derivative method (HPSD). A strong linear relationship exists between these indicators (ΔT , and $\Delta T'$) and the imposed heat-pulse velocity, HPVI. 168

Fig. 7.3. Location of probes used in the willow experiment. Using just three sets of conventional probes, we were able to test and compare five different heat-pulse methods (CHP, T-max, HRM, CAG, HPSG and HPSD). Here, T is the temperature difference recorded following application of the 1-2 s heat pulse..... 169

Fig. 7.4. A comparison between sap flux density measurements obtained with the new Symmetrical Gradient (TR_{SG}) and Symmetrical Derivative (TR_{SD}) heat-pulse methods, versus branch transpiration calculated using a big-leaf model (TR_{model}). 171

Fig. 7.5. Scatter plots showing the relationship between sap flux density obtained from the new Symmetrical Gradient (TR_{SG}) and Symmetrical Derivative (TR_{SD}) methods and branch transpiration estimated by big-leaf model (TR_{model}). 171

Fig. 7.6. Comparing the temporal evolution of the heat pulse velocity from the new Symmetrical Gradient (SG) and Symmetrical Derivative (SD) methods and from the traditional compensation (CM) and T-max (TM) methods in the willow tree..... 172

Fig. 7.7. Linear correlations between the heat-pulse velocity from the new Symmetrical Gradient (SG) and Symmetrical Derivative (SD) methods and from the compensation method (HPVCM) in the willow tree. 173

-
- Fig. 8.1.** Inputs and outputs of the soil-plant-atmosphere model. Variations in the soil water content are calculated as the sum of the inputs: irrigation amount (IA) + effective precipitation (P_e) minus the sum of the outputs: transpiration (TR) + evaporation (ER) + drainage below the rootzone (D) 181
- Fig. 8.2.** Main diagram of the Simulink model to estimate soil water content from the evapotranspiration (ET_o), irrigation and precipitation inputs. $\Theta_{tai}(n)$ is a vector composed of the soil water content in each layer in day n. 182
- Fig. 8.3.** Soil and plant water stress models (ER vs. EP and TR vs. TP)..... 186
- Fig. 8.4.** Generalized crop coefficient (K_c) curve. DOY = day of year..... 190
- Fig. 8.5.** Identification and validation data for irrigation and no irrigation periods. DOY = day of year. SWC = soil water content..... 190
- Fig. 8.6.** Dynamics of the soil water content (SWC) simulated with CROPSYST and the proposed SPA model. 198
- Fig. 8.7.** Trajectories for the actual (dotted line) and the simulated (solid line) soil water content (SWC). One-step validation results. DOY = day of year. 201
- Fig. 8.8.** Trajectories for the actual (dotted line) and the simulated (solid line) soil water content (SWC). N-step validation results. DOY = day of year. 202
- Fig. 8.9.** Temporal evolution of the soil water content (SWC) when no irrigation was applied. DOY = day of year. 205
- Fig. 8.10.** Temporal evolution of the soil water content (SWC) when irrigation amounts are calculated as 100% of the crop evapotranspiration (ET_c) in the previous day. DOY = day of year. 205
- Fig. 8.11.** PID control scheme..... 207
- Fig. 8.12.** Temporal evolution of A: the soil water content (SWC, A) and B: the irrigation amounts (IA) and potential evapotranspiration (ET_o) when PID irrigation controller is applied. 207
- Fig. 8.13.** Simulink model for the simulation of the proportional, integral and derivative (PID) + feedforward ET_c irrigation controller. 208

Fig. 8.14. Comparison of the trajectories of the soil water content (SWC) when applying PID and when applying PID with feedforward ET_c . IA = irrigation amount. DOY = day of year. 208

Fig. 8.15. Comparing soil water content trajectories (A) and irrigation amounts (B) of the MPC and PID controllers assuming no precipitations. DOY = day of year..... 209

Fig. 8.16. Comparing soil water content trajectories (A) and irrigation amounts (B) of the MPC and PID controllers assuming precipitation events. DOY = day of year. 210

Fig. 8.17. Soil water content (SWC) trajectories (A) and irrigation amounts (IAs) applied (B) by the MPC with (MPCp) and without (MPCnp) the predictions of changes in the set point. 212

Fig. 8.18. Soil water content (SWC, A) and irrigation amounts (IA, B) when PID was applied in a real field experiments, from DOY 186 to 199. Setpoint was set to 180 mm. 214

Fig. 8.19. Soil water content (SWC, A) and irrigation amounts (IA, B) when PID was applied in a real field experiments, from DOY 208 to 220. Setpoint was set to 180 mm. 215

Tables

Table 2.1. Applied water and water balance characteristics in irrigation treatments. ...	47
Table 2.2. Yearly values of water stress integral (S_{ψ}) in each treatment during the irrigation periods.	51
Table 2.3. Average yield, water productivity and fruit quality parameters for 2005. ...	52
Table 2.4. Average yield, water productivity and fruit quality parameters for 2006. ...	52
Table 2.5. Average yield, water productivity and fruit quality parameters for 2007. ...	52
Table 2.6. Temporal variability analysis for all parameters listed by Tukey's test.	54
Table 2.7. Pearson's correlation coefficients among studied parameters for the 3-year period.	54
Table 3.1. Irrigation treatments. The aimed irrigation amount at different main phenophases is shown in terms of % of the irrigation needs.	68
Table 3.2. Main water balance components for the irrigation period at main phenophases.	71
Table 3.3. Irrigation water applied, actual water stress ratio and water savings for each treatment at different phenophases.	76
Table 3.4. Yield components and fruit quality parameters.	85
Table 3.5. Water stress integral, stomatal conductance integral, yield and fruit quality parameters for the entire study period (2007-2008) (Normalized data).	86
Table 4.1. Total irrigation amounts (IA) and water savings (WS) as compared to the control for each treatment. The experimental period was from day of year 152 to day of year 286. See text for details on the treatments.	105
Table 4.2. Correlation coefficients among between the studied parameters.	110

Table 4.3. Yield and fruit quality parameters.	112
Table 8.1. Variables and parameters of the SPA model.	184
Table 8.2. Variables and parameters of the SPA model.	198
Table 8.3. Identified values the four models of the crop coefficient (K_c).....	200
Table 8.4. Maximum and averaged relative errors for 1-step and N-step validation ..	203
Table 8.5. Irrigation ammount (IA) and mean squared error (MSE) for the tested irrigation controllers.	214

Symbols and abbreviations

Abbreviations	Description
AIC	automatic irrigation controller
CAG	calibrated gradient method
CHP	compensation heat pulse
CRM	coefficient of residual mass
CRP	control de riego de la plantación
CU	control unit
DI	deficit irrigation
FDR	frequency domain reflectometry
FI	full irrigation
HPSD	heat pulse symmetrical derivative method
HPSG	heat pulse symmetrical gradient method
HPV	heat pulse velocity
HRM	heat ratio method
IA	irrigation amount
LFDI	low frequency deficit irrigation
LVDT	linear variable displacement transducer
MIMO	multiple inputs multiple outputs
MLD	mixed logical dynamical
MPC	model predictive control
MSE	mean squared error
MU	measurement unit
NI	normally irrigated
OI	overirrigated
PCA	principal component analysis
PC _i	i-th principal component
PEC	pump and electrovalve controller
PID	proportional-integral-derivative
RDI	regulated deficit irrigation
RIA	red de información agroclimática
SISO	single input single output
SDI	sustained deficit irrigation
SDI ₅₃	treatment irrigated at 53% ET _c
SDI ₆₇	treatment irrigated at 67% ET _c
SDI ₇₇	treatment irrigated at 77% ET _c
SPA	soil-plant-atmosphere
TDV	trunk diameter variations
WUE	water use efficiency

Symbols/variables	Description	Unit
DOY	day of the year	(Day)
ECa	apparent electrical conductivity	(mS m ⁻¹)
ED	equatorial diameter	(mm)
E_{IS}	efficiency of the irrigation system	(-)
E_p	daily total tree transpiration	(L day ⁻¹)
E_{pNI}	Ep of normally irrigated tree	(L day ⁻¹)
E_{pOI}	Ep of overirrigated tree	(L day ⁻¹)
ET _c	crop evapotranspiration	(mm)
ET _o	potential evapotranspiration	(mm)
FC	field capacity	(mm)
ID	irrigation dose	(mm)
ID _{NI}	ID for normally irrigated trees	(mm)
ID _{OI}	ID for overirrigated trees	(mm)
IN	irrigation needs	(mm)
K_c	crop coefficient	(-)
K_{ci}	i-th crop coefficient	(-)
K_r	reduction coefficient	(-)
K_{SD}	proportionality constant for HPSD method	(cm s °C ⁻¹ h ⁻¹)
K_{SG}	proportionality constant for HPSG method	(cm °C ⁻¹ h ⁻¹)
LAI	leaf area index	(-)
MDS	maximum daily shrinkage	(mm)
MI	maturity index	(°Brix L g ⁻¹)
MXSD	daily maximum stem diameter	(mm)
n_i	sampling day	(day)
PD	polar diameter	(mm)
P_e	effective precipitation	(mm)
p_{max}	maximum root depth	(mm)
PT	peel thickness	(mm)
REW	relative extractable water	(mm)
S_g	integrated stomatal conductance	(mmol m ⁻² s ⁻¹)
S_{RI}	relative ratio of S_ψ	(-)
SWC	soil water content	(mm)
S_ψ	water stress integral	(MPa)
TA	titratable acidity	(TA, g L ⁻¹)
T _c	crop evapotranspiration	(mm)
P_e	effective precipitation	(mm)
TRmodel	tree transpiration from Big Leaf model	(L h ⁻¹)

TR_{SD}	sap flux density from HPSD method	$(L\ h^{-1}\ m^{-2})$
TR_{SG}	sap flux density from HPSG method	$(L\ h^{-1}\ m^{-2})$
TSS	total soluble solids content	(°Brix)
WP	water productivity	$(kg\ mm^{-1})$
WS	water savings	(mm)
θ_v	volumetric soil water content	$(m^3\ m^{-3})$
$\theta_{v,min}$	minimum soil water content	(mm)
$\theta_{v,max}$	soil water content at field capacity	(mm)
t_Z	time delay in CHP method	(s)
t_M	time delay in T-max method	(s)
Ψ_i	Ψ_{stem} in sampling day ni	(MPa)
Ψ_{stem}	midday stem water potential	(MPa)
e_{rMAX}	maximum relative error	(-)
\bar{e}_r	averaged relative error	(-)
$\overline{\Delta T}$	averaging of the temp. difference signal	(°C)
$\Delta T'_{max}$	max. slope of the temp. difference curve	$(°C\ s^{-1})$

Variable names in roman characters for the SPA model (Chapter 8)

Symbols/variables	Description	Unit
dbulb	irrigation bulb diameter	(mm)
D_i	drainage from layer i	(mm)
EP	potential evapotranspiration	(mm)
ER	actual evapotranspiration	(mm)
FC	field capacity	(mm)
FC_{rat}	field capacity ratio	$(mm\ mm^{-1})$
IA	irrigation amount	(mm)
K_{LAI}	Extinction coefficient for solar radiation	(-)
K_{rain}	rainfall reduction coefficient	$(mm\ mm^{-1})$
LAI	leaf area index	(-)
LAI_{max}	maximum LAI	(-)
L_i	depth of layer i	(mm)
p	root depth	(mm)
p_{max}	max root depth	(mm)
P	precipitation	(mm)
P_e	effective precipitation	(mm)

RG_{LAI}	LAI growth ratio	(-)
RG_{root}	root growth ratio	(-)
rw	readily available water	(-)
SWC_i	soil water content in layer i	(mm)
SWC_{act}	actual soil water content	(mm)
SWC_{mod}	modeled soil water content	(mm)
SWC_{ref}	reference for soil water content	(mm)
$SWC_{ini, rat}$	Initial soil water content ratio	(-)
TP	potential transpiration	(mm)
TP_i	potential transpiration in layer i	(mm)
TR	actual transpiration	(mm)
tr	water stress threshold	(-)
WP	wilting point	(mm)
WP_{rat}	wilting point ratio	(mm mm ⁻¹)
ΔSWC_i	daily variations of SWC in layer i	(mm)

Abstract

Freshwater is a vital resource in agriculture, particularly in dry regions such as southern Spain. The use of irrigated crops can increase greatly agricultural production, making it a crucial tool in the fight against world hunger. This need is becoming urgent considering the prospects for world population growth and food shortages in the less developed countries. There is also a growing demand from other economic sectors also competing for water resources. These issues previously mentioned justify the need for a sustainable and rational use of water, which motivates the main objective of this thesis: to develop new strategies and techniques that provide significant irrigation water savings in fruit tree orchards, while improving production and crop quality.

Several studies have shown the advantages and shortfalls of deficit irrigation as one of these strategies. Deficit irrigation consists in reducing the water applied to the plants respect to the potential maximum, without causing significant decreases in crop performance. The reported results, which are varied, depend mainly on the timing of watering restrictions during the growing season, crop type and local conditions. In the first part of this thesis we show the effects of different deficit irrigation strategies on yield and fruit quality in orange orchards located in the Guadalquivir River Valley.

An alternative way to rationalize irrigation is the implementation of precise irrigation technologies by using automatic irrigation controllers based on feedback. In this case, the irrigation dose applied is calculated from measurements of soil, plant or atmosphere variables related to the water status of the plant. In this work we have developed and field tested two of these controllers. One of them was used to daily irrigate mature olive trees, in which the irrigation dose was estimated from sap flow measurements in the trunk of representative trees. The second irrigation controller, based on weather and soil moisture measurements, was evaluated in an almond orchard, demonstrating to be useful in reducing water losses by drainage, evaporation and runoff.

One of the most innovative and promising approaches for the automation of irrigation is based on the measurement of sap flow in conductive organs of a plant. A proper application of this approach requires sensors that can reliably measure broad ranges of sap flow. Most of the commercially available sensors work well in rather restrictive ranges, i.e. they are not reliable in the case of very low or very high sap

flows. One of the main contributions of this thesis was the development and evaluation of two new methods for measuring sap flow, capable of a measurement range wider than those of most current methods, and suitable for the measurement of reverse flows. This is of great interest for the study of phenomena related to hydraulic lift in the root system of fruit trees.

Later, we show our research on modelling the soil-plant-atmosphere system and on the design of irrigation strategies based on regulating the soil moisture content, in particular proportional-integral-derivative and model-based predictive controllers. The mathematical model used was implemented in a graphical and intuitive way and can be used to perform simulations and to develop advanced model-based controllers. The simulation results of different control strategies were evaluated and compared. One of these controllers was also successfully tested on an almond orchard in two different periods during of an irrigation season. These results show that the use of techniques and tools from control theory may have a major impact on improving the irrigation systems and the efficient use of the water resources.

Resumen

El agua dulce es un recurso fundamental en agricultura, especialmente en regiones secas como el sur de España. El uso de cultivos de regadío puede incrementar enormemente la producción agrícola, lo que la convierte en una herramienta crucial en la lucha contra el hambre en el mundo. Esta necesidad empieza a ser urgente, si tenemos en cuenta las perspectivas de crecimiento poblacional mundial y la escasez de alimentos en los países menos desarrollados. A esto se le une la creciente demanda por parte de otros sectores económicos que compiten también por los recursos hídricos. Todo lo anterior justifica la necesidad de un uso sostenible y racional del agua. En este marco se encuadra el objetivo principal de esta tesis: desarrollar nuevas estrategias y técnicas que permitan ahorros significativos de agua para el riego de frutales, a la par que mejoren la producción y calidad de la cosecha.

Numerosos estudios han revelado las ventajas e inconvenientes del riego deficitario como una de estas estrategias. La estrategia de riego deficitario consiste en reducir el agua aplicada a las plantas respecto a la teóricamente máxima sin perjudicar significativamente el rendimiento del cultivo. Los resultados publicados en la literatura son dispares y varían dependiendo principalmente de la distribución en el tiempo de las restricciones de riego, del tipo de cultivo y de las condiciones locales. En la primera parte de esta tesis se muestran los efectos de distintas estrategias de riego deficitario sobre la producción y calidad del fruto en plantaciones de naranjos del Valle del Guadalquivir.

Otra de las vías para la racionalización del riego es la implantación de tecnologías de riego de precisión con el uso de controladores de riego automático basados en realimentación. En este caso, la dosis de riego a aplicar se calcula a partir de medidas de variables del suelo, planta o atmósfera relacionadas con el estado hídrico de las plantas. En este trabajo de tesis se han desarrollado y evaluado en campo dos de estos controladores. Con uno de ellos se aplicó un riego diario en un olivar adulto, con dosis de agua estimadas a partir de medidas de flujo de savia en el tronco de árboles representativos. El segundo controlador de riego, basado en medidas meteorológicas y

de humedad en el suelo, se evaluó en una plantación de almendros, demostrándose su utilidad para reducir las pérdidas de agua por drenaje, evaporación y escorrentía.

Uno de los enfoques más innovadores y prometedores para la automatización del riego es el basado en la medida del flujo de savia en órganos conductores de la planta. Su correcta aplicación requiere de sensores capaces de medir de forma fiable rangos amplios del flujo de savia. La mayor parte de los sensores disponibles en el mercado funcionan bien en rangos más restrictivos, es decir, no son fiables para el caso de flujos de savia muy bajos o muy altos. Una de las principales contribuciones de esta tesis ha sido el desarrollo y evaluación de dos nuevos métodos de medida de flujo de savia capaces de ampliar el rango de medida respecto de los métodos actuales, permitiendo, además, medir flujos inversos, lo cual es de sumo interés para el estudio de fenómenos relacionados con la elevación hidráulica en raíces de árboles frutales.

Más adelante se muestran nuestros trabajos de modelización del sistema suelo-planta-atmósfera y de diseño de estrategias de riego basadas en el uso de reguladores de la humedad en suelo, en particular del tipo proporcional-integral-derivativo y predictivo basado en modelo. El modelo matemático que presentamos se ha implementado en un entorno gráfico e intuitivo, apto para realizar simulaciones y para el desarrollo de controladores avanzados basados en modelo. Se evaluaron y compararon los resultados en simulación de diferentes estrategias de control. Uno de estos controladores fue también ensayado con éxito en una parcela de almendros, en dos periodos diferentes de una campaña de riego. En el último capítulo de esta tesis mostramos que el uso de técnicas y resultados de teoría de control puede tener un gran impacto en la mejora de los sistemas de riego y el uso eficiente de los recursos hídricos.

Chapter 1

Introduction

1.1. The need for better water management

Water is a scarce resource¹, and its rational use is compulsory. Problems derived from lack of water will likely increase, if long-term predictions on global climate change are right. Meteorological records suggest significant increases in temperature and decreases in annual precipitation, which will entail a reduction of the available water resources of the XXI century². Industry and tourism, among others productive activities, compete for this resource increasing its profitability and productivity. Nowadays, the economic sector that most fresh water consumes is agriculture: ca. 70% of the total resources, against the 20% used by industry and the 10% for domestic use. Data for Spain and Andalusia shows a similar distribution at national and regional scales (Fig. 1.1). Irrigated agriculture is of crucial importance in the economy of Andalusia. The irrigated surface in the region accounts for only 23% of the total agricultural surface, with an average water consumption of 4.761 hm³ year⁻¹, but it generates 57% of the total yield and 60% of the agricultural employment (*Plan Nacional de Regadíos, Horizonte 2008*). Considering the expected increase in world population³, it is urgent to find solutions to ensure enough food supply. This can be only achieved by increasing the world agricultural yield and water productivity, mainly from the irrigated areas as suggested by the mentioned data.

¹ The world's consumption of water is doubling every 20 years, which is more than twice the rate of our population increase (Clothier y col., 2008).

² Climate change, water and food security. FAO Water Reports 36, 201.

³ World population will hit 7 billion by 2012 and 9 billion by 2050 (ONU, 2008).

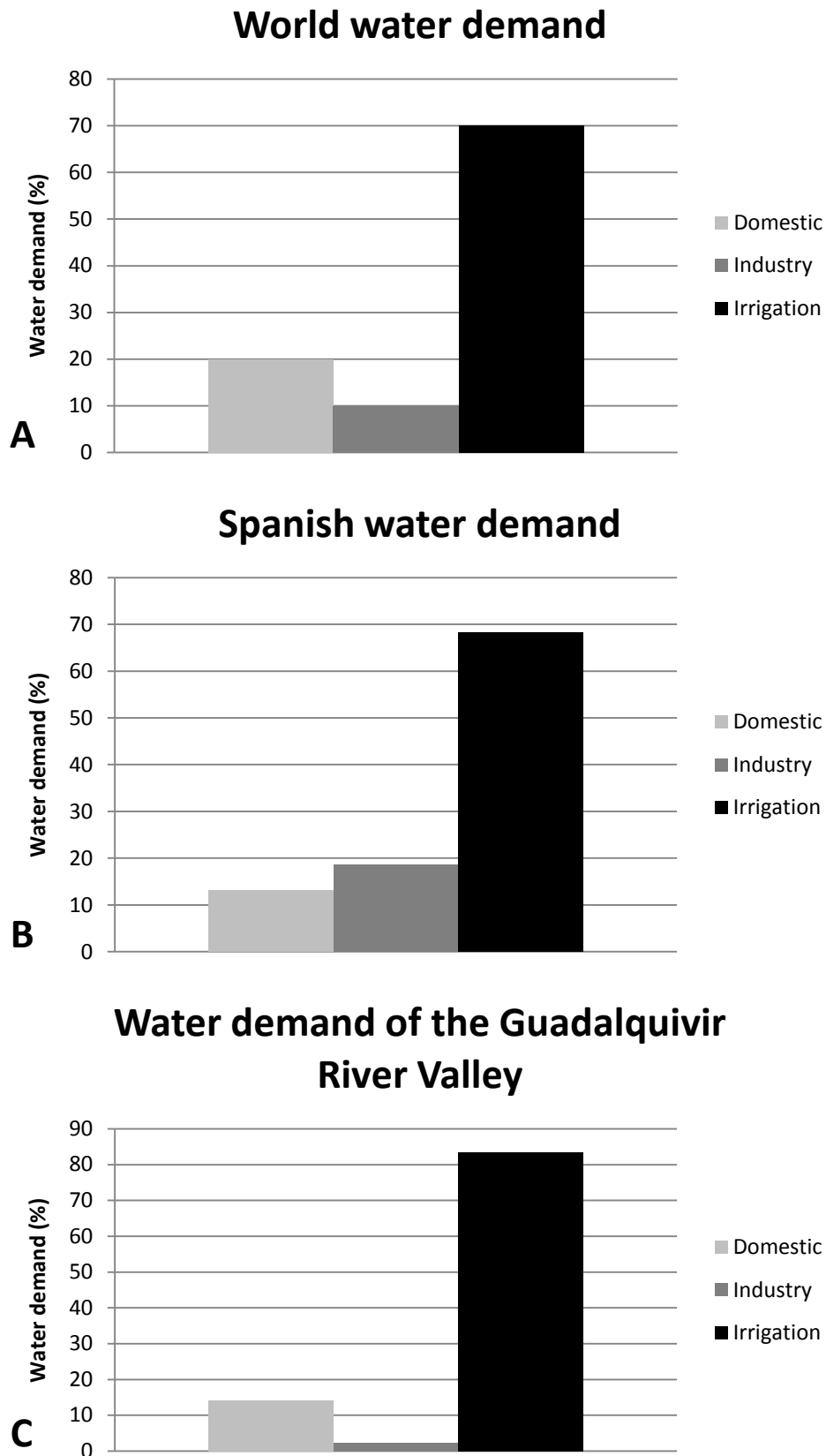


Fig. 1.1. World (A), national (B) and regional (C) water demand distributions by sectors.

This justifies the need to improve our understanding of the dynamics of the water used by the plants in order to develop methods aimed at optimizing water consumption. Indeed, this is the main motivation of this doctoral thesis.

1.2. Background

Archaeological discoveries have identified evidence of irrigation since ancient times. A form of water management called basin irrigation began at about the same time in Egypt and Mesopotamia ca. 8000 years ago (Taylor and Ashcroft, 1972), using the water of the flooding Nile or Tigris/Euphrates rivers. Nowadays, deficit irrigation (DI) strategies have proved to be efficient for achieving significant water savings with minimum reductions in crop performance. They are, in fact, the most advisable irrigation strategies for arid and semi-arid regions. The effects of DI in the performance of different fruit tree species are documented in a variety of publications which outline the advantages and shortfalls of this practice. Some authors reported that the effects of deficit irrigation on yield mainly depend on the growth stage of the crop (Doorenbos and Kassam, 1979; Ginestar and Castel, 1996; García-Tejero *et al.*, 2008). On the other hand, the negative effects from yield reductions may be partially mitigated by improvements in fruit quality (Sánchez-Blanco *et al.*, 1989; González-Altozano and Castel, 2000; Verreyne *et al.*, 2001). Furthermore, both the irrigation strategy and the cultivar definitely affect the yield response to deficit irrigation (Ginestar and Castel 1996; Treeby *et al.*, 2007; Pérez-Pérez *et al.* 2010). Different deficit irrigation strategies have been proposed, which differ mainly on the criteria for water distribution during the irrigation season. Among the most widely used are sustained deficit irrigation (SDI), which applies a constant water restriction throughout the season; regulated deficit irrigation (RDI), which involves the application of water shortages depending of crop growth stage; and low frequency deficit irrigation (LFDI), based on cycles of irrigation withholding and rewatering, designed according to a targeted crop water status, as determined from plant-based measurements (leaf or stem water potential, sap flow, trunk diameter fluctuations...). See Ruiz-Sanchez *et al.* (2010), for details on these and other DI strategies.

As early as 1859, Charles Darwin made a first reference to regulated deficit irrigation, perhaps the first documented one. Thus, in his famous work "The Origin of Species" noted that: "In some few cases it has been discovered that a very trifling change, such as a little more or less water at some particular period of growth, will determine whether or not a plant will produce seeds".

The work by Fereres and Soriano (2007) summarizes the principles of and the need for deficit irrigation. Later, Ruiz-Sanchez *et al.* (2010) reviewed the use of DI in fruit trees growing in Spain. These references provide an extensive bibliography on SDI and RDI strategies. To the best of our knowledge, very little research has been made on the effect of the LFDI strategy on the physiological response, water productivity and yield of fruit trees. Among the very few papers on this subject, Hutton *et al.* (2007) addressed the question of timing irrigation to suit citrus phenology. They, however, did not use any physiological criteria to fix the intervals between irrigation supplies.

A different approach for optimizing irrigation is the use of automatic irrigation controllers based on feedback, feed-forward strategies or a combination of both. Feedback is a mechanism, process or signal that is looped back to control a system within itself. Irrigation controllers use the information of the consequences of previous actions to calculate the next irrigation dose. In feed-forward strategies, the controllers use known or estimated values of future disturbances to compensate their effects in advance. In the field of automatic irrigation, measurements of soil, plant or atmosphere variables related to the plant water status provides the feedback and feed-forward signals. Feedback control can be said to have originated with the float valve regulators of the Hellenic and Arab worlds (Mayr, 1975), however it does not appear to have spread to medieval Europe. It seems rather to have been reinvented during the industrial revolution, where level, temperature and finally Watt's centrifugal governor were developed (Dickinson and Jenkins, 1927). Since then, automatic control has been applied in almost all engineering fields with great success; see Bennett (1996) for a brief history of automatic control, although the impact in agriculture, and in particular in precision irrigation, is limited.

Most of the irrigation controllers available on the market require the irrigation dose to be provided by the user. Only then, they are able to switch on/off the irrigation pump and to open or close the valves to apply the irrigation doses to every sector of the

orchard. Very few automatic irrigation controllers are able to calculate autonomously the irrigation dose. Most are based on measurements of soil matric potential (Luthra *et al.*, 1997; Klein, 2004; Miranda *et al.*, 2005). These devices are relatively inexpensive and easy to use, but ground water measurements imply certain limitations: they require a large number of sensors and do not take into account the plant status and response. Protocols for automatic irrigation controllers have been reported based on trunk diameter variation (Goldhamer and Fereres, 2004; Garcia-Orellana *et al.*, 2007) or sap flow measurements (Fernández *et al.*, 2001, 2008). Both methods are considered having a great potential for irrigation control (Fereres *et al.*, 2003; Jones, 2004). Unfortunately, most of the commercially available sap flow sensors are not reliable both for very low and very high sap flows.

Recently, there has been an increasing interest on developing mathematical models representing both, the dynamics of water in the soil-plant-atmosphere (SPA) system and crop performance. Among the most popular models are WAVE (Vanclooster *et al.*, 1994), SPASMO (Green, 2001), SWAP (Van Dam, 2000; Van Dam *et al.*, 2008), MACRO (Larsbo and Jarvis, 2003), CROPGRO (Boote *et al.*, 1998), WOFOST (Van Diepen *et al.*, 1989) and DSSAT (Hoogenboom *et al.*, 2004). The utility of these models both for understanding the simulated process and for optimizing related practices has been widely proved. They are able to simulate the effect of irrigation strategies, climate conditions or diseases on crop performance. Unfortunately, the current models show certain limitations. The great variability of every component of the soil-plant-atmosphere system makes difficult having good quality input data. This issue limits the accuracy of the results, especially when extrapolating situations very different from those occurred during the identification process. Another problem is that these models usually require the identification of many parameters, which means that they are not user-friendly models. Furthermore, they are often too complex, so their use requires a specific training that can be given to a reduced number of users and are not suitable for designing advanced irrigation controllers based on these models.

Recent research in modelling has provided a better understanding of the SPA system. It is now possible to test automatic irrigation controllers in computer simulations prior to their use in field experiments. These controllers can be based on

simple laws such as on / off strategies in which irrigation is switched on or off when certain threshold values are overcome or based on more advanced laws, such as proportional-integral derivative (PID) or model predictive controllers (MPC). In a PID controller, the control signal is generated as a weighted sum of three terms: the error between the process variable and the setpoint, the integral of recent errors, and the rate by which the error has been changing. MPC is based on the use of a model to predict the mathematical evolution of the system, on the minimization of a cost function based on this prediction and on the use of a receding horizon strategy. These controllers, although successfully and extensively used in other areas of science and industry, see for example Astrom and Hägglund (2006) and Camacho and Bordons (1997), have been seldom applied in agriculture. However, we might find promising examples, especially in the management of greenhouses environmental control (Rodriguez *et al.*, 2008; Piñón *et al.*, 2005; El Ghoumari *et al.*, 2005).

In the next section we show the hypothesis and objectives of this thesis, which aims to cover some of the mentioned gaps of the current knowledge. The reader can find additional publications to those mentioned here in the Introduction section of each chapter of this thesis.

1.3. Hypothesis and objectives

The main objective of this thesis is to provide new techniques to optimize the irrigation water consumption in woody crops as well as to get an insight of the soil-plant-atmosphere system. To this end, identification, modelling and control tools from control theory as well as deficit irrigation strategies have been applied. We present results from experiments with three important species in Andalusia, with contrasting water use behaviours: orange, olive and almond trees. Next, the hypothesis and corresponding objectives of this thesis are presented.

Hypothesis 1. Different DI strategies have a different impact on water productivity and yield quality.

Objective 1. To evaluate the effects of various DI strategies on fruit yield and fruit quality in citrus orchards of the Guadalquivir River Valley.

Hypothesis 2. Irrigation of woody crops can be controlled from sap flow measurements in trees under the orchard irrigation conditions and in control, fully-irrigated trees.

Objective 2. To design, implement and test the software and hardware of an automatic irrigation controller, able to calculate and apply suitable irrigation doses to mature olive trees from sap flow measurements in the trunk of deficit and fully irrigated trees.

Hypothesis 3. Precise irrigation needs can be estimated from weather data and soil water content measurements, and used to minimize water losses by evaporation, drainage and runoff.

Objective 3. To design, implement and test the software and hardware of an automatic irrigation controller suitable for fruit tree orchards, able to calculate and apply daily irrigation from soil water content and weather measurements. The device was tested in an almond orchard.

Hypothesis 4. Any sap flow method suitable to optimize irrigation must be able to measure low transpiration values.

Objective 4. To model, simulate and test new sap flow methods with a better performance than the currently available ones, especially for estimating low sap flow values. The method was evaluated both in computer simulations and in the stem of a willow tree.

Hypothesis 5. Simplified models able to design control laws could overcome the shortfall of current simulation models based on the SPA system, which are not suitable for the design and simulation of automatic irrigation controllers.

Objective 5. To design and implement a SPA model in a commercial simulation platform and validate it with a model widely used in agronomy and with data from field experiments.

Hypothesis 6. Irrigation controllers based on feedback of measurable variables of the SPA system such as soil water content, weather forecasts and dynamic models of the SPA system can optimize irrigation water use.

Objective 6. To design, implement and test both in simulation and in field experiments automatic irrigation controllers based on well known techniques from control theory.

1.4. Outline

Since most of the results of this thesis have already been reported by the author in scientific journals and workshops, we considered appropriate to structure the thesis into chapters corresponding to the most important publications by the author (Section 1.5), directly related to the hypothesis and objectives previously mentioned (Section 1.3).

Thus, Chapters 2, 3 and 4 deal with the development of experiments aimed to study three different deficit irrigation strategies and their effect on yield and fruit quality, namely sustained deficit irrigation, regulated deficit irrigation and low frequency deficit irrigation with withholding & rewatering cycles. We evaluated the effect caused by the applied deficit irrigation strategies during a whole irrigation season in three different orchards located in the Guadalquivir River Valley. We estimated water productivity, water savings and the physiological response of the crop (stem water potential, stem diameter variations, stomatal conductance...). At the end of the season, we determined the effects on yield and in the organoleptic properties of the fruits.

In Chapter 5 we designed and tested an automatic irrigation control system for fruit tree orchards, denominated CRP. Control was based on sap flow measurements in the trunk as a feedback and sap flow readings in overirrigated irrigated trees were used as a reference. The controller was successfully tested in an olive orchard (*Olea europea* cv. Manzanilla de Sevilla), in the experimental farm “La Hampa”, belonging to the Consejo Superior de Investigaciones Científicas (CSIC) and located in the municipality of Coria del Rio.

In Chapter 6 we developed an automatic irrigation system in an almond orchard, in which we had plant physiological sensors (sap flow and dendrometers), soil moisture sensors and a nearby weather station. The controller used weather data as a measurement of the disturbance to be compensated in the system and soil moisture data as a feedback to prevent flooding situations, regulating the irrigation intervals to maintain the soil water content levels between threshold values defined in previous

trials. The automatic irrigation system was evaluated in an almond orchard belonging to the Centro Las Torres-Tomejil IFAPA (TM Alcalá del Río, Seville).

In Chapter 7, we introduce new methods to estimate plant water consumption from sap flow measurements in trees. Sap flow monitoring is one of the most promising approaches to automate precision irrigation systems. We developed field experiments in plants, in which we compared our new methods against other heat-pulse techniques, to evaluate the proposed solutions.

In Chapter 8 we show the design, identification, simulation and validation processes of a representative mathematical model of this system. We used the model to design and tune both classical proportional-integral-derivative and model-based advanced controllers. In particular, we developed model based predictive controllers. In addition, an automatic irrigation controller based on a proportional-integral-derivative control law was applied in a real case, specifically in the almond orchard described in chapter 6.

Finally, in Chapter 9 we present concluding remarks and future work.

1.5. Publications by the author

Most of the results presented in this thesis have already been reported by the author in scientific journals and workshops. Major publications that have contributed to the achievement of this thesis are listed below:

Fernández JE, Diaz-Espejo A, Torres-Ruiz JM, Muriel JL, Romero R, Morales-Sillero A, Martín-Palomo MJ. 2009. Seasonal Changes of Hydraulic Conductance of Mature Olive Trees under Different Water Regimes. *Acta Hort. (ISHS)* 846:263-270.

Fernández JE, Romero R, Díaz-Espejo A, Cuevas MV, Muriel JL, Montaña JC. 2008. A device for Scheduling irrigation in fruit tree orchards from sap flow readings. *Acta Horticulturae*, 792: 283-290. (Chapter 5).

- Fernández JE, Romero R, Díaz-Espejo A, Muriel JL, Cuevas MV, Montaña JC. 2008. Design and testing of an automatic irrigation controller for fruit tree orchards based on sap flow measurements. *Australian Journal of Agricultural Research* 59, 589–598. (Chapter 5).
- Fernández JE, Romero R, García I, Muriel JL. 2010. An Automatic Controller for High Frequency Irrigation Based on FDR Measurements Combined with the Crop Coefficient Approach. *The Third International Symposium on Soil Water Measurement Using Capacitance, Impedance and TDR (Murcia, Spain)*
- García-Tejero I, Jiménez-Bocanegra JA, Durán-Zuazo VH, Romero R, Muriel JL. 2010. Positive Impact of Deficit Irrigation on Physiological Response and Fruit Yield in Citrus Orchards: Implications for Sustainable Water Savings. *Journal of Agricultural Science and Technology Vol 4, No.3.* (Chapter 2).
- García-Tejero I, Jiménez-Bocanegra JA, Martínez G, Durán-Zuazo VH, Romero R, Muriel JL. 2010. Positive Impact of Regulated Deficit Irrigation on Yield and Fruit Quality in a commercial Citrus Orchard. *Agricultural Water Management Vol 97, 614-622.* (Chapter 3).
- García-Tejero I, Romero R, Jiménez-Bocanegra JA, Martínez G, Durán-Zuazo VH, Muriel JL. 2010. Response of citrus trees to deficit irrigation during different phenological periods in relation to yield, fruit quality, and water productivity. *Agricultural Water Management Vol 97, 689-699.* (Chapter 4).
- Martínez G, Vanderlinden K, Jiménez JA, Romero R, García I, Muriel JL. 2007. Uso de un sensor de inducción electromagnética para detectar zonas con un manejo diferenciado del suelo. *Estudios de la Zona No Saturada del Suelo Vol. VIII. ZNS'2007.*
- Romero R, Green S, Muriel JL, Garcia I, Clothier B. 2011. Improving Heat-Pulse Methods to Extend the Measurement Range Including Reverse Flows. *VIII International Workshop on Sap Flow (Volterra, Italy).* Submitted. (Chapter 7).
- Romero, R, Martín-Palomo MJ, Muriel JL, Díaz-Espejo, A, Fernández JE. 2010. Water Consumption in Young and Mature Olive Trees As Affected by the Irrigation System. *28th International Horticultural Congress. 28th International*

-
- Horticultural Congress (28). Num. 28. Lisbon. International Society for Horticultural Science (ISHS), 691-692.
- Romero R, Muñoz de la Peña D, Muriel JL, Fernández JE. 2011. Modeling and control of the soil water content in an almond orchard. *Computers and Electronics in Agriculture*. Submitted. (Chapter 8).
- Romero R, Muriel JL, García I. 2009a. Automatic Irrigation System in Almonds and Walnuts Trees Based on Sap Flow Measurements. *Acta Hort. (ISHS)* 846:135-142. (Chapter 6).
- Romero R, Muriel JL, García I. 2009b. A simple Soil-Plant-atmosphere model in Simulink for irrigation control testing. VI International Symposium on Irrigation of Horticultural Crops (Viña del Mar, Chile). Submitted. (Chapter 8).
- Romero R, Muriel JL, García I, Muñoz de la Peña D. 2010. Modelo suelo-planta-atmósfera para experimentación de control de riego. *Proceedings of the XXXI Jornadas de Automática*, Jaén, Spain, Sept. 2010. (Chapter 8).
- Torres-Ruiz JM, Fernández JE, Diaz-Espejo A, Muriel JL, Romero R, Martín-Palomo MJ, Morales-Sillero A. 2011. Stomatal Control and Hydraulic Conductivity in 'Manzanilla' Olive Trees under Different Water Regimes. *Acta Hort. (ISHS)* 888:149-155.

1.6. References

- Astrom KJ, Hägglund T. 2006. *Advanced PID control: ISA - The Instrumentation, Systems, and Automation Society*. 461 p.
- Bennett S. 1996. A brief history of automatic control. *IEEE Control Systems Magazine* 16(3):17-25.
- Boote KJ, Jones JW, Hoogenboom G. 1998. *Simulation of crop growth: CROPGRO model*.
- Camacho EF, Bordons C. 2004. *Model predictive control: Springer Verlag*. 405 p.

- Dickinson H, Jenkins R. 1927. James Watt and the Steam Engine: Clarendon. Oxford.
- Doorembos J, Kassam A. 1979. Yield response to water. Rome: FAO 33.
- El Ghoumari MY, Tantau HJ, Serrano JS. 2005. Non-linear constrained MPC: Real-time implementation of greenhouse air temperature control. *Comput Electron Agric* 49(3):345-356.
- Fereres E, Goldhamer DA, Parsons LR. 2003. Irrigation water management of horticultural crops. *Hortscience* 38(5):1036-1042.
- Fereres E, Soriano MA. 2007. Deficit irrigation for reducing agricultural water use. *Journal of Experimental Botany* 58(2):147-159.
- Fernández JE, Green SR, Caspari HW, Díaz-Espejo A, Cuevas MV. 2008. The use of sap flow measurements for scheduling irrigation in olive, apple and Asian pear trees and in grapevines. *Plant and Soil* 305(1-2):91-104.
- Fernández JE, Palomo MJ, Díaz-Espejo A, Clothier BE, Green SR, Girón IF, Moreno F. 2001. Heat-pulse measurements of sap flow in olives for automating irrigation: tests, root flow and diagnostics of water stress. *Agric Water Manage* 51(2):99-123.
- García-Orellana Y, Ruiz-Sánchez MC, Alarcón JJ, Conejero W, Ortuño MF, Nicolás E, Torrecillas A. 2007. Preliminary assessment of the feasibility of using maximum daily trunk shrinkage for irrigation scheduling in lemon trees. *Agric Water Manage* 89(1-2):167-171.
- García-Tejero I, Jiménez JA, Reyes MC, Carmona A, Pérez R, Muriel JL. 2008. Aplicación de caudales limitados de agua en plantaciones de cítricos del valle del Guadalquivir. *Fruticultura Profesional* 173:5-17.
- Ginestar C, Castel JR. 1996. Responses of young clementine citrus trees to water stress during different phenological periods. *Journal of Horticultural Science* 71(4):551-559.
- Goldhamer DA, Fereres E. 2004. Irrigation scheduling of almond trees with trunk diameter sensors. *Irrigation Science* 23(1):11-19.

-
- Gonzalez-Altozano P, Castel JR. 2000. Effects of regulated deficit irrigation on 'Clementina de Nules' citrus trees II. Vegetative growth. *J Am Soc Hort Sci* 75:388-392.
- Green S. 2001. Pesticide and nitrate movement through Waikato and Franklin soils. Interim Progress Report, HortRes, 2002/007, Palmerston North, NZ.
- Hoogenboom G, Jones J, Wilkens P, Porter C, Batchelor W, Hunt L, Boote K, Singh U, Uryasev O, Bowen W. 2004. Decision support system for agrotechnology transfer version 4.0 [CD-ROM]. University of Hawaii, Honolulu, HI 1:235-265.
- Hutton R, Landsberg J, Sutton B. 2007. Timing irrigation to suit citrus phenology: a means of reducing water use without compromising fruit yield and quality? *Australian Journal of Experimental Agriculture* 47(1):71-80.
- Jones HG. 2004. Irrigation scheduling: advantages and pitfalls of plant-based methods. *Journal of Experimental Botany* 55(407):2427-2436.
- Klein I. 2004. Scheduling Automatic Irrigation by Threshold-Set Soil Matric Potential Increases Irrigation Efficiency While Minimizing Plant Stress. *Acta Hort (ISHS)* 664:361-368.
- Larsbo M, Jarvis N. 2003. MACRO 5.0: a model of water flow and solute transport in macroporous soil: technical description: Department of Soil Sciences, Swedish Univ. of Agricultural Sciences.
- Luthra SK, Kaledhonkar MJ, Singh OP, Tyagi NK. 1997. Design and development of an auto irrigation system. *Agric Water Manage* 33(2-3):169-181.
- Mayr O. 1975. *The origins of feedback control*: MIT press. Cambridge. MA. 176 p.
- Miranda FR, Yoder RE, Wilkerson JB, Odhiambo LO. 2005. An autonomous controller for site-specific management of fixed irrigation systems. *Comput Electron Agric* 48(3):183-197.
- Pérez-Pérez JG, García J, Robles JM, Botía P. 2010. Economic analysis of navel orange cv. 'Lane late' grown on two different drought-tolerant rootstocks under deficit irrigation in South-eastern Spain. *Agric Water Manage* 97(1):157-164.

-
- Piñón S, Camacho EF, Kuchen B, Pena M. 2005. Constrained predictive control of a greenhouse. *Comput Electron Agric* 49(3):317-329.
- Rodriguez F, Guzman JL, Berenguel M, Arahall MR. 2008. Adaptive hierarchical control of greenhouse crop production. *Int J Adapt Control Signal Process* 22(2):180-197.
- Ruiz Sánchez MC, Domingo Miguel R, Castel Sánchez JR. 2010. Review. Deficit irrigation in fruit trees and vines in Spain. *Plant Soil* 120:299-302.
- Sánchez-Blanco MJ, Torrecillas A, León A, Delamor F. 1989. The Effect of Different Irrigation Treatments on Yield and Quality of Verna Lemon. *Plant and Soil* 120(2):299-302.
- Taylor SA, Ashcroft GL. 1972. *Physical edaphology: the physics of irrigated and nonirrigated soils*: San Francisco, CA (EUA). WH Freeman.
- Treeby MT, Henriod RE, Bevington KB, Milne DJ, Storey R. 2007. Irrigation management and rootstock effects on navel orange *Citrus sinensis* (L.) Osbeck fruit quality. *Agric Water Manage* 91(1-3):24-32.
- van Dam JC. 2000. Field-scale water flow and solute transport: SWAP model concepts, parameter estimation and case studies. PhD-thesis, Wageningen University, Wageningen, The Netherlands. 167 p.
- van Dam JC, Groenendijk P, Hendriks RFA, Kroes JG. 2008. Advances of modeling water flow in variably saturated soils with SWAP. *Vadose Zone Journal* 7(2):640-653.
- van Diepen CA, Wolf J, van Keulen H, Rappoldt C. 1989. WOFOST: a simulation model of crop production. *Soil Use and Management* 5(1):16-24.
- Vanclooster M, Viaene P, Diels J. 1994. WAVE: a mathematical model for simulating water and agrochemicals in the soil and vadose environment: reference and user's manual (release 2.0): Katholieke Universiteit Leuven.
- Verreyne JS, Rabe E, Theron KI. 2001. The effect of combined deficit irrigation and summer trunk girdling on the internal fruit quality of 'Marisol' Clementines. *Scientia Horticulturae* 91(1-2):25-37.

Chapter 2

Impact of sustained deficit irrigation on yield, water productivity and fruit quality in a commercial citrus orchard, cv. Salustiana

Part of this chapter is published in:

García-Tejero I, Jiménez-Bocanegra JA, Durán-Zuazo VH, Romero R, Muriel JL. 2010. Positive Impact of Deficit Irrigation on Physiological Response and Fruit Yield in Citrus Orchards: Implications for Sustainable Water Savings. *Journal of Agricultural Science and Technology* Vol 4, No.3.

Abstract. This work analyses the impact of three sustained deficit irrigation (SDI) treatments, with different levels of water reduction, on the yield of a 12-year-old orange orchard (*Citrus Sinensis* L. Osbeck, cv. Salustiana) from 2004 to 2007. In addition, a control treatment was established in which 100% of the irrigation needs (IN, mm) was supplied. The three SDI treatments were irrigated at 77%, 67% and 53% of IN, respectively. For each treatment, midday stem water potential (Ψ_{stem} , MPa) values were measured every 10-15 days. Then, the water stress integral (S_{Ψ} , MPa), i.e. the cumulative integral of Ψ_{stem} over the studied period, was used to evaluate the global water status of the plant. Yield and fruit quality were analyzed at harvest. Data were normalized to take into account the temporal variability of the results due to changing weather conditions during the studied years. Significant differences between treatments were found both in total soluble solids and titratable acidity. These variables showed significant regression coefficients with the values of the integrated Ψ_{stem} . These results led us to conclude that, in mature orange trees grown under the evaluated conditions, SDI has significant effects on fruit quality. On the contrary, the effects of the tested SDI treatments on yield were not significant. Thus, in the SDI treatment in which 53% of the irrigation needs were supplied, we got $14.9 \pm 9.9\%$ decrease in yield, as compared with the yield obtained in the control treatment, but this difference was not statistically significant. A global rescaled distance cluster analysis was performed both to summarize main relationships between the evaluated

variables and to establish a correlation matrix. Finally, a classification tree was derived and principal-component analysis was undertaken. This allowed us to identify and evaluate the variables that better explain the effect of irrigation treatments on the crop. In conclusion, the tested SDI strategies increased water productivity and fruit quality with non significant reductions in yield. They can be considered, therefore, as advisable strategies for orange orchards (*Citrus Sinensis* L. Osbeck, cv. Salustiana) in our region.

2.1. Introduction

From 70% to 80% of the worldwide water usage is associated with agriculture, the greater percentages corresponding to arid and semi-arid areas. This has created competition for water with other sectors, such as industry or tourism, in which water is more commercially valuable than in agriculture. However, the socio-economic value of irrigated land in Andalusia exceeds 3.5-fold the value in extensive agriculture on non-irrigated land (Berbel and Gutiérrez, 2004).

The current area cropped with citrus in Andalusia (74,000 ha) has increased by 2.04% annually for the last 25 years. The expected production of citrus in the region will be close to 2.3 million tons by 2015 (30% of the national production). Of the total area of citrus in Andalusia, 51,500 ha are dedicated to sweet orange, covering the Salustiana and Valencia cultivars almost 20% of that area.

The average annual irrigation water consumed in Andalusia is close to 4,761 hm³, with about 10% diverted to citrus groves (García-Tejero *et al.*, 2008).

Weather forecasts for the 21st century predict significant increments in temperature and major reductions in the annual precipitation, which may led to an estimated 17% decline in the available water resources for agriculture worldwide. An increase in potential evapotranspiration (ET_o, mm) of over 20% is expected in the Guadalquivir river valley by the year 2050. The biggest increases will occur in the most western areas where the majority of arable land is concentrated (Rodríguez Díaz *et al.*, 2007).

Under such restrictive conditions, finding new cultivation strategies is becoming a priority. They must be focussed on reducing water consumption and on making more efficient the use of the available water resources. Thus, maximizing the use of water saving techniques and improving crop productivity is crucial for a rational agriculture.

This can be achieved with deficit irrigation (DI) strategies, i.e. by applying lower amounts of irrigation water than those needed by the crop.

Plants undergo stress when the water taken up by the roots fails to compensate for the transpiration driven by atmospheric conditions. When the water stored in the soil is being depleted the actual crop evapotranspiration (ET_c , mm) decreases. This usually affects photosynthesis and lowers carbon assimilation (Hsiao, 1973). Consequently, vegetative development and crop yield are reduced (González-Altozano and Castel, 2000).

In recent years, several contributions have documented the advantages of using deficit irrigation (DI) strategies to improve water saving and fruit quality in citrus trees (Southwick and Davenport, 1986; Ginestar and Castel, 1996; González-Altozano and Castel, 1999, 2000; Muriel *et al.*, 2006; García-Tejero *et al.*, 2007, 2008). Shalhevet and Bielorai (1978) and Doorenbos and Kassam (1979) reported that the response of the citrus trees to water stress depends strongly on the phenological stage of the crop. Other authors agreed with that statement, and also outlined the importance of the pedoclimatic characteristics of the orchard (Ginestar and Castel, 1996, and Treeby *et al.*, 2007, in orange orchards; Sánchez-Blanco *et al.*, 1989, in lemon orchards). Thus, a water deficit at the end of the fruit growing period increases juice acidity and soluble-solid contents (González-Altozano and Castel, 1999; Hutton *et al.*, 2007). Other authors have shown that a reduction in the available soil water during flowering could decrease yield, because it may affect the fruit-setting process (Doorenbos and Kassam, 1979; Castel and Buj, 1990). Pérez-Pérez *et al.* (2008) reported that water stress during flowering and fruit setting reduces the number of fruits. Concerning fruit weight and fruit diameter, the response of fruit weight and fruit diameter to water stress is species-dependent. Thus, it has been reported that DI conditions are responsible for a greater number of smaller fruits, since the lack of water reduces fruit weight and diameter (Treeby *et al.*, 2007). Peng and Rabe (1998), however, worked with 'Satsuma' and found that fruit size was not affected by water deficit.

The term water productivity (WP, $\text{kg}\cdot\text{L}^{-1}$) refers to the crop production per unit of water applied, rather than per unit of irrigated surface (Feres and Soriano, 2007). The effects of DI on yield and fruit quality in orange groves will depend mainly on the

plant material, and the intensity, duration, and timing of the imposed water deficits (Vaux and Pruitt, 1983; Ginestar and Castel, 1996). In any case, the correct application of any DI strategy should boost WP with a minimum yield decrease. Sustained deficit irrigation (SDI) is a widely used DI strategy. Basically, SDI consists on applying a reduced percentage of ET_c all throughout the irrigation season. The aim of this work was to evaluate the impact of SDI treatments with different levels of water stress on yield and fruit quality in a commercial citrus orchard, cv. Salustiana, under non-tillage soil management. The work, which lasted for three years (2004-2007), was focused on evaluating plant-water relations in the orchard with the aim of improving WP.

2.2. Material and methods

2.2.1. Experimental site

This work was made in a commercial orchard located in the Guadalquivir River Valley, SW Spain ($37^{\circ} 44' 57''$ N, $5^{\circ} 10' 6''$ W), planted with 12-year-old orange trees (*Citrus sinensis*, L. Osbeck, cv Salustiana) grafted on Citrange Carrizo (*Citrus sinensis*, L. Osbeck x *Poncirus trifoliata*, L. Raf.). The trees, spaced 6 m x 4 m, were, on average, 3.25 m in height and 4.0 m in diameter. They were planted on ridges 0.4 m high and 4 m wide, with 2 m between ridges. The orchard was under non-tillage conditions. From October to May grass covered the row between ridges. In October, immediately after pruning the trees, the grass was mechanically cut and left on the soil orchard. Later in the year, from the beginning of the period of high atmospheric demand, herbicides were used to keep the soil free of weeds.

The soil is a calcareous sandy-clay loam fluvisol (FAO, 1998) with an effective depth of 0.6 m. At deeper depths, the soil has high contents of clay and calcic carbonate. In the top 0.6 m soil layer, textural values are $56.65 \pm 5.0\%$ sand, $21.99 \pm 3.0\%$ silt, and $21.39 \pm 2.5\%$ clay. The soil is rich in calcium ($75.4 \text{ cmol kg}^{-1}$) and poor in both nitrogen (460 mg kg^{-1}) and organic matter (1.0 %). The water-holding capacity is 107 mm on average and the bulk density ranges from 1.23 to 1.30 Mg m^{-3} . Nutrients were applied twice per week from the end of March to October. Each treatment received a total of 150 kg ha^{-1} of N, 70 kg ha^{-1} of P_2O_5 and 110 kg ha^{-1} of K_2O .

The climate is typically Mediterranean, with dry, hot summers and mild, wet winters. Average annual ET_o and rainfall values are 1400 mm and 534 mm, respectively (period 1971-2000). Rainfall is distributed mainly from late autumn to early spring, with November to February being the wettest months. Temperature in winter rarely falls below 0 °C; in July and August may peak to over 40 °C.

2.2.2. Irrigation treatments and experimental design

Four irrigation treatments were applied over three consecutive years (2005-2007): 1) control, where water was applied to satisfy 100% of the irrigation needs (IN, mm); 2) SDI77, at 77% of IN; 3) SDI67, at 67% of IN; 4) SDI53, at 53% of IN. Each year, the treatments were implemented from May-June to October-November. Irrigation in each treatment was controlled automatically, with a head-unit programmer and electro-hydraulic valves.

The irrigation system consisted of two laterals per tree row with self-compensating drippers 1 m apart (8 drippers per tree). The discharge rate of the drippers depended on the treatment: control, 3 L h⁻¹; SDI77, 2.3 L h⁻¹; SDI67, 2 L h⁻¹; SDI53, 1.6 L h⁻¹.

Five 288 m² plots per treatment were distributed in a randomized complete block design. Each plot consisted of three rows with four trees per row. Measurements were made in the two central trees of each plot, termed here as sample trees.

Seasonal values of ET_o were calculated with the FAO56 Penman-Monteith equation (Allen *et al.*, 1998), with data from an automatic weather station nearby the orchard. Irrigation needs (IN, mm) were weekly calculated as:

$$IN = \left[\sum_{k=1}^7 ET_o^k \right] \cdot K_c \cdot K_r - P_e \quad \text{Eq. 2.1}$$

where K_c is the crop coefficient, K_r is a reduction coefficient accounting for the percentage of ground surface covered by the crop and P_e is the effective precipitation. Although the use of monthly values of K_c may lead to more accurate estimations of ET_c than one single K_c value for the whole season, we assumed $K_c = 0.7$ all throughout the

season, because this is the usual practice in the region. This will help growers to adopt our results. We considered $K_r = 1$ after Fereres and Castel (1981), since more than 50% of the ground surface was covered by the canopies of the trees.

2.2.3. Plant measurements

Values of Ψ_{stem} were obtained with a pressure chamber (Scholander et al., 1965) following Turner (1988). Once every 10-15 days, two mature leaves were sampled from the north quadrant of each one of two sample trees of each plot. Measurements were made between 12.00 and 14.00 Greenwich Mean Time (GMT). S_Ψ was estimated according to a modified equation derived from that proposed by Myers (1988), which integrates the water-potential values over the period for which the trees are stressed:

$$S_\Psi = \sum_{i=1}^{i=t} \left| \Psi_{i+1} \cdot (n_{i+1} - n_i) + \frac{1}{2} (\Psi_i - \Psi_{i+1}) \cdot (n_{i+1} - n_i) \right| \quad \text{Eq. 2.2}$$

Ψ_i and Ψ_{i+1} are the Ψ_{stem} values measured in two sampling days (n_i and n_{i+1}).

The assumption implicit in the calculation of S_Ψ is that stressing conditions reflected in Ψ_{stem} reduce the growth rate. S_Ψ is an approximation of the integral of the rate. For example, the increment of the basal area reached at the end of the growing period will be a function of S_Ψ calculated over the complete period.

At the end of each season, the total fruit weight of each of the two sample trees of each plot was determined. For each treatment, WP was calculated by dividing the yield (kg) by the volume of water applied (L).

For each SDI treatment, we also studied the relationships between the relative ratio of S_Ψ (S_{RI}) and the total applied irrigation amounts (IAs, % IN), S_{RI} was defined as:

$$S_{\text{RI}ij} = \left| 1 - \frac{S_{\Psi ij}}{S_{\Psi(\text{control})j}} \right| \quad \text{Eq. 2.3}$$

where subindices i and j stand for treatment and year, and $S_{\Psi(\text{control})j}$ is the S_Ψ of the control treatment in each year.

Fruit-quality characteristics were analysed after harvest. Ten fruits from each of the two sample trees of each plot were used for analysis. For each fruit we measured equatorial (ED, mm) and polar (PD, mm) diameters, peel thickness (PT, mm), fruit weight and juice content. Total soluble solids content (TSS, °Brix) was measured with a digital refractometer PR-101. Titratable acidity (TA, g L⁻¹) was determined by titrating the samples with NaOH 0.1 N by the colorimetric method, using phenolphthalein as indicator solution. Maturity index (MI, °Brix L g⁻¹) was then calculated by dividing TSS by TA. This is a key parameter to determine the optimal time for harvesting.

2.2.4. Statistical analysis

Data of each year were subjected to a one-way variance analysis (ANOVA; SPSS statistical package; SPSS, Chicago, IL, USA) with four irrigation treatments and ten replicates per treatment, using Tukey's test for mean separations ($P < 0.05$). With this method, yearly values of yield, WP and fruit quality were compared between treatments. A similar analysis was carried out with the whole dataset (2004 to 2007) to evaluate the temporal variability by comparing the same parameters between years.

An overall analysis was made for evaluating the correlations between the studied parameters. Datasets were previously normalized following Sterk and Stein (1997), whose methodology allows a dataset to be analysed when different conditions have occurred during sampling (in our case, different years differing in meteorological conditions). Then, the Pearson's correlation coefficient was calculated for the whole period. When applied to two variables, the coefficient is defined as the covariance of the two variables divided by the product of their standard deviations. With a value within ± 1 , the coefficient informs on the correlation (linear dependence) between the variables.

A classification tree (Rawls and Pachepsky, 2002) was derived using the R software (Team RDC, 2008) to determine the relationships between the variables and to group the complete dataset into the different irrigation strategies. The classification tree is based on the calculation of the deviations of each variable from its mean value and the corresponding deviation of each group from the mean of the group for different thresholds. The variable and threshold that give the maximum deviations are selected

and classification is continued in this manner until determining a minimum number of elements belonging to a particular group.

We also used the R software to make a principal component analysis (PCA). The PCA (Ihaka and Gentleman, 1996) is a factor analysis protocol used to identify variables or underlying factors that better explain the correlation or covariance matrix of several variables (Davis, 2002). Thus, linear combinations of the factors or components may explain a large part of the found variability, thus reducing the number of variables required to explain the total variability.

2.3. Results

2.3.1. Water relations

The main components of the water balance (P_e , ET_c and IA) in the irrigation treatments are shown in Table 2.1 and Fig. 2.1. Rainfall values registered during each irrigation period were quite similar except for 2005, when the P_e was 89% and 84% lower than in 2006 and 2007 respectively, thus increasing the water deficit ($ET_c - P_e$) to as much as 679 mm, 8% higher than in 2006 and 22% higher than in 2007. Rainfall was very low during the period of highest atmospheric demand from mid-June to mid-September. For all treatments, IA was quite close to the aimed amounts, except in 2007.

2.3.2. Plant-water measurements

The influence of IA on Ψ_{stem} is shown in Fig. 2.2. In 2005 and 2007, lack of water at the end of August (DOY 240) caused a reduction in the IAs, which led to a decrease of Ψ_{stem} down to -1.5 MPa and -1.8 MPa in 2005 and 2007 respectively. The greatest variability of Ψ_{stem} along the season was found in the SDI53 treatment. Maximum value of -0.5 MPa for Ψ_{stem} was recorded in the control treatment in 2005.

The seasonal pattern of the plant water status, as indicated by Ψ_{stem} , in the SDI treatments did not appreciably differ from control. Significant differences were found between treatments, but only during the period of highest atmospheric demand from mid-June to mid-September. Differences were more evident between the SDI53 and the control treatments. These differences were reflected in S_ψ . Thus, the control treatment

Table 2.1. Applied water and water balance characteristics in irrigation treatments.

		Years	2005	2006	2007	<i>Average</i>
		IP ¹ (DOY)	152-282	114-279	133-312	158
P_e ² (mm)		During IP	13	115	81	70
		Annual	296	436	347	360
ET _c (mm)		During IP	692	745	639	692
		Annual	1026	1041	935	1001
control		IA (mm)	704	653	658	672
		IA ³ (% IN)	104	104	118	108
		WB ⁴	25	23	100	49
Irrigation treatments	SDI77	IA (mm)	540	501	504	515
		IA (% ET _c)	80	80	90	83
		WB (mm)	-139	-129	-54	-107
	SDI67	IA (mm)	469	436	438	448
		IA (% ET _c)	69	69	78	72
		WB (mm)	-210	-194	-120	-175
SDI53	IA (mm)	376	348	351	358	
	IA (% ET _c)	55	55	63	58	
	WB (mm)	-303	-282	-207	-264	

¹Irrigation Period; ²Effective precipitation; ³Irrigation amount; ⁴Water balance (=IA+ P_e -ET_c)
SDI77, low deficit irrigation; SDI67, moderate deficit irrigation; SDI53 severe deficit irrigation.
DOY, day of year

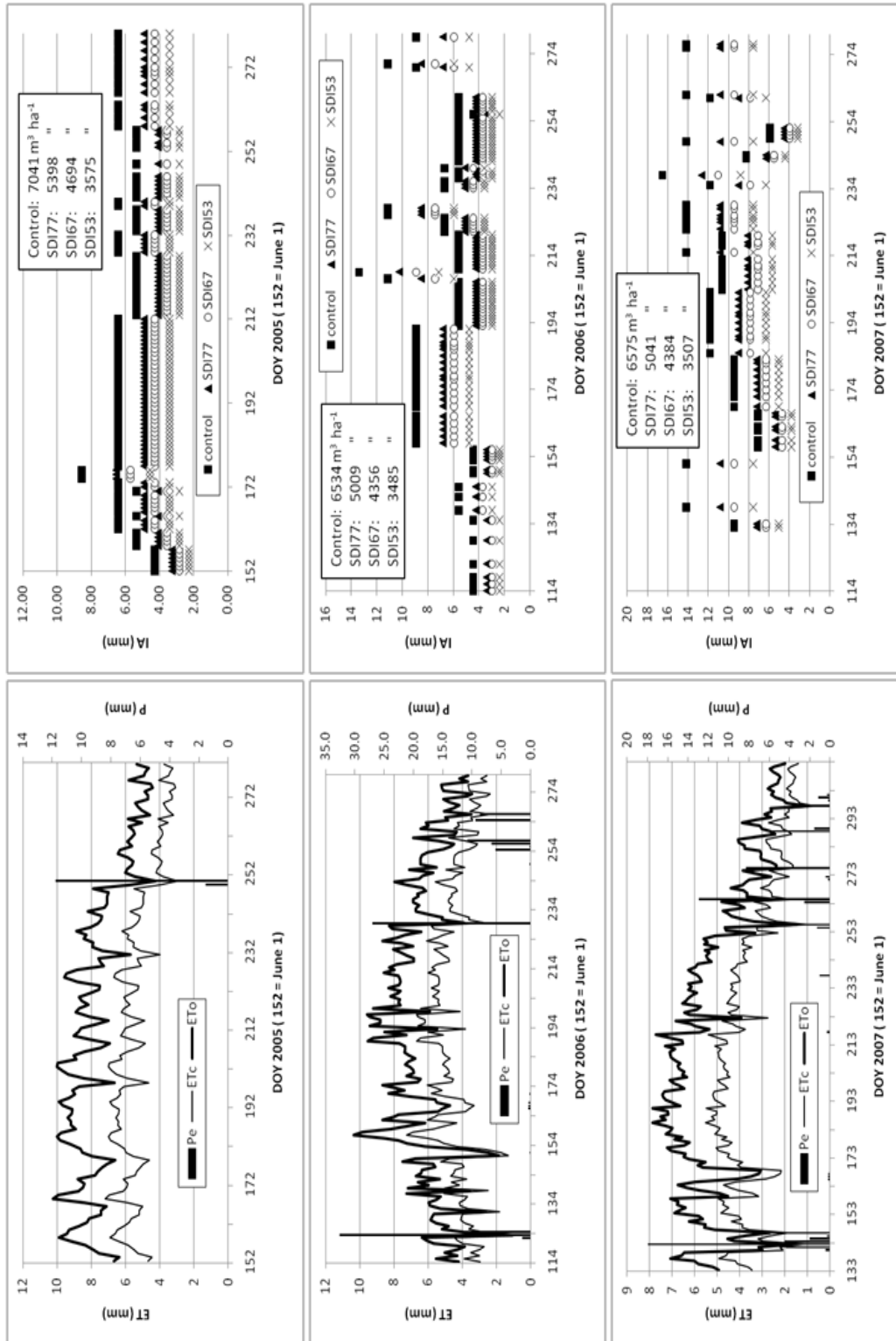


Fig. 2.1.1. Effective precipitation (Pe), crop (ET_c) and potential (ET_o) evapotranspiration, and irrigation amounts (IA) for each treatment during the tree experimental years. DOY = day of year.

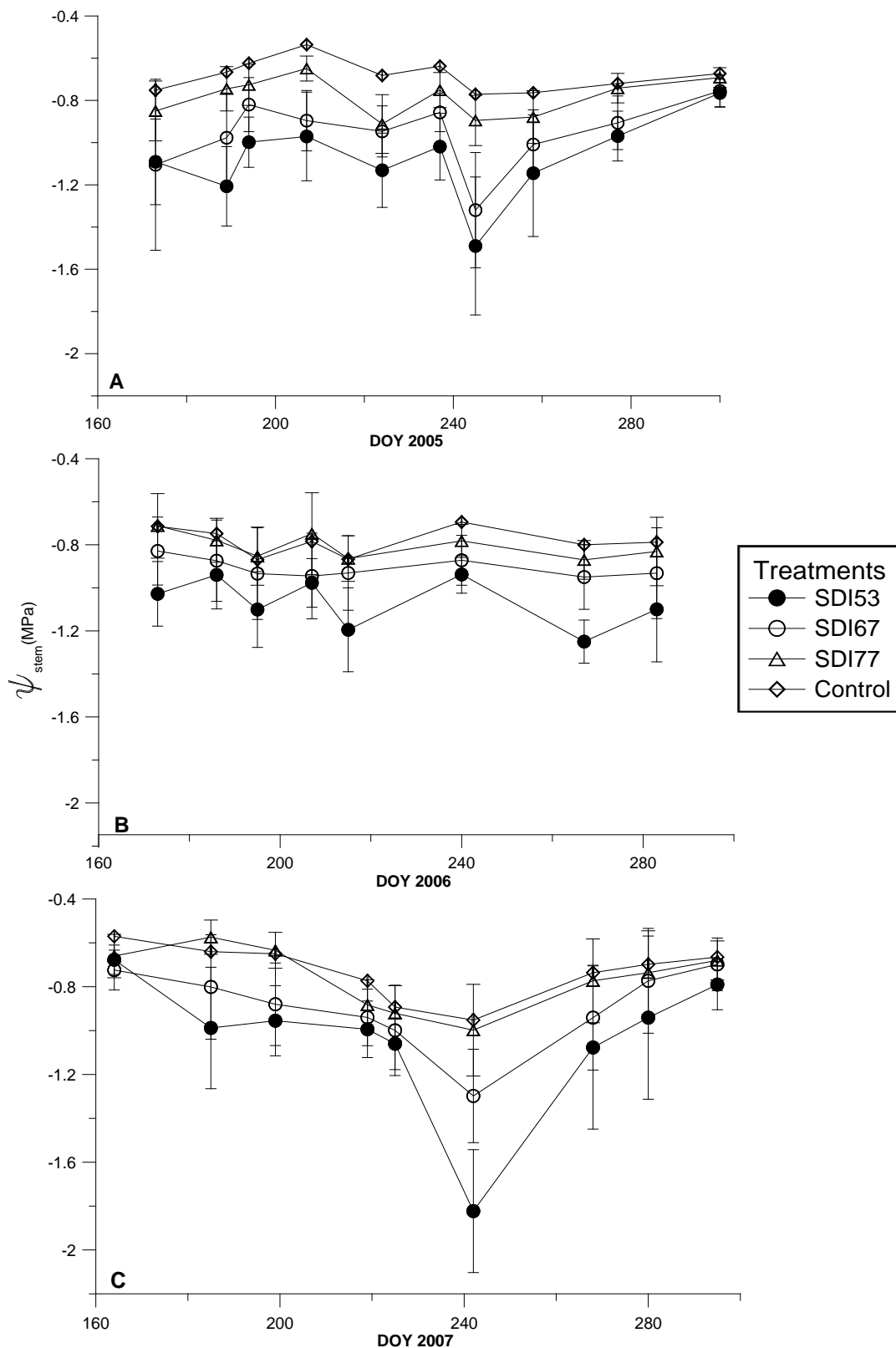


Fig. 2.2. Seasonal patterns of midday stem water potential (Ψ_{stem}) for each irrigation treatment and experimental year. Each point represents the average of 20 readings. Vertical bars represent the standard deviation. DOY = day of year.

gave the lowest S_{Ψ} values, which were statistically different from those corresponding to the SDI53 and SDI67 treatments (Table 2.2). The overall analyses revealed that, on average, the SDI77 treatment did not give S_{Ψ} values significantly different from those in the control treatment. This suggests that the $S_{\Psi} = 91.3$ MPa can be established as a threshold value for accumulated water stress in the considered period.

In 2007, a year with high IAs, Ψ_{stem} , and consequently S_{Ψ} were quite similar in the SDI77 and control treatments. This was not surprising, considering that the IAs were enough to satisfy IN in both treatments.

Fig. 2.3 shows the relationship between S_{RI} and IA (expressed as percentage of IN) in the SDI treatments. A negative tight linear correlation ($r^2 = 0.85$) was found, suggesting that this ratio is a good indicator of the plant-water relationship.

2.3.3. Effects of irrigation treatments on yield, fruit quality, and water productivity

In 2005 significant differences were found between treatments regarding fruit weight, TSS, and TA (Table 2.3). The fruits produced by the SDI53 trees were smaller and lighter than those of the control treatment. Both TA and TSS were greater in the deficit treatments, especially in SDI53. Although the yield response was not statistically significant, it was lower in all SDI treatments than in the control treatment, especially in SDI53, for which 21% yield reduction was observed (Table 2.3).

In 2006 TSS and TA were the only variables for which significant differences between treatments were found (Table 2.4). Differences were also found in other parameters such as peel thickness, fruit weight and maturity index, but these were not significant.

In 2007, TSS, TA and peel thickness (PT) were the variables most affected by water stress, and statistically differed in SDI53 with respect to the control treatment (Table 2.5). The results for the other variables were statistically similar, their differences being less relevant than in previous years. There were non significant differences in most of the variables between the SDI77 and control treatments, due to the fact that irrigation needs were nearly satisfied in SDI77 treatment this year.

Table 2.2. Yearly values of water stress integral (S_{Ψ}) in each treatment during the irrigation periods.

Treatment	Year			
	2005	2006	2007	Average
	S_{Ψ} (MPa)			
SDI53	137.8 ^a ± 19.1	122.3 ^a ± 8.9	106.1 ^a ± 9.8	122.1 ^a ± 18.5
SDI67	122.3 ^b ± 10.2	105.5 ^b ± 15.3	95.2 ^b ± 12.2	107.8 ^b ± 16.7
SDI77	101.3 ^c ± 4.3	93.2 ^c ± 5.8	79.2 ^c ± 5.9	91.3 ^c ± 10.6
Control	88.9 ^d ± 5.7	85.3 ^c ± 11.7	75.2 ^c ± 11.4	83.1 ^c ± 11.3

Within each column, different letters indicate significant differences at $P < 0.05$ by Tukey's test.

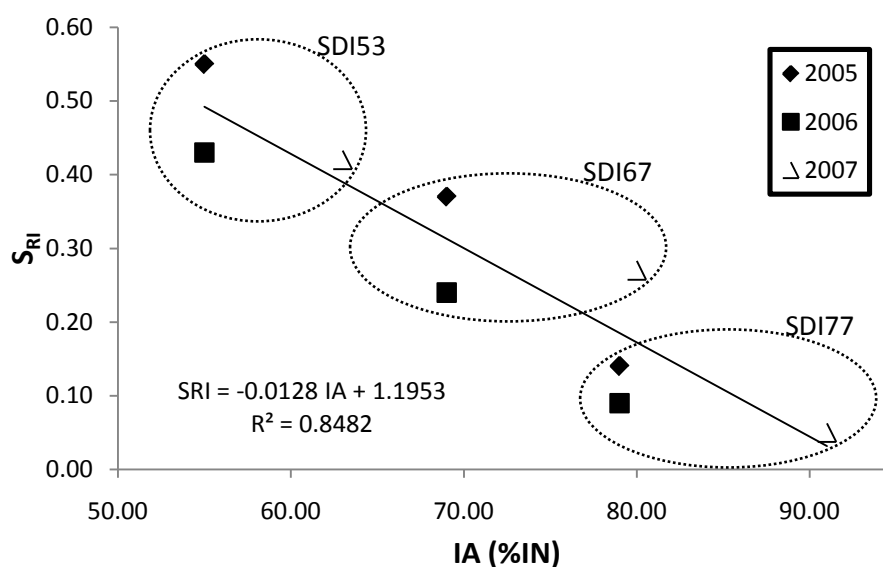


Fig. 2.3. Linear correlation between relative ratio of water stress integral (S_{RI}) and irrigation amounts (IA) in stressed treatments during the irrigation period normalized at 130 days (days of year 164-292). IN = irrigation needs.

Table 2.3. Average yield, water productivity and fruit quality parameters for 2005.

Treatment	Yield (kg tree ⁻¹)	WP (kg mm ⁻¹)	Fruit weight (g)	Juice content (%)	TSS (°Brix)	TA (g L ⁻¹)	MI (TSS/TA)	ED	PD (mm)	PT
SDI53	88.3 ^a	1.00E-02 ^a	279.3 ^a	44.8 ^a	11.8 ^d	0.92 ^a	12.8 ^a	86.5 ^a	83.6 ^a	8.51 ^a
SDI67	100.7 ^a	8.75E-03 ^b	293.5 ^{ab}	45.2 ^a	11.2 ^c	0.81 ^b	13.9 ^a	87.3 ^a	85.1 ^{ab}	8.50 ^a
SDI77	99.1 ^a	7.92E-03 ^c	290.7 ^{ab}	46.3 ^a	10.3 ^b	0.80 ^b	13.2 ^a	86.5 ^a	84.6 ^{ab}	8.18 ^a
control	111.3 ^a	6.67E-03 ^d	316.9 ^b	45.0 ^a	9.6 ^a	0.71 ^b	13.9 ^a	89.3 ^a	88.0 ^b	8.42 ^a

Within each column, different letters indicate significant differences at $P < 0.05$ by Tukey's test. WP, water productivity; TSS, total soluble solids; TA, titratable acidity; MI, maturity index; ED equatorial diameter; PD, polar diameter; PT, peel thickness.

Table 2.4. Average yield, water productivity and fruit quality parameters for 2006.

Treatment	Yield (kg tree ⁻¹)	WP (kg mm ⁻¹)	Fruit weight (g)	Juice content (%)	TSS (°Brix)	TA (g L ⁻¹)	MI (TSS/TA)	ED	PD (mm)	PT
SDI53	119.6 ^a	1.33E-02 ^a	203.9 ^a	44.6 ^a	11.1 ^c	0.64 ^c	17.2 ^a	76.1 ^a	73.7 ^a	7.25 ^a
SDI67	126.7 ^a	1.21E-02 ^b	207.5 ^a	45.6 ^a	10.4 ^b	0.58 ^b	17.5 ^a	76.5 ^a	74.3 ^a	7.11 ^a
SDI77	113.9 ^a	9.17E-03 ^c	206.1 ^a	45.1 ^a	9.8 ^a	0.54 ^a	18.0 ^a	75.2 ^a	76.0 ^a	7.06 ^a
control	124.0 ^a	7.92E-03 ^d	211.8 ^a	44.9 ^a	10.1 ^{ab}	0.59 ^b	18.3 ^a	76.7 ^a	75.5 ^a	7.03 ^a

Within each column, different letters indicate significant differences at $P < 0.05$ by Tukey's test. WP, water productivity; TSS, total soluble solids; TA, titratable acidity; MI, maturity index; ED equatorial diameter; PD, polar diameter; PT, peel thickness.

Table 2.5. Average yield, water productivity and fruit quality parameters for 2007.

Treatment	Yield (kg tree ⁻¹)	WP (kg mm ⁻¹)	Fruit weight (g)	Juice content (%)	TSS (°Brix)	TA (g L ⁻¹)	MI (TSS/TA)	ED	PD (mm)	PT
SDI53	76.0 ^a	8.75E-03 ^a	209.6 ^a	48.8 ^a	12.5 ^c	1.12 ^b	11.3 ^a	76.6 ^a	70.9 ^a	6.33 ^b
SDI67	81.7 ^a	7.50E-03 ^b	217.5 ^a	49.6 ^a	11.7 ^b	1.04 ^{ab}	11.4 ^a	77.2 ^a	71.7 ^a	5.66 ^a
SDI77	82.0 ^a	6.67E-03 ^c	205.8 ^a	49.0 ^a	10.9 ^a	1.03 ^{ab}	10.7 ^a	75.3 ^a	70.6 ^a	5.46 ^a
control	95.7 ^a	5.83E-03 ^d	211.9 ^a	47.9 ^a	10.6 ^a	0.95 ^a	11.2 ^a	74.8 ^a	70.4 ^a	5.58 ^a

Within each column, different letters indicate significant differences at $P < 0.05$ by Tukey's test. WP, water productivity; TSS, total soluble solids; TA, titratable acidity; MI, maturity index; ED equatorial diameter; PD, polar diameter; PT, peel thickness.

WP (Tables 2.3-2.5) averaged per treatment, ranged from 0.006 to 0.011 kg L⁻¹ in the control and SDI53 treatments, respectively. WP in control treatment was very similar during the three study years. The highest values were registered in 2006, due to the high yield in all treatments compared to the other years (Tables 2.3-2.5).

2.3.4. Temporal variability of data and the overall analysis

The results of the temporal variability analysis show significant differences in yield, fruit quality, and WP (Table 2.6). The different conditions registered in each study year promoted significant variations in the collected data. For this reason, the datasets of each year were normalized prior to the global analysis. This allows us to study the relationships between the different parameters and the defined irrigation treatments regardless of temporal variability.

Significant regression coefficients (Table 2.7) were found between S_{ψ} and TSS, TA and PT. This set of relationships confirmed the results found over the three studied seasons (Tables 2.3-2.5) on the effects that crop water stress has on fruit quality. Regression coefficients were also significant between fruit weight and other variables such as juice content, TSS, TA, MI, ED, PD and PT. Significant relationships were found between TA and TSS, MI, ED and PD.

The classification tree showed good agreement with the separation of treatments (Fig. 2.4). The treatment misclassification rate was lower than 20%. Although all variables were included in the classification procedure, only a few of them were relevant: S_{ψ} , TSS, ED, yield, fruit weight, TA and PT. The first threshold, set by S_{ψ} , created the two main branches of the tree with the less stressed treatments in the left branch and the most stressed treatments in the right one. An exception occurred in the left branch with the SDI67 treatment, corresponding to points that showed a low S_{ψ} and high TSS during the second season. As expected, the main separation between treatments SDI77 and control was established by their S_{ψ} , and, at the second level of separation, by their ED. This showed that fruits from treatment SDI77 had a smaller ED than those produced by the control treatment. TSS characterizes the major difference between SDI53 and SDI67 treatments, being its concentration higher in the SDI53 treatment. This can be linked to the lower amount of water supplied to the SDI53

treatment. The second most important difference between these two treatments was the

Table 2.6. Temporal variability analysis for all parameters listed by Tukey's test.

Year	Yield (kg tree ⁻¹)	WP (kg mm ⁻¹)	Fruit weight (g)	Juice content (%)	TSS (°Brix)	TA (g L ⁻¹)	MI (TSS/MI)	ED	PD	PT
2005	99.8 ^a	1.29E-02 ^a	295.1 ^a	45.3 ^a	10.7 ^b	0.81 ^b	13.5 ^b	87.4 ^b	85.3 ^c	8.40 ^c
2006	121.0 ^b	1.04E-02 ^b	207.4 ^b	45.1 ^a	10.3 ^a	0.58 ^a	17.8 ^c	76.1 ^a	74.9 ^b	7.11 ^b
2007	83.9 ^a	7.08E-03 ^c	211.2 ^b	48.2 ^b	11.4 ^c	1.03 ^c	11.2 ^a	76.0 ^a	70.9 ^a	5.75 ^a

Within each column, different letters indicate significant differences at $P < 0.05$. WP, water productivity; TSS, total soluble solids; TA, titratable acidity; MI, maturity index; ED equatorial diameter; PD, polar diameter; PT, peel thickness.

Table 2.7. Pearson's correlation coefficients among studied parameters for the 3-year period.

	S_{Ψ}	Yield	Fruit weight	Juice weight	TSS	TA	MI	ED	PD
Yield	NS								
Fruit weight	NS	-0.260**							
Juice weight	NS	NS	-0.302**						
TSS	0.752**	NS	-0.279**	NS					
TA	0.422**	NS	-0.353**	NS	0.584**				
MI	NS	NS	0.182*	NS	NS	-0.716**			
ED	NS	-0.286**	0.773**	-0.194*	NS	-0.206*	NS		
PD	NS	-0.209*	0.629**	NS	-0.344**	-0.373**	NS	0.634**	
PT	0.217*	NS	0.381**	-0.445**	NS	NS	0.189*	0.433**	0.317**

TSS, total soluble solids; TA, titratable acidity; MI, maturity index; ED equatorial diameter; PD, polar diameter; PT, peel thickness;

NS, no significant; * and ** significant at $P < 0.05$ and 0.01 level respectively.

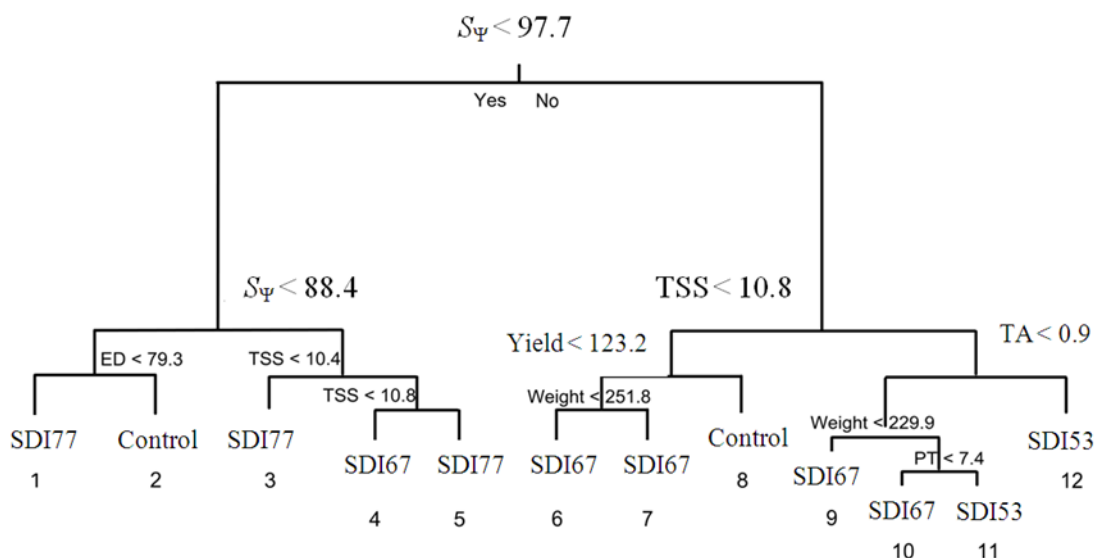


Fig. 2.4. Classification tree for all studied treatments (SDI53, SDI67, SDI77 and control) and parameters: water stress integral (S_{Ψ} , MPa); total soluble solids (TSS, °Brix); titratable acidity (TA, g l⁻¹); weight (g); yield (kg tree⁻¹); equatorial diameter (ED, mm); peel thickness (PT, mm).

level of TA. As in the case of TSS, the TA level was higher in the SDI53 treatment than in the SDI67 treatment, according to the water stress observed. Finally, a third level of difference between SDI53 and SDI67 treatments was characterized by the PT, this being also directly related to the amount of water supplied in both treatments. In summary, low-stress treatments affected mainly S_{Ψ} and fruit shape, while high-stress treatments affected mainly juice characteristics.

The PCA showed a good reproduction of the total dataset variability with few components (Fig. 2.5). The first principal component (PC1) represented 67% of the total variability found in the whole dataset, while the second (PC2) and third (PC3) constituted 19% and 13% of the total variability. This shows that only the first three components were responsible for the total variability.

Fig. 2.5 shows the distribution of the variables used in the PCA and their loadings on the three main PC. At first inspection it appears that yield, fruit weight, and S_{Ψ} were the variables with notable loadings. Considering PC1, yield had the highest loading, (-0.98), in contrast to fruit weight (0.20). The remaining variables ranged from -0.06 to 0.06 and were therefore negligible. On the PC2, fruit weight had the highest loading, (-0.89), and only yield (-0.21) and S_{Ψ} (0.38) had notable effects. With respect to PC3, S_{Ψ} showed the highest loading, (0.92), followed by fruit weight, (0.38). However, as with PC1 and PC2, the relationship between them was weak. Therefore, main results given by the PCA were: i) yield, fruit weight and S_{Ψ} explained a large part of the variability found in the total dataset; and ii) yield, fruit weight and S_{Ψ} can be considered independent from the standpoint of a PCA.

2.4. Discussion

WP data showed a clear linear correlation with the IAs applied ($r^2 = 0.72$), in agreement with Ahuja *et al.* (2008).

According to our results, an irrigation-water saving of 157 mm on average in the SDI77 treatment, compared to the control, did not bring out any significant response in

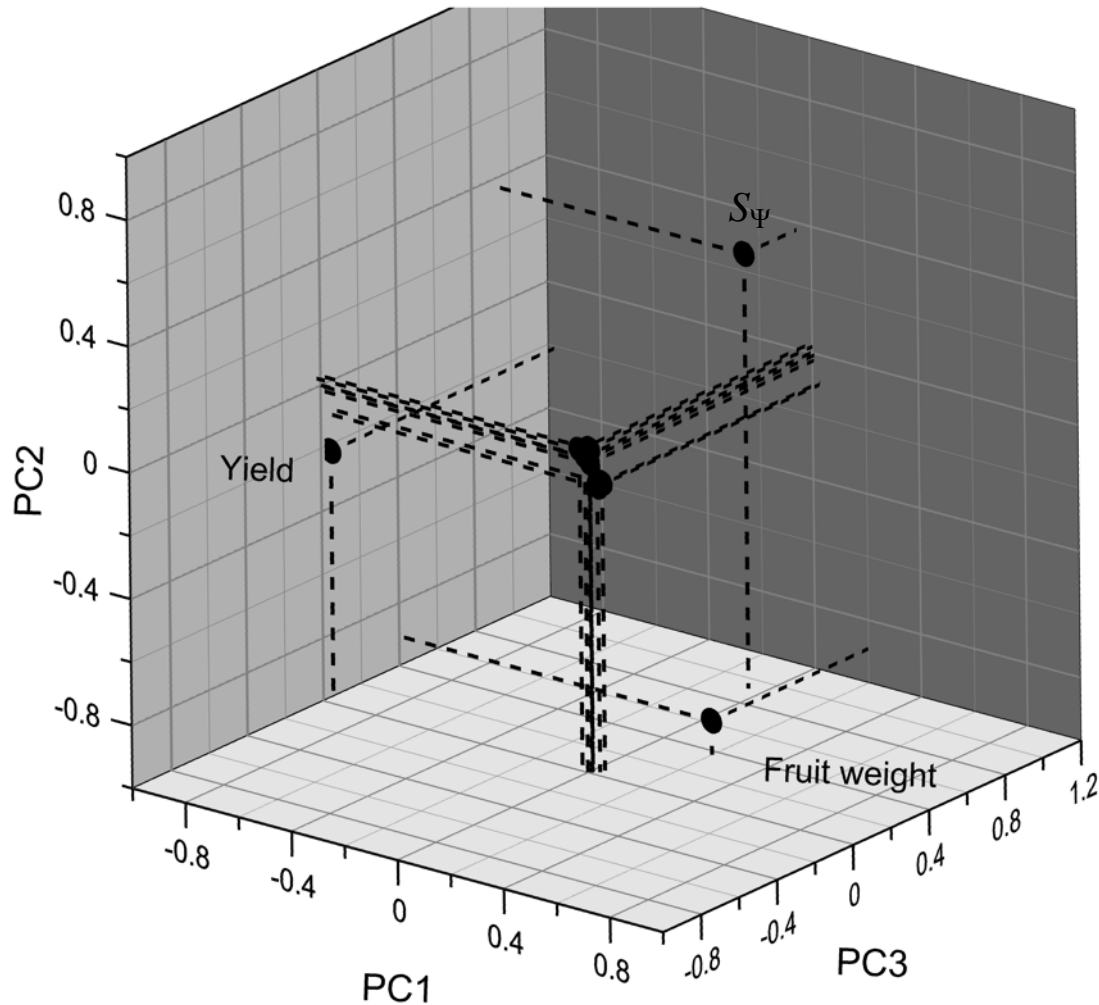


Fig. 2.5. Loadings of the studied variables (yield, fruit weight and water stress integral, S_{ψ}) to the first three principal components (PC1, PC2 and PC3).

the water status of the trees (Tables 2.1-2.2). Despite of this significant reduction in supplied water, no appreciable decrease in fruit yield was observed. In the SDI53 and SDI67 treatments there were no significant differences in yield, although it is noteworthy that we observed differences that were appreciable and that the changes were related to the water deficit undergone by the trees in each treatment. In these two treatments we found significant differences in the water status of the trees (Table 2.2)

. The SDI treatments registered the highest S_{RI} in 2005 (Fig. 2.3). Furthermore, the differences between treatments were clearer than in other years.

Vélez *et al.* (2007) were unable to detect any significant differences in either the final production or the fruit weight or in the number of fruits per tree in mandarin “Clementine of Nules”, in response to a regulated deficit irrigation (RDI) strategy based on daily changes in trunk diameter. According to González-Altozano and Castel (1999),

values for Ψ_{stem} must exceed a threshold of -1.3 MPa to exert a significant effect on final crop production. This might partly explain why none of the three studied years showed any statistical significant difference in yield between irrigation treatments. In fact, Ψ_{stem} values of trees grown under the most severe SDI treatments showed Ψ_{stem} levels lower than the threshold value just occasionally. Under more severe water-stress conditions, Ginestar and Castel (1996) observed important differences in yield. They evaluated a treatment in which the available water was 50% of the crop water needs during the irrigation season.

The effects in parameters such as fruit weight, juice content, maturity index, fruit diameter or peel thickness showed no statistically significant differences between treatments (Tables 2.3-2.5).

Under our experimental conditions, the effects of the irrigation treatments were more evident in the organoleptic characteristics of the fruit, including TA and TSS (Tables 2.3-2.5). Similar results have been reported by other authors, such as Vélez *et al.* (2007), Ginestar and Castel (1996), González-Altozano and Castel (1999), Hutton *et al.* (2007), Treeby *et al.* (2007) and Pérez-Pérez *et al.* (2008). Furthermore, Hockema and Etxeberria (2001) showed that water stress leads to increased TSS and TA, but this is not a result of fruit dehydration but rather of the osmoregulatory response caused by the lack of water (Yakushiji *et al.*, 1998).

Regarding the relations between water stress and fruit weight, significant differences were detected only in 2005, when S_{Ψ} showed the highest values. In average, however, significant correlations were not found between S_{Ψ} and fruit weight. Several significant relations were found between weight and other parameters more affected by water stress (TSS or TA). Several authors have also reported relations between the water stress and fruit size. Treeby *et al.* (2007) observed that water stress boosted the number of fruits while reducing fruit size. Vélez *et al.* (2007) reported a decrease in the weight of the fruit and a slight increase in the number of fruits per tree, although none of these differences could be considered significant. Similar results were observed in the present work. Although we observe fruit weight reductions in SDI treatments, which were compensated with an increase in the number of fruits, the differences were not significant.

2.5. Conclusions

Irrigation water savings of up to 55% of IN had no significant impact on tree yield, but rather affected other key factors (TSS and TA) that have direct relevance for the final quality of the harvested product. The seasonal pattern of S_{Ψ} in different irrigation treatments was consistent with the water deficit imposed in each treatment. Any water deficit considerably boosts S_{Ψ} , which results in a strong negative correlation between S_{RI} and IAS, indicating that S_{Ψ} and S_{RI} can be used as reliable stress indexes.

Our results indicate that the main effects of water stress are reflected in organoleptic fruit parameters, with strong correlations between TSS and S_{Ψ} and between TA and S_{Ψ} . Water stress effect was less obvious in other morphological variables such as fruit weight, ED or PT, although these also registered significant correlations. Furthermore, the main result given by the PCA analysis was that yield, fruit weight, and S_{Ψ} explain a large part of the variability found in the total dataset.

The higher increase in WP was detected in SDI53 treatment, with not significant decrease in yield within the three studied years. However, the low values of Ψ_{stem} detected in this treatment suggest an excessive stress that could result in reductions of yield in the future. A longer experiment is required to confirm the long-term effect of this water stress. On the other hand, the SDI67 and SDI77 treatments did not cause significant Ψ_{stem} reductions. We demonstrate in this work the potential of these treatments to increase WP and fruit quality (TSS and TA) with non significant reductions of yield. For this reason, and considering the problem of water scarcity in Andalusia, we strongly recommend these strategies for orange orchards (*Citrus Sinensis* L. Osbeck, cv. Salustiana) in our region.

2.6. References

Ahuja L, Saseendran S, Reddy V, Yu Q. 2008. Synthesis, actions, and further research to improve response of crop system models to water stress. Response of crops to limited water: understanding and modeling water stress effects on plant growth processes 1:411.

-
- Allen RG, Pereira LS, Raes D, Smith M. 1998. Crop evapotranspiration-Guidelines for computing crop water requirements-FAO Irrigation and drainage paper 56. FAO, Rome 300:6541.
- Berbel J, Gutiérrez C. 2004. I Estudio de sostenibilidad del regadío del Guadalquivir. FERRAGUA. Spain.
- Castel J, Buj A. 1990. Response of Salustiana oranges to high frequency deficit irrigation. *Irrigation Science* 11(2):121-127.
- Davis JC. 2002. *Statistics and Data Analysis in Geology (Third Edition)*. John Wiley & Sons. p 678.
- Doorembos J, Kassam A. 1979. *Yield response to water*. Rome: FAO 33.
- FAO. 1998. *World Reference Base for Soil Resources*. Rome: Food and Agriculture Organization of the United Nations.
- Fereres E, Castel JR. 1981. *Drip Irrigation Management*. Division of Agricultural Sciences. University of California. Leaflet N° 21259. 2,11-24.
- Fereres E, Soriano MA. 2007. Deficit irrigation for reducing agricultural water use. *Journal of Experimental Botany* 58(2):147-159.
- García-Tejero I, Jiménez JA, Muriel JL, Martínez G. 2007. Planificación y desarrollo de estrategias de riego deficitario en una plantación de naranjos: influencia de la variabilidad espacial de las propiedades del suelo. *Book of Abstracts XXV Congreso Nacional de Riegos*. Pamplona. Spain. p 63.
- García-Tejero I, Jiménez JA, Reyes MC, Carmona A, Pérez R, Muriel JL. 2008. Aplicación de caudales limitados de agua en plantaciones de cítricos del valle del Guadalquivir. *Fruticultura Profesional* 173:5-17.
- Ginestar C, Castel JR. 1996. Responses of young clementine citrus trees to water stress during different phenological periods. *Journal of Horticultural Science* 71(4):551-559.

- Gonzalez-Altozano P, Castel JR. 1999. Effects of regulated deficit irrigation on 'Clementina de Nules' citrus trees I. Yield and fruit quality effect. *J Am Soc Hort Sci* 74:749-758.
- Gonzalez-Altozano P, Castel JR. 2000. Effects of regulated deficit irrigation on 'Clementina de Nules' citrus trees II. Vegetative growth. *J Am Soc Hort Sci* 75:388-392.
- Hockema BR, Etxeberria E. 2001. Metabolic contributors to drought-enhanced accumulation of sugars and acids in oranges. *Journal of the American Society for Horticultural Science* 126(5):599-605.
- Hsiao TC. 1973. Plant responses to water stress. *Annu Rev Plant Physiol Plant Molec Biol* 24:519-570.
- Hutton R, Landsberg J, Sutton B. 2007. Timing irrigation to suit citrus phenology: a means of reducing water use without compromising fruit yield and quality? *Australian Journal of Experimental Agriculture* 47(1):71-80.
- Ihaka R, Gentleman R. 1996. R: a language for data analysis and graphics. *Journal of computational and graphical statistics* 5:299-314.
- Muriel J, Jiménez J, García I, Vaquero I. 2006. Relaciones hídricas en una plantación de naranjos (*Citrus sinensis*, L. cv. Navelino) bajo estrategias de riego deficitario mantenido. VIII Simposium Hispano Portugués de Relaciones Hídricas en las Plantas:17–21.
- Myers BJ. 1988. Water stress integral—a link between short-term stress and long-term growth. *Tree Physiology* 4(4):315.
- Peng Y, Rabe E. 1998. Effect of differing irrigation regimes on fruit quality, yield, fruit size and net CO₂ assimilation of Mihowase Satsuma. *Journal of horticultural science & biotechnology* 73(2):229-234.
- Pérez-Pérez J, Romero P, Navarro J, Botía P. 2008. Response of sweet orange cv 'Lane late' to deficit-irrigation strategy in two rootstocks. II: Flowering, fruit growth, yield and fruit quality. *Irrigation Science* 26(6):519-529.

-
- Rawls W, Pachepsky YA. 2002. Soil consistence and structure as predictors of water retention. *Soil Science Society of America journal* 66(4):1115-1126.
- Rodríguez Díaz J, Weatherhead E, Knox J, Camacho E. 2007. Climate change impacts on irrigation water requirements in the Guadalquivir river basin in Spain. *Regional Environmental Change* 7(3):149-159.
- Sánchez-Blanco MJ, Torrecillas A, León A, Delamor F. 1989. The Effect of Different Irrigation Treatments on Yield and Quality of Verna Lemon. *Plant and Soil* 120(2):299-302.
- Scholander PF, Bradstreet ED, Hemmingsen E, Hammel H. 1965. Sap pressure in vascular plants. *Science* 148(3668):339.
- Shalhevet J, Bielorai H. 1978. Crop water requirements in relation to climate and soil. *Soil Science* 125(4):240-247.
- Southwick SM, Davenport TL. 1986. Characterization of water stress and low temperature effects on flower induction in citrus. *Plant Physiology* 81(1):26-29.
- Sterk G, Stein A. 1997. Mapping wind-blown mass transport by modeling variability in space and time. *Soil Science Society of America Journal* 61(1):232-239.
- Team RDC. 2008. R: A language and environment for statistical computing. R Foundation for Statistical Computing Vienna Austria ISBN 3(10).
- Treeby MT, Henriod RE, Bevington KB, Milne DJ, Storey R. 2007. Irrigation management and rootstock effects on navel orange *Citrus sinensis* (L.) Osbeck fruit quality. *Agric Water Manage* 91(1-3):24-32.
- Turner NC. 1988. Measurement of plant water status by the pressure chamber technique. *Irrigation Science* 9(4):289-308.
- Vaux H, Pruitt WO. 1983. Crop-water production functions. *Advances in irrigation* 2:61-67.
- Velez J, Intrigliolo D, Castel J. 2007. Scheduling deficit irrigation of citrus trees with maximum daily trunk shrinkage. *Agric Water Manage* 90(3):197-204.

Yakushiji H, Morinaga K, Nonami H. 1998. Sugar accumulation and partitioning in Satsuma mandarin tree tissues and fruit in response to drought stress. *American Society for Horticultural Science (USA)* 123:719-726.

Chapter 3

Impact of regulated deficit irrigation on yield, water productivity and fruit quality in a commercial citrus orchard, cv. Navelina

Part of this chapter is published in:

García-Tejero I, Romero R, Jiménez-Bocanegra JA, Martínez G, Durán-Zuazo VH, Muriel JL. 2010. Response of citrus trees to deficit irrigation during different phenological periods in relation to yield, fruit quality, and water productivity. *Agricultural Water Management* Vol 97, 689-699.

Abstract. In 2007 and 2008, four strategies of regulated deficit irrigation (RDI) and a control treatment were implemented in 11-year-old citrus trees (*Citrus sinensis* L. Osb. cv. Navelina) grafted onto carrizo citrange (*Citrus sinensis* L. Osb. x *Poncirus trifoliata* L. Osb.). Irrigation in the control treatment was aimed at guarantying 100% of the irrigation needs (IN, mm). The four RDI treatments were defined based on irrigation amounts (IA, mm) calculated as a percentage of the control (70% for moderate water stress and 56% for severe water stress), varying in each of the following growth phases: flowering (from 50% of opened flowers to fruit setting), fruit growth and fruit maturation. Midday stem water potential (Ψ_{stem} , MPa) and stomatal conductance (g_s , $\text{mmol}\cdot\text{m}^{-2}\cdot\text{s}^{-1}$) measurements were made in each of the considered treatments. Both the water stress integral (S_Ψ , MPa) and the stomatal conductance integral (S_g , $\text{mmol}\cdot\text{m}^{-2}\cdot\text{s}^{-1}$) were calculated for all treatments and used for quantifying the water-stress levels suffered by the trees. Reference equations were formulated to quantify the correlations between the supplied irrigation amounts (IA) or S_Ψ and S_g and yield and fruit-quality parameters. Significant differences in yield between the control and the RDI treatments were found in the second year of the experiment. In the first year the differences were not significant. The greater differences were found in treatments with severe water stress applied during both the flowering and fruit growth phases. When severe water stress was allowed during the fruit maturation phase, the effects were especially evident in fruit-quality parameters (total soluble solids content and titratable acidity). The best results were obtained with the RDI strategy characterized by moderate deficit irrigation (70% of control) during flowering and fruit growth and severe deficit irrigation (56% of control) during fruit maturation. This strategy saved $1030 \text{ m}^3 \text{ ha}^{-1}$ with

respect to the control, with not significant effect in yield. It also improved fruit quality parameters as TSS and TA. The RDI strategy with severe deficit irrigation at flowering and fruit growth, and moderate deficit irrigation during maturation allowed water savings of up to 1375 m³ ha⁻¹ in 2008, but yield was reduced by 22%. Water productivity, however, increased 30% as compared to the control.

3.1. Introduction

Water deficits conditions are common in the Guadalquivir River Valley (SW Spain). Therefore, irrigation is needed for commercial production of crops such as citrus trees. The increasing demand for food-related agricultural products, fodder, and fuel, due to population growth, makes compulsory agricultural practices focused to a more efficient use of water. In this context, there is an increasing challenge for scientists to develop innovative crop-management practices for a use of the soil, water and agrochemicals oriented to improve the sustainability of agricultural systems (Anapalli *et al.*, 2008). Water productivity (WP, kg of marketable yield ·L⁻¹ of water consumed by the crop) can be improved either by increasing yield or reducing crop water consumption (Feres *et al.*, 2003). Deficit irrigation (DI) has been widely investigated as a valuable and sustainable production strategy in dry regions. Any rational DI strategy saves water and increases WP. Different DI strategies cause different effects on the crop. In general photosynthetic rates are lowered, reducing carbon assimilation (Hsiao, 1973) and exerting a negative impact on the crop development and production (González-Altozano and Castel, 2000a). Any DI strategy must be designed to achieve the best compromise between the negative impact of the reduced water supplies and the advantages of water and energy saving. It is known that the response of citrus trees to DI depends on a variety of factors, such as the phenological stage, intensity and duration of the water stress period, crop physiological status, irrigation-water quality, plant genotype, and the degree of stress endured by the crop (Doorenbos and Kassam, 1979; Ginestar and Castel, 1996; García-Tejero *et al.*, 2008). It has also been described that DI may increase fruit quality (Sánchez-Blanco *et al.*, 1989, in Verna lemon trees; González-Altozano and Castel, 2000b, in cv. Clementina de Nules; Verreynne *et al.*, 2001, in cv. Marisol Clementines).

Among the most widely used methods to evaluate the water status of a plant is the measurement of leaf- or stem-water potential. Still, there is some controversy concerning the time and method of measurement (Gonzalez-Altozano and Castel, 2003). These measurements offer information on the water-retention force by the plant, but do not indicate the crop physiological response to the imposed water stress. Some authors proposed the use of cumulative plant evapotranspiration or transpiration as a good integrator of the effects of water stress on various plant physiological processes (Verasan and Philips, 1978). Plant transpiration is related to stomatal conductance (g_s , $\text{mmol}\cdot\text{m}^{-2}\cdot\text{s}^{-1}$), this being a key variable for the plant, because of its influence in some main physiological processes. Values of stomatal conductance may vary over a wide range, as they are affected by several meteorological variables, *e.g.* radiation and vapour-pressure deficit of the air, and depend on the plant water status (Anapalli *et al.*, 2008).

The aim of this work was to evaluate the impact of different deficit irrigation strategies on yield, fruit quality, and WP in a commercial 11-year-old orchard of citrus trees (*Citrus sinensis* L. Osb. cv. Navelina) grafted onto carrizo citrange (*Citrus sinensis* L. Osb. x *Poncirus trifoliata* L. Osb.). We evaluated four RDI strategies, which supplied reduced amounts of water at flowering, fruit growth and fruit maturation. The experiment lasted two irrigation seasons, 2007 and 2008. We also characterized main soil-plant-water variables to evaluate the crop response to each RDI strategy.

3.2. Material and methods

3.2.1. Experimental site

This work was made in a commercial orchard of the Guadalquivir river valley, SW Spain ($37^{\circ} 44' 5''$ N; $5^{\circ} 12' 35''$ W), planted with 11-year-old 'Navelina' orange trees (*Citrus sinensis*, L. Osbeck) grafted on 'Citrango Carrizo' (*Citrus sinensis*, L. Osbeck x *Poncirus trifoliata*, L. Raf.). The trees, spaced 6 m x 5 m, were ca. 3 m in height and ca. 4 m in diameter. They were planted on NW-SE oriented, 0.3 m high ridges. The experiments involved 0.9 ha under conventional management practices. The shaded ground surface area was 42% of the total.

The soil is a typical fluvisol (FAO, 1998) with an effective depth of 1.5 m. Roots grow predominantly within the top 0.6 m soil layer, which has 35% sand, 40% silt and 25% clay. The organic matter content was below 1.5%. The soil was slightly limey (10.6% of CO_3) with a high cation-exchange capacity (>15 meq / 100 g) and a C:N ratio of 10.5. The soil water content at field capacity and wilting point are $230 \text{ mm}\cdot\text{m}^{-1}$ and $100 \text{ mm}\cdot\text{m}^{-1}$, respectively. The water holding capacity for the root zone is 78 mm. The trees were fertigated. Each treatment received a total of $240 \text{ kg}\cdot\text{ha}^{-1}$ of N, $65 \text{ kg}\cdot\text{ha}^{-1}$ of P_2O_5 and $179 \text{ kg}\cdot\text{ha}^{-1}$ of K_2O . These amounts agree with legal policies published for agricultural integrated production for citrus in Andalusia, the region in which the experimental orchard was located (BOJA, No. 113, 2000).

The climate is typically Mediterranean, with dry, hot summers and mild, wet winters. Average annual ET_0 and rainfall values are 1400 mm and 534 mm, respectively (period 1971-2000). Rainfall is distributed mainly from late autumn to early spring, with November to February being the wettest months. Temperature in winter rarely falls below 0°C and in July and August may peak to over 40°C .

3.2.2. Irrigation treatments and experimental design

Four RDI treatments were applied during two seasons (2007-2008). They were based on supplying a certain percentage of the irrigation needs (IN) during flowering, fruit growth and fruit maturation. Details are shown in Table 3.1. In addition, a control treatment aimed at 100% of IN was established all throughout each irrigation season. Each year, the treatments were implemented from early April to harvest, in mid-December. Water meters were used to measure the actual IAs supplied to each treatment.

The irrigation system consisted of two laterals per tree row each with one self-compensating dripper 1 m apart. The discharge rate and the number of drippers per tree were adjusted as a function of the IN for each treatment: 1) in the control treatment we

Table 3.1. Irrigation treatments. The aimed irrigation amount at different main phenophases is shown in terms of % of the irrigation needs.

Treatments	Main phenophases		
	Flowering	Fruit growth	Fruit Maturation
RDI-676	56	70	56
RDI-677	56	70	70
RDI-667	56	56	70
RDI-776	70	70	56
control	100	100	100

used ten 2.3 L h⁻¹ drippers per tree; 2) when IA was aimed at 70% of the IN we used ten 1.6 L h⁻¹ drippers per tree, with a total discharge rate of 69.6% of the control; 3) when IA was aimed at 56% of the IN we used eight 1.6 L h⁻¹ drippers per tree with a total discharge rate of 55.6% of the control).

Five plots per treatment were distributed in a randomized complete block design. Each plot consisted of three rows with four trees per row. Measurements were made in the two central trees of each plot, termed here as sample trees. The experimental plots were located in the central part of the orchard, surrounded by trees.

Daily values of potential evapotranspiration (ET_o) were calculated with the FAO56 Penman-Monteith equation (Allen *et al.*, 1998) and data from an automatic weather station nearby the orchard. Every week we calculated IN according to the ET_o values of the precedent week (Doorenbos and Pruitt, 1974):

$$IN = \left[\sum_{k=1}^7 ET_o^k \right] \cdot K_c \cdot K_r - P_e \quad \text{Eq. 3.1}$$

where K_c is the crop coefficient, K_r is a reduction coefficient accounting for the percentage of ground surface covered by the crop (Castel, 1991) and P_e is the effective precipitation. K_c values were 0.5 from March to May, 0.55 from June to October and 0.5 in November and December. We calculated $K_r = 0.84$. During the fruit growth period the soil water content was measured at 0.1 m intervals from 0.05 m down to 0.95 m, using TDR probes (TRIME-T, IMKO GmbH, Germany). Two access tubes per treatment were located close to the drippers, in the wetted soil volumes.

3.2.3. Plant measurements

Midday stem water potential (Ψ_{stem} , MPa) values were measured with a pressure chamber (Scholander *et al.*, 1965) following Turner (1988). Once every 10-15 days, two mature leaves were sampled from the north quadrant of each one of two sample trees of each plot. Measurements were made around 12.00 Greenwich Mean Time (GMT). S_{Ψ} was estimated according to a modified equation derived from that proposed by Myers (1988), which integrates the water-potential values over the period for which the trees are stressed:

$$S_{\Psi} = \sum_{i=1}^{i=t} \left| \Psi_{i+1} \cdot (n_{i+1} - n_i) + \frac{1}{2} (\Psi_i - \Psi_{i+1}) \cdot (n_{i+1} - n_i) \right| \quad \text{Eq. 3.2}$$

Ψ_i and Ψ_{i+1} are the Ψ_{stem} values measured in two sampling days (n_i and n_{i+1}).

On the same days when Ψ_{stem} was measured, g_s was monitored in two sunny leaves per tree, using a diffusion porometer AP-4 (Delta-T Devices, Cambridge, UK). The stomatal conductance integral (S_g , $\text{mmol} \cdot \text{m}^{-2} \cdot \text{s}^{-1}$), i.e. the accumulated stomatal conductance during the irrigation period, was calculated as:

$$S_g = \sum_{i=1}^t \left| g_{i+1} \cdot (n_{i+1} - n_i) + \frac{1}{2} \cdot (g_i - g_{i+1}) \cdot (n_{i+1} - n_i) \right| \quad \text{Eq. 3.3}$$

where: g_i and g_{i+1} are the g_s values measured in two sampling days (n_i and n_{i+1}).

At the end of each season the total fruit weight of each of the two sample trees of each plot was determined. One sample of 100 fruits per tree was collected to determine average fruit weight. Fruit number per tree was determined by dividing the yield of each tree by the average fruit weight.

Fruit-quality characteristics were analysed after harvest. Ten fruits from each of the two sample trees of each plot were used for analysis. For each fruit we measured equatorial diameter (ED, mm), polar diameter (PD, mm), peel thickness (PT mm) and juice content. Total soluble solids content (TSS, °Brix) was measured with a digital refractometer PR-101. Titratable acidity (TA, g L^{-1}) was determined by titrating the

samples with NaOH 0.1 N by the colorimetric method, using phenolphthalein as indicator solution. Maturity index (MI, °Brix L g⁻¹) was then calculated by dividing TSS by TA. This is a key parameter to determine the optimal time for harvesting.

3.2.4. Statistical analysis

Data of each year were subjected to a one-way variance analysis (ANOVA; SPSS statistical package; SPSS, Chicago, IL, USA) with five irrigation treatments and ten replicates per treatment, using Tukey's test for mean separations ($P < 0.05$). With this method, yearly values of yield, WP, Sg, S_{ψ} and fruit quality were compared between treatments. A similar analysis was carried out with the whole dataset (2007 and 2008). The annual datasets were previously normalized following Sterk and Stein (1997). Linear correlations were also established among S_{ψ} and Sg, and fruit yield parameters.

3.3. Results

3.3.1. Water conditions

Details on the length of each irrigation season, ET_c , P_e , and IN for each considered phenophase, are given in Table 3.2. The pattern of ET_c and rainfall was very similar in both seasons (Table 3.2 and Fig. 3.1). Both in 2007 and 2008, there was an irregular distribution of rainfall at flowering and fruit maturation. In 2008, rainfall at flowering delayed the beginning of the irrigation season 49 days with respect to the previous year. This was the cause for the lower IN in 2008 than in 2007 (Table 3.2 and Fig. 3.2). Rainfall was negligible in the fruit growth periods of both experimental years. In this period was when the greatest ET_o values were registered, as usual in the area. IN during the irrigation period was 346 mm in 2007 and 326 mm in 2008. However, during the fruit growth period, IN was higher in 2008 (291 mm) than in 2007 (251 mm). This caused the application of a greater amount of irrigation water during this period in 2008 (Table 3.3). In 2008, the IN calculated for the period of fruit maturation was negative (Fig. 3.2), i.e. P_e was greater than ET_c . However, we had to irrigate because of the erratic rainfall distribution (Fig. 3.3). The rainfall events recorded in this period unable us to impose the aimed water deficits in the RDI treatments.

Table 3.2. Main water balance components for the irrigation period at main phenophases.

Season	Phenophase			Total
	2007	Flowering	Growth	
IP (days) ¹	89	96	33	218
DOY ²	77-165	166-261	262-294	91-294
ET _c (mm) ³	157.14	259.89	48.16	477.54
P _e (mm) ⁴	84.38	8.82	26.04	184.38
IN (mm) ⁵	72.76	251.07	22.12	345.95

Season	Phenophase			Total
	2008	Flowering	Growth	
IP (days) ¹	75	96	14	185
DOY ²	91-165	166-261	262-275	77-275
ET _c (mm) ³	143.44	294.43	19.7	457.57
P _e (mm) ⁴	101.46	3.22	26.6	131.28
IN (mm) ⁵	41.98	291.21	-6.9	326.29

¹Irrigation Period, ²Day of the year, ³Estimated crop evapotranspiration,

⁴Effective precipitation, ⁵Irrigation Needs (ET_c-P_e).

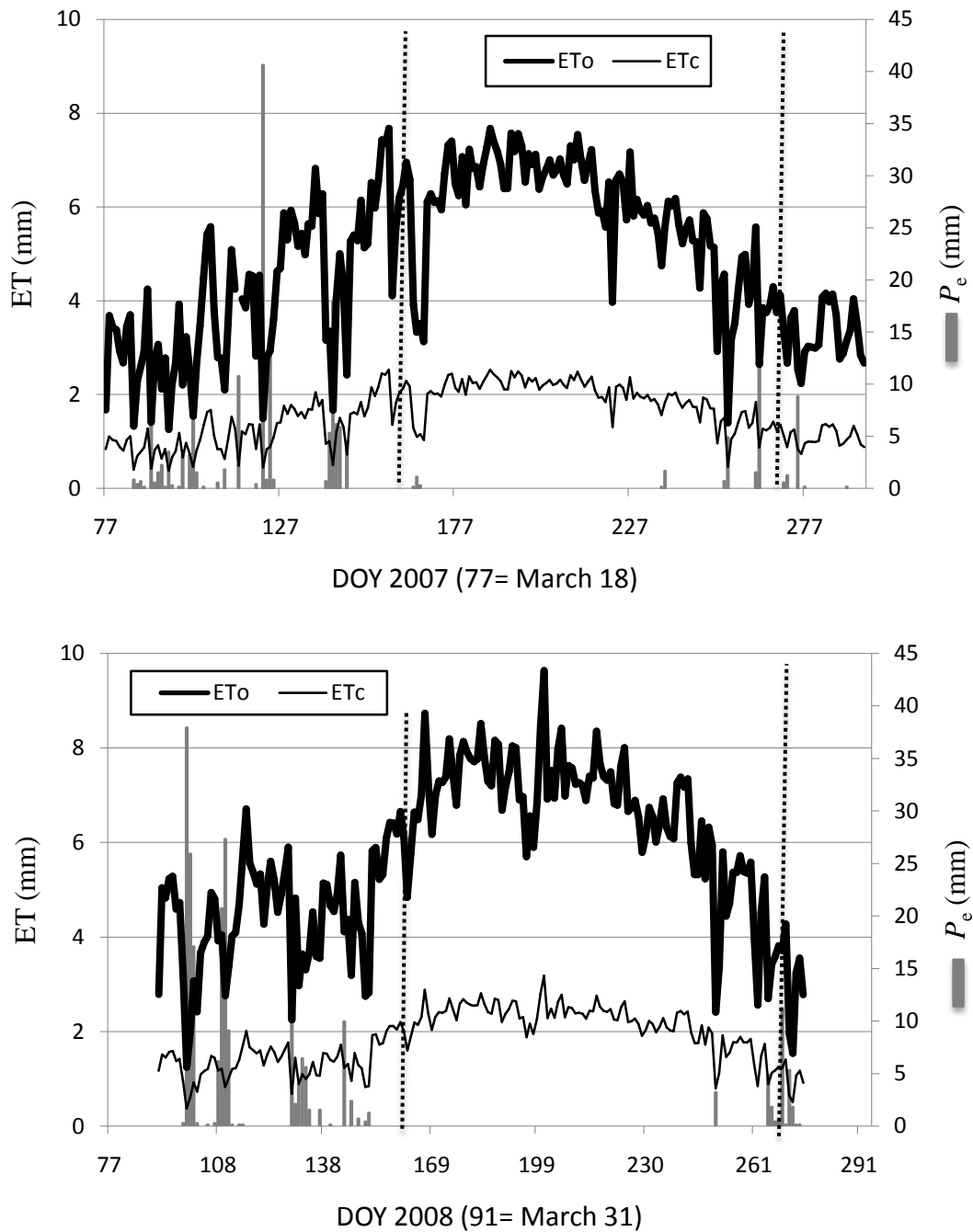


Fig. 3.1. Effective precipitation (P_e), crop (ET_c) and potential (ET_o) evapotranspiration during the experimental years. DOY = day of year.

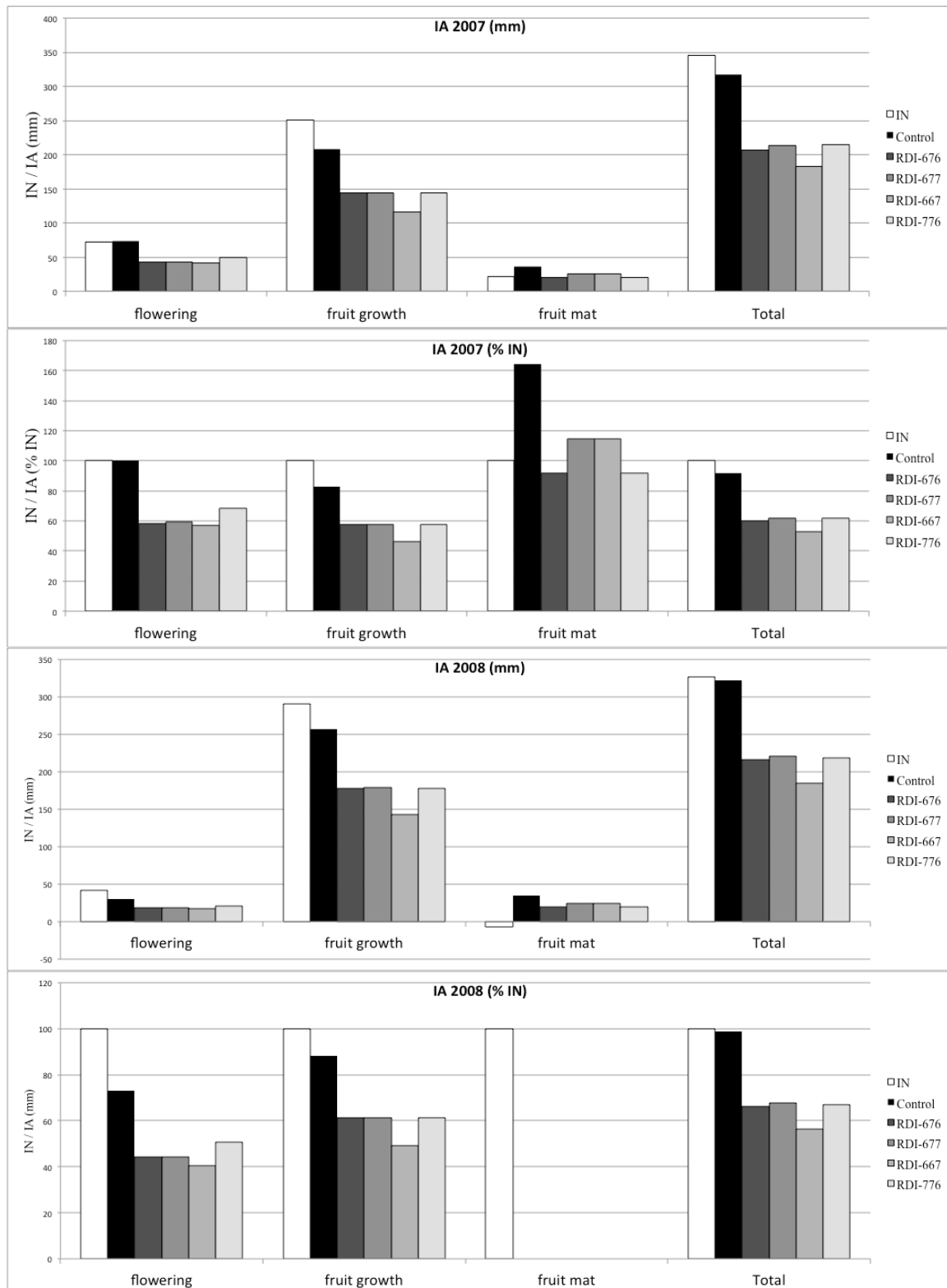


Fig. 3.2. Irrigation amounts (IA) in mm and as percentage of the irrigation needs (IN) during the irrigation periods on 2007 and 2008.

The total IA in each treatment was similar in both years (Table 3.3). RDI-667 was the most restrictive treatment (55% of IN on average). The total IA in the RDI-676, RDI-677, and RDI-776 treatments was similar ($64\pm 1\%$ of IN on average), although the water distribution according to the phenological periods differed among treatments. For the control treatment, the average IA for the two experimental years amounted to $95\pm 3\%$ of IN.

For the RDI treatments, TDR measurements showed water depletions in the soil profile according to the reduced water supplies (Fig. 3.4). The control treatment maintained moisture contents close to 80% of field capacity on average, with slight decreases in 2008. As shown in Fig. 3.3, the IAs applied during the flowering and fruit growth periods were slightly below the actual INs of the crop. Data in the figure shows little differences in soil water contents (SWC) between the control and the RDI treatments. This is striking, since it does not agree with differences in supplied water (Table 3.3). Possibly the soil variability, together with other limitations of soil moisture measurements, reduced the reliability of our SWC measurements. Taking this into account, data in Fig. 3.4 show that SWC values in the RDI-667 treatment were especially low during the fruit growth period, being between 15 and 30% lower than those recorded in the control treatment. The highest SWC were measured in the control treatment, both in 2007 and 2008 seasons. However, due to the high variability of the data, the differences between RDI-776 and control treatments were not significant in 2007. We did not find significant differences either in SWC among the RDI-677, RDI-776, and control treatments during 2008.

3.3.2. Plant water status and gas exchange

In both seasons, Ψ_{stem} was very similar in all the treatments at the end of the flowering period (Fig. 3.5). This was expected because we were, at that time, at the end of the rainy season. This explains that the differences in SWC between treatments were not enough to cause significant differences in the water status. Both at fruit growth and fruit maturation, RDI trees showed more negative values of Ψ_{stem} than the control trees. However the differences were only significant between control and RDI-667 during the fruit growth period. In the RDI-776 treatment, in which moderate stress was applied during flowering and fruit growth (IA = 70% of control), Ψ_{stem} decreased significantly at

the end of the fruit maturation period, when severe stress was applied (IA= 56% of control).

Concerning gas exchange, the most restrictive treatment, RDI-667, showed the lowest g_s values and the control treatment the highest ones (Fig. 3.6). Differences between treatments were not significant, likely because of the high variability of g_s .

Box and whisker plots of S_g and S_ψ for each treatment and season are shown in Fig. 3.7. It was notable that treatments with similar water-stress levels during the fruit growth period (RDI-676, RDI-677 and RDI-776) showed similar values both of S_g and S_ψ in 2007 and 2008. The differences in water-stress levels in these treatments occurred during flowering and fruit maturation. Rainfall in these periods might explain why these differences were not enough to affect S_g and S_ψ .

Significant linear correlations were found between IA and S_g and S_ψ (Fig. 3.8) in 2007 and 2008. The coefficients of determination were particularly high between IA and S_g in 2007 ($r^2 = 0.751$) and between IAs and S_ψ in 2008 ($r^2 = 0.837$).

3.3.3. Yield, fruit quality and water productivity

We found clear relations between yield (average per treatment, normalized for each year) and the annual IA (Fig. 3.9). On the other hand, these differences were not clear in the box and whisker plots, especially in 2007 (Fig. 3.10). This was mainly due to a high variability of the yield data of each treatment. However, in 2008, significant differences were found between the control treatment and the RDI-676 and RDI-677 treatments. The biggest differences were for RDI-667, with an average yield reduction of 15% in 2007 and 26% in 2008, as compared to the control treatment (Table 3.4). In the rest of the RDI treatments yield reductions were also observed, but the differences were not always statistically significant.

In 2008, when the differences were greater, severe water stress applied during the flowering period was reflected in the final fruit number per tree (Table 3.4). This is clear for treatment RDI-677, in which the fruits per tree were significant lower than in the control treatment.

Table 3.3. Irrigation water applied, actual water stress ratio and water savings for each treatment at different phenophases.

Season		2007				2008			
		Phenophase				Phenophase			
Treat.		Flowering	Growth	Maturity	Total	Flowering	Growth	Maturity	Total
RDI-676	IA (mm) ¹	42.3	144.7	20.3	207.3	18.7	178.1	19.2	216
	IA (% IA control)	57.95	69.50	55.77	65.27	60.91	69.35	55.65	67.08
	IA (% IN) ²	58.14	57.63	91.77	59.92	44.55	61.16	-	66.20
	WS (mm) ³	30.7	63.5	16.1	110.3	12	78.7	15.3	106
RDI-677	IA (mm)	43.4	144.8	25.3	213.5	18.7	178.7	24	221.4
	IA (% IA control)	59.45	69.55	69.51	67.22	60.91	69.59	69.57	68.76
	IA (% IN)	59.65	57.67	114.38	61.71	44.55	61.36	-	67.85
	WS (mm)	29.6	63.4	11.1	104.1	12	78.1	10.5	100.6
RDI-667	IA (mm)	41.7	115.9	25.3	182.9	17.1	143.5	24	184.6
	IA (% IA control)	57.12	55.67	69.51	57.59	55.70	55.88	69.57	57.33
	IA (% IN)	57.31	46.16	114.38	52.87	40.73	49.28	-	56.58
	WS (mm)	31.3	92.3	11.1	134.7	13.6	113.3	10.5	137.4
RDI-776	IA (mm)	49.7	144.7	20.3	214.7	21.3	178.1	19.2	218.6
	IA (% IA control)	68.08	69.50	55.77	67.60	69.38	69.35	55.65	67.89
	IA (% IN)	68.31	57.63	91.77	62.06	50.74	61.16	-	67.00
	WS (mm)	23.3	63.5	16.1	102.9	9.4	78.7	15.3	103.4
control	IA (mm)	73	208.2	36.4	317.6	30.7	256.8	34.5	322
	IA (% IA control)	100.00	100.00	100.00	100.00	100.00	100.00	100.00	100.00
	IA (% IN)	100.33	82.93	164.56	91.81	73.13	88.18	-	98.69
	WS (mm)	0	0	0	0	0	0	0	0

¹IA, Irrigation amount; ²IN, Irrigation needs; ³WS, Water Savings (related to control treatment); *Average of water supplied to each treatment referred to control treatment during the irrigation period.

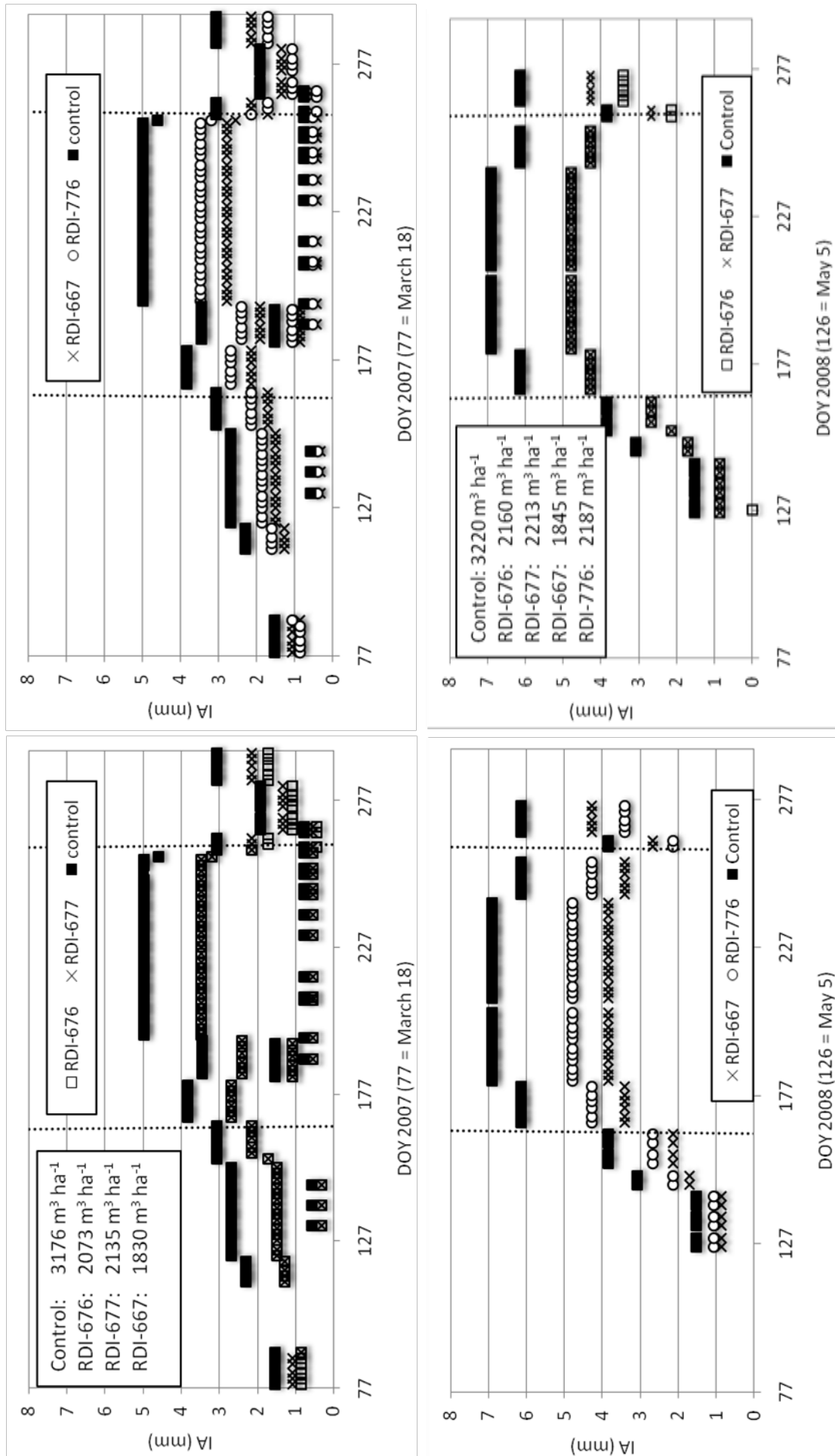


Fig. 3.3. Irrigation amounts (IA) for each treatment during the experimental years. DOY = day of year.

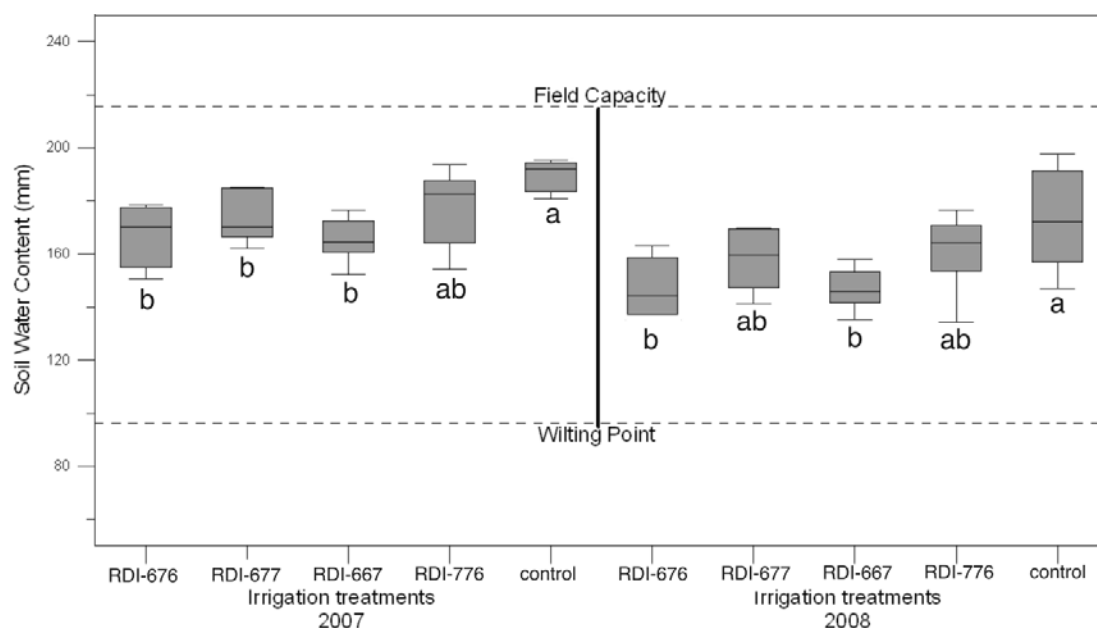


Fig. 3.4. Soil water content in the root zone for each treatment at the end of the fruit growth period of 2007 and 2008. The line inside the box shows the median and the letters after each box-whiskler plot show statistical differences at $P < 0.05$ level.

On the other hand, when these water restrictions were applied during the fruit growth or fruit maturation periods, i.e. in the RDI-676, RDI-667 and RDI-776 treatments, fruit weight rather than fruit number per tree was the affected variable. Particularly, RDI-667 presented significant differences in fruit weight with the control treatment. As mentioned above, this was the treatment in which yield was most affected. RDI-776 was the treatment with the highest number of fruits in both experimental years, although these differences were not significant.

Table 3.4 also shows the effects on fruit morphological parameters (ED, PD, and fruit weight). Not significant relations were found between these parameters and the IA applied in the treatments.

Regarding the effect of water stress on organoleptic properties, fruit quality was affected mainly in treatments with higher stressed levels during the fruit growth and fruit maturation periods (RDI-676, RDI-667, and RDI-776). In these treatments we registered increases both in TSS and TA, coupled with small decreases in MI. These effects were particularly significant in the RDI-667 treatment, in which the most severe reductions in IA were applied. Results from the RDI-776 treatment shows that a severe reduction of IA during fruit maturation improved juice quality without excessively lowering MI.

For the entire study period (2007-2008), our results show significant differences between some of the treatments for S_{ψ} , S_g , yield, fruit weight, TSS, TA, and ED (Table 3.5). This overall analysis confirmed the results in the year-by-year analysis, especially for the second experimental year, when the rise in TSS and TA values registered in the RDI-667 and RDI-776 treatments was especially noticeable. Concerning yield parameters, only the most water limited treatment (RDI-667) showed significant differences in yield, mainly due to a significant decrease in fruit weight. The rest of the treatments did not show significant differences in yield, fruit weight or fruit number when considering the whole experimental period (2007-2008).

In 2007 values of WP in the tested deficit irrigation treatments were similar, but significantly higher than in the control treatment (Fig. 3.11). In 2008 WP was reduced in all the RDI treatments, but they again were significantly higher than in the control treatment.

3.3.4. Plant water status and gas exchange versus yield and fruit quality

We analysed the relationships between both yield and fruit-quality parameters and S_g and S_{ψ} , to define which of those parameter was most related to the crop response to DI.

The S_{ψ} values showed strong linear correlation with TSS only (Fig. 3.12). Other parameters, such as PD, MI, and juice content showed no significant correlations when considering the whole dataset, but were statistically significant when considering each year separately. Therefore, in 2007 year, the juice content ($r^2 = 0.71$) and PD ($r^2 = 0.80$) had a significant correlation with S_{ψ} (regressions not shown). MI also showed significant correlations with S_{ψ} , with r^2 values of 0.76 in 2007 and 0.52 in 2008.

Values of S_g were closely correlated with some yield and fruit parameters (Fig. 3.13), especially with fruit weight ($r^2 = 0.78$), TA ($r^2 = 0.92$), PD ($r^2 = 0.79$) and MI ($r^2 = 0.76$).

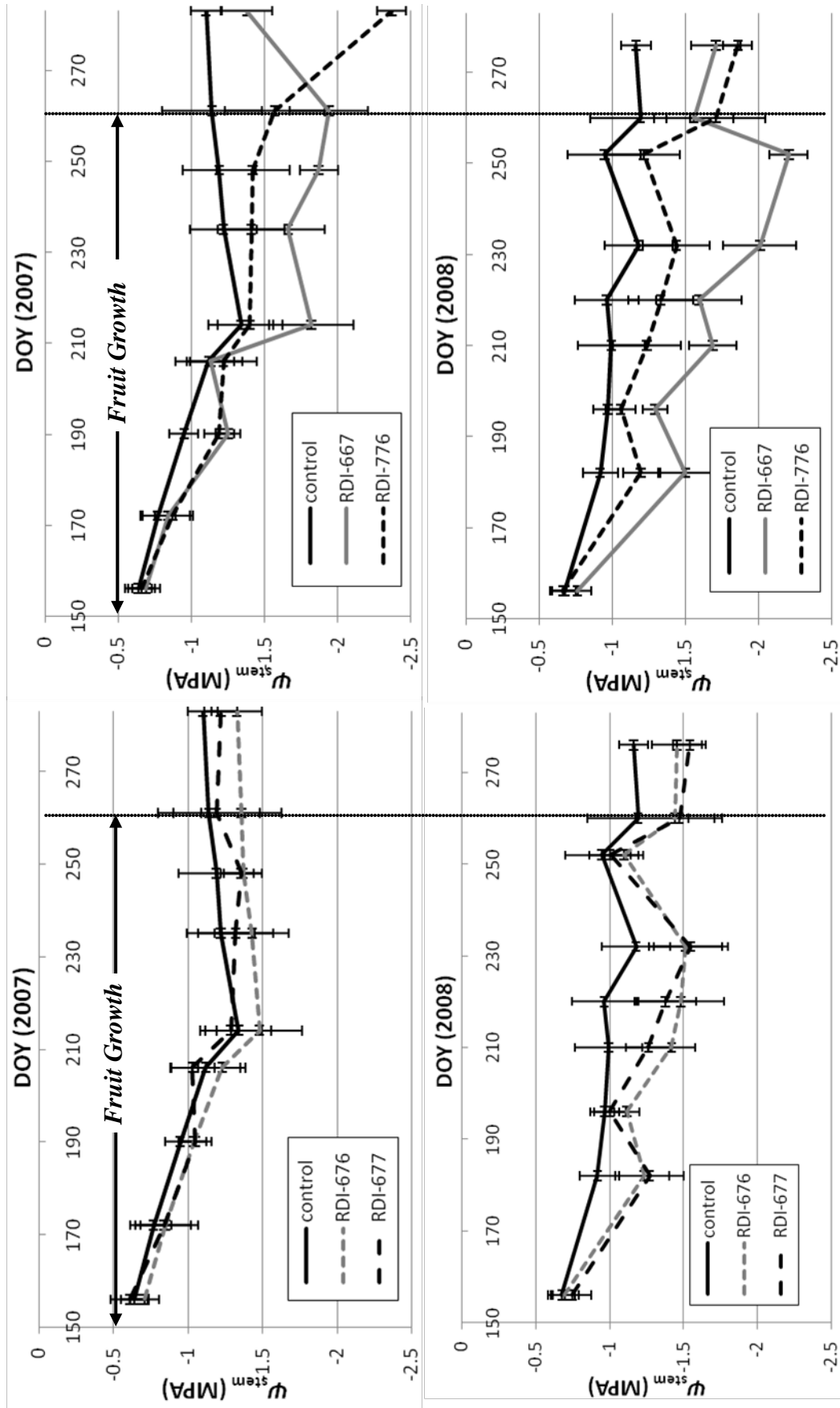


Fig. 3.5. Evolution of midday stem water potential (ψ_{stem}) in each treatment during the fruit growth and fruit maturation periods of the experimental years. Vertical bars indicate the standard deviation in each treatment (ten repetitions per treatment). DOY = day of year.

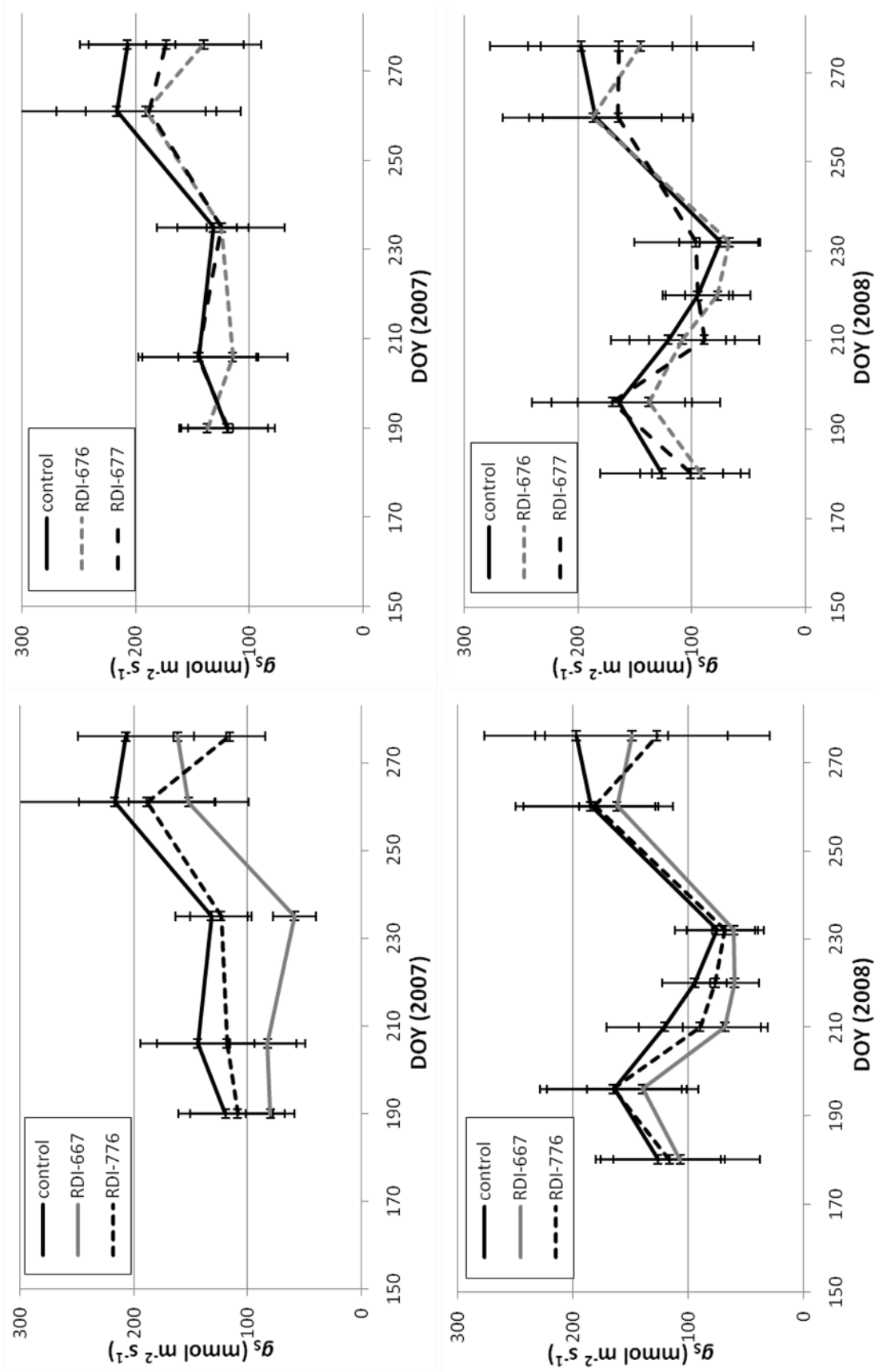


Fig. 3.6. Evolution of stomatal conductance (g_s) in each treatment during the fruit growth and fruit maturation periods of the experimental years. Vertical bars indicate the standard deviation in each treatment (ten repetitions per treatment). DOY = day of year.

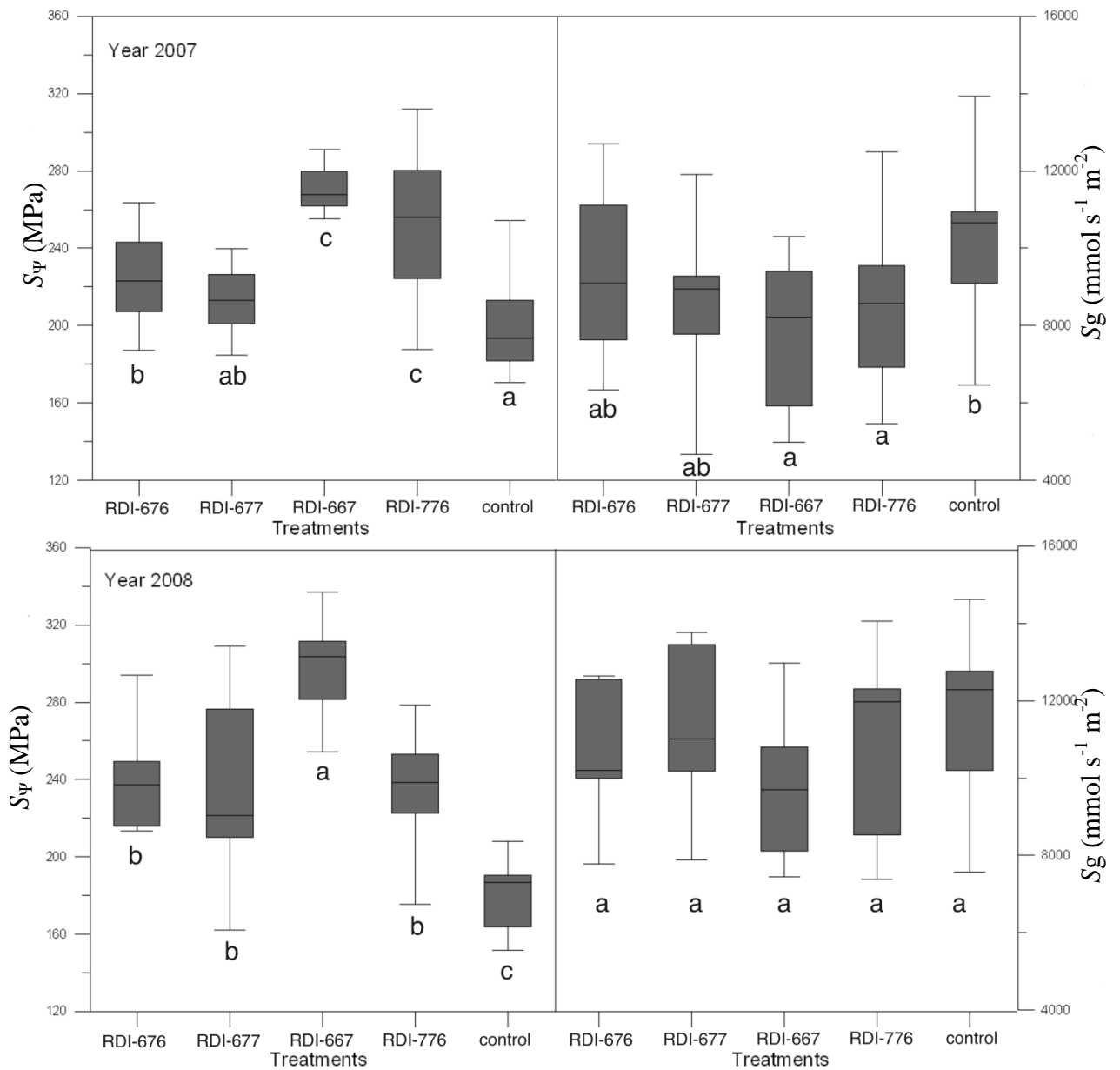


Fig. 3.7. Box and whisker plots for water stress integral (S_{ψ}) and stomatal conductance integral (S_g) during the studied years. Vertical lines indicate the standard deviation for each treatment.

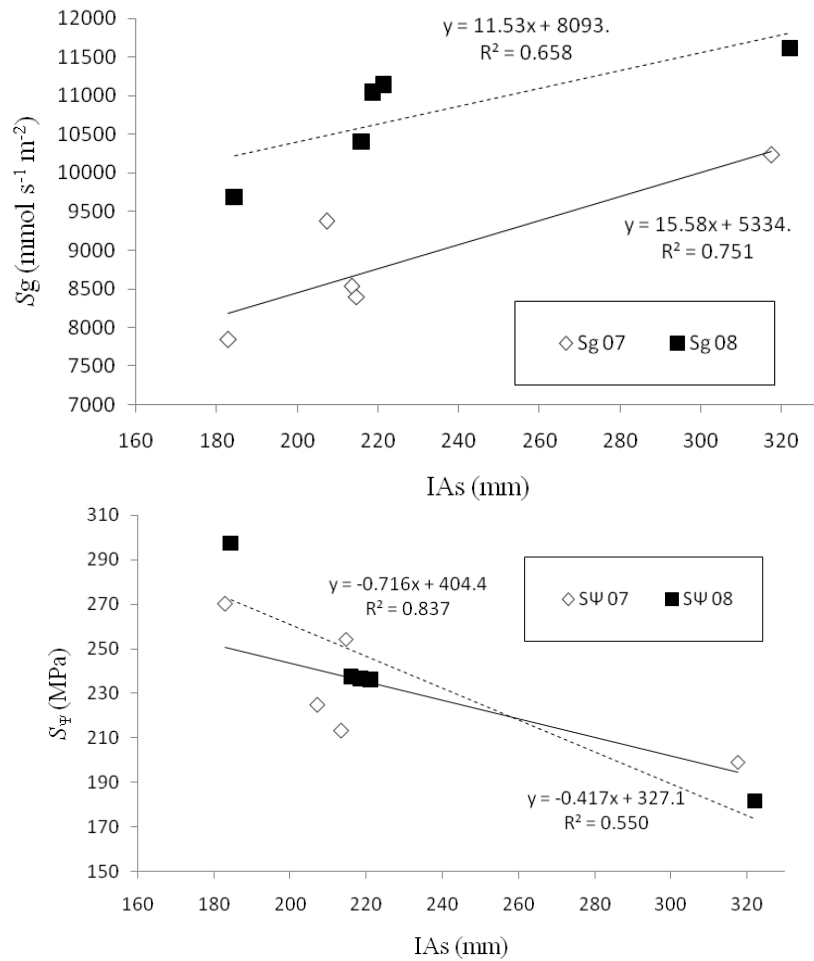


Fig. 3.8. Linear relationships among irrigation amounts (IAs) and water stress integral (S_{ψ}) and stomatal conductance integral (Sg) in control and RDI treatments during the irrigation period.

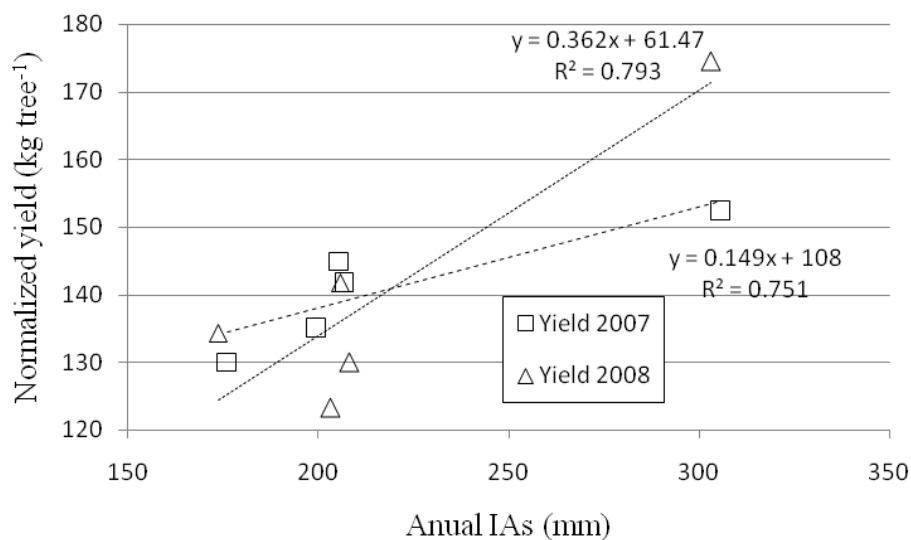


Fig. 3.9. Yield vs. annual irrigation amounts (IAs). Yield was normalized to take into account the temporal variability of the results due to changing weather conditions during the studied years.

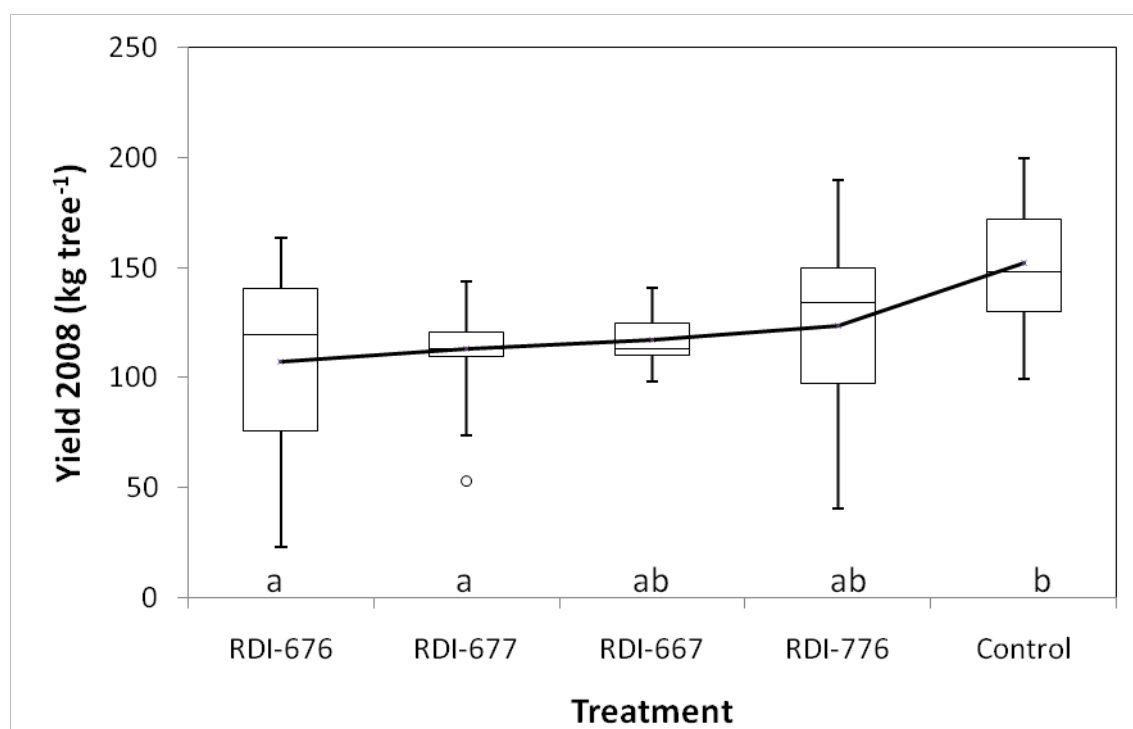
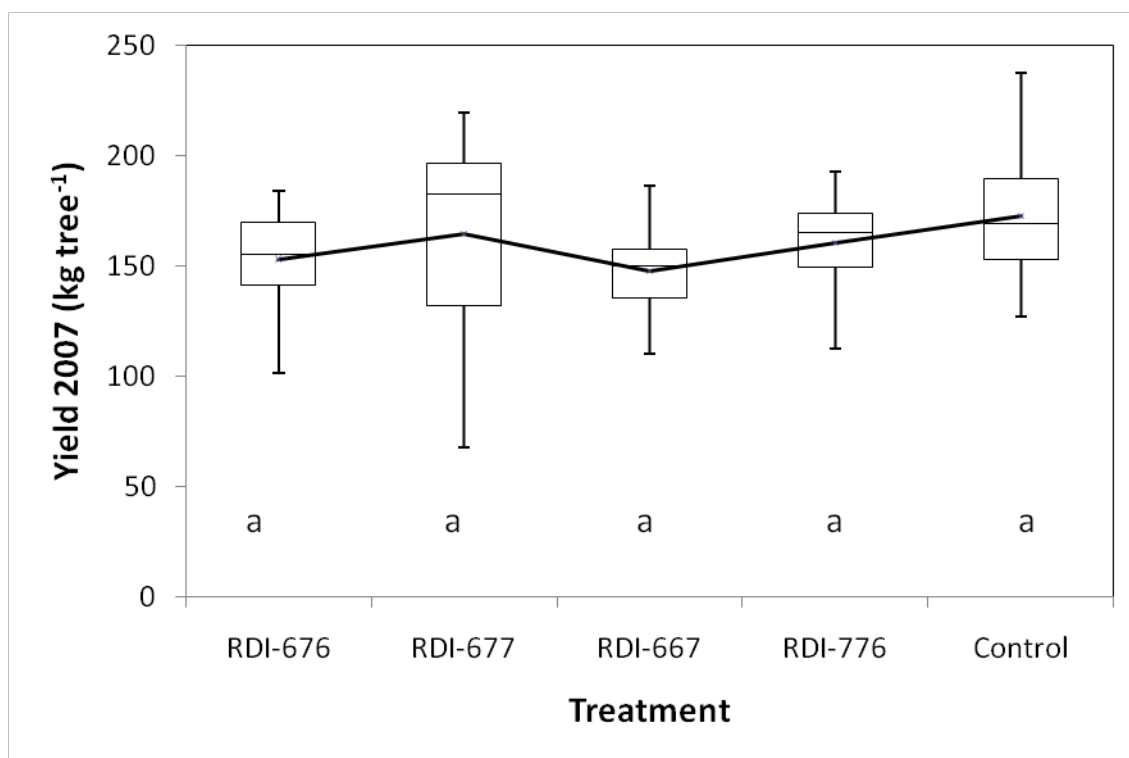


Fig. 3.10. Box and whisker plot for yield (years 2007 and 2008). The line inside the box shows the median and the letters after each box-whisker plot show statistical differences at $P < 0.05$ level.

Table 3.4. Yield components and fruit quality parameters.

Season 2007	Treatments				
	RDI-676	RDI-677	RDI-667	RDI-776	control
Yield (kg tree ⁻¹)	153.1	164.39	147.5	160.65	172.77
Fruit weight (g)	209.22 ^a	218.39 ^a	207.65 ^a	215.54 ^a	267.64 ^b
Fruits tree ⁻¹	735	758	722	765	667
Juice Weight (%)	39.77	40.05	37.67	37.96	39.19
TSS (°Brix)	12.88 ^b	12.78 ^b	14.04 ^b	13.11 ^b	11.26 ^a
T.A. (g L ⁻¹)	1.32 ^{abc}	1.25 ^{ab}	1.55 ^c	1.41 ^{bc}	1.15 ^a
M.I.	9.75 ^{ab}	10.22 ^b	9.06 ^a	9.29 ^a	9.79 ^{ab}
E.D. (mm)	75.00 ^a	75.80 ^{ab}	74.89 ^a	75.98 ^{ab}	89.79 ^b
P.D. (mm)	79.70 ^{ab}	79.23 ^b	76.36 ^a	77.76 ^a	84.04 ^{ab}
Rind (mm)	6.00	6.28	6.69	6.13	6.60
Season 2008	Treatments				
	RDI-676	RDI-677	RDI-667	RDI-776	control
Yield (kg tree ⁻¹)	131.33	118.23	117.1	154.69	157.92
Fruit weight (g)	268.69 ^{ab}	285.68 ^b	214.22 ^a	262.43 ^{ab}	272.99 ^b
Fruits tree ⁻¹	509 ^{ab}	424 ^a	554 ^{ab}	620 ^b	588 ^b
Juice Weight (%)	46.83	45.73	46.28	45.00	45.93
TSS (°Brix)	13.19 ^b	12.98 ^b	14.82 ^c	13.40 ^b	11.24 ^a
T.A. (g L ⁻¹)	0.96 ^b	0.85 ^{ab}	1.12 ^c	0.96 ^c	0.74 ^a
M.I.	13.86 ^{ab}	15.71 ^b	13.23 ^a	14.29 ^{ab}	15.27 ^{ab}
E.D. (mm)	81.24 ^{ab}	83.99 ^b	75.82 ^a	80.85 ^{ab}	82.48 ^b
P.D. (mm)	86.85	88.51	85.82	84.31	86.30
Rind (mm)	6.72	7.21	6.76	6.76	6.47

Within each row, different letters indicate significant differences at $P < 0.05$ by Tukey's test. TSS, total soluble solids; TA, titratable acidity; MI, maturity index; ED, equatorial diameter; PD, polar diameter; PT, peel thickness.

Table 3.5. Water stress integral, stomatal conductance integral, yield and fruit quality parameters for the entire study period (2007-2008) (Normalized data).

	Treatments				
	RDI-676	RDI-677	RDI-667	RDI-776	control
S_{ψ}	130.8 ^{bc}	123.8 ^b	160.1 ^d	138.9 ^c	109.4 ^a
S_g	7918 ^{ab}	7846 ^{ab}	6851 ^a	7589 ^{ab}	8536 ^b
Yield (kg tree ⁻¹)	150.2 ^{ab}	149.2 ^{ab}	139.7 ^a	166.5 ^{ab}	174.3 ^b
Fruit weight (g)	206.8 ^{ab}	218.1 ^b	182.5 ^a	206.8 ^{ab}	233.9 ^b
Fruits tree ⁻¹	726	684	765	805	745
Juice Weight (%)	41.0 ^a	40.6 ^a	39.8 ^a	39.3 ^a	40.3 ^a
TSS (°Brix)	14.1 ^b	13.9 ^b	15.6 ^c	14.3 ^b	12.1 ^a
TA (g L ⁻¹)	1.3 ^{abc}	1.2 ^{ab}	1.5 ^c	1.3 ^{bc}	1.1 ^a
MI	12.0 ^a	13.1 ^a	11.3 ^a	12.0 ^a	12.7 ^a
ED (mm)	75.8 ^{ab}	77.5 ^b	73.1 ^a	76.1 ^{ab}	79.2 ^b
PD (mm)	84.6 ^a	85.2 ^a	83.4 ^a	82.3 ^a	86.5 ^a
PT (mm)	6.7 ^a	7.1 ^a	7.1 ^a	6.8 ^a	6.9 ^a

Within each row, different letters indicate significant differences at $P < 0.05$ by Tukey's test.

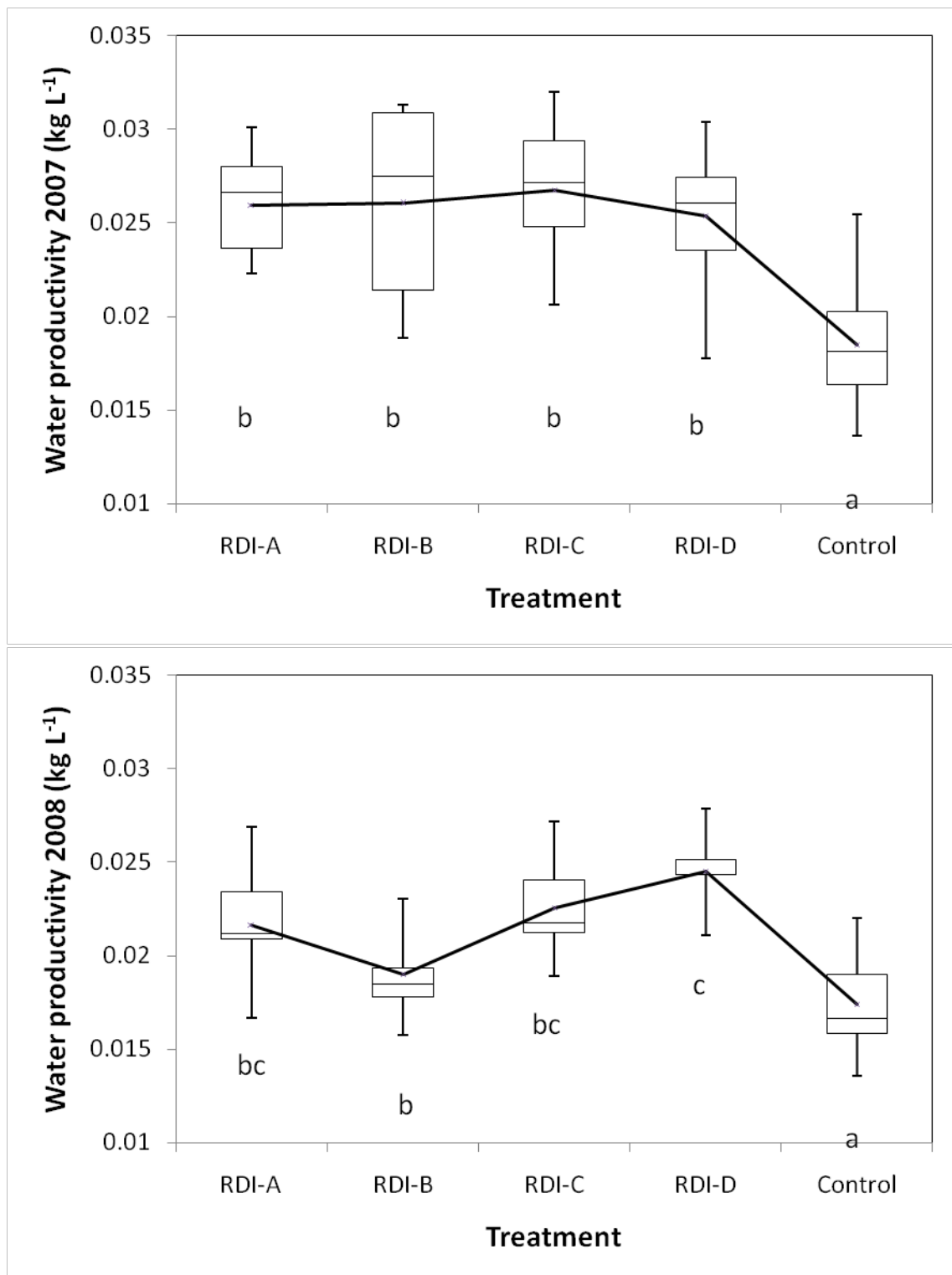


Fig. 3.11. Box and whisker plot for water productivity (years 2007 and 2008). The line inside the box shows the median and the letters after each box and whisker plot show statistical differences at $P < 0.05$ level.

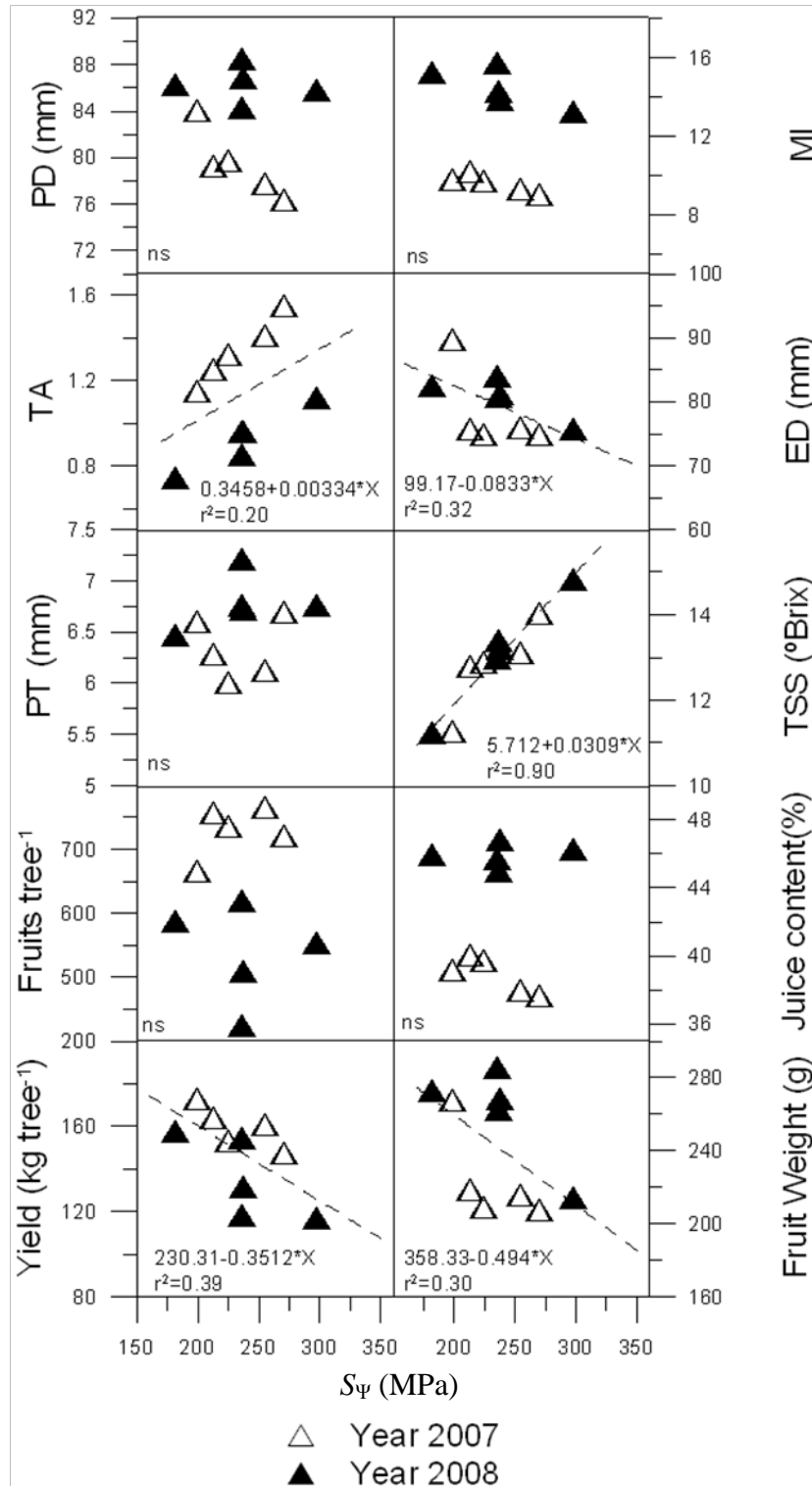


Fig. 3.12. Relationships among water stress integral (S_{ψ} , MPa) and yield and fruit quality parameters (years 2007 and 2008). PT, peel thickness; TSS, total soluble solids; MI maturity index; TA, titratable acidity; ED and PD equatorial and polar diameter respectively.

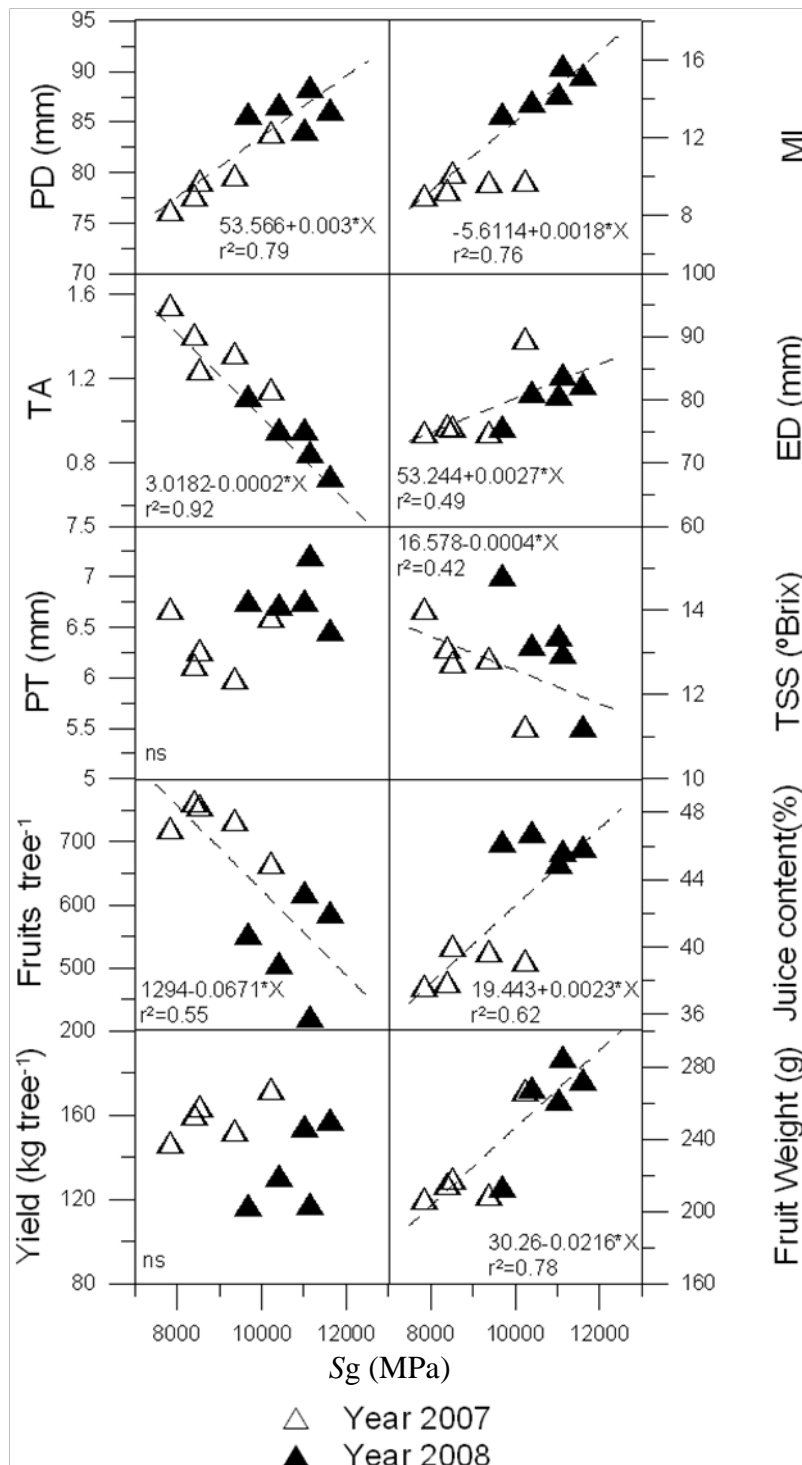


Fig. 3.13. Relationships among stomatal conductance integral (S_g , $\text{mmol s}^{-1} \text{m}^{-2}$) and yield and fruit quality parameters (years 2007 and 2008). PT, peel thickness; TSS, total soluble solids; MI maturity index; TA, titratable acidity; ED and PD equatorial and polar diameter

3.4. Discussion

In terms of the threshold value for midday Ψ_{stem} in citrus trees, the control treatment registered values ranging between -0.6 and -1.3 MPa, in periods of minimum and maximum evapotranspiration demand, respectively. These values are close to those reported by Ortuño *et al.* (2006a). According to De Swaef *et al.* (2009), Ψ_{stem} directly reflects the plant's water status, bearing strong relationships with the sap-flow rate or daily radial-stem growth. Many authors have found similar results for Ψ_{stem} (Goldhamer *et al.*, 1999; Naor and Cohen, 2003; Nortes *et al.*, 2005), a parameter which usefulness for irrigation management is widely accepted (Shackel *et al.*, 1997; Naor, 2000).

In general, g_s is not sensitive to the irrigation treatment until a certain threshold of Ψ_{stem} is reached. In this context, Ortuño *et al.* (2004), observed in well-irrigated lemon trees greater fluctuations in g_s than in Ψ_{stem} . In other experiment, Ortuño *et al.* (2006b) observed that Ψ_{stem} was more sensitive to water stress than g_s , since significant differences between treatments were found in Ψ_{stem} a week before than in g_s .

Our results suggest that both S_Ψ and S_g are good indicators of potential effects caused by water stress in some of the fruit quality parameters such as TA and TSS. Nevertheless, S_g showed better results when considering the relations obtained each year than that of the two years experimental period. In contrast, treatments with similar S_Ψ or S_g showed different effects on yield and fruit-quality parameters. This could have been due both to changing meteorological conditions and to the stress distribution over the phenological periods. Differences on water distribution along the irrigation season, depending on the irrigation strategy, had a greater effect on the response of the citrus tree than the annual IA applied in each treatment.

Several pieces of work have shown that certain levels of water stress increases TSS and TA in citrus trees (Bielorai, 1982; Kuriyama *et al.*, 1981; Yakushiji *et al.*, 1998; Hockema and Etxeberria, 2001). In this context Pérez-Pérez *et al.* (2009) pointed out that a reduction of IA during fruit maturation period in 'Lane late' sweet orange significantly increased TSS and TA, without changes in MI, PD, and peel thickness. Moreover, this irrigation reduction lowered juice parameters and ED. Ginestar and Castel (1996) observed that withholding of irrigation during the fruit maturation of young clementine citrus trees in two consecutive years caused a reduction of yield, fruit weight and fruit

number, although fruit number differences were not significant. Gonzalez-Altozano and Castel (1999) documented similar results in two treatments with reductions of 50% and 75% of irrigation during fruit maturation of 10-year-old clementine citrus trees in the first experimental year. In the second year, these authors observed reductions in yield and fruit weight and increments in fruit number. Nevertheless, only fruit weight differences were significant. Hutton *et al.* (2007) tested DI by applying different irrigation interval treatments during fruit growth and fruit maturation periods in 'Valencia' orange trees during two consecutive years. In their experiment, the development of more vegetative shoot growth by trees growing under increasing water deficit in late summer increased the number of potential fruiting sites for flowering in the following season. This was seen in the increase in fruit count per tree recorded for trees grown under longer irrigation intervals. This also could explain the results of Gonzalez-Altozano and Castel (1999) reported above. Hutton *et al.* (2007) also observed that the increased crop load (number of fruits per tree) and periodic water stress during fruit growth period contributed to the smaller fruit size recorded in trees irrigated at the longer intervals. Consequently, the increased fruit numbers did not result in significant increases in fruit mass per tree. They observed yield differences between years were much greater than between irrigation treatments.

The higher number of fruits in our RDI-776 treatment could be explained because the water limitations during fruit maturation. Gonzalez-Altozano and Castel (2003) also documented that prolonged moderated deficit irrigation in autumn promoted higher flowering during next spring.

González-Altozano and Castel (2003) observed significant effects on yield, because of a decrease in fruit number when the crop underwent moderate to severe water stress. However, this strategy did not affect either the fruit weight or the organoleptic properties. When a severe reduction in water supplied by irrigation was applied during the fruit-growing period, the fruit number was not affected but fruit weight, and thus yield, was reduced, although only fruit weight differences were significant.

Our results in 2008 suggest that any severe water stress (IA < 57% of IN) at flowering affected mainly the fruit number, thus reducing yield. Nevertheless, the differences were only significant in treatment RDI-667. Furthermore, when a similar

reduction in IA was maintained during fruit growth the fruit weight significantly decreased. Deficit irrigation during fruit maturation affected the organoleptic fruit characteristics. DI strategies were influenced by the spring and autumn rainfall, suggesting that its application could be appropriate from mid-spring to the end of summer, coinciding with late flowering and the final fruit growth period, respectively.

Increasing WP may be a mean of achieving a rational use of water in agriculture. Taking into account that the available water for irrigated land is a limiting factor in many world areas (Ali and Talukder, 2008), strategies such as DI have shown that water productivity can be enhanced (Ali *et al.*, 2007; Jalota *et al.*, 2006) and could be associated with acceptable commercial production. Nowadays, the low importance given to improving WP must be related to the reduced water costs in Mediterranean agricultural areas (Lorite *et al.*, 2004), where water represents only less than 10% of the total production costs, a clear contradiction with the Common Agricultural Policy and the water Framework Directive (García-Vila *et al.*, 2008). Our WP results were particularly good for the RDI-776 treatment during 2008, when the highest water productivity was achieved (0.025 kg L^{-1}). Thus, this DI strategy offered the best results, with water savings greater than 30% (Table 3.3) and non-significant yield losses (Table 3.4). The total yearly IAs in the RDI-676, RDI-677 and RDI-776 treatments were similar ($64\% \pm 1\%$ of IN), but the different periods in which IA was more severely reduced had significant effects on yield, and hence in final water productivity (Tables 3.3-3.4 and Fig. 3.11).

3.5. Conclusions

Although all the tested RDI treatments increased WP, our results show that RDI-776 is the best strategy for *Citrus sinensis* L. Osb. cv. Navelina trees grown in the area. This treatment allowed $1200 \text{ m}^3 \text{ Ha}^{-1}$ (37% IN) of water savings per year on average with no significant effect in yield. It also improved significantly fruit quality parameters as TSS and TA.

In the rest of the tested RDI treatments, with a greater reduction of irrigation water at flowering (44% of control), mainly fruit number was affected. Furthermore, maintaining this reduction during the fruit growth period caused a significant loss in fruit weight and some changes in fruit quality parameters, such as an increase of TSS and TA.

Our results suggest that both S_{ψ} and S_g are good indicators of potential effects caused by water stress in some fruit quality parameters as TA and TSS, although S_g showed better results when considering the relations obtained each year than that of the two years experimental period. In contrast, treatments with similar S_{ψ} or S_g showed different effects on yield and fruit-quality parameters, probably due to changing meteorological conditions and to the stress distribution over the phenological periods. Differences on water distribution along the irrigation season, depending on the irrigation strategy, had a greater effect on the response of the citrus tree than the annual IA applied in each treatment.

3.6. References

- Ali M, Hoque M, Hassan A, Khair A. 2007. Effects of deficit irrigation on yield, water productivity, and economic returns of wheat. *Agric Water Manage* 92(3):151-161.
- Ali M, Talukder M. 2008. Increasing water productivity in crop production--A synthesis. *Agric Water Manage* 95(11):1201-1213.
- Allen RG, Pereira LS, Raes D, Smith M. 1998. Crop evapotranspiration--Guidelines for computing crop water requirements--FAO Irrigation and drainage paper 56. FAO, Rome 300:6541.
- Anapalli SS, Ahuja, L.R., Ma, L., Timlin, D.J., Stockle, C.O., Boote, K.J., Hoogenboom, G. 2008. Current Water Deficit Stress Simulations in Selected Agricultural System Simulation Models. In: Ahuja LR, Reddy, V.R., Saseendran, S.A., Yu, Q., editor. *Response of Crops to Limited Water: Understanding and Modeling Water Stress Effects on Plant Growth Processes*. Madison, WI: American Society of Agronomy, Crop Science Society of America, Soil Science Society of America. p 1-38.
- Bielorai H. 1982. The effect of partial wetting of the root zone on yield and water use efficiency in a drip-and sprinkler-irrigated mature grapefruit grove. *Irrigation Science* 3(2):89-100.

- BOJA. 2000. Orden de 21 de septiembre de 2000 por la que se aprueba el Reglamento Específico de Producción Integrada de Cítricos. Sevilla: Consejería de Agricultura y Pesca. 30 de Septiembre de 2000, 15287-15297.
- Castel J. 1991. El riego de los cítricos. *Hortofruticultura* 5:41-52.
- De Swaef T, Steppe K, Lemeur R. 2009. Determining reference values for stem water potential and maximum daily trunk shrinkage in young apple trees based on plant responses to water deficit. *Agric Water Manage* 96(4):541-550.
- Doorembos J, Kassam A. 1974. Crop water requirements. FAO Irrigation and drainage paper 24.
- Doorembos J, Kassam A. 1979. Yield response to water. Rome: FAO 33.
- FAO. 1998. World Reference Base for Soil Resources. Rome: Food and Agriculture Organization of the United Nations.
- Fereres E, Goldhamer DA, Parsons LR. 2003. Irrigation water management of horticultural crops. *Hortscience* 38(5):1036-1042.
- García-Tejero I, Jiménez JA, Reyes MC, Carmona A, Pérez R, Muriel JL. 2008. Aplicación de caudales limitados de agua en plantaciones de cítricos del valle del Guadalquivir. *Fruticultura Profesional* 173:5-17.
- García-Vila M, Lorite I, Soriano M, Fereres E. 2008. Management trends and responses to water scarcity in an irrigation scheme of Southern Spain. *Agric Water Manage* 95(4):458-468.
- Ginestar C, Castel JR. 1996. Responses of young clementine citrus trees to water stress during different phenological periods. *Journal of Horticultural Science* 71(4):551-559.
- Goldhamer DA, Fereres E, Mata M, Girona J, Cohen M. 1999. Sensitivity of continuous and discrete plant and soil water status monitoring in peach trees subjected to deficit irrigation. *J Am Soc Hortic Sci* 124:437-444.

-
- Gonzalez-Altozano P, Castel JR. 1999. Effects of regulated deficit irrigation on 'Clementina de Nules' citrus trees I. Yield and fruit quality effect. *J Am Soc Hort Sci* 74:749-758.
- Gonzalez-Altozano P, Castel JR. 2000a. Effects of regulated deficit irrigation on 'Clementina de Nules' citrus trees II. Vegetative growth. *J Am Soc Hort Sci* 75:388-392.
- González-Altozano P, Castel JR. 2000b. Effects of regulated deficit irrigation in 'Clementina de Nules' citrus trees growth, yield and fruit quality. *Acta Hort* 537:749-758.
- González-Altozano P, Castel JR. 2003. Riego deficitario controlado en " Clementina de Nules". I: efectos sobre la producción y la calidad de la fruta. *Spanish Journal of Agricultural Research*(2):81-92.
- Hockema BR, Etxeberria E. 2001. Metabolic contributors to drought-enhanced accumulation of sugars and acids in oranges. *Journal of the American Society for Horticultural Science* 126(5):599-605.
- Hsiao TC. 1973. Plant responses to water stress. *Annu Rev Plant Physiol Plant Molec Biol* 24:519-570.
- Hutton R, Landsberg J, Sutton B. 2007. Timing irrigation to suit citrus phenology: a means of reducing water use without compromising fruit yield and quality? *Australian Journal of Experimental Agriculture* 47(1):71-80.
- Jalota S, Sood A, Chahal G, Choudhury B. 2006. Crop water productivity of cotton (*Gossypium hirsutum* L.)-wheat (*Triticum aestivum* L.) system as influenced by deficit irrigation, soil texture and precipitation. *Agric Water Manage* 84(1-2):137-146.
- Kuriyama T, Shimoosako M, Yoshida M, Shiraishi S. The effect of soil moisture on the fruit quality of Satsuma mandarin (*Citrus unshiu* Marc); 1981. *International Society of Citriculture*. p 524-527.

-
- Lorite I, Mateos L, Fereres E. 2004. Evaluating irrigation performance in a Mediterranean environment. *Irrigation Science* 23(2):77-84.
- Myers BJ. 1988. Water stress integral—a link between short-term stress and long-term growth. *Tree Physiology* 4(4):315.
- Naor A. 2000. Midday stem water potential as a plant water stress indicator for irrigation scheduling in fruit trees. *Acta Hort* 537:447-454.
- Naor A, Cohen S. 2003. Sensitivity and Variability of Maximum Trunk Shrinkage, Midday Stem Water: Potential, and Transpiration Rate in Response to Withholding Irrigation from Field-grown Apple Trees. *Hortscience* 38(4):547-551.
- Nortes PA, Pérez-Pastor A, Egea G, Conejero W, Domingo R. 2005. Comparison of changes in stem diameter and water potential values for detecting water stress in young almond trees. *Agric Water Manage* 77(1-3):296-307.
- Ortuño M, Alarcón J, Nicolás E, Torrecillas A. 2004. Comparison of continuously recorded plant-based water stress indicators for young lemon trees. *Plant and Soil* 267(1):263-270.
- Ortuño MF, García-Orellana Y, Conejero W, Ruiz-Sánchez MC, Alarcón JJ, Torrecillas A. 2006a. Stem and leaf water potentials, gas exchange, sap flow, and trunk diameter fluctuations for detecting water stress in lemon trees. *Trees-Structure and Function* 20(1):1-8.
- Ortuño MF, García-Orellana Y, Conejero W, Ruiz-Sánchez MC, Mounzer O, Alarcón JJ, Torrecillas A. 2006b. Relationships between climatic variables and sap flow, stem water potential and maximum daily trunk shrinkage in lemon trees. *Plant and Soil* 279(1-2):229-242.
- Pérez-Pérez J, Robles J, Botía P. 2009. Influence of deficit irrigation in phase III of fruit growth on fruit quality in 'lane late' sweet orange. *Agric Water Manage* 96(6):969-974.

-
- Sanchez-Blanco MJ, Torrecillas A, Leon A, Delamor F. 1989. The Effect of Different Irrigation Treatments on Yield and Quality of Verna Lemon. *Plant and Soil* 120(2):299-302.
- Scholander PF, Bradstreet ED, Hemmingsen E, Hammel H. 1965. Sap pressure in vascular plants. *Science* 148(3668):339.
- Shackel K, Ahmadi H, Biasi W, Buchner R, Goldhamer D, Gurusinghe S, Hasey J, Kester D, Krueger B, Lampinen B and others. 1997. Plant Water Status as an Index of Irrigation Need in Deciduous Fruit Trees. *HortTechnology* 7(1):23-29.
- Steppe K, Dzikiti S, Lemeur R, Milford JR. 2006. Stomatal oscillations in orange trees under natural climatic conditions. *Annals of botany* 97(5):831.
- Sterk G, Stein A. 1997. Mapping wind-blown mass transport by modeling variability in space and time. *Soil Science Society of America Journal* 61(1):232-239.
- Thompson R, Gallardo M, Valdez L, Fernandez M. 2007. Determination of lower limits for irrigation management using in situ assessments of apparent crop water uptake made with volumetric soil water content sensors. *Agric Water Manage* 92(1-2):13-28.
- Turner NC. 1988. Measurement of plant water status by the pressure chamber technique. *Irrigation Science* 9(4):289-308.
- Verasan VP, Ronald E. 1978. Effects of Soil Water Stress on Growth and Nutrient Accumulation in Corn. *Agronomy Journal* 70(4):613-618.
- Verreyne JS, Rabe E, Theron KI. 2001. The effect of combined deficit irrigation and summer trunk girdling on the internal fruit quality of 'Marisol' Clementines. *Scientia Horticulturae* 91(1-2):25-37.
- Yakushiji H, Morinaga K, Nonami H. 1998. Sugar accumulation and partitioning in Satsuma mandarin tree tissues and fruit in response to drought stress. *American Society for Horticultural Science (USA)* 123:719-726.

Chapter 4

Impact of sustained and low frequency deficit irrigation on the physiological response, water productivity and fruit yield of citrus trees cv. Navelina

Part of this chapter is published in:

García-Tejero I, Jiménez-Bocanegra JA, Martínez G, Durán-Zuazo VH, Romero R, Muriel JL. 2010. Positive Impact of Regulated Deficit Irrigation on Yield and Fruit Quality in a commercial Citrus Orchard. *Agricultural Water Management* Vol 97, 614-622.

Abstract. This work was carried out in a citrus orchard of the Guadalquivir River Valley, with 11-year-old citrus trees (*Citrus sinensis* L. Osbeck, cv. Navelina) grafted on Citrange Carrizo (*Citrus sinensis* L. Osbeck x *Poncirus trifoliata* L. Raf.) under three irrigation treatments: (1) control, in which 111% of the irrigation needs (IN, mm) were replaced by irrigation; (2) a low frequency deficit irrigation (LFDI) treatment with withholding & rewatering cycles, in which trees were irrigated to replace 100% of the IN when midday stem water potential (Ψ_{stem} , MPa) values approached -2.0 MPa, and irrigation was withheld when Ψ_{stem} values were similar to those in the control trees. This resulted in a 65% of the total crop IN and six withholding&rewatering cycles during the irrigation season; and (3) a sustained deficit irrigation (SDI) approach in which total water supplies amounted to 58% of the crop IN. Midday stem-water potential and stomatal conductance (g_s , $\text{mmol m}^{-2} \text{s}^{-1}$) were measured during the dry period (from mid-June to mid-September), as well as trunk diameter fluctuations from which we derived the maximum daily shrinkage (MDS, mm) and the daily maximum stem diameter (MXSD, mm). This allowed us to evaluate the impact of the irrigation treatments in the plant-water status and to establish main relationships among the recorded variables during the fruit growth and fruit maturation periods. The lowest Ψ_{stem} and g_s values were registered in the treatments with lower irrigation supplies (SDI and LFDI). Compared with the control treatment, MDS values were significantly higher in the SDI treatment and in the withholding periods of the LFDI treatment and the opposite was observed with the MXSD values. In the LFDI trees, values of Ψ_{stem} , g_s , MDS and MXSD

fluctuated in agreement with the withholding&rewatering cycles. Thus Ψ_{stem} and g_s values decreased and MDS values increased during the withholding periods, and the opposite behaviour followed the rewatering events. The g_s values were markedly influenced by weather conditions. Tight relationships between Ψ_{stem} and g_s , and between Ψ_{stem} and MDS were found. The LFDI treatment promoted 40% water saving with an 18% of reduction in yield only. In addition, this treatment improved fruit quality.

4.1. Introduction

In arid and semi-arid areas, such as those of the Mediterranean basin in which citrus are widely grown, the sustainable use of water in agriculture is a challenge (Araus, 2004; Ruiz Sánchez *et al.*, 2010). The area devoted to citrus orchards in Andalusia, the south region of Spain, is of ca. 74000 ha. Most orchards are irrigated with an average of 6500 m³ ha⁻¹ yr⁻¹. The increasing demand of water from other sectors (industry, tourism, etc.) is putting pressure for a more rational use of water in agriculture. This can be achieved by improving the crop water productivity (WP), i.e. by maximizing the marketable yield per unit of water applied.

Deficit irrigation (DI) of fruit tree orchards allows significant water savings and WP increase (Feres and Soriano, 2007). Many authors have pointed out the advantages of DI for improving water productivity in citrus orchards (González and Castel, 2000; Muriel *et al.*, 2006; García-Tejero *et al.*, 2007, 2008). A reliable monitoring of the tree water status is required for applying most DI strategies, since episodes of severe water stress that may affect negatively yield and fruit quality must be avoided. In this context, stem water potential (Ψ_{stem}) and stomatal conductance (g_s) are among the most useful plant-based measurements to monitor the plant response to limiting water conditions (Romero *et al.*, 2006; Pérez-Pérez *et al.*, 2008a, 2008b, 2009). The measurement of these variables, however, cannot be automated, i.e. they cannot be continuously monitored. By contrast, trunk diameter variations (TDV) are also related to the tree water stress and they can be automatically recorded. In fact, TDV-derived indices such as the maximum daily shrinkage, MDS (Ortuño *et al.*, 2006, 2009; Velez *et al.*, 2007; Conejero *et al.*, 2007), and the daily maximum stem diameter, MXSD (Cuevas *et al.*, 2010; Moriana *et al.*, 2010; Fernández *et al.*, 2010, 2011) have been successfully used both to derived information on the tree water stress and to control irrigation in a variety of fruit tree species including

citrus. A variety of DI strategies have been used with different woody crops, such as grapevine (García-Escudero *et al.*, 1991, 1997, Rubio *et al.*, 2004, Yuste *et al.*, 2005, Intrigliolo and Castel, 2008), apricot trees (Ruiz-Sánchez *et al.*, 2000 and Pérez-Pastor *et al.*, 2009), almond trees (Girona *et al.*, 2005 and Goldhamer *et al.*, 2006), apple trees (Girona *et al.*, 2009) and olive trees (Moriana *et al.*, 2003 and Iniesta *et al.*, 2009). This subject was extensively reviewed by Ruiz-Sanchez *et al.* (2010). To our knowledge, very little research has been made on the effect of sustained deficit irrigation (SDI) and low frequency deficit irrigation (LFDI) strategies on the physiological response, water productivity and fruit yield of citrus trees. These two DI strategies, however, are among the most widely used irrigation strategies in citrus orchards of the Guadalquivir River Valley, as well as in many other areas where water for irrigation is scarce. Hutton *et al.* (2007) addressed the question of timing irrigation to suit citrus phenology. The intervals between irrigation applications were fixed by the authors and not based on the physiological response of the trees. Gomes *et al.* (2004) studied the effect of water stress on transpiration, g_s and leaf water potential of 1-year-old 'Pera' orange trees in pots. They compared a LFDI and a full irrigation (FI) treatment, but they did not reported results on water use efficiency or fruit yield.

The main objectives of this research were to evaluate the impact of a SDI (58% of the irrigation needs, IN) and a LFDI (65% of IN, withholding&rewatering periods of 15-29 days) strategy on the physiological response, water productivity and fruit yield of mature citrus trees under field conditions in the Guadalquivir River Valley, and to explore the feasibility of these strategies as sustainable practices for improving WP in Mediterranean areas in which citrus trees are cropped under water scarcity conditions.

4.2. Material and methods

4.2.1. Experimental site

This research was carried out in a commercial orchard located in the Guadalquivir River Valley, SW Spain (37°29'19"N, 5°50'43"W) planted with 11-year-old orange trees (*Citrus sinensis*, L. Osbeck, cv. Navelina) grafted on Citrange Carrizo (*Citrus sinensis*, L.

Osbeck x *Poncirus trifoliata*, L. Raf.). The trees, spaced 6 m × 4 m, were, on average, 2.5 m in height and 3.2 m in diameter.

The soil was a texture-contrast duplex soil. The top 0.9 m layer was a typical fluvisol (FAO, 1998) with textural values of 70% sand, 19% silt and 11% clay, a water holding capacity of 99 mm. The organic-matter content was below 1%. Below there was a dense clay layer. Most of the roots were in the top 0.4 m of soil. The climate in the area is typically Mediterranean, with dry, hot summers and mild, wet winters. Average annual values of potential evapotranspiration (ET_o) and rainfall (R) values are 1400 mm and 534 mm, respectively (period 1971-2000). Rainfall occurs mainly from late autumn to early spring, with November to February being the wettest months. Temperature in winter rarely falls below 0 °C, and maximum values can go over 40 °C in July and August.

4.2.2. Irrigation treatments and experimental design

The irrigation needs (IN) for the orchard conditions were calculated as

$$IN = \left[\sum_{k=1}^7 ET_o^k \right] \cdot K_c \cdot K_r - P_e \quad \text{Eq. 4.1}$$

where ET_o was calculated with the FAO56 Penman-Monteith equation (Allen *et al.*, 1998) and data from an automatic weather station nearby the orchard. K_c is the crop coefficient and K_r is a reduction coefficient accounting for the percentage of ground surface covered by the crop. P_e is the effective precipitation. We used the K_c values reported by Fernández-Gómez *et al.* (1999), i.e. 0.45 in January and February, 0.5 from March to May, 0.55 from June to October and 0.5 in November and December. A K_r value of 0.7 was calculated after Fereres and Castel (1981), corresponding to the 35% of the ground surface covered by the canopies of the trees.

In 2008, the experimental year, we applied three irrigation treatments: 1) control, in which the trees were irrigated three time per week with the aim of replacing the crop water needs, i.e. 100% of IN; 2) SDI, a sustained deficit irrigation in which the trees were irrigated with the same frequency than the control trees, but scaled to a total irrigation supply of 60% of IN; 3) LFDI, a low frequency deficit irrigation consisting on

withholding irrigation until midday $\Psi_{\text{stem}} \approx -2.0$ MPa and then irrigating, three times per week also, until no differences on Ψ_{stem} with the control trees were found. The duration of the withholding&rewatering cycles varied from 15 to 29 days.

The irrigation season started in May (early fast-growth fruit period) and ended in November (after fruit-maturity period). For all treatments, the irrigation system consisted of two laterals per tree row with self-compensating drippers 1 m apart (8 drippers per tree). The discharge rates of the drippers were 2.2 L h^{-1} in the control and LFDI trees, and 1.3 L h^{-1} in the SDI trees.

Three 576 m^2 plots per treatment were distributed in a randomized complete block design. Each plot consisted of three rows with 8 trees per row. Measurements were made in the four central trees of each plot, termed here as sample trees.

4.2.3. Measurements

Midday stem-water potential was measured with a pressure chamber (Scholander *et al.*, 1965), following Turner (1988). Once every 7-10 days, two mature leaves were sampled from the north quadrant of each one of the sample trees of each plot. Measurements were made around 12.00 Greenwich Mean Time (GMT).

On the same days in which Ψ_{stem} was measured, g_s was monitored in two sunny leaves per tree, using a diffusion porometer AP-4 (Delta-T Devices, Cambridge, UK).

Three trees per treatment were instrumented with linear variable displacement transducers, LVDTs (Model 2.5 DF; Solartron Metrology, Bognor Regis, UK) installed in the main trunk at about 0.25 m from the ground. The LVDTs were mounted on holders built of aluminium and INVAR—an alloy comprising 64% Fe and 35% Ni that has minimal thermal expansion (Li *et al.*, 1989). Measurements were taken every 30 s and recorded every 15 min on a datalogger. We used these records to calculate the maximum daily shrinkage (MDS) as the difference between the maximum trunk diameter and minimum trunk diameter recorded on the day.

Measurements of the volumetric soil water content in the wetted soil volumes (irrigation bulbs) (SWC, mm) were made with a capacitance probe (C-probe Systems

LTD, UK). We used two access tubes per treatment, located in the soil of one sample tree per plot, at 0.01 m from the closer dripper and 1 m. apart from the trunk. Measurements in each tube were made at 10, 30, 60 and 90 cm depth, every 15 min.

The total fruit weight of each sample tree was determined at the end of the season. For each treatment, WP was calculated as the yield (kg) divided by the volume of water applied (L).

Fruit-quality characteristics were analysed after harvest. Ten fruits from each sample tree were used for analysis. For each fruit we measured equatorial (ED, mm) and polar (PD, mm) diameters, peel thickness (PT, mm), fruit weight and juice content. Total soluble solids contents (TSS, °Brix) were measured with a digital refractometer PR-101. Titratable acidity (TA, g L⁻¹) was determined by titrating the samples with NaOH 0.1 N by the colorimetric method, using phenolphthalein as indicator solution. The maturity index (MI, °Brix L g⁻¹) was then calculated by dividing TSS by TA.

For evaluating the impact of the considered DI strategies, yield and fruit quality variables were subjected to analysis with one-way variance by Tukey's test at level of $P < 0.05$.

4.3. Results

4.3.1. Water supplies

During the studied period (DOY 152-286 in 2008), the seasonal values of ET_o , ET_c and P_e were 776, 299 and 47 mm, respectively. Rainfall was very low during the period of greatest atmospheric demand (from mid-June to mid-September, Fig. 4.1A). Most rainfall events were recorded from mid-September to mid-October. The irrigation amounts (IA, mm) amounted to 280 mm in control (111% IN), 145 mm in SDI (58% IN) and 165 mm in LFDI (65% IN) (Fig. 4.1B, Table 4.1).

The SWC dynamics (Fig. 4.2) was consistent with the applied IA in each treatment. In the control treatment the SWC at 30 cm depth was nearly constant during the studied period (Fig. 4.2A). In the SDI treatment SWC values decreased for most of the dry period, until the first rainfall events in late summer (DOY 260). Afterwards, SWC

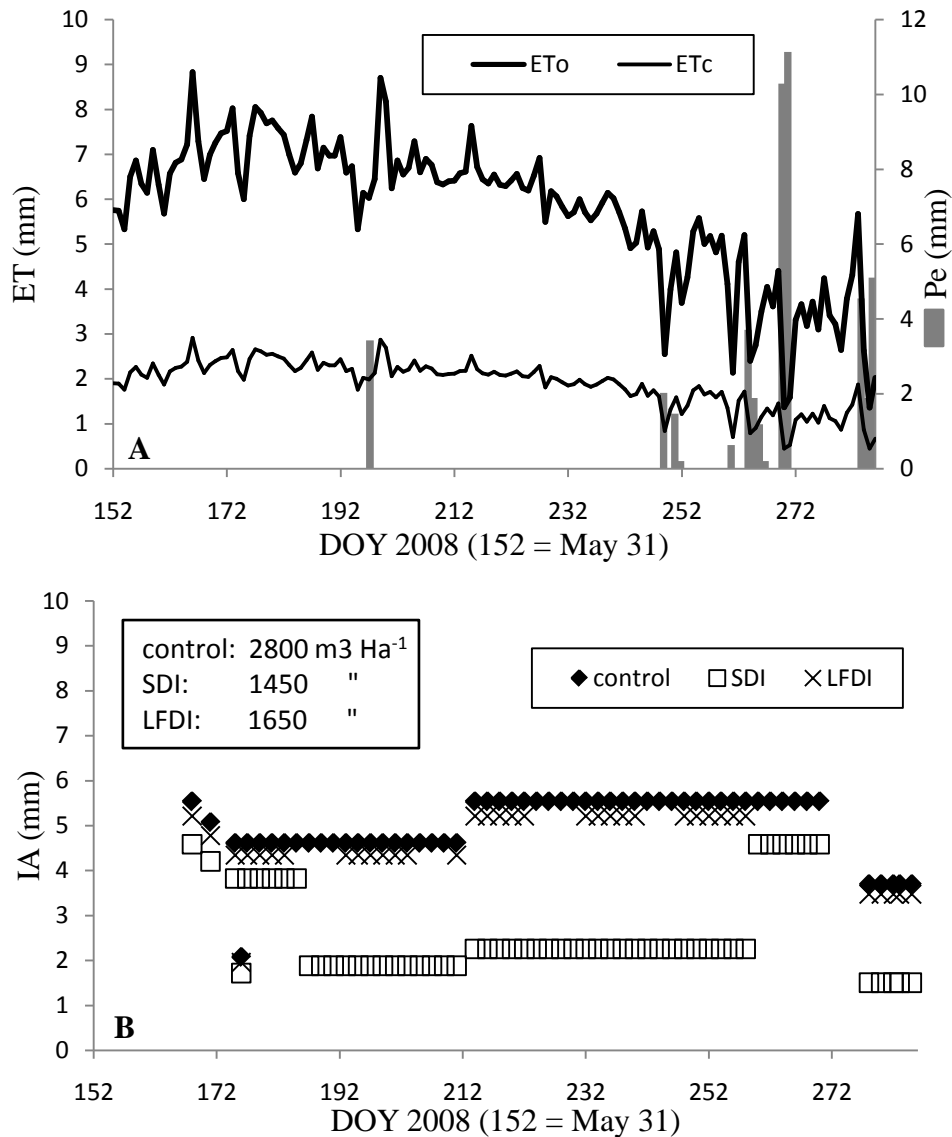


Fig. 4.1. Effective precipitation (P_e), crop (ET_c) and potential (ET_o) evapotranspiration (A), and irrigation amounts (IA) for each treatment (B) during the irrigation season. DOY = day of year.

Table 4.1. Total irrigation amounts (IA) and water savings (WS) as compared to the control for each treatment. The experimental period was from day of year 152 to day of year 286. See text for details on the treatments.

	Treatments		
	Control	SDI	LFDI
IA (mm)	280	145	165
IA (%IN)	111	58	65
WS (mm)	0	135	115

IN = irrigation needs

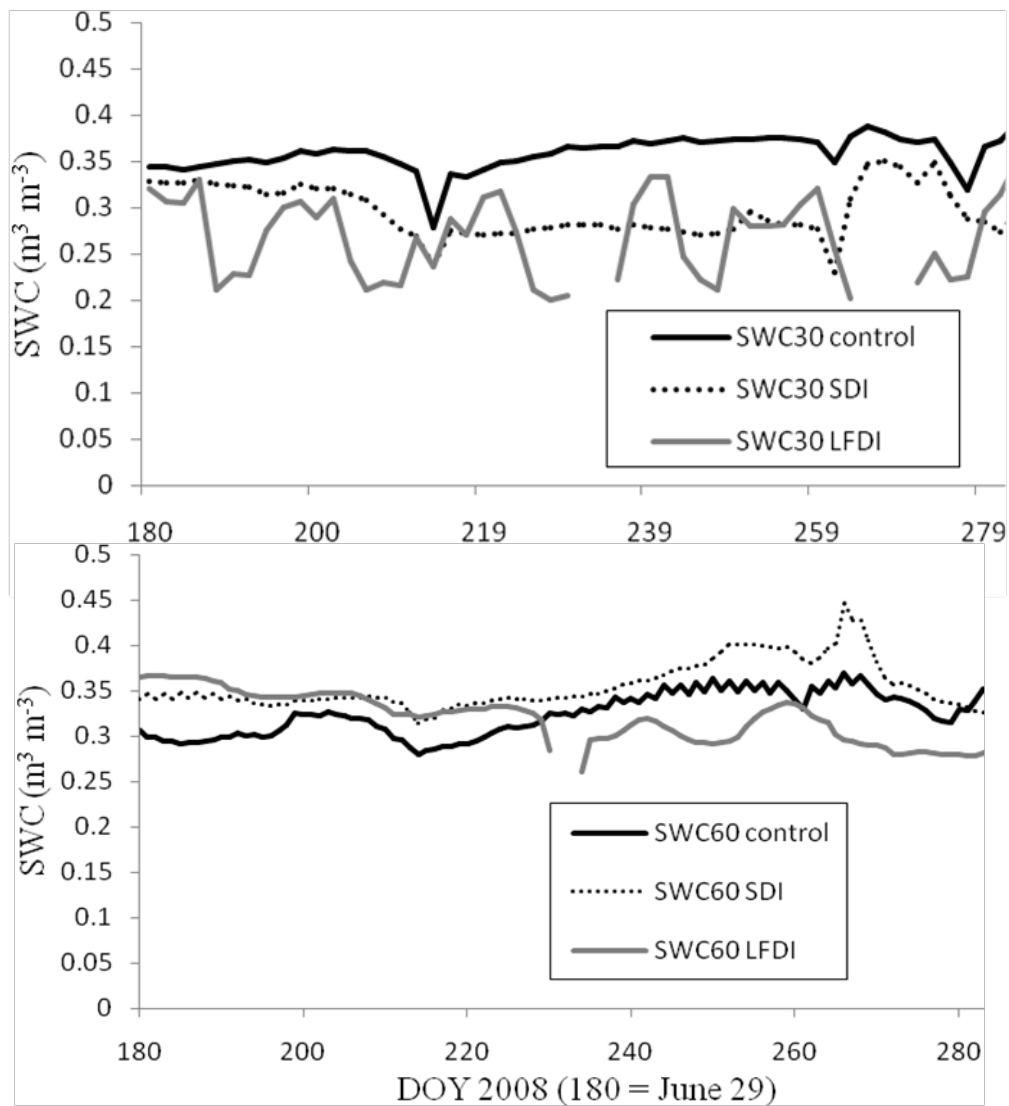


Fig. 4.2. Dynamics of soil water content (SWC) in each treatment at 30 and 60 cm depth. SDI: Sustainable deficit irrigation; LFDI: Low frequency deficit irrigation. DOY = day of year.

increased up to values close to those measured in the control treatment. For the LFDI treatment the SWC values at 30 cm depth fluctuated according to the irrigation events. Thus, the SWC values decreased drastically in the first 48 h after withholding irrigation. At 60 cm depth (Fig. 4.2B), SWC in control and SDI treatments was nearly constant for most of the dry season. Fluctuations also occurred in the LFDI treatment at 60 cm depth, although less markedly than at 30 cm depth. The decreases in SWC at 60 cm were delayed 2-3 days respect to the decreases at 30 cm.

4.3.2. Plant-based measurements

The time courses of the studied physiological variables (Ψ_{stem} , g_s and MDS, Fig. 4.3) were consistent with the IAs applied in each treatment (Fig. 4.1). The g_s values showed a large temporal variability (Fig. 4.3B), likely due to the variability of meteorological conditions.

In the control treatment we recorded values of Ψ_{stem} between -0.7 and -1.3 MPa throughout the studied period (Fig. 4.3A). For the SDI treatment Ψ_{stem} followed a decreasing trend (from -1.2 MPa to -2.0 MPa during the dry period), according to the decreasing available water in the soil of this treatment (Fig. 4.2). The first rainfall events after the dry season, from DOY 262 (Fig. 4.1A), increased SWC in all plots (Fig. 4.2) and the differences between treatments on Ψ_{stem} disappeared (Fig. 4.3). In the LFDI treatment Ψ_{stem} values markedly depended on the withholding&rewatering cycles. For each cycle, Ψ_{stem} values were close to those of the control treatment after the recovery irrigations, showing that these were enough for the LFDI trees to recover from water stress.

For the control trees, the average value of g_s for the dry period (DOY 185-246) was $121 \text{ mmol m}^{-2} \text{ s}^{-1}$ (Fig. 4.3B). The low values of g_s in all the treatments on DOY 258 were probably due to the particularly low solar radiation conditions in this measurement day (data non shown). Values of g_s in the SDI treatment during the dry season were significantly lower than in the control treatment. In this treatment, g_s showed a decreasing trend, from 107 to $34 \text{ mmol m}^{-2} \text{ s}^{-1}$. This agrees with the cumulative stress during that period (Fig. 4.3A). In the LFDI treatment g_s fluctuated, according to the

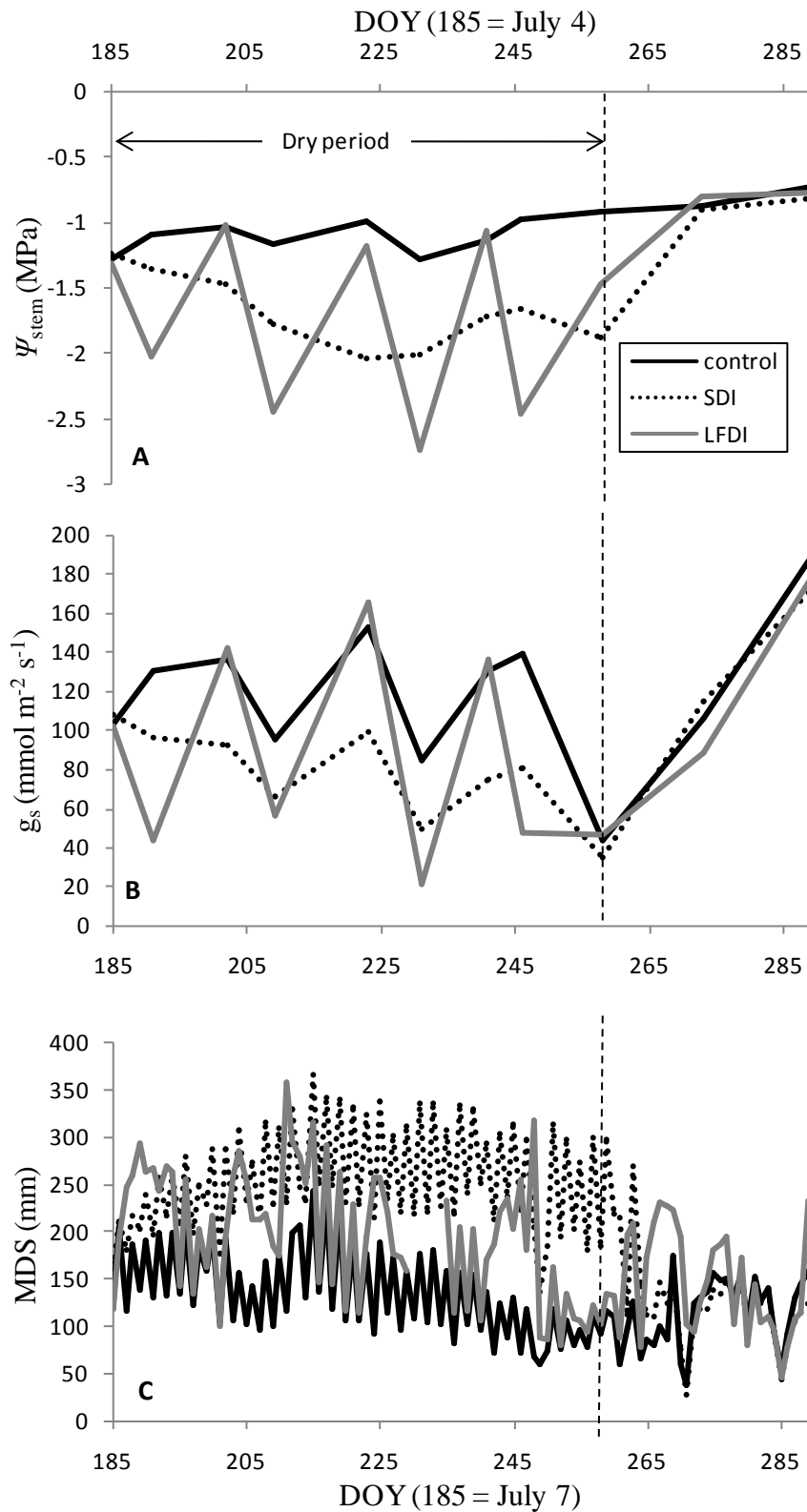


Fig. 4.3. Dynamics for stem water potential (A), stomatal conductance (B) and maximum daily shrinkage (C) in each treatment during the irrigation period. DOY = day of year.

withholding&rewatering cycles, from 166 to 21 mmol m⁻² s⁻¹. As for Ψ_{stem} , differences on g_s between treatments disappeared after the autumn rainfalls.

Values of MDS in the control treatment varied from 100 to 200 μm (Fig. 4.3C) for most of the dry season. The greatest values corresponded to the non-irrigation days. The MDS values in the control decreased, as the ET_o , from early August. In the SDI trees the MDS trend mimicked that of ET_o (Fig. 4.1), and values were usually greater than in the control trees, likely because of the most severe water stress levels reached by the SDI trees. In the LFDI trees the MDS values increased with soil drying between two recovery irrigation periods, and decreased when the trees were irrigated. After the dry season, i.e. after the occurrence of the rainfall events from DOY 262, differences on MDS between treatments disappeared.

The correlation coefficients (r) of the relationships between Ψ_{stem} , g_s , MDS and SWC at 30 cm (SWC30) and 60 cm (SWC60) depth are shown in Table 4.2. The results obtained between MDS and the other parameters were especially significant (Table 4.2). Highest correlation coefficients were obtained between the Ψ_{stem} and the SWC at 30 cm depth ($r = -0.53$), Ψ_{stem} and g_s ($r = 0.75$), and MDS and Ψ_{stem} ($r = -0.63$). This suggests that these parameters (i.e. Ψ_{stem} , g_s , SWC30 and MDS) offer certain information about the crop water status when an irrigation deficit is applied. Nevertheless, the moderate values of the correlation coefficients suggest that no direct relationships should be assumed between these variables. These results show that the relationships between the considered variables should be explained with more complex multiparametric models.

We also measured the maximum stem diameter (MXSD, mm), which showed different seasonal patterns, in each treatment (Fig. 4.4). The dry period coincided with the fruit growth stage. This explains the limited trunk growth showed in Fig. 4.4 for the control trees from DOY 179 to DOY 242. Only at the end of this period, coinciding with the fruit maturity phase, there was a slight increase in trunk diameter. After harvesting, from DOY 268, net trunk growth was negligible. In relation to the SDI treatment, we observed a significant decrease of the MXSD values due to the accumulated water stress of these trees. The MXSD trend in the SDI trees changed with the first rainfall events at

Table 4.2. Correlation coefficients among between the studied parameters.

	MDS	SWC30	SWC60	Ψ_{stem}
MDS				
SWC30	-0.41**			
SWC60	NS	NS		
Ψ_{stem}	-0.63**	-0.53**	NS	
g_s	-0.25*	0.21*	NS	0.75**

MDS: Maximum daily shrinkage; SWC30: soil water content at 30 depth; SWC60: soil water content at 60 of depth; Ψ_{stem} : stem water potential; g_s : stomatal conductance;

NS: no significant; * and ** significant correlations at $P < 0.05$ and $P < 0.01$, respectively.

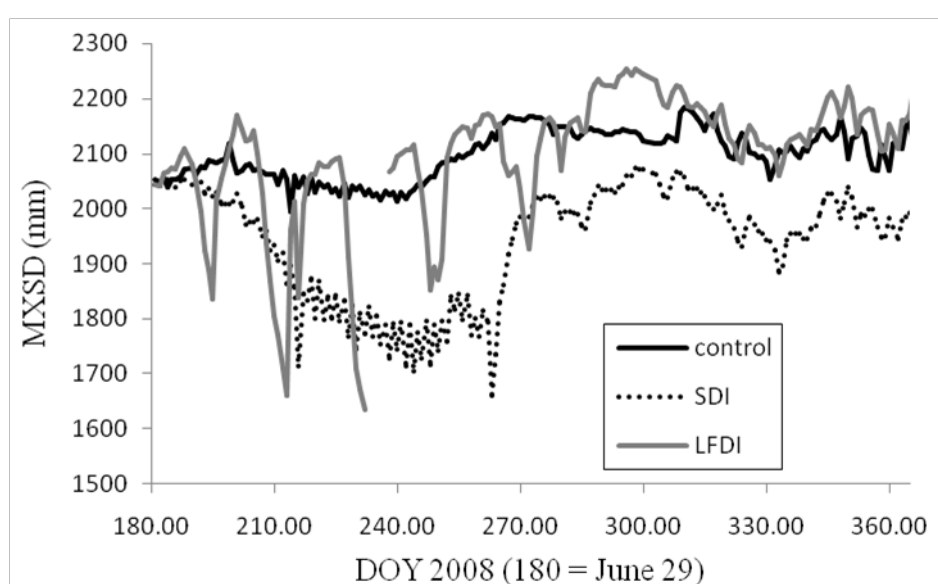


Fig. 4.4. Temporal evolution of the daily maximum stem diameter (MXSD) in each treatment during the studied period. SDI: Sustainable deficit irrigation; LFDI: Low frequency deficit irrigation. DOY = day of year.

the end of the dry period. This increment confirms the recovery of these trees suggested by the Ψ_{stem} and g_s observations (Fig. 4.3). Finally, the MXSD values registered in LFDI trees showed decline and recovery periods according to the irrigation events in this treatment. At the end of the season the LFDI trees showed a net growth similar to that in control trees. Likely, the depletion of SWC together with high atmospheric demand led to negligible growth and progressive dehydration of tissues at the end of the withholding periods, which causes the marked decreases of MXSD recorded in the LFDI trees at the end of the periods in which irrigation was withheld. The comparison of Figs. 4.2, 4.3 and

4.4 suggests that higher correlation coefficients might be obtained with MXSD versus SWC30, Ψ_{stem} and g_s (data not shown) than with MDS.

We also measured the maximum stem diameter (MXSD, mm), which showed different seasonal patterns, in each treatment (Fig. 4.4). The dry period coincided with the fruit growth stage. This explains the limited trunk growth showed in Fig. 4.4 for the control trees from DOY 179 to DOY 242. Only at the end of this period, coinciding with the fruit maturity phase, there was a slight increase in trunk diameter. After harvesting, from DOY 268, net trunk growth was negligible. In relation to the SDI treatment, we observed a significant decrease of the MXSD values due to the accumulated water stress of these trees. The MXSD trend in the SDI trees changed with the first rainfall events at the end of the dry period. This increment confirms the recovery of these trees suggested by the Ψ_{stem} and g_s observations (Fig. 4.3). Finally, the MXSD values registered in LFDI trees showed decline and recovery periods according to the irrigation events in this treatment. At the end of the season the LFDI trees showed a net growth similar to that in control trees. Likely, the depletion of SWC together with high atmospheric demand led to negligible growth and progressive dehydration of tissues at the end of the withholding periods, which causes the marked decreases of MXSD recorded in the LFDI trees at the end of the periods in which irrigation was withheld. The comparison of Figs. 4.2, 4.3 and 4.4 suggests that higher correlation coefficients might be obtained with MXSD *versus* SWC30, Ψ_{stem} and g_s (data not shown) than with MDS.

4.3.3. Yield and fruit quality response

Table 4.3 shows the effects of the water treatments on yield and fruit quality parameters. Yield was lower both in LFDI and SDI than in the control treatment, the decreases being due to both lower fruit weight and reduced number of fruits per tree. Concerning juice content, decreases of 17% in SDI and 10% in LFDI, were recorded, as compared to the control. There were also significant effects on fruit organoleptic properties. Significant increases of total soluble solids and titratable acidity were registered both in the SDI and LFDI treatments. We also observed increases of maturity index in SDI and LFDI, although only in the LFDI treatment the differences were significant.

Table 4.3. Yield and fruit quality parameters.

	Treatments		
	Control	SDI	LFDI
Yield (kg tree ⁻¹)	152.6 ^a	91.4 ^c	124.4 ^b
Fruit weight (g)	264.7 ^a	228.1 ^b	237 ^b
Fruits per tree	577 ^a	495 ^b	497 ^b
Juice weight (%)	47.5 ^a	39.9 ^c	43.5 ^b
TSS (°Brix)	10.3 ^b	12.6 ^a	13.3 ^a
TA (g L ⁻¹)	1.2 ^b	1.5 ^a	1.5 ^a
MI	8.3 ^b	8.8 ^b	9.2 ^a
ED (mm)	79.4 ^a	72.6 ^b	72.7 ^b
PD (mm)	84.6 ^a	80.3 ^b	79.2 ^b
Peel thickness (mm)	6.2 ^a	8.7 ^b	6.4 ^a

SDI: Sustainable deficit irrigation; LFDI: Low frequency deficit irrigation;
TSS: total soluble solids; TA: titratable acidity; MI: maturity index;
ED: equatorial diameter; PD: polar diameter.

Values of WP were 0.03 kg L⁻¹ in LFDI, 0.025 kg L⁻¹ in SDI and 0.024 kg L⁻¹ in control. These results show that greatest WP values did not only depend on the amount of water supplied, but also on the irrigation strategy.

4.4. Discussion

The MDS values observed in the SDI trees and during the withholding periods and in the LFDI treatment along the season were significant higher than in the control trees (Fig. 4.3C). This agrees with the levels of water stress suffered by the trees (Fig. 4.3A). This is in accordance with the results reported by Ortuño (2004a) for young lemon trees and Ginestar (1995) for mandarin trees. These authors concluded that when Ψ_{stem} was higher than -2.5 MPa an increase in MDS was associated with a decrease in Ψ_{stem} . On the other hand, Ortuño *et al.* (2004b), in an experiment with young lemon trees, found differences in MDS values the second day after the IAs were significantly restricted, i.e. soon after the increase in water stress. The water depletion was 25% lower in the deficit irrigation treatment compared with the control treatment.

Steppe *et al.* (2006) reported fluctuations in g_s measured in young orange trees, even with stable atmospheric conditions. The observed fluctuations in g_s were accompanied by lower fluctuations in Ψ_{stem} , as observed in our experiment. Stomatal

oscillations have been observed in several species, including orange trees (Dzikiti *et al.*, 2007; Westhoff *et al.*, 2009; Zimmermann *et al.*, 2010). Zimmermann *et al.* (2010) showed a strong correlation between the frequency (and amplitude) of the oscillations and the wind speed. An increase in wind speed obviously reduces the hydration boundary layer on the leaves and, in turn, increases temporarily local transpiration causing a reduction of turgor pressure in the leaf tissues. This phenomenon may explain the fluctuation of the g_s values we observed in the field (Fig. 4.3B).

Our results show that MDS could be a reliable and sensitive indicator of water stress for a rational control of DI strategies in commercial citrus orchards. Similar findings were obtained in previous experimental works (Ortuño *et al.*, 2006), showing high significant correlations between MDS and Ψ_{stem} ($r = 0.77$) in young lemon tree. The same can be deduced from the review works by Ortuño *et al.* (2010) and Fernández and Cuevas (2010). Our results also suggest that MXSD could also be an advisable indicator of water stress for the DI trees. Other authors have found a better performance on MXSD than MDS as an indicator of water stress in fruit tree orchards. This is the case of Cuevas *et al.* (2010) and Fernández *et al.* (2011) in mature olive trees with heavy crop load.

Regarding g_s , the significant differences between treatments showed in Fig. 4.3B is in accordance with Gomes *et al.* (2004). The authors studied the effects of a LFDI treatment on g_s of orange trees. They reported significant differences on the g_s values of the LFDI trees after seven days without irrigation, as compared with those full irrigated. On the tenth day after rewatering the g_s values of the stressed trees were not significant different from those in the non stressed trees.

Yield was significant lower in the SDI trees than in the control trees, the decreases being due to a reduction in both fruit weight and No. fruits per tree. Several authors have described the agronomic effects of DI, showing important differences among species. Thus, the applications of SDI strategies in vineyards have shown a general increase in yield and, in some instances, also some beneficial effects on fruit ripening (García-Escudero *et al.*, 1991, 1997; Rubio *et al.*, 2004; Yuste *et al.*, 2005; Intrigliolo and Castel, 2008). In apricot trees (Ruiz-Sánchez *et al.*, 2000; Pérez-Pastor *et al.*, 2009) SDI applied throughout the growing season affected productivity and limited vegetative and reproductive growth. In almond trees, Girona *et al.* 2005 considered more interesting a

regulated deficit irrigation (RDI) strategy with a 60% saving of water compared with the control treatment than a SDI treatment receiving 30% less water than control. However, in an experiment made in California, Goldhamer *et al.* (2006) indicated that, for the same level of applied water, yield was less affected under SDI than under RDI. RDI and SDI strategies were applied to apple trees (*Malus domestica* L.) in a trial in Lleida with DI (50% of the control) applied during the last stage of fruit growth and FI the rest of the growing season (Girona *et al.*, 2009). During the three year period, RDI did not reduce fruit size or yield, while SDI during the whole year drastically reduced fruit size. In the same way, Moriana *et al.* (2003) compared the yield response of mature olive trees (cv. Picual) growing in Cordoba, south Spain, under SDI (75% ET_c) and RDI (75% ET_c except in midsummer period when no irrigation was applied) with a control (100% ET_c). The results illustrated that the average reductions in crop evapotranspiration and yield in both DI strategies with respect to the control were similar. Although the plant water status in the SDI trees was better than in the RDI trees, the difference was not sufficient to recommend one of the two strategies as the other since the yield was the same and SDI used greater amount of water. Iniesta *et al.* (2009) tested the same treatments (FI, SDI and RDI) in an olive orchard (cv. Arbequina) in Cordoba by. In both DI treatments IAs amounted to 25% of the control. The results from 2004 to 2006 showed that a reduction of seasonal irrigation application of around 75% caused a decrease in seasonal ET (30-35%) and in radiation use efficiency, leading to moderate ($\approx 15\%$) reductions in oil yield. The water use efficiency (WUE) for oil production in SDI and RDI was higher than in FI, and the oil yield was similar in both deficit treatments. Therefore, both irrigation strategies were recommended for olive orchards, to reduce IA with moderate reductions in oil yield.

In our LFDI treatment both, fruit size and fruit number, were lower than in the control treatment. We compared these results with those obtained by Hutton *et al.* (2007). Hutton *et al.* reduced irrigation in Valencia orange trees (*Citrus sinensis* L. Osbeck on *Poncirus trifoliata* L. Raf. rootstock) by up to 33% relative to a FI treatment by extending the intervals between applications from 3 to 17 days during fruit growth stages II and III. The development of more vegetative shoot growth by trees growing under increasing water deficit (longer irrigation interval) in late summer increased the number of potential fruiting sites for flowering in the following season and this was seen in the increase in

fruit per tree recorded for trees grown under longer irrigation intervals. However, the increased crop load (number of fruits per tree) and periodic water stress during fruit growth stage II contributed to the smaller fruit size recorded in trees irrigated at the longer intervals. Consequently, the increased fruit numbers did not result in significant increases in fruit mass per tree. Yield differences (kg tree^{-1}) between years were much greater than between irrigation treatments. The apparent discrepancies with our results might probably due to a lower stress of the trees in the Hutton *et al.* experiment, since they observed higher values of Ψ_{stem} (up to -2.3 MPa) than those we measured in the LFDI trees (up to -2.7 MPa).

In the SDI and LFDI treatments irrigation was reduced respect to control trees during both, the flowering and the fruit growth periods. This explains the reductions of both the number of fruits per tree and the fruit size. It is well known that the yield response of citrus trees to water stress strongly depends on the phenological stage of the crop, being growth and flowering the most critical periods for water stress (Ginestar and Castel, 1996). This explains that reductions in IA during the flowering period promoted a decrease in the fruit number, due to problems related to the fruit setting process (Castel and Buj, 1990; Pérez *et al.*, 2008a, 2008b). In relation to the growth period, an applied water stress during this stage caused a considerable reduction in fruit size (Velez *et al.*, 2007; Treeby *et al.*, 2007).

According to González-Altozano and Castel (1999), values for Ψ_{stem} must exceed the threshold of -1.3 MPa to exert a significant effect on final crop production. In our experiments, trees grown under SDI and LFDI treatments showed Ψ_{stem} values lower than this threshold. Ginestar and Castel (1996) also observed important differences in yield in a treatment in which the available water was 50% of the crop water needs during any period of the year.

The increases of total soluble solids, acidity and titratable maturity index in the SDI and LFI treatments is also in agreement with findings by other authors testing DI strategies in citrus trees (González-Altozano and Castel 1999; Hutton *et al.*, 2007; Yakushiji *et al.*, 1998).

4.5. Conclusions

Significant water savings can be achieved in commercial citrus orchards under DI irrigation, with a reduced impact in yield and fruit quality. In our case, water savings amounted to 41% for the LFDI treatment, as compared to the fully irrigated control treatment. The reduction in yield was 18% only, and the quality parameters TSS, TA and MI improved. In the SDI treatment, water savings were slightly higher than in the LFDI treatment (48%), but yield reduction was substantially higher (40% reduction). Dendrometric sensors offer continuous monitoring and automatic data recording and transfer, and their sensitivity and robustness are appropriate for the control of precise irrigation in commercial citrus orchards. For these reasons, the MDS and MXSD indices seems to be an advantageous alternative to stem water status monitoring, for the assessment of tree water stress.

4.6. References

- Allen RG, Pereira LS, Raes D, Smith M. 1998. Crop evapotranspiration-Guidelines for computing crop water requirements-FAO Irrigation and drainage paper 56. FAO, Rome 300:6541.
- Araus J. 2004. The problems of sustainable water use in the Mediterranean and research requirements for agriculture. *Annals of Applied Biology* 144(3):259-272.
- Castel J, Buj A. 1990. Response of Salustiana oranges to high frequency deficit irrigation. *Irrigation Science* 11(2):121-127.
- Conejero W, Alarcón J, García-Orellana Y, Abrisqueta J, Torrecillas A. 2007. Daily sap flow and maximum daily trunk shrinkage measurements for diagnosing water stress in early maturing peach trees during the post-harvest period. *Tree Physiology* 27(1):81.
- Cuevas MV, Torres-Ruiz JM, Álvarez R, Jiménez MD, Cuerva J, Fernández JE. 2010. Assessment of trunk diameter variation derived indices as water stress indicators in mature olive trees. *Agric Water Manage* 97(9):1293-1302.

- Dzikiti S, Steppe K, Lemeur R, Milford J. 2007. Whole-tree level water balance and its implications on stomatal oscillations in orange trees [*Citrus sinensis* (L.) Osbeck] under natural climatic conditions. *Journal of Experimental Botany* 58(7):1893.
- FAO. 1998. World Reference Base for Soil Resources. Rome: Food and Agriculture Organization of the United Nations.
- Fereres E, Castel JR. 1981. Drip Irrigation Management. Division of Agricultural Sciences. University of California. Leaflet N° 21259. 2, 11-24.
- Fereres E, Soriano MA. 2007. Deficit irrigation for reducing agricultural water use. *Journal of Experimental Botany* 58(2):147-159.
- Fernández JE, Cuevas MV. 2010. Irrigation scheduling from stem diameter variations: A review. *Agricultural and Forest Meteorology* 150(2):135-151.
- Fernández JE, Torres-Ruiz JM, Díaz-Espejo A, Montero A, Álvarez R, Jiménez MD, Cuerva J, Cuevas MV. 2011. Use of maximum trunk diameter measurements to detect water stress in mature 'Arbequina' olive trees under deficit irrigation. *Agric Water Manage* 98(12):1813-1821.
- Fernández-Gómez R, Avila-Alabarces, R., López-Rodríguez, M., Gavilán-Zafra, P. Oyonarte-Gutierrez, N.A. 1999 Manual de Riego para Agricultores. Fundamentos del riego (módulo 1). Ed Consejería de Agricultura y Pesca, Junta de Andalucía.
- García-Escudero E, López R, Santamaría P, Zaballa O. 1997. Ensayos de riego localizado en viñedos productivos de cv "Tempranillo". *Vitic Enol Profes* 50:35-47.
- García-Escudero E, Santamaría P, López R, Palacios L. 1991. Aplicación de dosis moderadas de agua en el proceso de maduración del cv Tempranillo en Rioja. *Vitivinicultura* 2(1):30-34.
- García-Tejero I, Jiménez JA, Muriel JL, Martínez G. 2007. Planificación y desarrollo de estrategias de riego deficitario en una plantación de naranjos: influencia de la variabilidad espacial de las propiedades del suelo. Book of Abstracts XXV Congreso Nacional de Riegos. Pamplona. Spain. p 63.

- García-Tejero I, Jiménez JA, Reyes MC, Carmona A, Pérez R, Muriel JL. 2008. Aplicación de caudales limitados de agua en plantaciones de cítricos del valle del Guadalquivir. *Fruticultura Profesional* 173:5-17.
- Ginestar C. 1995. Efectos del estrés hídrico en distintos períodos fenológicos en plantaciones de cítricos jóvenes regadas por goteo: Doctoral thesis. Universidad Politécnica de Valencia, Spain. 183 p.
- Ginestar C, Castel JR. 1996. Responses of young clementine citrus trees to water stress during different phenological periods. *Journal of Horticultural Science* 71(4):551-559.
- Girona J, DCJ, Bonastre N., Paris C., Mata M., Arbonés A., Marsal J. 2009. Evaluation of different irrigation strategies on apple (*Malus domestica*). Physiological and productive results. Viña del Mar, Chile. Proc VI International Symposium on Irrigation of Horticultural Crops. p 54.
- Girona J, Mata M, Marsal J. 2005. Regulated deficit irrigation during the kernel-filling period and optimal irrigation rates in almond. *Agric Water Manage* 75(2):152-167.
- Goldhamer DA, Viveros M, Salinas M. 2006. Regulated deficit irrigation in almonds: effects of variations in applied water and stress timing on yield and yield components. *Irrigation Science* 24(2):101-114.
- Gomes MMA, Lagôa AMMA, Medina CL, Machado EC, Machado MA. 2004. Interactions between leaf water potential, stomatal conductance and abscisic acid content of orange trees submitted to drought stress. *Brazilian Journal of Plant Physiology* 16(3):155-161.
- Gonzalez-Altozano P, Castel JR. 1999. Effects of regulated deficit irrigation on 'Clementina de Nules' citrus trees I. Yield and fruit quality effect. *J Am Soc Hort Sci* 74:749-758.
- Gonzalez-Altozano P, Castel JR. 2000. Effects of regulated deficit irrigation on 'Clementina de Nules' citrus trees II. Vegetative growth. *J Am Soc Hort Sci* 75:388-392.

-
- Hoppula KI, Salo TJ. 2007. Tensiometer-based irrigation scheduling in perennial strawberry cultivation. *Irrigation Science* 25(4):401-409.
- Hutton R, Landsberg J, Sutton B. 2007. Timing irrigation to suit citrus phenology: a means of reducing water use without compromising fruit yield and quality? *Australian Journal of Experimental Agriculture* 47(1):71-80.
- Iniesta F, Testi L, Orgaz F, Villalobos F. 2009. The effects of regulated and continuous deficit irrigation on the water use, growth and yield of olive trees. *European Journal of Agronomy* 30(4):258-265.
- Intrigliolo DS, Castel JR. 2008. Effects of irrigation on the performance of grapevine cv. Tempranillo in Requena, Spain. *American Journal of Enology and Viticulture* 59(1):30.
- Li S, Huguet J, Schoch P, Orlando P. 1989. Response of peach tree growth and cropping to soil water deficit at various phenological stages of fruit development. *J Hort Sci* 64(5):541-552.
- Moriana A, Girón IF, Martín-Palomo MJ, Conejero W, Ortuño MF, Torrecillas A, Moreno F. 2010. New approach for olive trees irrigation scheduling using trunk diameter sensors. *Agric Water Manage* 97(11):1822-1828.
- Moriana A, Orgaz F, Pastor M, Fereres E. 2003. Yield responses of a mature olive orchard to water deficits. *Journal of the American Society for Horticultural Science* 128(3):425-431.
- Muriel J, Jiménez J, García I, Vaquero I. 2006. Relaciones hídricas en una plantación de naranjos (*Citrus sinensis*, L. cv Navelino) bajo estrategias de riego deficitario mantenido. VIII Simposium Hispano Portugués de Relaciones Hídricas en las Plantas: 17–21.
- Ortuño MF. 2004. Medidas de flujo de savia y variaciones micrométricas del tronco como indicadores del estado hídrico del limonero: Doctoral thesis. Universidad de Murcia. Spain. 289 p.

- Ortuño MF, Alarcón J, Nicolás E, Torrecillas A. 2004. Comparison of continuously recorded plant-based water stress indicators for young lemon trees. *Plant and Soil* 267(1):263-270.
- Ortuño MF, Brito JJ, García-Orellana Y, Conejero W, Torrecillas A. 2009. Maximum daily trunk shrinkage and stem water potential reference equations for irrigation scheduling of lemon trees. *Irrigation Science* 27(2):121-127.
- Ortuño MF, Conejero W, Moreno F, Moriana A, Intrigliolo DS, Biel C, Mellisho CD, Pérez-Pastor A, Domingo R, Ruiz-Sánchez MC. 2010. Could trunk diameter sensors be used in woody crops for irrigation scheduling? A review of current knowledge and future perspectives. *Agric Water Manage* 97(1):1-11.
- Ortuño MF, García-Orellana Y, Conejero W, Ruiz-Sánchez MC, Alarcón JJ, Torrecillas A. 2006. Stem and leaf water potentials, gas exchange, sap flow, and trunk diameter fluctuations for detecting water stress in lemon trees. *Trees-Structure and Function* 20(1):1-8.
- Pérez-Pastor A, Domingo R, Torrecillas A, Ruiz-Sánchez MC. 2009. Response of apricot trees to deficit irrigation strategies. *Irrigation Science* 27(3):231-242.
- Pérez-Pérez J, Romero P, Navarro J, Botía P. 2008a. Response of sweet orange cv 'Lane late' to deficit irrigation in two rootstocks. I: water relations, leaf gas exchange and vegetative growth. *Irrigation Science* 26(5):415-425.
- Pérez-Pérez J, Romero P, Navarro J, Botía P. 2008b. Response of sweet orange cv 'Lane late' to deficit-irrigation strategy in two rootstocks. II: Flowering, fruit growth, yield and fruit quality. *Irrigation Science* 26(6):519-529.
- Pérez-Pérez J, Robles J, Botía P. 2009. Influence of deficit irrigation in phase III of fruit growth on fruit quality in 'lane late' sweet orange. *Agric Water Manage* 96(6):969-974.
- Romero P, Navarro J, Pérez-Pérez J, García-Sánchez F, Gómez-Gómez A, Porrás I, Martínez V, Botía P. 2006. Deficit irrigation and rootstock: their effects on water relations, vegetative development, yield, fruit quality and mineral nutrition of *Clemenules mandarin*. *Tree Physiology* 26(12):1537.

-
- Rubio J, Albuquerque MV, Yuste J. 2004. Influence of water stress and crop load on the physiology and the productivity of Tempranillo under semiarid conditions. *Acta Hort (ISHS)* 640:99-106.
- Ruiz-Sánchez MC, Domingo Miguel R, Castel Sánchez JR. 2010. Review. Deficit irrigation in fruit trees and vines in Spain. *Plant Soil* 120:299-302.
- Ruiz-Sánchez MC, Torrecillas, A., Pérez-Pastor, A. and Domingo, R. 2000. Regulated deficit irrigation in apricot trees. *Acta Horticulturae* 537:759-766.
- Scholander PF, Bradstreet ED, Hemmingsen E, Hammel H. 1965. Sap pressure in vascular plants. *Science* 148(3668):339.
- Seckler DW. 1996. The new era of water resources management: from "dry" to "wet" water savings: *Issues in Agriculture* No. 8 CGIAR. 17 p.
- Steppe K, Dzikiti S, Lemeur R, Milford JR. 2006. Stomatal oscillations in orange trees under natural climatic conditions. *Annals of botany* 97(5):831.
- Treeby MT, Henriod RE, Bevington KB, Milne DJ, Storey R. 2007. Irrigation management and rootstock effects on navel orange *Citrus sinensis* (L.) Osbeck fruit quality. *Agric Water Manage* 91(1-3):24-32.
- Turner NC. 1988. Measurement of plant water status by the pressure chamber technique. *Irrigation Science* 9(4):289-308.
- Velez J, Intrigliolo D, Castel J. 2007. Scheduling deficit irrigation of citrus trees with maximum daily trunk shrinkage. *Agric Water Manage* 90(3):197-204.
- Westhoff M, Reuss R, Zimmermann D, Netzer Y, Gessner A, Geßner P, Zimmermann G, Wegner L, Bamberg E, Schwartz A. 2009. A non invasive probe for online monitoring of turgor pressure changes under field conditions. *Plant Biology* 11(5):701-712.
- Yakushiji H, Morinaga K, Nonami H. 1998. Sugar accumulation and partitioning in Satsuma mandarin tree tissues and fruit in response to drought stress. *American Society for Horticultural Science (USA)* 123:719-726.

Yuste J, Asenjo J, Albuquerque M, Rubio J. 2005. Relationships among Physiology, Growth and Production as Affected by Water Regime and Vine Spacing of 'Tempranillo' Grapevines. *Acta Horticulturae* 689:343-348.

Zimmermann U, Rüger S, Shapira O, Westhoff M, Wegner L, Reuss R, Gessner P, Zimmermann G, Israeli Y, Zhou A. 2010. Effects of environmental parameters and irrigation on the turgor pressure of banana plants measured using the non invasive, online monitoring leaf patch clamp pressure probe. *Plant Biology* 12(3):424-436.

Chapter 5

An automatic irrigation controller for fruit tree orchards, based on sap flow measurements

Part of this chapter is published in:

Fernández JE, Romero R, Díaz-Espejo A, Cuevas MV, Muriel JL, Montaña JC. 2008. A device for Scheduling irrigation in fruit tree orchards from sap flow readings. *Acta Horticulturae*, 792: 283-290.

Fernández JE, Romero R, Díaz-Espejo A, Muriel JL, Cuevas MV, Montaña JC. 2008. Design and testing of an automatic irrigation controller for fruit tree orchards based on sap flow measurements. *Australian Journal of Agricultural Research* 59, 589–598.

Abstract. We designed and tested an automatic irrigation control system for fruit tree orchards, denominated CRP. At the end of each day, the device calculates the irrigation dose (ID) from sap flow readings in the trunk of trees irrigated to replenish the crop water needs, relative to similar measurements made in overirrigated trees. It then acts on the pump and electrovalve to supply an ID enough to maintain the soil close to its field capacity during the irrigation period. Remote control of the system is possible from any computer or smartphone connected to the Internet. We tested the CRP in an olive orchard in southern Spain. The device was robust and able to filter and amplify the output voltages of the heat-pulse velocity probes and to calculate reliable sap flow data. It calculated and supplied daily irrigation amounts to the orchard according to the specified irrigation protocol. The remote control facility showed to be useful for getting real-time information both on the CRP behaviour and the applied IDs, and for changing parameters of the irrigation protocol. For our conditions, olive trees with big root systems growing in a soil with a remarkable water-holding capacity, the approach mentioned above for calculating ID had not enough resolution to replace the daily crop water consumption. The device, however, was able to react when the soil water content fell below the threshold for soil water deficit. The threshold value was identified with simultaneous measurements of stem water potential in the instrumented trees. Our results suggest a change in the irrigation

protocol that will allow the CRP to apply a recovery irrigation whenever that threshold is reached, making the device suitable for applying a deficit irrigation strategy in the orchard.

5.1. Introduction

Demands from other water-user sectors, apart from agriculture, are increasing pressure to improve irrigation practices (Feres and Evans, 2006). As a response, new approaches and technologies to optimise irrigation scheduling are being developed. Those based on monitoring a key variable in the plant have the potential advantage of integrating, in a single measurement, not only the plant's response to the prevailing soil and atmospheric water conditions, but also the effect of the plant's physiological mechanisms controlling water use. Thus, canopy temperature, water content in the trunk, trunk diameter variations, and sap flow readings are currently considered promising plant-based variables for irrigation control (Feres *et al.*, 2003; Jones, 2004). An additional advantage of these variables for irrigation scheduling is that they can be automated.

Infrared thermometry has been used since the sixties, both to monitor plant stress and to provide useful information for irrigation control (Jackson, 1982; Hatfield, 1983). Recent improvements have increased the potential of the technique as a tool for irrigation scheduling (Jones, 1999; Alves and Pereira, 2000; Lobo *et al.*, 2004). However, the use of this technique in fruit tree orchards has to overcome the difficulty of the high variability induced by the canopies' covering just part of the orchard floor. Monitoring water content changes in the stem of some species by automatable techniques, such as time-domain reflectometry (TDR), has long been used for detecting the onset of water stress (Constant and Murphy, 1990; Holbrook and Sinclair, 1992). It seems, however, that simpler and less expensive sensors are required before farmers adopt this approach for irrigation control (Nadler *et al.*, 2006).

Extensive research has been carried out recently to improve irrigation control based on trunk diameter variations and sap flow in the trunk. Continuous monitoring of trunk diameter by linear variable displacement transducers (LVDT sensors) for assessing tree's response to irrigation water deficits has been studied in a variety of fruit tree species. In olive, the technique has been evaluated by Moriana and Feres (2002) and Moreno *et al.* (2006). An example of irrigation control based on the use of LVDT sensors

in almond trees was published by Goldhamer and Fereres (2004). Recently, García-Orellana *et al.* (2007) have evaluated the feasibility of scheduling irrigation of lemon trees from the maximum daily trunk shrinkage. Sap flow readings are being widely used to determine both water consumption and the dynamics of transpiration and water uptake by main roots. Among the different sap flow methods, the compensation heat-pulse (CHP) method has been used in various fruit tree species, including kiwifruit (Green *et al.*, 1989), apple (Green *et al.*, 1989, 2003), pear (Caspari *et al.*, 1993), apricot (Alarcon *et al.*, 2000, 2003; Nicolás *et al.*, 2005), lemon (Ortuño *et al.*, 2004), and olive (Moreno *et al.*, 1996; Fernández *et al.*, 2001, 2003, 2006a,b; Giorio and Giorio, 2003; Williams *et al.* 2004). Comparisons between sap flow and trunk diameter readings as water stress indicators in fruit trees, and between these two variables and more-traditional water-stress indicators such as leaf- or stem-water potential and stomatal conductance, have been carried out by Ortuño *et al.* (2004, 2005, 2006a, b), Conejero *et al.* (2007) and Intrigliolo and Castel (2006a, b), among others. These papers outline the high potential of the two variables.

Most of the irrigation controllers available on the market require the irrigation dose (ID) to be provided by the user. Only then are they able to switch the irrigation pump on and off and to open and close electrovalves to apply the input ID to each sector of the orchard. In this work, we consider an automatic irrigation controller (AIC) to be a device able to calculate ID by itself, based on one or several recorded variables, and to act on the irrigation system so that the calculated ID is supplied to the crop. These processes must be carried out automatically. Very few AICs have been developed so far. Most of them are based on soil matric potential measurements (Luthra *et al.*, 1997; Klein, 2004; Miranda *et al.*, 2005). These are relatively inexpensive, user-friendly devices, but soil moisture monitoring implies certain limitations: a high number of sensors may be required to cope with the spatial variability within the orchard, and they do not take plant performance into account. To our knowledge, an AIC based on either LVDT or sap flow readings has not yet been developed, although irrigation protocols based on both approaches have been suggested (Fernández *et al.*, 2001; Goldhamer and Fereres, 2004; García-Orellana *et al.*, 2007). The ‘Pepista’ system (Pelloux *et al.*, 1990) uses trunk diameter variations to control irrigation, but it requires criteria for data interpretation.

Nadezhdina and Cermak (1997) reported an AIC based on what they call *sap flow index* (see Nadezhdina, 1999, for details), but a commercial version was not released.

The aim of the present work was to design and build an AIC for fruit tree orchards, based on sap flow measurements in the trunk of representative trees, and to test the performance of the device after installing it in an olive orchard, both for amplifying and filtering output signals from the thermocouples of the sap flow sensors and for calculating the ID according to the specified irrigation protocol. Water status, both in the instrumented trees and soil, was monitored throughout the field test, and results compared with the calculated IDs.

5.2. Materials and methods

5.2.1. Irrigation controller

We named the AIC developed in this work CRP, the Spanish acronym for *crop irrigation controller*. The CRP has been designed to adjust the ID daily to maintain the soil around field capacity. The ID values are automatically calculated from sap flow readings in the trunk of trees irrigated to supply the crop water needs, denominated normally irrigated (NI) trees, relative to similar measurements made in overirrigated (OI) trees, used as reference trees. The CRP was built in our laboratory during 2005, and tested in an olive orchard in 2006, as described below.

The CRP has three main physical components:

a) The measurement unit (MU). This part of the CRP is installed in the orchard, and records sap flow in one NI and one OI tree. The MU uses the heat-pulse velocity (HPV) system of Green (1998) for sap flow readings. This system employs the CHP method. The CRP tested here had three MUs, each with three sets of HPV probes (Tranzflo NZ Ltd, Palmerston North, New Zealand) per tree. These, together with the corresponding heat-pulse controllers and the power supply system, were the only components of the CRP not designed in our laboratory. The main characteristics of the HPV probes are described in Green *et al.* (2003). Each set of probes has two temperature probes, inserted at $x'=5$ mm upstream and $x=10$ mm downstream of the heater. Each temperature probe consists of four thermocouples, at 5, 12, 22, and 35 mm below the

cambium. Heat pulses were fired for 1 s every 30 min throughout the testing period. After each heat pulse, output signals from each HPV probe are amplified and filtered to derive t_z values, the time intervals for the coincidence of temperatures at points x' and x (see appendixes 5.A1 and 5.A2). The four t_z values from each set of probes are stored in an EEPROM.

b) The control unit (CU). This is a standard PC located close to the head of the irrigation system, wired to each of the three MUs, using RS485 communication protocol. This allows up to 32 devices to communicate at half-duplex on a single pair of wires at distances up to 1200 m, more than enough for our experimental set-up. For operating, the CU runs the software described in the appendix 5.A3. Every night, at 23:45 hours, the CU gets the t_z values measured by each MU that day. After saving these values, the CU uses them to calculate the sap flow values (Q , L hour⁻¹) for each HPV probe set and time of measurement. The Q values are saved, and then used to calculate the total tree transpiration for the day (E_p , L day⁻¹). The CU then computes the ID for the next day as described below, and sends this value to the pump & electrovalve controller.

c) The pump & electrovalve controller (PEC). This device, also located close to the head of the irrigation system, is wired to the CU, from which it receives the calculated ID. The role of the PEC is to switch the irrigation pump on and off, and to open and close the electrovalve of the irrigation sector for a time sufficiently long to supply the ID. In addition, the PEC reads pulses from a flow meter installed after the electrovalve, enabling the system to control the supply of water either by volume or by time (software details in appendix 5.A4).

Fig. 5.1 shows the tasks carried out by each of the main components of the CRP. The number of MUs and electrovalves controlled can be customised depending on orchard requirements. The number of HPV probe sets per tree, the depth of the thermocouples within each probe, and other parameters related to sap flow monitoring, can also be changed.

We used a remote desktop of Windows XP to access the CU via the Internet from home or office, for remote control of the CRP functions, including parameter changing and program debugging.

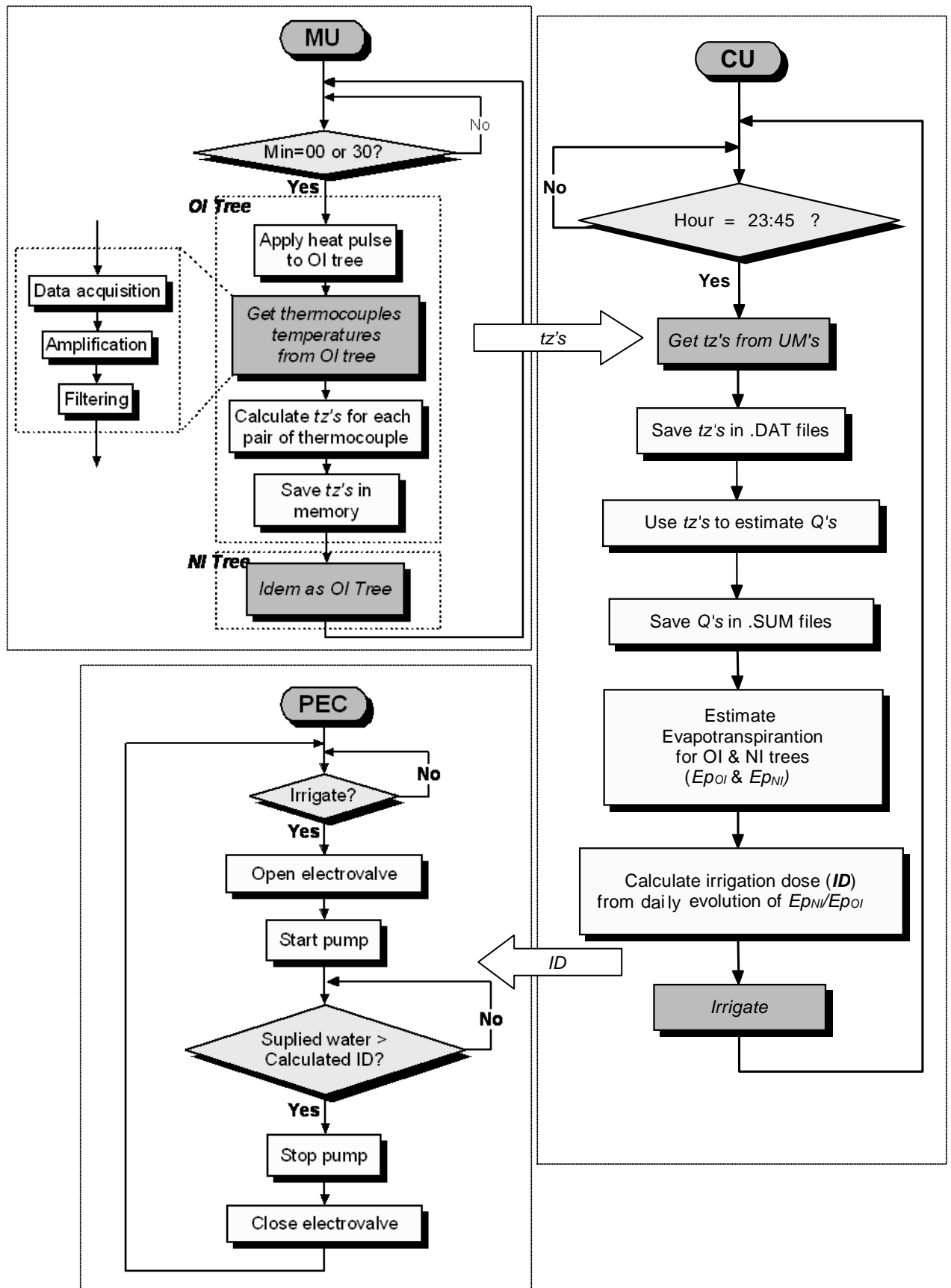


Fig. 5.1. Flow diagram showing the tasks of the three main physical components of the CRP: the measuring unit (MU), the control unit (CU), and the pump & electrovalve controller (PEC). See text for details.

The irrigation protocol was as follows: the soil in the orchard must be around field capacity on the first two days of the irrigation period. On these two days, the CRP does not calculate the ID; instead, its value is defined by the user. At 23:45 hours on the first day of the irrigation period, the CU collects the t_z values from each MU and calculates E_p of that day, for each NI tree (E_{pNI}) and each OI tree (E_{pOI}). The CU then calculates the transpiration ratio between the two types of tree (E_{pNI}/E_{pOI}). The following day, the CU does the same, and compares the resulting value with the one calculated on the previous day. From this comparison, the CU automatically adjusts the ID for the next day (the third of the irrigation period): if $(E_{pNI}/E_{pOI})_{DOY} \cong (E_{pNI}/E_{pOI})_{DOY-1}$ (where DOY denotes ‘day-of-year’), the ID applied on the current day could have been either enough to cover the water needs of the NI trees or too high. Accordingly, the ID of the next day is reduced. If $(E_{pNI}/E_{pOI})_{DOY} \neq (E_{pNI}/E_{pOI})_{DOY-1}$, the CU assumes the ID applied on the current day was not enough to cover the demand of the NI trees, and increases the ID for the next day. This procedure is repeated each day of the irrigation period, with the following rules:

1) If the transpiration ratios of two consecutive days are considered different, that is, $|(E_{pNI}/E_{pOI})_{DOY-1} - (E_{pNI}/E_{pOI})_{DOY}| > 0.05(E_{pNI}/E_{pOI})_{DOY-1}$; then the CU increases the ID by 10% on the next day, and by 20% on the following days.

2) If $|(E_{pNI}/E_{pOI})_{DOY-1} - (E_{pNI}/E_{pOI})_{DOY}| \leq 0.05(E_{pNI}/E_{pOI})_{DOY-1}$, then the CU reduces the ID by 10% on the first day, and by 20% on the following days.

5.2.2. Field trial

We tested the CRP in an olive orchard (*Olea europaea* cv. ‘Manzanilla de Sevilla’) of *La Hampa*, an experimental farm of the Spanish Research Council (CSIC) close to Seville, Spain (37° 17’ N, 6° 3’ W, elevation 30 m). The trees, planted at 7 m x 5 m, were 38 years old. The soil is a sandy loam (Xerochrept) with a depth of about 2 m. The soil texture is quite homogeneous, with average values of 73.5% coarse sand, 4.7% fine sand, 14.8% clay, and 7.0% silt. Laboratory measurements showed that the volumetric soil water content (θ_v , $m^3 m^{-3}$) for -0.1 and -1.5 MPa soil matric potential was $0.33 m^3 m^{-3}$ and $0.10 m^3 m^{-3}$, respectively. Field measurements, however, showed that θ_v values close to the emitters a few hours after irrigation were rarely greater than $0.26 m^3 m^{-3}$.

We selected a plot with four rows each of eight trees for irrigation with the CRP. In March 2006, we installed the three MUs in the plot, at about 50, 75, and 100 m from the CU, located in the shed at the head of the irrigation system, next to the plot. The instrumented trees were representative of those in the plot, with an average canopy volume of 37 m^3 and a leaf area density (LAD) of about $1.6 \text{ m}^2 \text{ m}^{-3}$ at the end of the growing season. Each MU was powered by a 12 V, 216 Ah battery fed with a solar panel. For irrigating the NI trees, i.e. all trees in the plot except the three OI trees, we installed an irrigation system consisting of a single pipe per row, with five 3 L h^{-1} drippers per tree, 1 m apart. As explained above, ID_{NI} was calculated daily by the CU, except for the first two days of the irrigation period, which began on May 8, day-of-year (DOY) 128.

The OI trees were irrigated to 130% of the crop evapotranspiration (ET_c , mm), with an irrigation system similar to that described for the NI trees, but with drippers of 6 L h^{-1} discharge rate. We calculated ET_c with the crop coefficient approach recommended by the FAO (Allen *et al.*, 1998). Data for calculating the potential evapotranspiration (ET_o , mm) were collected with an automatic weather station located next to the orchard. For both the crop coefficient (K_c) and the coefficient related to the percentage of ground covered by the crop (K_r), we used the values recommended by Fernández *et al.*, (2006b) (K_c values were 0.76 in May, 0.70 in June, 0.63 in July and August, and 0.72 in September; K_r was 0.7). Values of ET_c were calculated twice a week during the whole testing period, and ID_{OI} was adjusted accordingly. We used a standard irrigation controller (Agronic 4000, Sistemas Electrònics PROGRÉS, S.A., Lérida, Spain) for supplying the calculated ID_{OI} . The CRP was kept running for 132 days, until September 16 (DOY 259). Herbicides were used to prevent weed growth in the orchard.

Stem water potential (Ψ_{stem} , MPa) was recorded at midday every 5-7 days throughout the irrigation period, in both the OI and the NI trees. A pressure chamber (Soilmoisture Equipment Corp., Santa Barbara, California, USA) was used to measure the xylem water potential at the petiole of leaves wrapped in aluminium foil some 2 hours before midday. Two leaves per tree ($n = 6$) were sampled from the base of shoots in the trunk or main branches.

Volumetric soil water content (θ_v , $\text{m}^3 \text{ m}^{-3}$) in the 0.2-2.0 m soil profile was monitored with a neutron probe (Troxler 3300, Research Triangle Park, NC, USA).

Access tubes were installed along the tree row, at distances of 0.5, 1.5, and 2.5 m from the trunk in the NI tree of MU2, and at 1.5 and 2.5 m from the trunk in the NI trees of MU1 and MU3. One single access tube per tree was installed in the OI trees, at 1.5 m from the trunk, since less variation of θ_v was expected in the OI trees than in the NI trees. Values of θ_v in the top 0.0-0.2 m were determined by gravimetry. Soil water profiles were recorded every 10-20 days through the testing period. A depth equivalent of water, expressed as the level of relative extractable water (REW, mm) was calculated from the measured θ_v values (Granier, 1987):

$$\text{REW} = \frac{\theta_v - \theta_{v,\min}}{\theta_{v,\max} - \theta_{v,\min}} \quad \text{Eq. 5.1}$$

where θ_v is the actual soil water content (mm), $\theta_{v,\min}$ the minimum soil water content measured in the soil (mm), and $\theta_{v,\max}$ the soil water content at field capacity (mm).

5.3. Results and discussion

5.3.1. CRP reliability

The CRP worked well, except for the heaters of the sap flow probes: nine heaters had to be replaced during the testing period. Most of them burnt out, suggesting an excess of current. We used one heat-pulse controller for each heater. With this configuration, and taking into account the heat-pulse controller characteristics, power output from the heater was 72 W, which means 72 J of energy delivered in a heat pulse of 1 s. The problem was solved simply by connecting two heaters to a single heat-pulse controller and increasing the heat pulse to 2 s. Thus, we had 64 J, but only 32 W, avoiding burnt-out heaters. Apart from that, we had 8 software faults in the 132 days of field trial, most of them at the beginning of the period. These were solved within a few hours, thanks to the remote control of the system.

The CRP was able to properly filter and amplify output voltages from the HPV probes. The curve shown in Fig. 5.2A was recorded with a high-performance digital multimeter (Keithley 2000, 0.1 μV resolution, accuracy of 0.003% reading), while that in

Fig. 5.2B was recorded with a standard digital multimeter (Iso-Tech IDM73, accuracy of 0.5% reading). The curve in Fig. 5.2B, despite having been highly amplified (note the different scaling) and measured with a low-precision multimeter, was less noisy than that in Fig. 5.2A, which proves the high amplification and filtering performance of the MU. The t_z value calculated by the MU (Fig. 5.2B) was similar to that derived from the curve recorded by the high-performance multimeter (Fig. 5.2A). In addition, we can expect the t_z value calculated by the MU to be more precise than that derived from the curve recorded by the high-performance multimeter, as the MU's curve was less noisy. We recorded several curves like that shown in Fig. 5.2, on different days of the field trial, always with similar results.

Fig. 5.3A shows the seasonal time course of ET_o and that of the E_p values calculated by the CRP in two OI trees, those in which the highest and lowest E_p values were recorded. Simple linear correlation analysis between the ET_o and E_p values in Fig. 5.3A showed $r^2 = 0.77$. Fig. 5.3B is the same, but for the NI trees; in this case, $r^2 = 0.71$. These correlation coefficient values are similar to the $r^2 = 0.73$ obtained by Fernández *et al.* (2001) in the same orchard when comparing ET_o with the E_p values calculated by the CHP method, using a CR10X data logger and HPV probes similar to those connected to the CRP. Other authors have found similar correlation coefficients for other species and conditions (Meiresonne *et al.* 1999; Zhang *et al.* 1999). These results prove the CRP was able to derive the t_z values from the output voltages of the HPV probes and to calculate reliable sap flow data, yielding daily E_p values as good as those calculated by the approach usually followed by most researchers when using the CHP method (Giorio and Giorio, 2003; Green *et al.*, 2003; Fernández *et al.*, 2006a). Fig. 5.3 also shows big differences of E_p between trees. As all instrumented trees had similar size and LAI (see tree characteristics in Materials and Methods), we can assume that these differences were mainly due to the probe location effect: sap flow records depends on the xylem characteristics in the location where the probes are inserted (Fernández *et al.*, 2001; Green *et al.*, 2003). Fig. 5.3, however, shows similar E_p dynamics for all trees, parallel to that of the ET_o . These results illustrates the main advantage of using the difference in the E_{pNI}/E_{pOI} ratio between two consecutive days for calculating the ID, as the CRP does: the sap flow recorded in either one or both of the trees connected to each

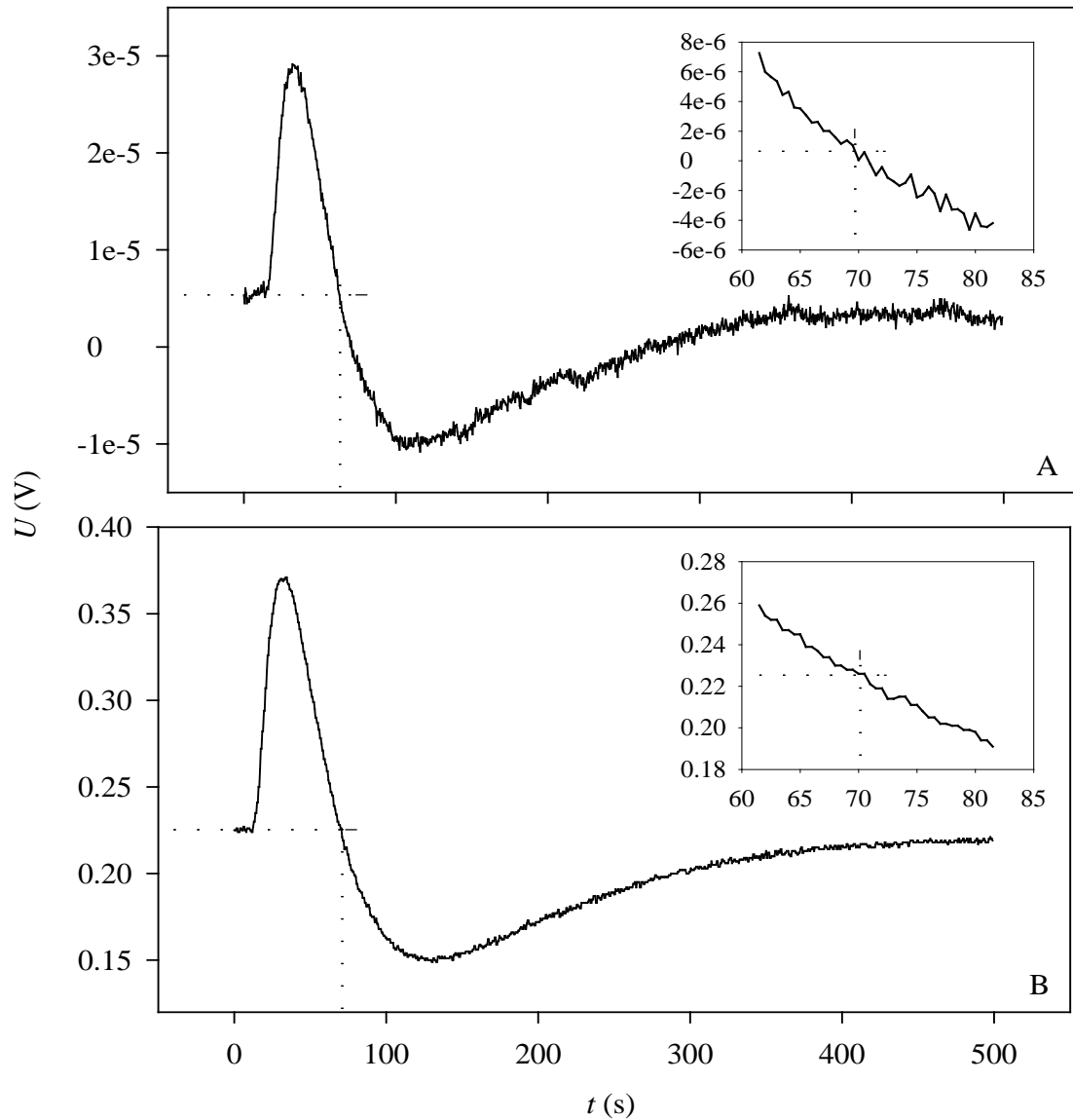


Fig. 5.2. Output voltage (U) from the outer pair of thermocouples of one of the probe sets monitored by the measurement unit 1, before (A) and after (B) being amplified and filtered by the CRP. Amplified sections of the graphs correspond to the calculated t_z values, indicated by the dashed lines. The X-axis shows the time (t) after the firing of the heat pulse.

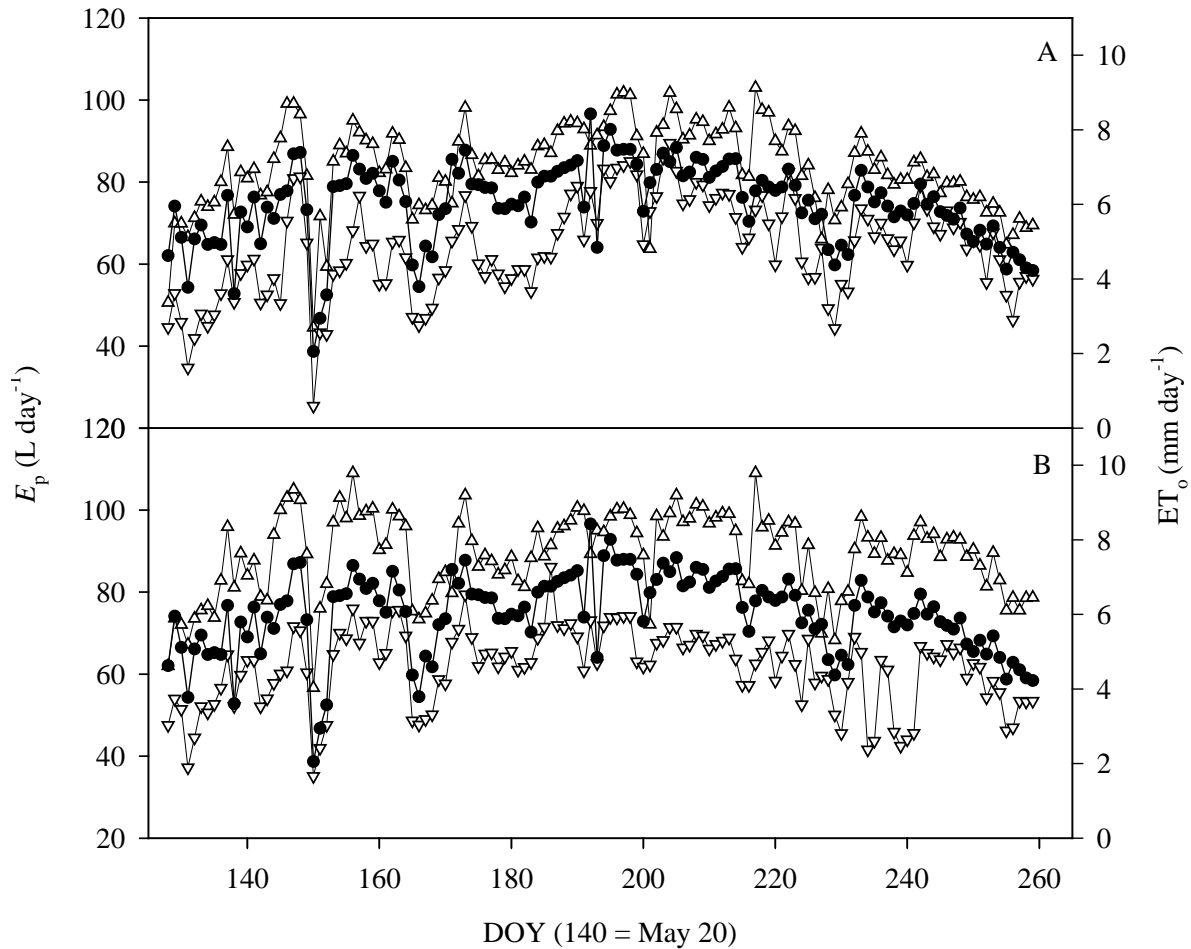


Fig. 5.3. Daily transpiration (E_p) values calculated by the CRP from the sap flow records in two OI trees — those for which the highest (Δ) and the lowest (∇) transpiration rates were estimated (A). Fig. B is the same but for the NI trees. Also shown are the potential evapotranspiration (ET_o) values estimated from the FAO56 Penman-Monteith equation and the data recorded by the weather station next to the orchard (\bullet). DOY = day of year.

MU can be over- or underestimated by the probe location effect, but this does not affect the dynamics of the E_{pNI}/E_{pOI} ratio.

5.3.2. CRP performance

The first value of E_{pNI}/E_{pOI} , calculated by the CRP on DOY 129, when the soil of both the OI and the NI trees was at about field capacity, was 0.89 (Fig. 5.4B). Variable weather conditions were recorded from DOY 145 to DOY 160. Low values of atmospheric demand, and consequently of ET_c , were recorded most of those days (Fig. 5.4C). Perhaps

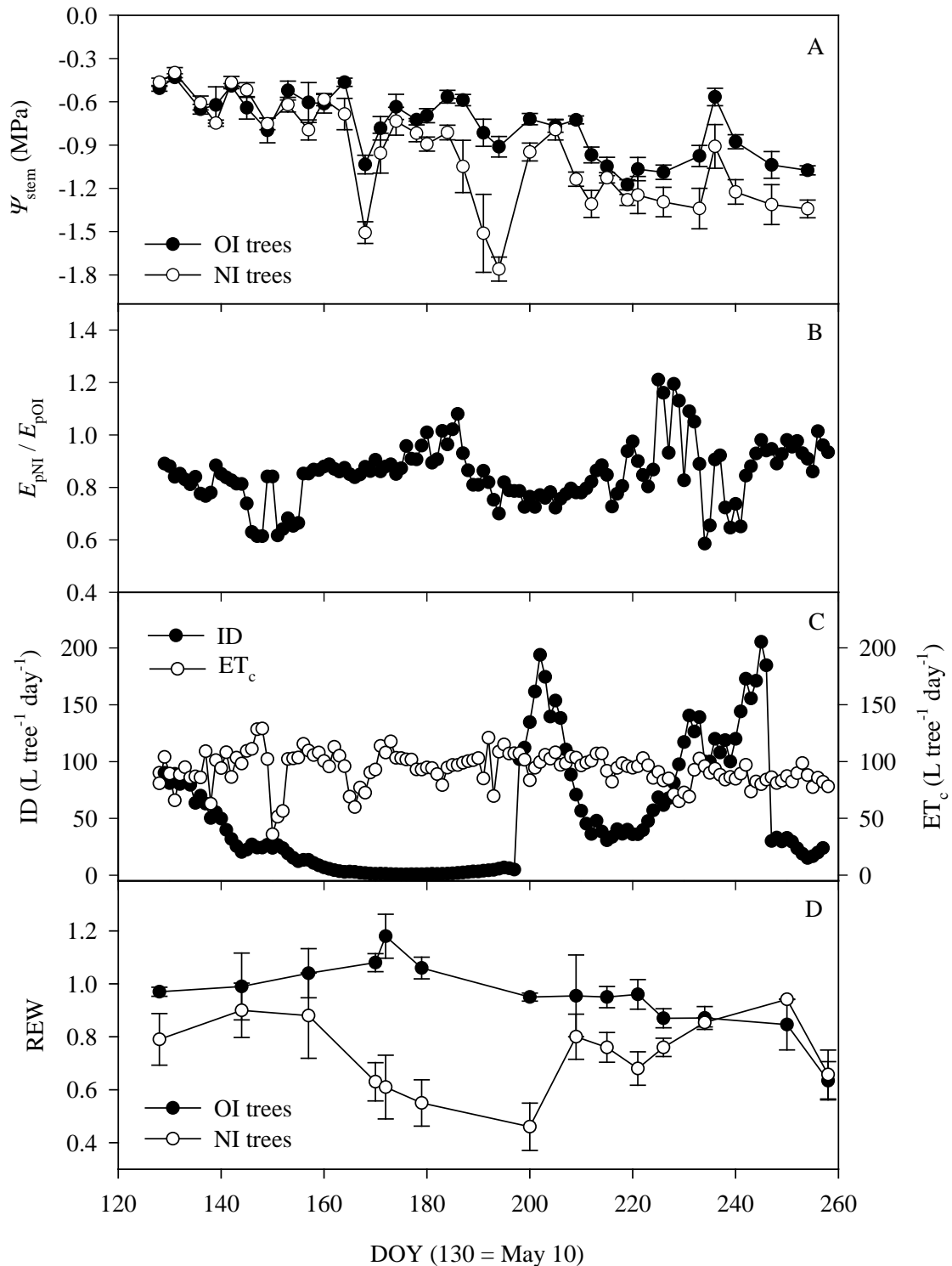


Fig. 5.4. Daily values of the transpiration ratio between the normally irrigated and overirrigated trees ($E_{\text{pNI}}/E_{\text{pOI}}$) determined by the CRP during the field trial (B), and the derived irrigation doses, ID (C). Irrigation began on day-of-year (DOY) 128. Water supply on DOY 199 corresponds to a recovery irrigation (see text for details). Also shown are the values of stem water potential measured at midday (Ψ_{stem}) in the instrumented trees ($n = 6$) (A) and the relative extractable water (REW) calculated from the soil water profiles measured in the rootzone of the instrumented trees ($n = 7$ for the NI trees and $n = 3$ for the OI trees) (D). Vertical bars represent \pm the standard error. The crop evapotranspiration values (ET_c), calculated as explained in the Materials and Methods section, are represented in panel C.

the variable atmospheric demand was responsible, at least in part, for the changing E_{pNI}/E_{pOI} values recorded on that period. Apart from that, on the first 46 days, the time course of the daily E_{pNI}/E_{pOI} values showed a slope of approximately zero, with $E_{pNI}/E_{pOI} = 0.85$ on DOY 175. Consequently, the IDs calculated by the CRP decreased from DOY 130 until DOY 176, when the calculated ID was just 0.58 L tree^{-1} (Fig. 5.4C).

This caused a decrease in the soil water content in the rootzone of the NI trees, with $REW \approx 0.57$ on DOY 176 (Fig. 5.4D). From DOY 177 to 187, differences between the E_{pNI}/E_{pOI} ratios of consecutive days were greater than 5% (Fig. 5.4B); from DOY 188 to 196, the E_{pNI}/E_{pOI} ratio decreased markedly nearly everyday, showing, for the first time since the beginning of the irrigation season, a clear response to the low water supplied to the NI trees. The daily evolution of the E_{pNI}/E_{pOI} ratio from DOY 177 to 196 yielded increasing IDs calculated by the CRP according to the irrigation protocol: by 10% on DOY 177 and by 20% on the following days. Due to the low ID on DOY 176, however, the ID on DOY 196 was only 6.71 L tree^{-1} , much lower than the ET_c value estimated for that day with the crop coefficient approach ($106.9 \text{ L tree}^{-1}$) (Fig. 5.4C). Both Ψ_{stem} (Fig. 5.4A) and the E_{pNI}/E_{pOI} ratio (Fig. 5.4B) decreased markedly in the NI trees from DOY 187, indicating that the soil water content was too low to prevent a significant increase in the trees' water stress. This made us apply a recovery irrigation of 102 L tree^{-1} on DOY 199, corresponding to the ET_c value estimated with the crop coefficient approach (Fig. 5.4C). From that day on, we left the CRP to control irrigation again as programmed. As shown in Fig. 5.4C, the ID increased for four consecutive days, reaching a maximum of $193.9 \text{ L tree}^{-1}$ on DOY 203, and then decreased. The average REW in the rootzone of the NI trees went from a minimum of 0.48 on DOY 196 to a maximum of 0.80 on DOY 209. According to this change in the soil water status, Ψ_{stem} of the NI trees recovered quickly, reaching values similar to those of the OI trees on DOY 205. It took longer, however, for the E_{pNI}/E_{pOI} ratio to recover. This agrees with what is already known about the behaviour of the olive tree after a recovery irrigation: the water potential of stressed olive trees recovers quickly after rewatering, but it takes longer for stomatal conductance to recover, the delay being related to the level of water stress previously reached (Ferreles *et al.* 1996; Fernández *et al.* 1997). Large daily fluctuations in the E_{pNI}/E_{pOI} ratio were often recorded from DOY 224 to 242, which led the CRP to calculate increasing IDs on nearly every day of that period (Fig. 5.4B,C). This caused a substantial increase in the soil water content of

the NI trees, reaching similar values to those of the OI trees from DOY 234. The lack of water available for irrigation on the farm from DOY 245 made us reduce the irrigation supplied to the OI trees to about one third of ET_c , and adjust the ID calculated by the CRP on DOY 248 to 30 L tree^{-1} . No significant changes were recorded from that day to the end of the irrigation season (September 16; DOY 259), apart from the decrease in both Ψ_{stem} and REW, for all the experimental trees, caused by the mentioned reduction in the irrigation amounts.

The time-course evolution both of the E_{pNI}/E_{pOI} ratio and Ψ_{stem} from the beginning of the irrigation season until DOY 187 (Fig. 5.4A,B), suggests that the NI trees were able to take up similar amounts of water from the soil as the OI trees until $REW \approx 0.50$, the value recorded on that day. The cumulated ET_c from DOY 128 to 187 amounted to 4520 L tree^{-1} , while the amount of water supplied in that period by the CRP to the NI trees was 1410 L tree^{-1} only. The difference, 3110 L tree^{-1} , should have been provided by the soil. Fernández *et al.* (2006b) estimated that the available water in the soil orchard is 170 mm, which means some 85 L of water per cubic metre of soil before $REW \approx 0.5$. Therefore, some 36 m^3 of rhizosphere should have been needed for each tree to be able to cover the mentioned difference. Taking into account that the average effective rootzone depth estimated from the soil water profiles measured during the irrigation period was 1.6 m, such rhizosphere could correspond to about 23 m^2 ground surface, of the 35 m^2 available to each tree. This is reasonable, since it agrees with observations on the root system distribution carried out in the same orchard by Fernández *et al.* (1991). Besides the relatively high amount of water available for each tree from the soil water reserves, the high capacity of the olive tree for taking up water from drying soils (Xiloyannis *et al.*, 1998) probably contributed to the delay in the Ψ_{stem} and E_{pNI}/E_{pOI} responses to the low IDs applied until DOY 187. It seems that, for our orchard conditions, $REW \approx 0.5$ is a threshold for soil water depletion at the beginning of the irrigation period, when the soil outside the irrigation bulbs is wetted after the rainy season. Later in the season, from about DOY 210, values of Ψ_{stem} in the NI trees were lower than those recorded before DOY 187, despite of the greater REW values recorded at that time (Fig. 5.4A,D). This cannot be attributed to differences in atmospheric demand only, because average ET_o values recorded in the two periods were similar (Fig. 5.3). We can assume that the volume of soil from which the roots could absorb water from DOY 210 was lower than at

the beginning of the irrigation period, being likely restricted to the irrigation bulbs. Under these conditions, any reduction in the volumetric soil water content within the irrigation bulbs has a greater impact on the amount of water taken up by the tree. We can expect, therefore, greater threshold REW values later in the irrigation period than at the beginning. These results suggest that the threshold value of $REW=0.25$ usually recommended for olive (Orgaz and Fereres, 2004) is too low.

The mentioned results suggests that the E_{pNI}/E_{pOI} ratio may not has enough resolution for the daily adjustment of ID to keep the soil around field capacity, in orchards where the soil has a medium-to-high soil water-holding capacity and the roots of trees explore large volumes of soil. The ratio, however, seems to be a sensitive indicator of a threshold value of water stress, even for those conditions, suggesting a potential for the automatic control of deficit irrigation.

Depending on the soil characteristics, a careful evaluation of the level to which the OI trees must be irrigated could be required. Thus, lack of oxygen in the rootzone, nitrogen deficiency because of excessive leaching losses, and anomalous leaf area development could make overirrigated trees to become non-representative of those in the orchard (Goldhamer and Fereres, 2001; Fernández *et al.* 2007). In addition, there are evidences of flooding causing a reduction in the recorded value of some plant-based water status indicators, including sap flow (Ortuño *et al.*, 2007). In this work we irrigated our OI trees to 130% of ET_c , to assure non-limiting soil water conditions all throughout the experiment. On the other hand, the fact that our experimental soil has no restrictions to percolation (Palomo *et al.*, 2002) made us to expect a negligible impact of the mentioned problems derived from overirrigating the trees.

Our results show that the increase or reduction of ID by 10% on the next day and 20% on the following days according to the differences of the E_{pNI}/E_{pOI} ratios of two consecutive days, was not always enough to match the changes on the crop water requirements. This was the case from DOY 177 to 196, Fig. 5.4C. We have found no evidences in the literature on the physiological bases to be taken into account for adjusting properly those percentages. There are, however, articles in which other authors evaluate, for different species, the results of working with similar percentages as those used in this work. Thus, Conejero *et al.* (2007) evaluated the use of sap flow and trunk

diameter readings for scheduling irrigation in young peach trees. They reduced irrigation by 10% when the signal intensities derived from the sensor readings was at or below unity on at least two or three consecutive days, and increased irrigation by 10% when the signal intensity exceeded unity. Their results show that the precision of water scheduling decreased during periods of increasing irrigation need, and that 10% irrigation increases were insufficient, or that irrigation should be scheduled more frequently than every three days. Another example is that of Velez *et al.* (2007), who used maximum daily trunk shrinkage (MDS) in mature ‘Clementina de Nules’ citrus trees to schedule deficit irrigation. The authors varied in ± 10 to 20% the water applied weekly, according to the evolution of the MDS ratio between overirrigated and control trees. By using this approach they managed to maintain the MDS ratio close to the target value, for most of the season.

Analysis of the E_{pNI}/E_{pOI} values showed that reducing the 5% threshold difference between $(E_{pNI}/E_{pOI})_{DOY}$ and $(E_{pNI}/E_{pOI})_{DOY-1}$ is not advisable: daily fluctuations were close to that value even on days with no significant changes in either the soil water content or the atmospheric demand. We cannot explain the unusually high fluctuations in the E_{pNI}/E_{pOI} ratio recorded from DOY 224 to 242. The system apparently worked well, and no significant changes in the environmental conditions occurred in that period, except for a 15 mm rainfall event on DOY 229, likely responsible for both the increase on Ψ_{stem} (Fig. 5.4A) and the decreased on ID (Fig. 5.4C) recorded on the following days. Except for period between DOY 224 and 242, the only case in which daily fluctuations of the E_{pNI}/E_{pOI} ratio were greater than 5% for several consecutive days was from DOY 187 (Fig. 5.4B), in agreement with the decrease in soil water content to below the threshold for soil water (Fig. 5.4D), and the marked decrease in Ψ_{stem} of the NI trees (Fig. 5.4A). This, together with the results discussed above, suggests the need for a change in the irrigation protocol: the CRP must apply a recovery irrigation when the E_{pNI}/E_{pOI} ratio decreases more than 5% for three consecutive days. The amount of water for the recovery irrigation must be set by the user, depending on the fruit tree species and orchard characteristics. For our experimental orchard, 100 L tree⁻¹ would be a reasonable amount (Fernández and Moreno 1999). The effect that this change in the irrigation protocol might have on CRP performance is still to be tested.

Monitoring the soil water status for scheduling irrigation can be recommended in some cases, especially for homogeneous, annual crops with reduced rootzones (Hoppula and Salo, 2007; Thompson *et al.* 2007). In the case of woody plants exploring big volumes of soil, soil water variability imposes limitations to this approach, especially because the number of required sensors may become unaffordable. In those cases, plant-based measurements may be especially useful for irrigation scheduling purposes, since they inform on the plant response to the soil and atmospheric conditions (Jones, 2004). Compared to irrigation scheduling methods based on the atmospheric demand, such as the crop coefficient method (Allen *et al.* 1998), plant-based measurements can increase the resolution of the calculated IDs, which is certainly an advantage for precise high-frequency irrigation. In addition, plant-based measurements such as sap flow and trunk diameter can be easily automated, which is particularly valuable for irrigation scheduling (Jones, 2007). Automatic irrigation controllers, such as the CRP, have an additional advantage: the device is able not only to measure the plant indicator automatically; it also processes the collected information and operates the irrigation system to apply the calculated ID. Still, the highly variable soil and crop conditions in many commercial orchards may limit the potential use of AICs such as the CRP. On those cases, however, the use of remote sensing techniques could inform on the variability of water stress within the orchard, helping to choose the most representative locations for the MUs, thus reducing the number of required sensors. See the work by Sepulcre-Cantó *et al.* (2007) for an example on the use of those techniques in olive and peach orchards.

5.4. Conclusions

The CRP proved to be a robust device able to calculate and supply daily irrigation amounts to the orchard, in accord with the specified irrigation protocol. It allows the user to interact with the device from any computer, PDA, or smartphone connected to the Internet, for consulting, changing parameters, or even taking full control of the irrigation practice. This is a clear advantage for irrigating orchards in remote areas. For the case studied in this work (olive trees with big root systems growing in a soil with a high water-holding capacity) the daily values of the E_{pNI}/E_{pOI} ratio had not enough resolution for the desired irrigation approach, intended to replace the daily crop water consumption. The CRP, however, was able to react to a sudden increase in the tree's water stress caused by

the soil water content falling below the threshold for soil water deficit, suggesting the device could be suitable for applying deficit irrigation in olive orchards with similar characteristics as our experimental orchard. This would require a small change in the irrigation protocol, suggested by our field results. The resolution of the E_{pNI}/E_{pOI} ratio could be greater when irrigating species with a lower capacity to take up water from drying soils, especially if these have a low water-holding capacity. Whether for those species and soils the CRP will be efficient to keep the soil close to its field capacity throughout the irrigation season is still to be tested.

5.5. References

- Alarcon JJ, Domingo R, Green SR, Nicolas E, Torrecillas A. 2003. Estimation of hydraulic conductance within field-grown apricot using sap flow measurements. *Plant and Soil* 251(1):125-135.
- Alarcón JJ, Domingo R, Green SR, Sánchez-Blanco MJ, Rodríguez P, Torrecillas A. 2000. Sap flow as an indicator of transpiration and the water status of young apricot trees. *Plant and Soil* 227(1-2):77-85.
- Allen RG, Pereira LS, Raes D, Smith M. 1998. Crop evapotranspiration-Guidelines for computing crop water requirements-FAO Irrigation and drainage paper 56. FAO, Rome 300:6541.
- Alves I, Pereira LS. 2000. Non-water-stressed baselines for irrigation scheduling with infrared thermometers: A new approach. *Irrigation Science* 19(2):101-106.
- Caspari HW, Green SR, Edwards WRN. 1993. Transpiration of well-watered and water-stressed Asian pear trees as determined by lysimetry, heat-pulse, and estimated by a Penman-Monteith model. *Agricultural and Forest Meteorology* 67(1-2):13-27.
- Conejero W, Alarcón J, García-Orellana Y, Nicolás E, Torrecillas A. 2007. Evaluation of sap flow and trunk diameter sensors for irrigation scheduling in early maturing peach trees. *Tree physiology* 27(12):1753.

- Constantz J, Murphy F. 1990. Monitoring moisture storage in trees using time domain reflectometry. *Journal of Hydrology* 119(1-4):31-42.
- Fereres E, Evans RG. 2006. Irrigation of fruit trees and vines: an introduction. *Irrigation Science* 24(2):55-57.
- Fereres E, Goldhamer DA, Parsons LR. 2003. Irrigation water management of horticultural crops. *Hortscience* 38(5):1036-1042.
- Fereres E, Ruz C, Castro J, Gómez JA, Pastor M. 1996. Recuperación del olivo después de una sequía extrema. *Proceedings of the XIV Congreso Nacional de Riegos. Aguadulce. Almería.* p 89-93.
- Fernández JE, Díaz-Espejo A, Infante JM, Durán P, Palomo MJ, Chamorro V, Girón IF, Villagarcía L. 2006. Water relations and gas exchange in olive trees under regulated deficit irrigation and partial rootzone drying. *Plant and Soil* 284(1-2):273-291.
- Fernández JE, Durán PJ, Palomo MJ, Díaz-Espejo A, Chamorro V, Girón IF. 2006. Calibration of sap flow estimated by the compensation heat pulse method in olive, plum and orange trees: relationships with xylem anatomy. *Tree Physiology* 26(6):719-728.
- Fernández JE, Green SR, Caspari HW, Díaz-Espejo A, Cuevas MV. 2008. The use of sap flow measurements for scheduling irrigation in olive, apple and Asian pear trees and in grapevines. *Plant and Soil* 305(1-2):91-104.
- Fernández JE, Moreno F. 1999. Water use by the olive tree. *Journal of crop production* 2(2):101-162.
- Fernández JE, Moreno F, Cabrera F, Arrue JL, Martín-Aranda J. 1991. Drip irrigation, soil characteristics and the root distribution and root activity of olive trees. *Plant and Soil* 133(2):239-251.
- Fernández JE, Moreno F, Girón IF, Blázquez OM. 1997. Stomatal control of water use in olive tree leaves. *Plant and Soil* 190(2):179-192.

-
- Fernández JE, Palomo MJ, Díaz-Espejo A, Clothier BE, Green SR, Girón IF, Moreno F. 2001. Heat-pulse measurements of sap flow in olives for automating irrigation: tests, root flow and diagnostics of water stress. *Agric Water Manage* 51(2):99-123.
- Fernández JE, Palomo MJ, Díaz-Espejo A, Girón IF. 2003. Influence of partial soil wetting on water relation parameters of the olive tree. *Agronomie* 23(7):545-552.
- García-Orellana Y, Ruiz-Sánchez MC, Alarcón JJ, Conejero W, Ortuño MF, Nicolás E, Torrecillas A. 2007. Preliminary assessment of the feasibility of using maximum daily trunk shrinkage for irrigation scheduling in lemon trees. *Agric Water Manage* 89(1-2):167-171.
- Giorio P, Giorio G. 2003. Sap flow of several olive trees estimated with the heat-pulse technique by continuous monitoring of a single gauge. *Environmental and Experimental Botany* 49(1):9-20.
- Goldhamer DA, Fereres E. 2001. Irrigation scheduling protocols using continuously recorded trunk diameter measurements. *Irrigation Science* 20(3):115-125.
- Goldhamer DA, Fereres E. 2004. Irrigation scheduling of almond trees with trunk diameter sensors. *Irrigation Science* 23(1):11-19.
- Granier A. 1987. Evaluation of transpiration in a Douglas-fir stand by means of sap flow measurements. *Tree Physiology* 3(4):309.
- Green SR. 1998. Flow by the heat-pulse method. HortResearch Internal Rep. 1998/22. HortResearch, Palmerston North, New Zealand.
- Green SR, Clothier B, Jardine B. 2003. Theory and practical application of heat pulse to measure sap flow. *Agronomy Journal* 95(6):1371-1379.
- Green SR, McNaughton KG, Clothier BE. 1989. Observations of night-time water use in kiwifruit vines and apple trees. *Agricultural and Forest Meteorology* 48(3-4):251-261.

- Hatfield JL. 1983. The utilization of thermal infrared radiation measurements from grain-sorghum crops as a method of assessing their irrigation requirements. *Irrigation Science* 3(4):259-268.
- Holbrook NM, Sinclair TR. 1992. Water-balance in the arborescent palm, sabal-palmetto .2. Transpiration and stem water storage. *Plant Cell and Environment* 15(4):401-409.
- Hoppula KI, Salo TJ. 2007. Tensiometer-based irrigation scheduling in perennial strawberry cultivation. *Irrigation Science* 25(4):401-409.
- Intrigliolo DS, Castel JR. 2006. Performance of various water stress indicators for prediction of fruit size response to deficit irrigation in plum. *Agric Water Manage* 83(1-2):173-180.
- Intrigliolo DS, Castel JR. 2006. Usefulness of diurnal trunk shrinkage as a water stress indicator in plum trees. *Tree Physiology* 26(3):303-311.
- Jackson R. 1982. Canopy temperature and crop water stress. *Advances in irrigation* 1:43-85.
- Jones HG. 1999. Use of infrared thermometry for estimation of stomatal conductance as a possible aid to irrigation scheduling. *Agricultural and Forest Meteorology* 95(3):139-149.
- Jones HG. 2004. Irrigation scheduling: advantages and pitfalls of plant-based methods. *Journal of Experimental Botany* 55(407):2427-2436.
- Jones HG. 2007. Monitoring plant and soil water status: established and novel methods revisited and their relevance to studies of drought tolerance. *Journal of Experimental Botany* 58(2):119.
- Klein I. 2004. Scheduling Automatic Irrigation by Threshold-Set Soil Matric Potential Increases Irrigation Efficiency While Minimizing Plant Stress. *Acta Hort (ISHS)* 664:361-368.

-
- Lobo FD, Oliva MA, Resende M, Lopes NF, Maestri M. 2004. Infrared thermometry to schedule irrigation of common bean. *Pesquisa Agropecuaria Brasileira* 39(2):113-121.
- Luthra SK, Kaledhonkar MJ, Singh OP, Tyagi NK. 1997. Design and development of an auto irrigation system. *Agric Water Manage* 33(2-3):169-181.
- Meiresonne L, Nadezhdina N, Cermak J, Van Slycken J, Ceulemans R. 1999. Measured sap flow and simulated transpiration from a poplar stand in Flanders (Belgium). *Agricultural and Forest Meteorology* 96(4):165-179.
- Miranda FR, Yoder RE, Wilkerson JB, Odhiambo LO. 2005. An autonomous controller for site-specific management of fixed irrigation systems. *Comput Electron Agric* 48(3):183-197.
- Moreno F, Conejero W, Martin-Palomo MJ, Girón IF, Torrecillas A. 2006. Maximum daily trunk shrinkage reference values for irrigation scheduling in olive trees. *Agric Water Manage* 84(3):290-294.
- Moreno F, Fernandez JE, Clothier BE, Green SR. 1996. Transpiration and root water uptake by olive trees. *Plant and Soil* 184(1):85-96.
- Moriana A, Fereres E. 2002. Plant indicators for scheduling irrigation of young olive trees. *Irrigation Science* 21(2):83-90.
- Nadezhdina N, Cermak J. 1997. Automatic control unit for irrigation systems based on sensing the plant water status. *Anais do Instituto Superior de Agronomia* 46:149-157.
- Nadezhdina N. 1999. Sap flow index as an indicator of plant water status. *Tree Physiology* 19(13):885-891.
- Nadler A, Raveh E, Yermiyahu U, Green S. 2006. Stress induced water content variations in mango stem by time domain reflectometry. *Soil Science Society of America Journal* 70(2):510-520.

- Nicolas E, Torrecillas A, Dell'Amico J, Alarcon J. 2005. The effect of short-term flooding on the sap flow, gas exchange and hydraulic conductivity of young apricot trees. *Trees-Structure and Function* 19(1):51-57.
- Orgaz F, Fereres E. 2004. Riego. *El Cultivo del Olivo*. 4th ed: Barranco D, Fernández Escobar R, Rallo L. Mundi Prensa, Madrid. p 251-272.
- Ortuño MF. 2004. Medidas de flujo de savia y variaciones micrométricas del tronco como indicadores del estado hídrico del limonero: Doctoral thesis. Universidad de Murcia. Spain. 289 p.
- Ortuño M, Alarcón J, Nicolás E, Torrecillas A. 2007. Water status indicators of lemon trees in response to flooding and recovery. *Biologia plantarum* 51(2):292-296.
- Palomo M, Moreno F, Fernández J, Díaz-Espejo A, Girón I. 2002. Determining water consumption in olive orchards using the water balance approach. *Agric Water Manage* 55(1):15-35.
- Pelloux G, Lorendeau J, Huguet J, Kuhlmann F. PEPISTA-Translation of plants behaviour by the measurement of diameters of stem or fruit as a self-adjusted method for irrigation scheduling; 1990. Deutsche Landwirtschafts-Gesellschaft (DLG). p 206-212.
- Sepulcre-Cantó G, Zarco-Tejada PJ, Jiménez-Muñoz J, Sobrino J, Soriano M, Fereres E, Vega V, Pastor M. 2007. Monitoring yield and fruit quality parameters in open-canopy tree crops under water stress. Implications for ASTER. *Remote sensing of environment* 107(3):455-470.
- Thompson R, Gallardo M, Valdez L, Fernandez M. 2007. Determination of lower limits for irrigation management using in situ assessments of apparent crop water uptake made with volumetric soil water content sensors. *Agric Water Manage* 92(1-2):13-28.
- Velez J, Intrigliolo D, Castel J. 2007. Scheduling deficit irrigation of citrus trees with maximum daily trunk shrinkage. *Agric Water Manage* 90(3):197-204.

Williams DG, Cable W, Hultine K, Hoedjes JCB, Yopez EA, Simonneaux V, Er-Raki S, Boulet G, de Bruin HAR, Chehbouni A and others. 2004. Evapotranspiration components determined by stable isotope, sap flow and eddy covariance techniques. *Agricultural and Forest Meteorology* 125(3-4):241-258.

Xiloyannis C, Dichio B, Nuzzo V, Celano G. 1998. L'olivo: pianta esempio per la sua capacità di resistenza in condizioni di estrema siccità. In *Seminari di Olivicoltura, Accademia Nazionale dell'olivo e dell'Olio, Tip Nuova Panetto e Petrelli, Spoleto (PG):79-111.*

Zhang H, Morison JIL, Simmonds LP. 1999. Transpiration and water relations of poplar trees growing close to the water table. *Tree Physiology* 19(9):563-573.

Appendix 5

5.A1. Filtering and amplification details

Output voltages from the HPV probes had maximum values of about 60 microvolts. An ICL7650B instrumentation amplifier incorporated in each MU multiplied input signals by a factor of 100. Additional amplification (for a gain of 27) was obtained thanks to an OP07 ultralow offset voltage operational amplifier. A tapered potentiometer was also included to correct the amplification offset. Eventually, a second-order Butterworth low-pass filter multiplied the signal by a factor of 2, eliminating noisy components.

5.A2. Measurement unit (MU)

Specifically designed software was downloaded to each of the three main components of the CRP (MU, CU, and PEC) for the system to work as explained in the Materials and Methods section. The “brain” of each MU is a PIC18F4525, C-programmed microcontroller. This device controls both the firing of heat pulses at the defined time intervals and the collection of differential temperatures from each pair of thermocouples in the HPV probes. These data are filtered firstly by the second-order Butterworth low-pass filter, and then selected by a control algorithm to obtain the t_z values, which are saved in the external EEPROM located on the MU board. The CU can read temperature values online.

5.A3 Control unit (CU)

A Visual Basic application was designed for CU operation. This allows the configuration of parameters related to the HPV probe characteristics and location in the trunk, as well as of those related to sap flow and ID calculation. The main code is dedicated to collecting, at the end of each day, the t_z values saved in the external EEPROM of the MUs. Wound width and correction factors for sap flow calculations were chosen according to calibration experiments made in the olive by Fernández et al. (2006a). After filtering wrong data, average values were used to calculate $(E_{pNI}/E_{pOI})_{DOY}$ and to derive ID. Clock synchronisation in MUs and CU was checked daily, using the PC clock as master. The

CU is also able to plot and save differential temperatures read by the HPV probes, i.e. differences in temperature between the downstream and upstream thermocouples. This helps to detect probe malfunction.

5.A4. Pump & electrovalve controller (PEC) software

The software for the PEC was written in C language, then compiled into a hex file, and finally loaded into a PIC16F877 microcontroller.

Chapter 6

An automatic controller for high frequency irrigation based on soil water content measurements combined with the crop coefficient approach

Part of this chapter is published in:

Romero R, Muriel JL, García I. 2009. Automatic Irrigation System in Almonds and Walnuts Trees Based on Sap Flow Measurements. *Acta Hort. (ISHS)* 846:135-142.

Abstract. The aim of this work was to evaluate the performance of a new automatic irrigation controller (AIC) in a 1 ha almond orchard during the irrigation season of 2009. The AIC was programmed to impose two irrigation treatments, one in which 100% of the crop water needs were replaced and another with 75% of that amount. Volumetric soil water contents (θ_v) were measured with FDR probes (EnviroSCAN) close to one representative tree per treatment. Data on precipitation and potential evapotranspiration were automatically collected by the AIC from a nearby weather station belonging to the *Red de Información Agroclimática* of the *Junta de Andalucía*. This information was used by the AIC to calculate ET_c with the crop coefficient approach, and to derive the daily irrigation amounts (IA) according to the established irrigation strategies. Then the AIC interacted with the irrigation system in the orchard to supply the calculated IA. While irrigating, θ_v data were wireless collected by the AIC every 5 min (Zigbee protocol). The device used this information to control in real time the electrovalves of the irrigation system in order to keep θ_v values between 80% and 100% of those corresponding to field capacity. This was intended both to avoid runoff and minimize evaporation losses. Remote connection to the AIC was implemented to allow supervision and control of the system from any computer connected to the internet. Main parameters related to the irrigation practice were stored by the AIC. Results showed a good performance of the device, being robust and able to calculate and supply the daily IA values all throughout the irrigation season, without any intervention from the user. The remote access utility to the data stored in the AIC was useful for supervising the irrigation practice in the orchard. It seems,

therefore, that the AIC is a suitable option for the management of high-frequency, precise irrigation in orchards, even if these are in remote areas.

6.1. Introduction

Continuous increments of water demand⁴ and the scarcity of its sources are increasing pressure to improve water-use productivity for both, agricultural and non-agricultural purposes (Feres and Soriano, 2007). On the other hand, the food shortage, on a global scale, provides the imperative to improve edible crop yields. Although irrigated areas accounted for approximately 18% of the world's cropped land in 2003 (FAOSTAT 2006), they produced approximately 40-45% of the global food (Morison *et al.*, 2008). So, it is well recognized the need to go further in getting a better understanding of the soil-plant-atmosphere system, mainly to develop more efficient irrigation practices (Fernández *et al.*, 2008). Some of the most promising practices are those based on new management tools to implement automatic irrigation systems that save water and increase water use efficiency (Feres and Evans, 2006).

Frequency domain reflectometry (FDR) sensors have been widely used for automatic irrigation. The working principle of FDR sensors is based on the electrical capacitance of a capacitor that uses the soil as a dielectric depending on the soil water content (Fernández *et al.*, 2000). A new approach, based on the use of low cost FDR sensors with wireless modules to implement sensors networks, is becoming popular in precision agriculture (Lopez Riquelme *et al.*, 2009). In orchards with high crop-water-stress variability, the use of electromagnetic induction devices may help to choose representative locations, and thus to reduce the number of required sensors. The apparent electrical conductivity (EC_a), measured with these devices, has been used for the spatial characterization of vadose zone soil properties, like soil salinity and texture (Rhoades *et al.*, 1976; 1999), soil water content (Kachanoski *et al.*, 1988) and soil physical properties (Carroll and Oliver, 2005).

⁴ The world's consumption of water is doubling every 20 years, which is more than twice the rate of our population increase (Clothier *et al.* 2008).

In this work we evaluated the performance of a new automatic irrigation controller (AIC) for fruit tree orchards. The system is based on FDR wireless sensors and meteorological data. The experimental platform was tested under field conditions in an orchard with mature almond trees, representative of commercial orchards in the area.

6.2. Materials and methods

6.2.1. Orchard characteristics

The experimental 1 ha orchard is located in the experimental farm of the IFAPA, planted with 9-year-old almond trees, at 18 km to the north of Seville (37° 30'N, 5° 57'W, ca. 10 m a.s.l.). The trees, spaced 6 m x 7 m, were, on average, 4.8 m in height and 5 m in diameter, with round shape crown. They were planted on ridges 0.5 m high and 2 m wide, with 4 m between ridges.

The soil is a silty loam typical fluvisol of 2.5 m depth, fertile, with organic matter content below 1.5 % and high cationic exchange capacity. Laboratory determinations showed volumetric water contents (θ_v) at field capacity (-0.3 MPa) and wilting point (-1.5 MPa) of $0.39 \text{ m}^3 \text{ m}^{-3}$ and $0.13 \text{ m}^3 \text{ m}^{-3}$, respectively. Field measurements, however, yielded θ_v values equal to 0.22 close to the emitters a few hours after irrigation, therefore we consider this value as the value for FC in field conditions.

The climate in the area is attenuated meso-mediterranean (FAO, 1963) with an average annual precipitation of 534 mm and ET_o of 1400 mm (period 1971-2000).

The orchard was divided into three plots, shown in Fig. 6.1. The irrigation system consisted of two laterals per tree row, one at each side of the trees, at 1 m from the trunk. The laterals had 4 L hour^{-1} drippers 1 m apart. The water supplied to each plot was controlled by an electrovalve connected to a pressurized pipe. The results of this work are focused in plots 1 and 2. These electrovalves were commanded by the AIC (see below) while irrigation amounts in plot 3 were estimated as in commercial orchards in the area.



Fig. 6.1. Location of the treatments in the IFAPA experimental farm (1 = 100% IN; 2 = 75% IN; 3 = Treatment normally carried out in the orchard, ca 70% IN).

We used an electromagnetic induction sensor (EM38-DD, Geonics Ltd., Missisagua, ON, Canada) for evaluating the homogeneity of the orchard soil. This device consists of two perpendicularly superposed EM38 sensors that simultaneously measure EC_a in the 0-0.75 m depth soil layer with the horizontal dipole, and down to 1.5 m with the vertical dipole (McNeill, 1980). The information provided by the EM38 helped us to choose representative locations within plots 1 and 2 (Fig. 6.2), where the testing of the AIC was carried out.

Harvesting was made on August 12th, and the yield of each plot determined for a seed humidity of 6%.

6.2.2. Evaluation of the AIC

Both in a1 and a2 (Fig. 6.2) we installed an EnviroSCAN probe (Sentek Sensor Technologies, Stepney, Australia) next to one of the drippers and at 1 m from the trunk of a representative tree, to record θ_v values at 0.1, 0.3, 0.5, 0.8 and 1.5 m depth. The probes

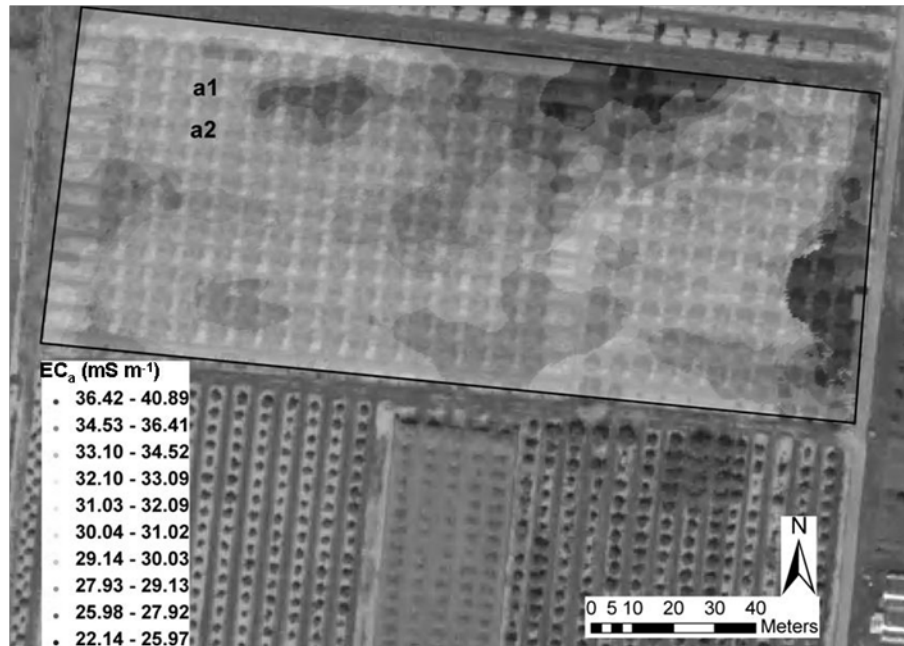


Fig. 6.2. Spatial variability of the soil electrical conductivity determined with an EM38-DD electromagnetic induction sensor in the area of orchard where the water treatments were imposed (marked area in Fig 1). Also shown are the representative locations for the 100% IN treatment (a1) and the 75% IN treatment (a2).

were calibrated after installation, by comparing the probe outputs with θ_v values derived from measurements with the gravimetric method.

The AIC automatically collected data on precipitation (P) and potential evapotranspiration (ET_o) from a nearby weather station belonging to the *Red de Información Agroclimática* (RIA) of the *Junta de Andalucía*, and used them to calculate the irrigation amounts (IA) in the orchard according to the established irrigation strategies (Section 3.2.3).

The AIC was programmed to supply the following IAs: in plot 1, IA = IN, being IN the irrigation needs (IN) to replace the crop water demand; in plot 2, IA = 0.75 IN. The device controlled the irrigation system for the whole irrigation season of 2009 (March 18 to Jul 31).

On October 18th, after the irrigation period, a trench was dug near the instrumented trees to study the root distribution by the trench method (van Noordwijk *et al.*, 2000). The trench was 2 m long (1 m at each side of the trunk), 2 m deep and 1.5 wide, and the studied wall was in the vertical of one of the laterals, being the drippers at

0.5 and at 1.5m from the beginning of the studied wall. Root distribution was recorded by overlaying the studied wall with a 0.1 m \times 0.1 m grid and counting the number and diameter of the roots.

6.2.3. Fundamentals of the AIC

The θ_v outputs were collected by the RT6 datalogger of the EnviroSCAN system. We incorporated a Zigbee wireless module (Baronti *et al.*, 2007) to the RT6 and designed an application that allowed the AIC to collect the θ_v outputs at any time. The main advantage of this approach, as compared to the use of the Sentek's software, is that the AIC had real time information on the soil water status, which allowed for a precise control of the water supply (see below). After collecting the θ_v and weather data, the AIC calculated IN as described below, and interacted with the electrovalves of the irrigation system to supply IN in plot 1 and 0.75 IN in plot 2. The AIC was remotely connected, so we could supervise and modify the control algorithms and the collected data from any computer connected to the internet.

The procedure to control irrigation, programmed in a user-friendly visual basic application, was as follows:

- 1) We fixed the time for the starting of the daily irrigation (10.00 am). At that time, the AIC started to interrogate the RIA website on the ET_o and R values of the previous day.
- 2) After collecting the ET_o and R values the AIC calculated IN as described in the FAO56 monograph (Allen *et al.*, 1998):

$$IN = \frac{1}{E_{IS}} (ET_o \cdot K_c \cdot K_r - P_e) \quad \text{Eq. 6.1}$$

where E_{IS} is the efficiency of the irrigation system; being a drip irrigation system, we consider $E_{IS} = 0.9$. K_c is the crop coefficient; we used representative values for almonds growing under conditions similar to those in our area (Sánchez-Blanco *et al.*, 1991). K_r is the coefficient related to the percentage of ground covered by the crop; in our case, $K_r = 1$ (Feres and Castel, 1981). P_e is

- the effective rainfall, considered here as 70% of P recorded by the weather station. This procedure has the advantage of considering the effect of the atmospheric demand on the crop water requirements, which is especially useful for species highly coupled with the atmosphere.
- 3) Then, the AIC opened the electrovalves to supply the required amount of water to each treatment, i.e. $IA = IN$ in plot 1 and $IA = 0.75 IN$ in plot 2. The system is designed to switch on & off the irrigation pump, but this was not necessary in our case, since water for irrigation was taken from a pressurized pipe, as mentioned in section 3.2.1.
 - 4) Every 5 min from the start of irrigation, the AIC read the θ_v values collected by the EnviroSCAN probes, and stopped irrigation when a fixed upper threshold value for θ_v was reached. In this work we used the $\theta_v = 0.2 \text{ m}^3 \text{ m}^{-3}$, the value for FC in field. This was aimed to avoid undesirable ponding conditions and to minimize evaporation losses.
 - 5) When θ_v decreased below a fixed low threshold value (80% of FC in our case), the system restarted the water supply.
 - 6) Steps 4 and 5 were repeated until the corresponding IA to each treatment was applied. The AIC worked on a time basis. The actual supplies were recorded by flow meters connected to the AIC, and the values stored.

6.3. Results and discussion

The AIC showed a good performance during the whole season. It calculated the daily IN values without our intervention, except for improvements in some of the algorithms. For both treatments, the cumulated IA supplied by the AIC showed a good agreement with the calculated values (Fig. 6.3), which shows that the device was able to control the opening and closing of the electrovalves properly. For the whole season, the water applied by irrigation was $4254 \text{ m}^3 \text{ ha}^{-1}$ in the 100% IN treatment and $3094 \text{ m}^3 \text{ ha}^{-1}$ in the 75% IN treatment.

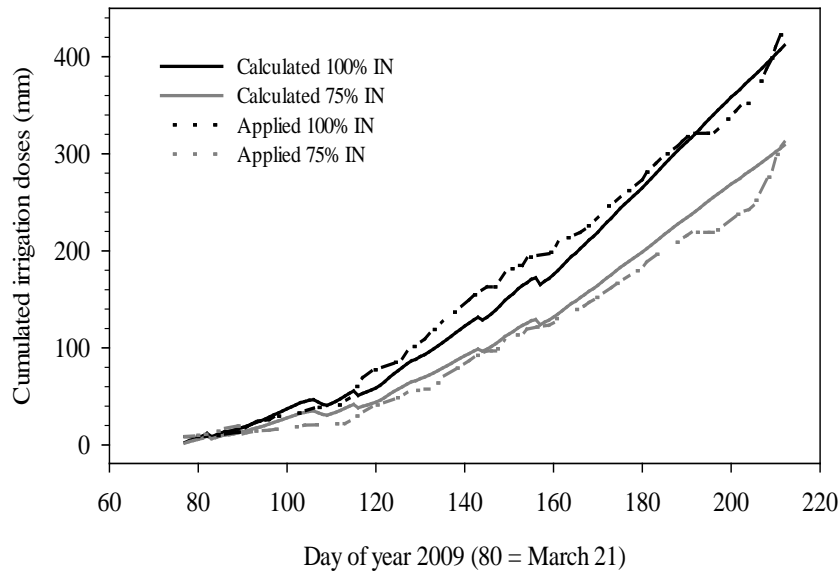


Fig. 6.3. Cumulated values of the water supplies made by the AIC in each treatment, as recorded by the flow meters. The irrigation needs calculated by the AIC with Eq. 1 (see text for details), are also shown.

The study on root distribution showed that most roots concentrated close to the drippers (Fig. 6.4), which suggests a good water-to-air equilibrium even in the volumes of the wet bulb with the greatest θ_v values. This shows that ponding conditions did not occur in the orchard, although we do not know whether this was due to the control of the water supplies by the AIC or to the hydraulic characteristics of the orchard soil.

Fig. 6.4 also shows that most of the roots were in the top 0.8 m of soil. Fig. 6.5 shows that in the 100% IN treatment the soil was close to FC all throughout the irrigation season, suggesting water losses below the maximum rooting depth. In the 75% IN treatment, however, θ_v values at 0.8 m were significantly lower (Fig. 6.5), which suggest that water losses by drainage, if any, were minimized in that treatment. This suggests that IAs in the 100% IN treatment were greater than the actual crop water needs. In fact, greater θ_v values were observed below the rootzone, at 1.5 m depth, in the 100% IN treatment than in the 75% IN treatment (Fig. 6.5). Both from visual observations in the trench dug for the study of the root system and data in Fig. 6.5 we assumed no influence of the water table in the root zone, despite of the proximity of the Guadalquivir river to the experimental orchard (Fig. 6.1). The seasonal evolution of the average θ_v values in the top 0.5 m of soil, where the maximum root densities were found (Fig. 6.4), shows little differences between the two irrigation treatments (Fig. 6.6). The relatively constant θ_v values recorded all throughout the season indicate that the water supplies in the 75% IN

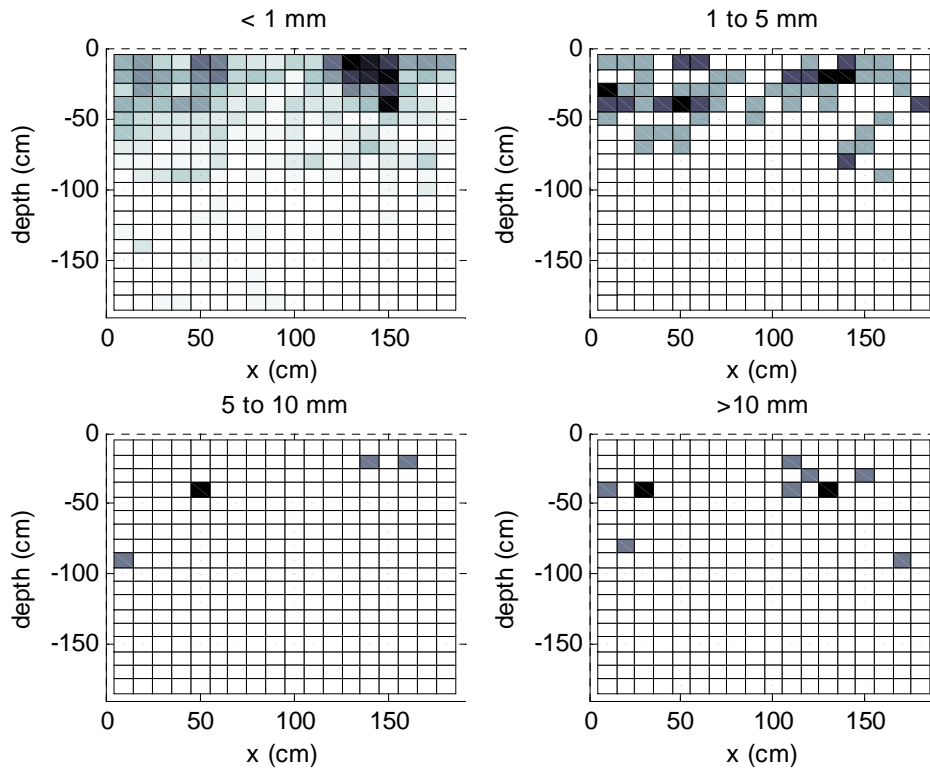


Fig. 6.4. Root distribution observed by the trench method in October 18th. The trench was dug in the vertical of the irrigation pipe. There was as a dripper at $x = 50$ cm and another at $x = 150$ cm.

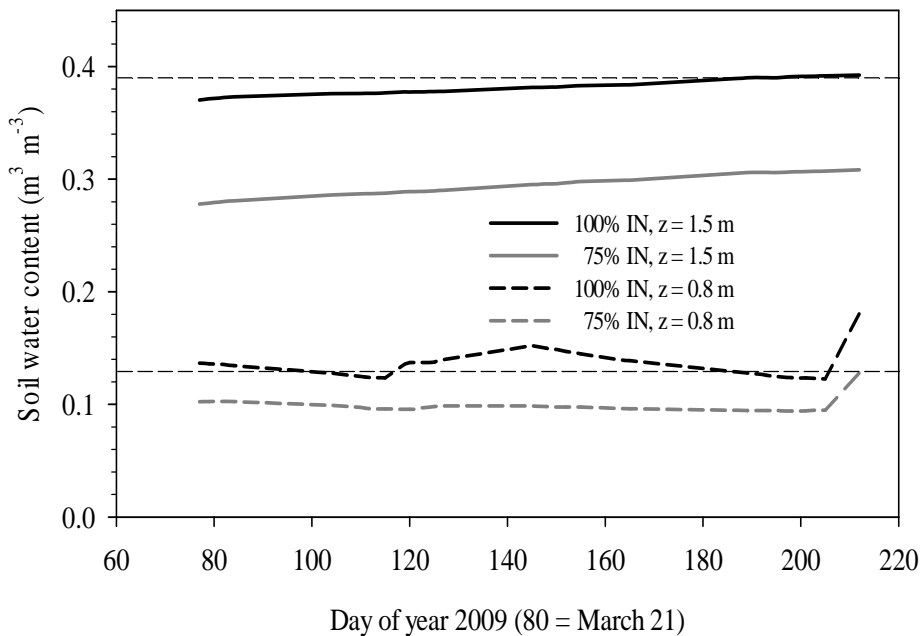


Fig. 6.5. Seasonal dynamics of the volumetric soil water content measured in both treatments at the maximum root depth (0.8 m) and at 1.5 m depth. See text for details on the treatments and on the measurements. Dashed lines represent the water contents at field capacity (-0.03 MPa) and wilting point (-1.5 MPa).

treatment were enough to replace the crop water needs. This agrees with the results on fruit production, since no statistical differences in yield were found between treatments (75% IN = $1787 \pm 390 \text{ kg ha}^{-1}$; 100% IN = $1906 \pm 210 \text{ kg ha}^{-1}$).

The usefulness of FDR measurements for irrigation management has been reported by several authors (Thompson *et al.*, 2007a, b). For reliable results, both *In situ* probe calibration and a number of probes according to the soil variability are required (Hidalgo *et al.*, 2003). Although the dynamics of the soil water content in the root zone is considered by some as sufficient to estimate the crop water needs (Fares and Alva, 2000), some authors recommend combining soil water measurements with plant-based measurements (Intrigliolo and Castel, 2004). Our results show that the control of IA in our orchard was improved by combining the IN values calculated with the crop coefficient approach and real time values of θ_v .

6.4. Conclusions

The tested prototype of the AIC proved to be robust and reliable enough for the automatic control of high-frequency irrigation in fruit tree commercial orchards. The device seems to be useful to minimize ponding conditions and water losses by drainage and evaporation from the soil surface, and it can be used for irrigating orchards in remote areas, through the internet. Our results show that IAs can be precisely controlled by combining soil water measurements with the crop coefficient approach, which takes into account the response of the crop to the atmospheric demand. Our results also show that standard K_c values derived for almond orchards are too high for our orchard conditions.

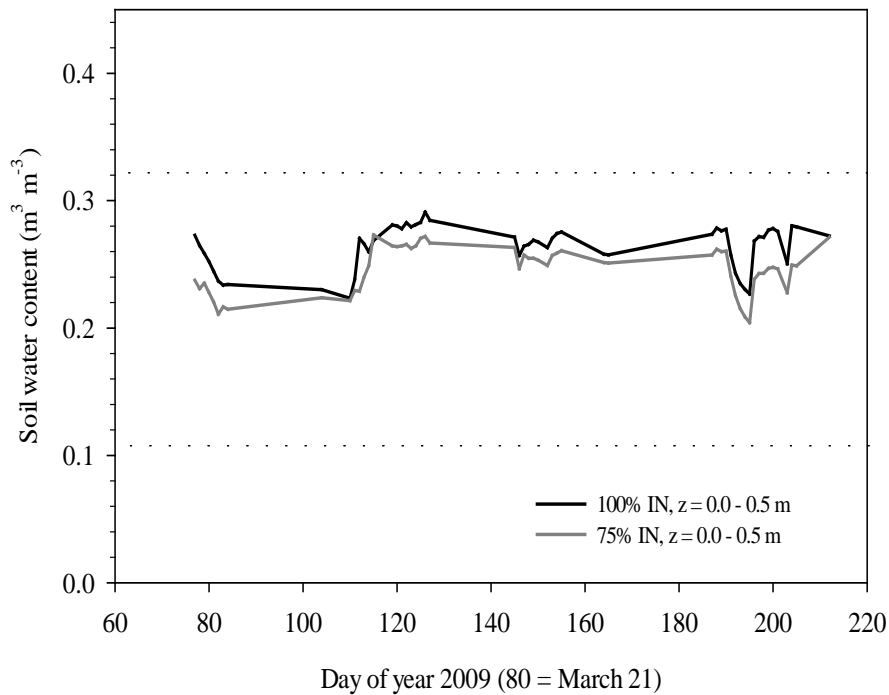


Fig. 6.6. Seasonal dynamics of the average volumetric soil water content in the top 0.5 m of soil of each treatment. See text for details on the treatments and on the measurements. Dashed lines as in Fig. 6.5.

6.5. References

- Allen RG, Pereira LS, Raes D, Smith M. 1998. Crop evapotranspiration-Guidelines for computing crop water requirements-FAO Irrigation and drainage paper 56. FAO, Rome 300:6541.
- Baronti P, Pillai P, Chook VWC, Chessa S, Gotta A, Hu YF. 2007. Wireless sensor networks: A survey on the state of the art and the 802.15. 4 and ZigBee standards. *Computer communications* 30(7):1655-1695.
- Carroll ZL, Oliver MA. 2005. Exploring the spatial relations between soil physical properties and apparent electrical conductivity. *Geoderma* 128(3-4):354-374.
- Clothier BE, Green SR, Deurer M. 2008. Preferential flow and transport in soil: progress and prognosis. *European Journal of Soil Science* 59(1):2-13.
- FAO. 1963. Carta bioclimática de la zona mediterránea. UNESCO-FAO.

- FAOSTAT. 2006. FAO Data for Agriculture: Statistics Database. FAOSTAT. Rome, Italy.
- Fares A, Alva AK. 2000. Evaluation of capacitance probes for optimal irrigation of citrus through soil moisture monitoring in an entisol profile. *Irrigation Science* 19(2):57-64.
- Fereres E, Castel JR. 1981. Drip Irrigation Management. Division of Agricultural Sciences. University of California. Leaflet N° 21259. 2, 11-24.
- Fereres E, Evans RG. 2006. Irrigation of fruit trees and vines: an introduction. *Irrigation Science* 24(2):55-57.
- Fereres E, Soriano MA. 2007. Deficit irrigation for reducing agricultural water use. *Journal of Experimental Botany* 58(2):147-159.
- Fernández JE, Green SR, Caspari HW, Díaz-Espejo A, Cuevas MV. 2008. The use of sap flow measurements for scheduling irrigation in olive, apple and Asian pear trees and in grapevines. *Plant and Soil* 305(1-2):91-104.
- Fernández JE, Van Noordwijk M, Clothier BE. 2000. Water Uptake. In: Smit AL, Bengough AG, Engels C, Van Noordwijk M, Pellerin S, Van de Geijn SC, editors. *Root Methods A Handbook*: Springer-Verlag Berlin Heidelberg New York. p 461-507.
- Hidalgo J, Pastor M, Hidalgo JC. 2003. Evaluación de una sonda FDR para la estimación de la evolución del contenido de agua en el suelo y para el control de riegos en olivar. In: Álvarez-Benedí J, Marinero P, editors. *Estudios de la Zona No Saturada del Suelo VI*. p 171-175.
- Intrigliolo DS, Castel JR. 2004. Continuous measurement of plant and soil water status for irrigation scheduling in plum. *Irrigation Science* 23(2):93-102.
- Kachanoski RG, van Wesenbeeck IJ, Gregorich EG. 1988. Estimating spatial variations of soil water content using noncontacting electromagnetic inductive methods. *Canadian Journal of Soil Science* 68(4):715-722.

-
- López Riquelme JA, Soto F, Suardíaz J, Sánchez P, Iborra A, Vera JA. 2009. Wireless sensor networks for precision horticulture in Southern Spain. *Comput Electron Agric* 68(1):25-35.
- McNeill JD. 1980. Electromagnetic terrain conductivity measurement at low induction numbers: Technical Note TN-6. Geonics Limited Mississauga, Ontario.
- Morison JIL, Baker NR, Mullineaux PM, Davies WJ. 2008. Improving water use in crop production. *Philosophical Transactions of the Royal Society B: Biological Sciences* 363(1491):639-658.
- Rhoades JD, Chanduvi F, Lesch SM. 1999. Soil salinity assessment: Methods and interpretation of electrical conductivity measurements: Irrigation and Drainage. Paper 57. Food & Agriculture Organization of the UN (FAO).
- Rhoades JD, Prather PAC. 1976. Effects of Liquid-phase Electrical Conductivity, Water Content, and Surface Conductivity on Bulk Soil Electrical Conductivity. *Soil Science Society of America Journal* 40(5):651-655.
- Sánchez-Blanco MJ, Ruiz-Sánchez MC, Planes J, Torrecillas A. 1991. Water relations of two almond cultivars under anomalous rainfall in non-irrigated culture. *Journal of Horticultural Science (United Kingdom)* 66:403-408.
- Thompson RB, Gallardo M, Valdez LC, Fernandez MD. 2007a. Determination of lower limits for irrigation management using in situ assessments of apparent crop water uptake made with volumetric soil water content sensors. *Agric Water Manage* 92(1-2):13-28.
- Thompson RB, Gallardo M, Valdez LC, Fernandez MD. 2007b. Using plant water status to define threshold values for irrigation management of vegetable crops using soil moisture sensors. *Agric Water Manage* 88(1-3):147-158.
- van Noordwijk M, Brouwer G, Meijboom F, Oliverira MRG, Bengough AG. 2000. Trench profile techniques and core break methods. In: A.L. Smit, A.G. Bengough, C. Engels, M. Van Noordwijk, S. Pellerin, S.C. Van de Geijn, editors. *Root Methods A Handbook* Springer-Verlag Berlin Heidelberg New York. p 211-234.

Chapter 7

Improving methods to measure sap flow

Part of this chapter is in:

Romero R, Green S, Muriel JL, Garcia I, Clothier B. 2011. Improving Heat-Pulse Methods to Extend the Measurement Range Including Reverse Flows. VIII International Workshop on Sap Flow (Volterra, Italy). Submitted.

Abstract. Traditional heat-pulse methods are not well suited to measuring either very high or very low sap flows and few methods can measure reverse flow. We have analysed two new methods that potentially extend the measurement range. Both methods can be used by modifying the analysis algorithm and adjusting the probe positions of common heat-pulse methods, with no change to existing equipment. The first method we will refer to as the *symmetrical gradient* method (HPSG). It consists of averaging the temperature difference signal of two probes ($\overline{\Delta T}$) that are equidistant from the heater. The second method we will refer to as the *symmetrical derivative* method (HPSD). It uses the same symmetrical probe configuration. However, the analysis is based on the maximum rate of change of the temperature difference curve (i.e. the derivative, $\Delta T'$). We use computer modelling to show that these two indicators ($\overline{\Delta T}$ and $\Delta T'_{max}$) are proportional to the heat-pulse velocity across a wide range of positive and negative flows. Hence, both metrics can be used to determine the actual sap flux density with acceptable measurement errors and good measurement sensitivity. We present results from field experiments on a willow tree (*Salix alba* L.) that was set up to compare our new methods against other heat-pulse techniques. We show that HPSG and HPSD both provide reliable data across a very wide range of flows. We are currently working on other field experiments to further refine our use of HPSG and HPSD to estimate tree transpiration and even to observe sap flow in roots.

7.1. Introduction

Various thermal methods are available to measure sap flow in the stem or roots of trees. These methods can be broadly divided into those based on heat balance and those based on heat pulse. Detailed reviews have been compiled by Fernandez *et al.* (2009), Campbell (1991), Swanson (1994), Čermák (1995), Smith and Allen (1996), Kostner *et al.* (1998) and Čermák and Nadezhdina (1998), amongst others. The main advantages of the heat-pulse method are that the instrumentation is simple, the probes are robust, and the measurements are reliable and accurate (Green, 1998). In the work described here, we used the Green's heat-pulse velocity (HPV) system that traditionally employs both the compensation and the T-max heat-pulse methods.

The compensation method (CHP) uses two temperature sensors placed asymmetrically upstream and downstream of a needle heater that is inserted radially into the conducting sapwood. A brief pulse of heat (1-2 s) is released from the needle and the time delay (t_z , s) for an equal temperature rise at both sensors is used to derive a heat pulse velocity. Alternatively, the T-max method (Cohen *et al.*, 1981) uses a single temperature sensor located downstream of the line heater, and the time delay (t_M , s) for a maximum rise at the downstream sensor is used to derive the heat-pulse velocity.

An important limitation of both techniques is that they do not work well at very low sap flux densities ($< 5 \text{ cm h}^{-1}$), as can occur, for example, during nocturnal transpiration in dry farming or deficit irrigation situations. In addition, these two traditional techniques cannot resolve reverse (or negative) sap flow, which may result from hydraulic redistribution (Bleby *et al.*, 2010; Nadezhdina *et al.*, 2010). Furthermore, under conditions of very high evaporative demand, the sap flux density in some plants can even exceed the limit of heat-pulse measurement.

Recently, Testi and Villalobos (2009) reported a modification to the compensation method, which they called the calibrated gradient method, CAG. This new method extends the low range of CHP to zero and even negative flows, although some improvements can be made for high and even moderate flows (Green *et al.*, 2008b). The heat ratio method (HRM) of Burgess *et al.* (2001) is an alternative heat-pulse method

developed to accurately measure low and reverse sap flow. This method uses the ratio of the temperature increase at points equidistant downstream and upstream from a line heater, evaluated some 60-120 s after the release of a heat pulse. Full details of the HRM configuration, corrections for wounding, and other operational factors are described by Burgess *et al.* (2001). The HRM method is sensitive to the direction of sap flow, being able to measure reverse flow in roots and other conductive organs, but it fails at higher flows (Green *et al.*, 2008b).

In order to extend the measurement range of heat pulse, we propose two new methods and compare their performance against more traditional heat-pulse methods.

7.2. Materials and methods

7.2.1. Two new heat-pulse methods

We present in this paper, for the first time, a practical analysis of two new heat-pulse methods, which potentially extend the measurement range of heat pulse:

- The first method, that we will call the *symmetrical gradient* (HPSG), follows a similar philosophy to the CAG, but employs a symmetrical layout of the sensors. The indicator ($\overline{\Delta T}$, °C) consists of averaging the difference in temperature signal (ΔT) between the two probes, for an as yet undetermined length of time after applying the heatpulse (Fig. 7.1).
- The second method we are proposing is called the *symmetrical derivative* (HPSD) method. It uses the same symmetrical installation of the temperature sensors and heater as in the HPSG method. However, in this case the indicator of sap flow is now the maximum rate of change (slope) of the ΔT curve (Fig. 7.1), i.e.: mathematically this is represented by $\Delta T'_{max} = \max_t \frac{d\Delta T(t)}{dt}$ (°C s⁻¹).

Computer simulations with the heat-pulse model of Green *et al.* (2003) show that the two new indicators ($\overline{\Delta T}$ and $\Delta T'_{max}$) have a very high linear correlation with heat-pulse velocity (Fig. 7.2). Linear correlations remain for a wide range of sap flux densities including reverse or negative flows. Another advantage of the new methods cf. CAG is that a zero value of the indicators means zero sap flow, owing to the symmetrical configuration of the probes.

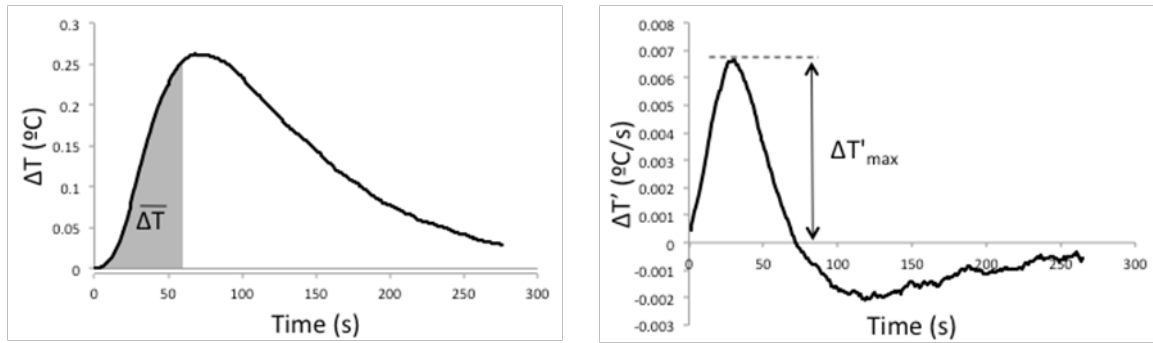


Fig. 7.1. Analysis scheme for two new heat-pulse methods. The left panel represents the Symmetrical Gradient method (HPSG) whereby the temperature difference signal is averaged over the first 60 s ($\overline{\Delta T}$). The right panel shows the Symmetrical Derivative method (HPSD) where we register the maximum value of the derivative of the temperature difference signal.

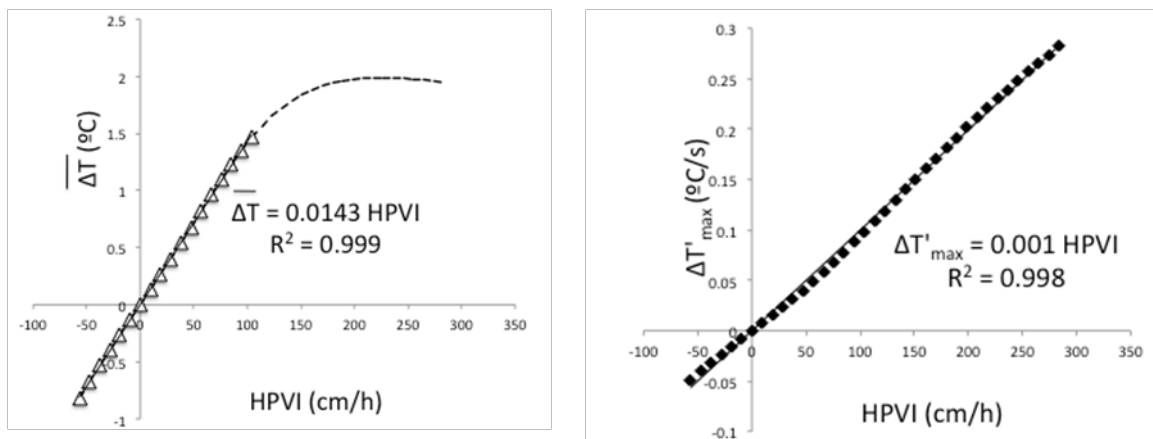


Fig. 7.2. Computer simulations of the performance of two new heat-pulse methods. The left panel shows the Symmetrical Gradient method (HPSG) and the right panel shows the Symmetrical Derivative method (HPSD). A strong linear relationship exists between these indicators ($\overline{\Delta T}$, and $\Delta T'$) and the imposed heat-pulse velocity, HPVI.

In practice, we have used conventional CHP equipment and simply altered the location of the temperature sensors relative to the heater probe, and modified the analysis routines. For the HPSG and HPSD methods, the temperature sensors were symmetrically installed at 10 mm either side of the heater (Fig. 7.3). In the case of the HPSG method, the heat-pulse velocity is estimated using the linear relation $HPV = K_{SG} \cdot \overline{\Delta T}$, where K_{SG} ($\text{cm } ^\circ\text{C}^{-1} \text{ h}^{-1}$) is a proportionality constant that can be obtained empirically or through computer modelling. In the case of the HPSD method, the heat-pulse velocity is estimated using the linear relationship $HPV = K_{SD} \cdot \Delta T'_{max}$, where K_{SD} ($\text{cm s } ^\circ\text{C}^{-1} \text{ h}^{-1}$) is a different

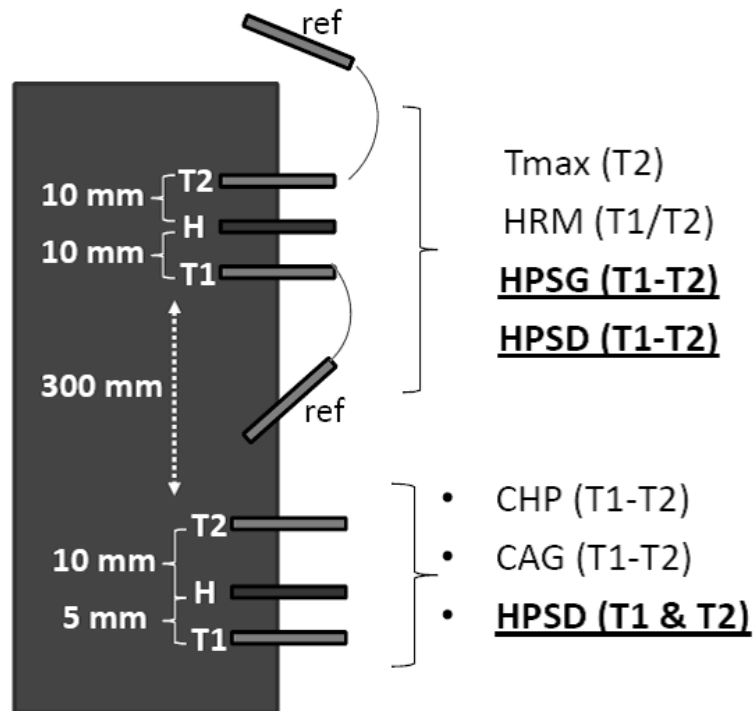


Fig. 7.3. Location of probes used in the willow experiment. Using just three sets of conventional probes, we were able to test and compare five different heat-pulse methods (CHP, T-max, HRM, CAG, HPSG and HPSD). Here, T is the temperature difference recorded following application of the 1-2 s heat pulse.

proportionality constant that can also be estimated empirically or from computer simulations.

7.2.2. Experimental site

A field experiment was set up in the branch of an 8-year-old willow tree (*Salix alba* L.) from December 2009 to February 2010. Three sets of probes were used to test the behaviour of these new methods against the more traditional approaches. The experimental set up is shown in Fig. 7.3. Each set of probes consists of a linear heater and two temperature sensors that were installed radially into the branch. The equipment was connected to a datalogger (model CR1000, Campbell Scientific, USA) powered with a 12V 7Ah battery charged by a 5W solar panel. Salient features of the HPV system are described in Green *et al.* (2003). In addition, we used a voltage regulator to reduce the effects of power fluctuations on the sap flow measurements. Using three sets of standard probes (model HP2TC, Tranzflo NZ Ltd, Palmerston North, NZ) located in the same

branch, we were able to test five different heat-pulse methods (CHP, T-max, CAG, HRM, HPSG and HPSD), by simply modifying the analysis routines performed by the data logger.

In practice, these new methods are working with very small temperature difference signals, and so it is essential to filter out any temperature ‘spikes’. Convoluted splines (Green, 2008a) were used to smooth the ‘raw’ temperature curves and, more importantly, to differentiate ΔT signals, as required for the HPSD method. While filtering is helpful for the HPSG method to improve the accuracy of the measurements, it is essential for the HPSD method because at very low flows the signal-to-noise ratio can exceed one.

7.3. Results and discussion

For the purpose of evaluation, we first used the big leaf model of Green (1993) to calculate transpiration losses from the willow branch. These calculations used meteorological data recorded from a nearby automatic weather station, and assumed a unit leaf area.

Fig. 7.4 compares the modelled transpiration against sap flux density measured using the new heat-pulse methods. From this graph, we can see that both methods essentially capture the daily dynamics of the transpiration. A scatter plot of the same data also reveals there to be a very strong linear correlation between these calculations of transpiration and data from our new heat-pulse methods (Fig. 7.5).

Furthermore, we also performed a comparison between our new heat-pulse methods and the more traditional CHP and T-max methods. From Fig. 7.6 it is clear that both of our new methods work equally well across the same range of sap flux densities compared with both the compensation and the T-max method. As expected, both of the new methods can resolve much lower flows than can be detected by the T-max method.

Finally, a scatter plot of data from the new methods compared with CHM also reveals a very strong linear relationship (Fig. 7.7).

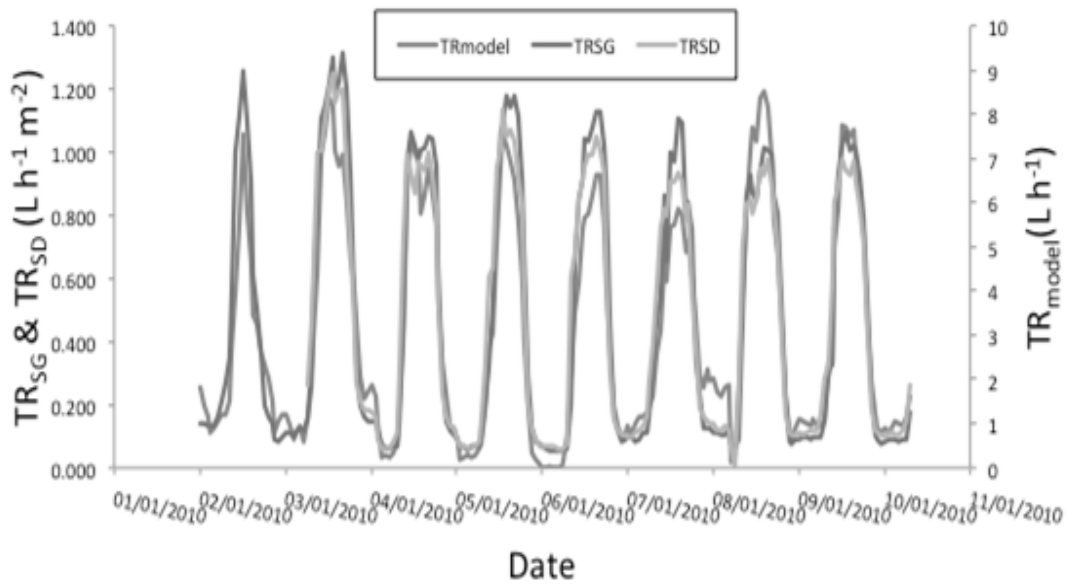


Fig. 7.4. A comparison between sap flux density measurements obtained with the new Symmetrical Gradient (TR_{SG}) and Symmetrical Derivative (TR_{SD}) heat-pulse methods, versus branch transpiration calculated using a big-leaf model (TR_{model}).

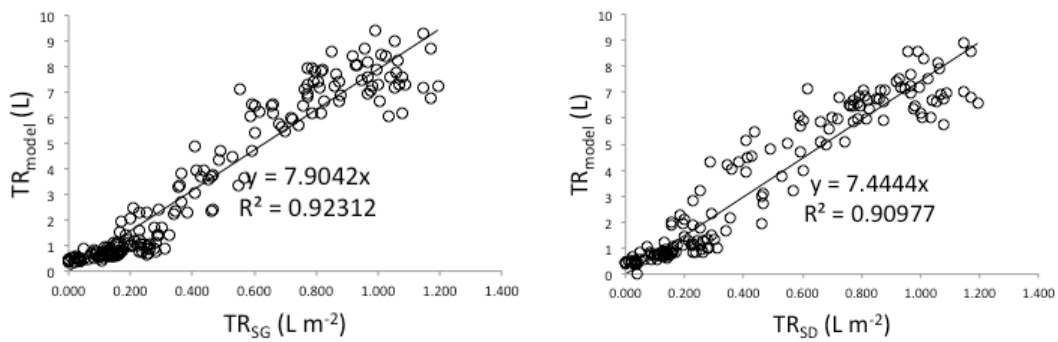


Fig. 7.5. Scatter plots showing the relationship between sap flux density obtained from the new Symmetrical Gradient (TR_{SG}) and Symmetrical Derivative (TR_{SD}) methods and branch transpiration estimated by big-leaf model (TR_{model}).

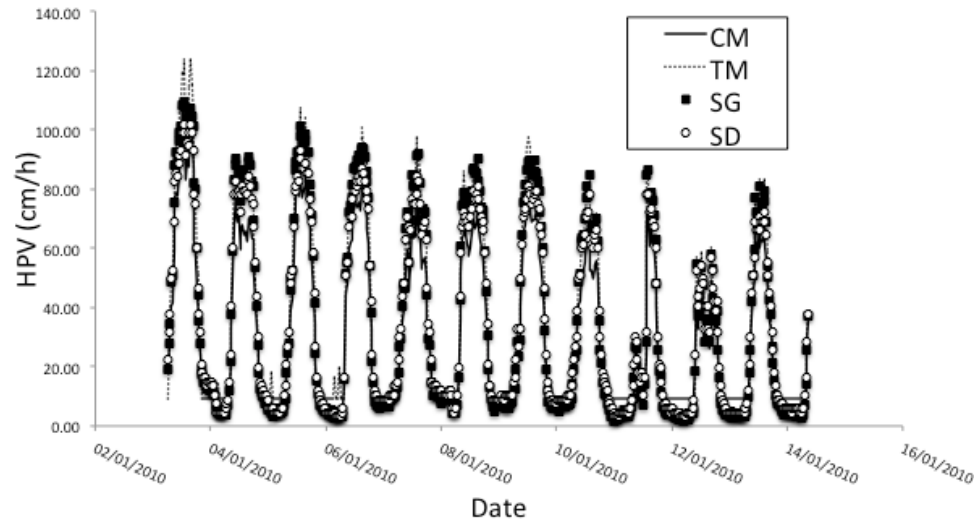


Fig. 7.6. Comparing the temporal evolution of the heat pulse velocity from the new Symmetrical Gradient (SG) and Symmetrical Derivative (SD) methods and from the traditional compensation (CM) and T-max (TM) methods in the willow tree.

7.4. Conclusions

Two new methods that extend the working range of heat pulse have been evaluated using field experiments and computer modelling. These new methods successfully capture the dynamic pattern of daily sap flow, as calculated using a big-leaf model for a single branch and as measured using traditional CHP and T-max methods. In both cases, we found a strong linear relationship between our new heat-pulse methods and corresponding data from other more traditional heat-pulse methods, across a wide range of sap flux densities where traditional approaches work well. In theory, these new methods are also well suited to low and even reverse flows.

With modern data loggers, the HPSG and HPSD methods are very simple to implement and offer an alternative practical approach to sap flow measurement across the full range of natural flows, including in the reverse direction. Although more experiments should be carried out to check and calibrate our two new methods, preliminary results presented here look to be very promising.

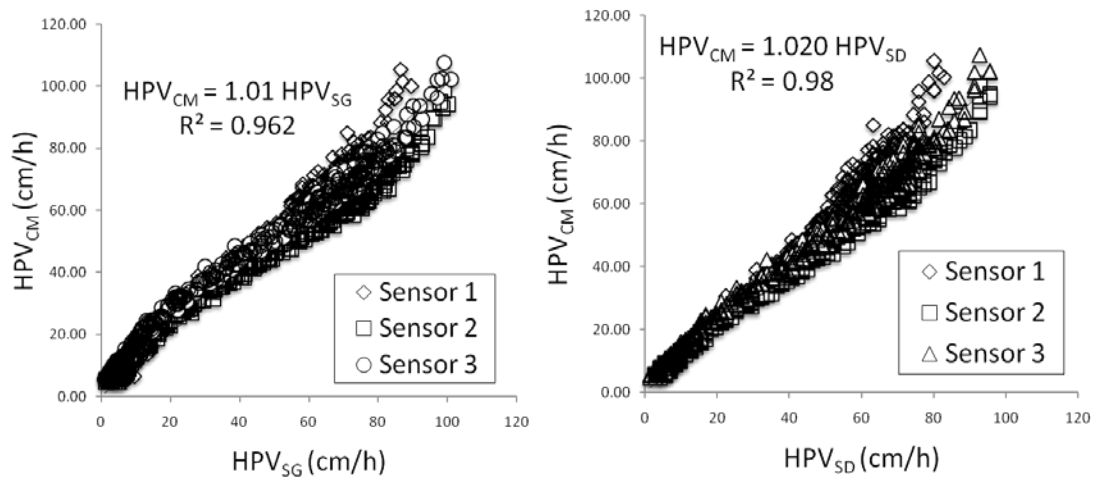


Fig. 7.7. Linear correlations between the heat-pulse velocity from the new Symmetrical Gradient (SG) and Symmetrical Derivative (SD) methods and from the compensation method (HPVCM) in the willow tree.

7.5. Acknowledgements

This work was funded by the Spanish Ministry of Science and Innovation, research project No. AGL2009-11310, the Regional Ministry of Innovation, Science and Enterprise of the Andalusian Government, Incentivos 2/2009, and the New Zealand Ministry of Agriculture and Forestry (SFF 08/054).

7.6. References

- Bleby TM, Mcelron AJ, Jackson RB. 2010. Water uptake and hydraulic redistribution across large woody root systems to 20 m depth. *Plant, Cell & Environment* 33:2132-2148.
- Burgess SSO, Adams MA, Turner NC, Beverly CR, Ong CK, Khan AAH, Bleby TM. 2001. An improved heat pulse method to measure low and reverse rates of sap flow in woody plants. *Tree Physiology* 21(9):589-598.
- Campbell GS. 1991. An overview of methods for measuring sap flow in plants. Collected summaries of papers at the 83rd annual meeting of the American Society of

- Agronomy, Division A-3: Agroclimatology and agronomic modelling Denver, Colorado, Oct27-Nov2, 1991.
- Čermák J. 1995. Methods for studies of water transport in trees, especially the stem heat balance and scaling. Proc 32nd Course in Applied Ecology, San Vito di Cadore, University of Padova, Italy, Sept 4-8, 1995.
- Čermák J, Nadezhdina N. 1998. Brief review of present techniques used for sap flow measurements in intact plants. Proc 4th International Workshop on Measuring Sap Flow in Intact Plants Židlochovice, Czech Republic, Oct 3-5, 1998 IUFRO Publications Publishing house of Mendel Univ Brno. p 4-11.
- Cohen Y, Fuchs M, Green GC. 1981. Improvement of the heat pulse method for determining sap flow in trees. *Plant, Cell & Environment* 4(5):391-397.
- Fernández JE, Čermák J, Cohen Y, Ferreira I, Nadezhdina N, Testi L. 2009. Methods to Estimate Sap Flow. ISHS Working Group on Sap Flow. www.wgsapflow.com/methods.pdf.
- Green SR. 1993. Radiation balance, transpiration and photosynthesis of an isolated tree. *Agricultural and Forest Meteorology* 64(3-4):201-221.
- Green SR. 1998. Measurements of sap flow by the heat-pulse method. An instruction manual for the HPV system. HortResearch internal report IR98. HortResearch Ltd, Palmerston North, New Zealand.
- Green SR, Clothier B, Jardine B. 2003. Theory and practical application of heat pulse to measure sap flow. *Agronomy Journal* 95(6):1371-1379.
- Green SR. 2008a. Measurement and modelling the transpiration of fruit trees and grapevines for irrigation scheduling. *Acta Hort* 792:321-332.
- Green SR, Clothier B, Perie E. 2008b. A Re-Analysis of Heat Pulse Theory across a Wide Range of Sap Flows. *Acta Hort (ISHS)* 846:95-104.
- Köstner B, Granier A, Čermák J. 1998. Sapflow measurements in forest stands: methods and uncertainties. *Ann Sci For* 55:13-27.

Nadezhdina N, David TS, David JS, Ferreira MI, Dohnal M, Tesa M, Gartner K, Leitgeb E, Nadezhdin V, Cermak J. 2010. Trees never rest: the multiple facets of hydraulic redistribution. *Ecohydrology* 3:431-444.

Smith DM, Allen SJ. 1996. Measurement of sap flow in plant stems. *Journal of Experimental Botany* 47(12):1833-1844.

Swanson RH. 1994. Significant historical developments in thermal methods for measuring sap flow in trees. *Agricultural and Forest Meteorology* 72(1-2):113-132.

Testi L, Villalobos FJ. 2009. New approach for measuring low sap velocities in trees. *Agricultural and Forest Meteorology* 149(3-4):730-734.

Chapter 8

Modeling and control of the soil water content in an almond orchard

Part of this chapter is published in:

Romero R, Muriel JL, García I, Muñoz de la Peña D. 2010. Modelo suelo-planta-atmósfera para experimentación de control de riego. Proceedings of the XXXI Jornadas de Automática, Jaén, Spain, Sept. 2010.

Romero R, Muñoz de la Peña D, Muriel JL, Fernández JE. 2011. Modeling and control of the soil water content in an almond orchard. Computers and Electronics in Agriculture. Submitted.

Abstract. In this chapter we present a soil-plant-atmosphere (SPA) model which can be used in a intuitive way to simulate water transport in a crop field and to design and test irrigation control strategies including model-based strategies. Using this model, we propose and test different controllers for precision irrigation based on classical proportional-integral-derivative (PID) control schemes, feedforward schemes and model predictive control (MPC). Our model requires daily potential evapotranspiration and rainfall inputs, and initial values for root depth and leaf area index, generating soil water content (SWC) outputs in every soil layer. Evaporation and transpiration, root and leaf area index growth and water balance models were implemented in Simulink blocks. We identified and validated the main parameters of the model with field data from an almond orchard during year 2010. We compared the performance of MPC and PID strategies to control SWC in simulations with our model. PID control showed several implementation advantages, although MPC showed better tracking results due to the incorporation of forecasts of potential evapotranspiration and precipitation and the changes in SWC references. We finally applied the PID strategy to control irrigation in a real almond orchard with promising results. This work is intended to be continued in a future practical implementation of the MPC strategy in our almond orchard.

8.1. Introduction

Several soil-plant-atmosphere (SPA) models have been developed in the past to simulate transport of water in soils. For a detailed review see Bastiaanssen *et al.*, 2007. Most of the models are programmed in FORTRAN (Green, 2001; Van Dam *et al.*, 2008) or similar non-graphical programming languages, so a medium-high level of knowledge about programming is required to use these models. Moreover, many of these models are not open source code, so it is difficult or even impossible to modify or improve them. In such cases, it is not easy to know exactly which equations and assumptions the authors used, how they were implemented in the code, or how those equations are interrelated. In addition, many parameters have to be introduced by the users in an often-tedious way. Another lack of the literature is that, in spite of the fact that many efforts have been done to model the SPA continuum; there are few references about controlling these systems. Automatic control theory has been extensively used in other areas of science and industry with great success, but it still has not been applied to agricultural research, in particular to precise irrigation. Several applications have been reported to greenhouses (Blasco *et al.*, 2007; Alimardani *et al.*, 2009; Hashimoto, 1980; Magliulo *et al.*, 2003; Beeson, 2011), and relatively simple applications to open air cultivation, especially on drip irrigation (Shock *et al.*, 2002; Nogueira *et al.*, 2003; Muñoz-Carpena *et al.*, 2008) and center pivots (O'Shaughnessy and Evett, 2010; Peters and Evett, 2008). Most of these results are based in proportional or on/off controllers and, in general, there are few applications of model-based control schemes such as model predictive control (MPC) to precise irrigation of open air orchards. However, several authors have shown the promising advantages of these controllers in other fields such as the environmental control of greenhouses (Rodriguez *et al.*, 2008; Piñón *et al.*, 2005; El Ghoumari *et al.*, 2005).

Model predictive control (MPC) was first proposed in the mid 70's of the past century (Richalet *et al.*, 1978; Cuttler and Ramaker, 1980). Since then, MPC has been widely applied in the refining and petrochemical industry. More than a specific kind of controller, model predictive control is a generic method that uses a mathematical model to predict the time evolution of a system and minimize a cost function based on this prediction. MPC is especially suitable for multivariable systems under restrictions and estimated perturbations, which is the case of irrigation problems in which weather forecasts are available. The crops considered in this thesis can be modelled as

multivariable hybrid systems subject to input constraints and measurable perturbations and hence MPC is particularly appropriate for designing precision irrigation control scheme.

Motivated by these issues, the aim of this chapter is twofold: first, to present a SPA model which can be used (and modified) in a very intuitive way, to simulate water transport and to design and test control strategies including model-based strategies; and second, to propose and test different control strategies for precision irrigation based on classical proportional-integral-derivative (PID) control schemes and MPC.

We will show the SPA model developed and structured in Simulink blocks as well as the underlying assumptions and equations. We will detail the identification and validation processes needed to use the model and how it was applied to a real field experiment. Then, we will present four control strategies: 1) a feed-forward control strategy, which calculates irrigation to compensate actual crop evapotranspiration (ET_c , mm); 2) a PID controller; 3) a PID with feed-forward; and 4) an MPC controller based on the identified SPA model. We analysed the performance of these strategies in simulation using the proposed SPA model. Finally, we will present the results of field experiments in which the ET_c compensation and PID controller were tested in an almond orchard located in the IFAPA Las Torres research centre.

8.2. Materials and methods

8.2.1. Experimental site

We carried out field experiments in the orchard described in section 6.2.1 both to test the proposed model of the SPA and to carry out a field experiment of a PID irrigation controller. The 1 ha orchard, planted with 9-year-old almond trees, is located in the experimental farm of the IFAPA, at 18 km to the north of Seville ($37^{\circ} 30'N$, $5^{\circ} 57'W$, ca. 10 m a.s.l.). The trees, spaced 6 m x 7 m, were, on average, 4.8 m in height and 5.0 m in diameter. The climate in the area is attenuated meso-mediterranean (FAO, 1963) with an average annual precipitation of 534 mm and ET_o of 1400 mm (period 1971-2000).

The soil is a silty loam typical fluvisol of 2.5 m depth, fertile, with organic matter content below 1.5 % and high cationic exchange capacity. Laboratory determinations

showed volumetric water contents (SWC) at field capacity (-0.3 MPa) and wilting point (-1.5 MPa) of $0.39 \text{ m}^3 \text{ m}^{-3}$ and $0.13 \text{ m}^3 \text{ m}^{-3}$, respectively. Field measurements, however, yielded SWC values equal to 0.22 close to the emitters 48 h after rainfall, therefore we consider this value as the value for field capacity (FC) in field conditions. The study on root distribution (section 6.2.2 and Fig. 6.4) showed that most roots concentrated close to the drippers, which suggests a good water-to-air equilibrium even in the volumes of the wet bulb with the greatest SWC values.

The irrigation system consisted of two laterals per tree row, one at each side of the trees, at 1 m from the trunk. The laterals had 4 L hour^{-1} drippers 1 m apart. The water supplied to the plot was controlled by two electrovalves connected to a pressurized pipe. These electrovalves were commanded by the automatic irrigation controller (AIC) described in sections 6.2.2 and 6.2.3.

8.2.2. SPA dynamic model

In general, an SPA model (Fig. 8.1) simulates the water transport through soil and plants to the atmosphere. Assuming a daily basis, the process can be summarized as follows. Most of the daily irrigation and effective precipitation is incorporated to the soil. Part of this water is retained in the soil and, when SWC is above a certain threshold, exceeding water is drained to deeper layers. During the day, trees consume some water from the soil for transpiration, through their roots to their leaves, and then to the atmosphere. Also some water is lost because direct evaporation from the soil to the atmosphere. Variations in the SWC of each layer can be calculated with a set of differential water balance equations, which account for irrigation (I , mm), effective precipitation (P_e , mm), actual evaporation (ER, mm) and transpiration (TR, mm) and drainage (D , mm). These set of equations are very difficult to implement, mainly because it is hard to define the value of each of these terms in continuous time. The drainage, precipitation, evaporation and so on depend in a highly nonlinear way of the state of the crop and in general they have a very high spatial and temporal variability. In addition, it is very hard to define the boundaries in which the water balances are studied.

We developed a discrete time mathematical model to obtain an approximate estimation of the behaviour of a given crop which can be used for doing predictions and design precision irrigation schemes on a daily time scale. The use of this time scale

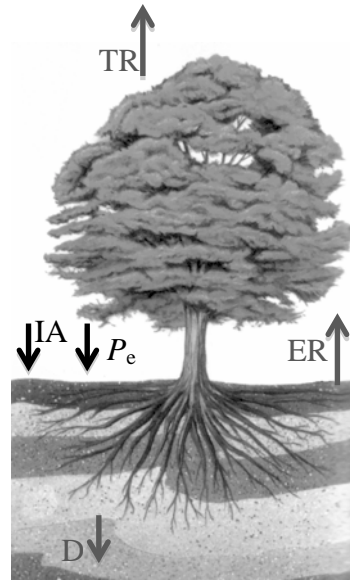


Fig. 8.1. Inputs and outputs of the soil-plant-atmosphere model. Variations in the soil water content are calculated as the sum of the inputs: irrigation amount (IA) + effective precipitation (P_e) minus the sum of the outputs: transpiration (TR) + evaporation (ER) + drainage below the rootzone (D)

allows obtaining an appropriate trade-off between precision and complexity of the resulting mathematical model, which in particular, is suitable for controller design purposes. Fig. 8.2 shows a Simulink implementation of the proposed model which consists of a series of blocks which represents several different physical processes of the SPA continuum.

The state of the proposed model is given by the SWC of a set of soil layers, the leaf area index (LAI), and the root depth (p , mm). The inputs are the potential evapotranspiration (ET_o , mm), irrigation amount (IA , mm) and effective precipitation (P_e , mm). SWC in each layer, LAI and p are accumulated in integrators. In particular, an herbaceous or fruit crop and a two-layer soil are represented. Using the model it is possible to predict not only the future value of the state variables, but also other processes such as evaporation, transpiration and drainage.

The interactions between processes in the Simulink model (Fig. 8.2) are represented by arrows connecting the blocks so the graph is very didactic and can be easily manipulated by the user. We present next the equations used in these blocks to evaluate each of the terms of the water balance of the SPA. Table 8.1 shows the symbol, units and definition of the variables and parameters, respectively, used in the proposed model.

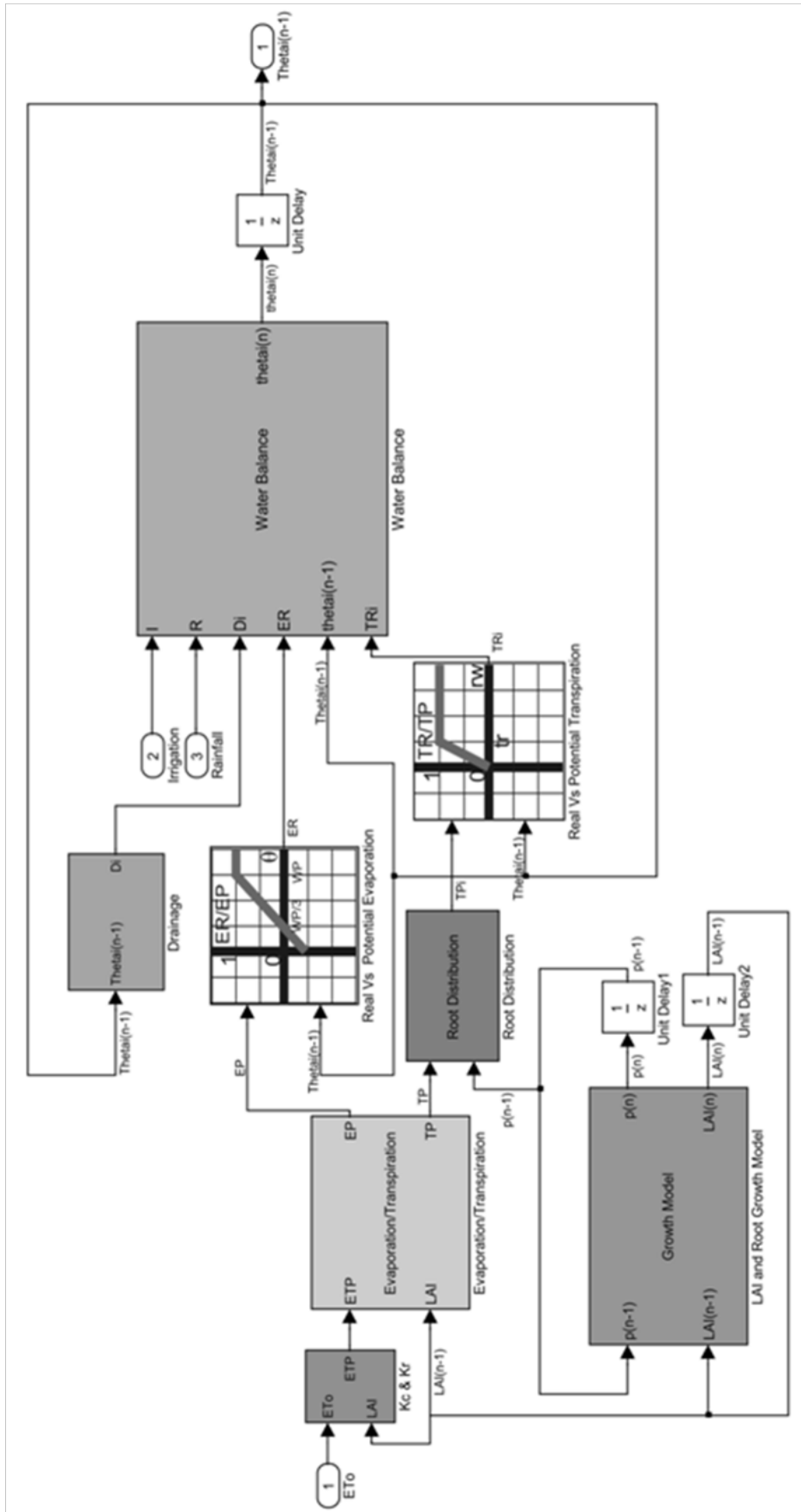


Fig. 8.2. Main diagram of the Simulink model to estimate soil water content from the evapotranspiration (ET_0), irrigation and precipitation inputs. $Thetai(n)$ is a vector composed of the soil water content in each layer in day n .

As previously mentioned, we model the soil water content in each layer with an integrator. The daily variations of the SWC in each layer (ΔSWC_1 and ΔSWC_2) are computed in the ‘*Water Balance block*’, in which the water balance equations are implemented in discrete time as follows:

$$\Delta\text{SWC}_1 = P_e + \text{IA} - \text{ER} - D_1 - \text{TR}_1 \quad \text{Eq. 8.1}$$

$$\Delta\text{SWC}_2 = D_1 - D_2 - \text{TR}_2 \quad \text{Eq. 8.2}$$

where, P_e is the effective precipitation, IA is the irrigation amount applied, ER is the evaporation, and D_i and TR_i represent the drainage and transpiration from layer i respectively.

In the ‘ K_c & K_r block’ the ET_0 values, received as input, are corrected by applying crop and reduction coefficients (K_c and K_r) to get the maximum crop evapotranspiration (ET_c , mm) as follows:

$$\text{ET}_c = \text{ET}_0 \cdot K_c \cdot K_r \quad \text{Eq. 8.3}$$

The coefficient K_c characterizes the specific crop (in relation to the reference crop) and the coefficient K_r accounts for the percentage of ground surface covered by the crop (Fereres and Castel, 1981).

Maximum crop evapotranspiration (ET_c) is partitioned in maximum soil evaporation (EP) and crop transpiration (TP) in the ‘*Evaporation/Transpiration block*’, according to the following equations (Brission *et al.*, 1992):

$$\text{EP} = \text{ET}_c e^{-K_{\text{LAI}} \cdot \text{LAI}} \quad \text{Eq. 8.4}$$

$$\text{TP} = \text{ET}_c \cdot \text{EP} \quad \text{Eq. 8.5}$$

Table 8.1. Variables and parameters of the SPA model.

Inputs		
Name	unit	Description
ET_o	mm	Potential evapotranspiration
P	mm	Precipitation
IA	mm	Irrigation amount
State		
Name	unit	Description
SWCi	mm	Water content in soil layer i
P	mm	Root depth
LAI		Leaf area index
Parameters identified from experimental data using least-squares		
Name	unit	Description
K_{LAI}	dimensionless	Extinction coefficient for solar radiation
d_{bulb}	mm	Irrigation bulb diameter
K_{rain}	mm mm ⁻¹	Precipitation reduction coef. (for the estimation of the effective precipitation)
FC_{rat}	mm mm ⁻¹	Field capacity ratio
WP_{rat}	mm mm ⁻¹	Wilting point ratio
$K_{c,i}$	mm mm ⁻¹	Crop coefficients
Parameters estimated using field measurements or from heuristics/crop knowledge		
Name	unit	Description
L_i	mm	Thickness layer i
K_r	mm mm ⁻¹	Reduction coefficient (ratio of ground surface covered by the crop)
P	mm	Root depth
p_{max}	mm	Maximum root depth (at the end of the crop development)
LAI_{max}	m ² leaf (m ² soil) ⁻¹	Maximum leaf area index (at the end of the crop development)
tr	mm mm ⁻¹	Threshold of available soil water below which there is water stress
RG_{root}	dimensionless	Root growth ratio
RG_{LAI}	dimensionless	LAI growth ratio
$SWC_{ini, rat}$	mm mm ⁻¹	Initial soil water content ratio (respect field capacity)

where K_{LAI} is the extinction coefficient for solar radiation and LAI is the leaf area index.

The root depth (p , mm) and the LAI are modelled as first order linear systems, which do not depend on the rest of the system variables:

$$\Delta p = RG_{root} \cdot (p_{max} - p) \quad \text{Eq. 8.6}$$

$$\Delta LAI = RG_{LAI} \cdot (LAI_{max} - LAI) \quad \text{Eq. 8.7}$$

where RG_{root} and RG_{LAI} are the root and LAI growth ratios and p_{max} , LAI_{max} are the maximum root depth and LAI. Note that the maximum values can be changed in order to account for the seasonal behaviour of the plant.

The ‘*Real vs. Potential Evaporation & Transpiration block*’ emulates an effect of the water deficit. When evaporation and transpiration deplete the SWC below a certain threshold, the retention forces of the soil compete for the water. Thus the potential evaporation and transpiration are reduced, according to the following pair of piece-wise affine functions (Feddes *et al.*, 2004), when SWC is depleted below the predefined water stress thresholds $\frac{\text{WP}_1}{3}$ and tr respectively, see Fig. 8.3.

$$\text{ER:} \begin{cases} \text{SWC}_1 < \frac{\text{WP}_1}{3} \rightarrow \text{ER} = 0 \\ \frac{\text{WP}_1}{3} \leq \text{SWC}_1 \leq \text{WP}_1 \rightarrow \text{ER} = \text{EP} \cdot \left(\frac{\text{SWC}_1 - \frac{\text{WP}_1}{3}}{\text{WP}_1 - \frac{\text{WP}_1}{3}} \right) \\ \text{SWC}_1 > \text{WP} \rightarrow \text{ER} = \text{EP} \end{cases} \quad \text{Eq. 8.8}$$

$$\text{TR}_i: \begin{cases} rw_i < \frac{\text{WP}_i}{3} \rightarrow \text{TR}_i = 0 \\ \text{WP}_i \leq rw_i \leq tr \rightarrow \text{TR} = rw_i \cdot \text{TP}_i \\ rw_i > tr \rightarrow \text{TR}_i = \text{TP}_i \end{cases} \quad \text{Eq. 8.9}$$

In these equations, SWC_i represent the soil water content in layer i , ER is the actual evaporation (mm), EP the potential evaporation (mm), WP the wilting point (mm), TR the actual transpiration (mm), TP the potential transpiration (mm), FC the field capacity (mm) and rw is the readily available water defined as follows:

$$rw = \frac{\text{SWC} - \text{WP}}{\text{FC} - \text{WP}} \quad \text{Eq. 8.10}$$

where the parameter tr represents the water stress threshold (in terms of rw) to calculate TR .

Water uptake by plants is distributed all along the soil profile according to the root distribution in the root distribution block. We assume that the potential

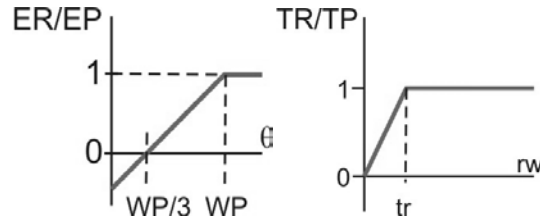


Fig. 8.3. Soil and plant water stress models (ER vs. EP and TR vs. TP).

transpiration in each layer is divided proportionally to the amount of roots in that layer. The ‘*Root Growth model*’ estimates the root depth, and then the ‘*Root Distribution block*’ divides the water uptake in each soil layer considering the amount of roots in it:

$$TR_i: \begin{cases} p \leq L_1 \rightarrow TP_1 = TP; TP_2 = 0 \\ p > L_1 \rightarrow TP_1 = TP \cdot \frac{L_1}{p}; TP_2 = TP - TP_1 \end{cases} \quad \text{Eq. 8.11}$$

where TP_i is the potential transpiration on layer i (mm), L_i the depth of layer i (m) and p the total root depth (m).

Finally, we modeled drainage between different layers in the ‘*Drainage block*’. We use the cascade “bucket” approach (Jothityangkoon *et al.*, 2001; Farmer *et al.*, 2003); that is, water accumulates in a layer until SWC exceeds field capacity, then drainage (D_i , mm) is generated to the layer below following the following equations:

$$D_i: \begin{cases} SWC_i \leq FC_i \rightarrow D_i = 0 \\ SWC_i > FC_i \rightarrow D_i = SWC_i - FC_i \end{cases} \quad \text{Eq. 8.12}$$

Eqs. 8.1-8.12 define the proposed SPA discrete time model based on a daily basis. Note that although the dynamics of the system are the water balance equations (modeled with integrators of the total intake), the relation between the state of the system, the inputs and the different terms of the balance equations is highly nonlinear. Under certain assumptions (in particular assuming constant root depth and LAI), the resulting model can be transformed into a hybrid dynamical system.

8.2.3. CROPSYST

To validate the proposed model, we compared it with the CROPSYST SPA model (Donatelli *et al.*, 1997). CROPSYST is a high precision SPA model based on partial differential equations, which has been widely used in agronomy. The code of CROPSYST is proprietary and in general is not appropriate for control purposes.

8.2.4. Model identification

In Table 8.1 we show a list of the parameters that define the proposed model. In order to use this model to carry out predictions or define an irrigation control law, these parameters must be identified. In general, each crop is different and the identification process must be done “ad hoc” for each application. The set of parameters shown in Table 8.1 can be divided into two different sets. The first set consists of the parameters that can be estimated from field measurements or from heuristic knowledge. The second set consists of those parameters that have to be identified using experimental data. We propose an identification procedure in two steps. First, a set of field experiments are carried out to identify the first set of parameters. Then, using experimental data, the rest of the parameters are defined.

The set of parameters that we propose to identify using field measurements are: L_i , K_r , tr , p_{\max} , LAI_{\max} , RG_{root} and RG_{LAI} . Each L_i can be set to describe a homogeneous layer of soil, with similar physical properties (textural classification). K_r can be calculated from the percentage of ground surface covered by the crop (Fererres and Castel, 1981). Finally, LAI and root related parameters can be obtained in previous independent experiments to define the LAI and root growth model. The LAI of a crop can be estimated using standard measurement methods such as those described in Jonckheere *et al.*, 2004, Weiss *et al.*, 2004 and Breda, 2003. Root depth can be measured from soil core samplings, trench wall methods or rhizotrons (Bengough *et al.*, 2000). In mature fruit trees during short periods (e.g. one irrigation season) LAI and p can be assumed constants ($LAI_{\max} = LAI_0$; $RG_{LAI} = 0$; $p_{\max} = p_0$; $RG_{\text{root}} = 0$).

In order to identify the second set of parameters, experimental data is needed, in particular, a historic set of all the inputs and outputs of the SPA system; that is, irrigation, precipitation, ET_0 and the resulting SWC trajectories, along a whole season or a long enough period. The values for SWC_i can be measured with soil water sensors

(TDR, FDR, neutron probes) or from gravimetric methods (Evelt *et al.*, 2008) while the weather conditions can be retrieved from historical data.

Following standard identification procedures, we propose to split the whole dataset recorded during the season in identification and validation data. Furthermore, we suggest to independently identify and validate the parameters for irrigation and non-irrigation periods in order to capture the dynamical behavior in this two different periods.

With the identification dataset we solved an optimization problem in MATLAB, in order to obtain the set of unknown parameters that minimized the mean squared (MSE) of the SWC in the root zone, defined as:

$$\text{MSE} = \frac{1}{N} \sum_{t=1}^N [\text{SWC}_{\text{act}}(t) - \text{SWC}_{\text{mod}}(t)]^2 \quad \text{Eq. 8.13}$$

where $\text{SWC}_{\text{act}}(t)$ and $\text{SWC}_{\text{mod}}(t)$ are the actual and the modeled SWC in the root zone in day t , respectively, and N the time length of the dataset in days. We used the function `fmincon` (constrained nonlinear minimization solver) and “active set” algorithm with the identification data set of irrigation and rainfall periods. MSE is a widely used indicator to quantify the difference between values implied by an estimator and the true values of the quantity being estimated. Note that in order to solve this optimization problem, we use all the parameters of the first set, which already were identified such as LAI or root depth.

One important parameter, which has to be identified, is K_c . In general, this parameter depends not only on the crop, but also on the time of the season. There are models in which K_c varies on a daily, monthly or even an annual basis. We propose to test several different parameterizations of the value of K_c along the identification period, which are the most common representations according to the usual practices of agronomist and FAO suggestions (FAO, 1998):

- One annual K_c for the whole season.
- A different constant value of K_c for each month considered. Since our experimental data finished on September 2010, we identified K_c from January to September.

- A piecewise linear curve obtained interpolating the values of K_c fixed at the central day of each month.
- K_c represented by a generalized curve (FAO56 Allen *et al.*, 1998), defined by the parameters shown in Fig. 8.4. The identified parameters were $K_{c,ini}$, $K_{c,med}$, $K_{c,end}$, t_{ini} , t_{dev1} , t_{dev2} and t_{end} .

We used the validation data set (Fig. 8.5) to simulate the model with the parameters identified as described. We compared the mean quadratic errors of the simulated SWC with the four models for K_c . First we run 1-step validations, in which the model estimates SWC from the actual SWC of the previous day. Then we run N-step validations, in which the model estimates SWC for the whole season from the actual SWC in the first day of the validation period. Identified parameters and validation results are shown in the results section.

8.2.5. PID control

Proportional-integral-derivative (PID) control is the most extended single-input single-output control loop in the industry. A PID controller tracks three terms: the error between the process variable and the setpoint (desired reference value), the integral of recent errors, and the rate by which the error has been changing. It computes its next corrective action from a weighted sum of those three terms (or modes), then outputs the results to the process and awaits the next measurement (Love, 2007). In this work we applied a PID to precise irrigation control of an almond orchard. We choose SWC in the root zone as the process variable to be controlled around a predefined set point. The code of the controller implemented in the field experiments is shown in the Appendix 8.A1.

We applied the Ziegler-Nichols tuning method (Ziegler and Nichols, 1942) for a first approximation of the proportional, integral and derivative coefficient of our PID controller. To do this, we simulated the proposed model (section 8.2.2) with a PID discrete controller in Simulink. Then coefficients were tuned to more conservative values. Finally, these coefficients were then used in the PID applied to the actual almond crop in the field experiments.

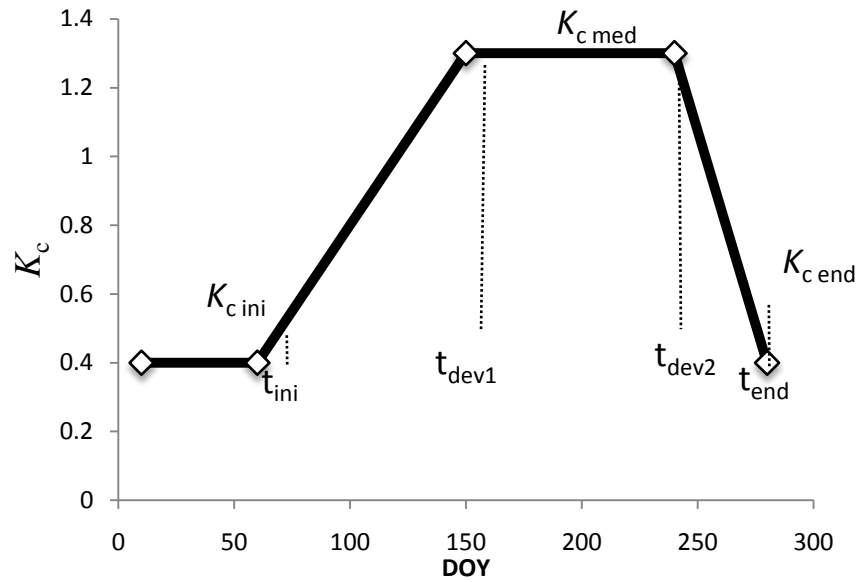


Fig. 8.4. Generalized crop coefficient (K_c) curve. DOY = day of year.

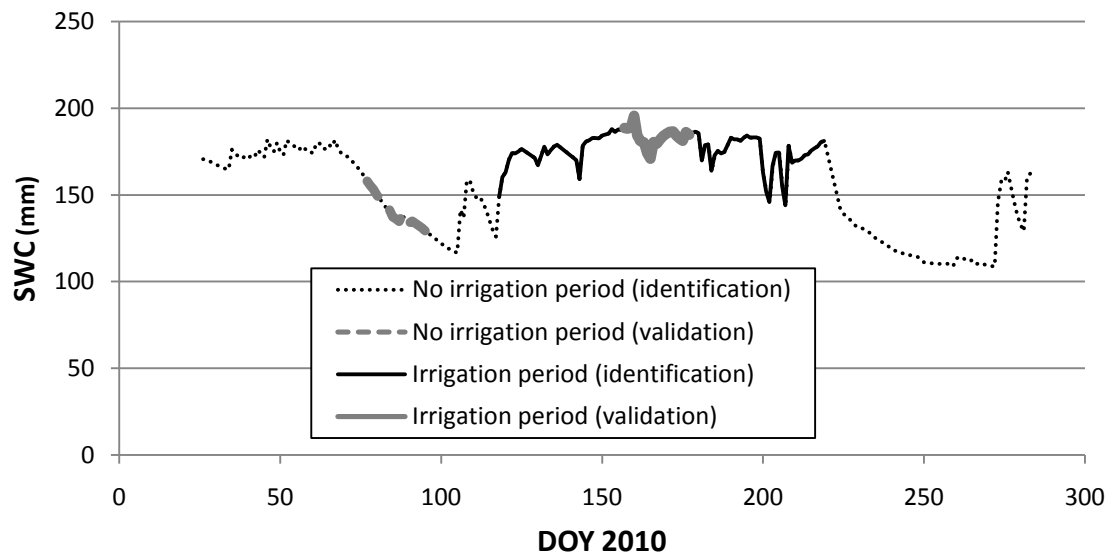


Fig. 8.5. Identification and validation data for irrigation and no irrigation periods. DOY = day of year. SWC = soil water content.

8.2.6. Model predictive control

An alternative to the PID technique is to use the knowledge of the system's dynamics to develop model-based controllers such as model predictive control (MPC), which is a generic method that relies on the following concepts:

- The use of a mathematical model to predict the evolution of a system over a finite period of time of N sampling instant (prediction horizon) given a future trajectory of the control inputs.
- Minimization of a cost function based on this prediction. The cost function depends on the predictions of the state and control actions.
- The use of a receding horizon strategy.

The idea is to obtain at each sampling instant the input trajectory (i.e. the optimal inputs over the entire prediction horizon), which minimizes the cost function based on the prediction of the system evolution. This is achieved by solving an optimization problem which also takes into account the constraints of the system. At the next time step the computation is repeated starting from the new state and over a shifted horizon, leading to a moving horizon policy, the so called receding horizon strategy.

MPC controllers can be defined for regulation or for reference tracking, which in general, is defined by the choosing of the cost function. Regulation MPC controllers penalize the deviation of the future state trajectories from a fixed equilibrium point. On the other hand, tracking controllers evaluate the cost based on the deviation from a desired state trajectory which can be time varying.

Over the last decade a solid theoretical foundation for MPC has emerged so that in real-life large-scale MIMO applications controllers with non-conservative stability guarantees can be designed routinely and with ease (Qin and Badgwell, 1997). However, the big drawback of MPC is the on-line computational effort, which may limit its applicability to relatively slow and/or small problems. For deterministic lineal models, the prediction of the future plant state is defined by linear functions of the initial state and the future inputs trajectories which leads to a quadratic program (QP) or a linear problem (LP) depending on the definition of the cost function. Nowadays, there are plenty of off-the-shelf efficient solvers for both LP and QP problems, which is one of the reasons of the success of MPC in the process industry (Camacho and Bordons,

2004), along with its inherent capability of including constraints, delays, and uncertainties explicitly into the controller formulation.

However, the model of the SPA system considered in this case is non linear and hence, standard MPC implementation techniques based on convex optimization algorithms cannot be applied. In particular, under certain assumptions, the SPA model belongs to the piecewise affine family. This class of systems leads to the use of modern hybrid MPC techniques, which we review next.

8.2.7. Hybrid MPC

The mathematical model of a system is traditionally associated with differential or difference equations, typically derived from physical laws governing the dynamics of the system under consideration. Consequently, most of the control theory and tools have been developed for such systems, in particular for systems whose evolution is described by smooth linear or nonlinear state transition functions. On the other hand, in many applications the system to be controlled is also constituted by parts described by logic, such as for instance on/off switches or valves, gears or speed selectors, and evolutions dependent on if-then-else rules. Often, the control of these systems is left to schemes based on heuristic rules inferred from practical plant operation.

MPC is denoted as hybrid MPC when it is based on models describing the interaction between continuous dynamics described by difference equations, and logical components described by finite state machines or if-then-else rules.

Bemporad and Morari (1999) introduced a class of hybrid systems in which logic, dynamics and constraints are integrated. They called them mixed logical dynamical (MLD) systems. The MLD formalism allows specifying the evolution of continuous variables through linear dynamic equations, of discrete variables through propositional logic statements and automata, and the mutual interaction between the two. The key idea of the approach consists of embedding the logic part in the state equations by transforming Boolean variables into 0-1 integers, and by expressing the relations as mixed-integer linear inequalities (see Bemporad and Morari, 1999; Torrisi and Bemporad, 2004 and references therein).

In order to obtain the model of SWC predictions, we have used a modelling language designed to describe hybrid models, called *hybrid system description language* (HYSDEL). In appendix 8.A2, we show the HYSDEL list used to model the SWC of a given crop field assuming that the LAI and the root depth are constant. This will allow us to use a set of available Matlab tools to simulate and design hybrid MPC controllers.

Controlling a system means to choose the command input signals so that the output signals tracks some desired reference trajectories. In Bemporad *et al.* (2000) and Bemporad and Morari (1999) the authors showed how mixed-integer programming (MIP) can be efficiently used to determine optimal control sequences. The Hybrid Toolbox for Matlab (Bemporad, 2004) can carry out simulations both in open-loop and in closed-loop, of hybrid systems controlled by MPC controllers. This toolbox includes the necessary mixed-integer solvers (or communication interfaces) needed to implement hybrid MPC controllers online. We use this toolbox to carry out the simulations of the MPC controller proposed next.

8.2.8. Model predictive control applied to crop fields

For the purpose of this thesis we focus on a tracking problem consisting in determining the optimal irrigation policies to drive the SWC trajectories as close as possible to a given reference or set point (SWC_{ref}). The predictions of the SWC are obtained from Eqs. 8.1-8.12. This set of equations provides a prediction of the future SWC in the first two layers of soil (SWC_1^{k+1} and SWC_2^{k+1}) from the current SWC (SWC_1^k and SWC_2^k), irrigation amount (IA^k), precipitation (P^k), atmosphere conditions (ET_0^k), leaf area index (LAI^k) and root depth (p^k) as follows:

$$[SWC_1^{k+1}, SWC_2^{k+1}] = f_{PWA}(SWC_1^k, SWC_2^k, IA^k, P^k, ET_0^k, LAI^k, p^k) \quad \text{Eq. 8.14}$$

This model is a discrete time nonlinear model subject to measured disturbances (P^k and ET_0^k).

In particular, the functions represented by the Eqs 8.8-8.10 are nonlinear, but assuming that LAI and root depth are constant along the whole prediction horizon, the

model becomes a piecewise affine (PWA) system, which is a particular case of hybrid systems. This class of systems has received a lot of attention in the last decade due to the advances in computational power and mixed-integer problems optimization algorithms. Although this class of optimization problems has in general a very high computational burden, in our application that is not an issue because the sampling time is very large (one full day).

The cost function considered in our MPC for irrigation of crop fields penalizes the infinity norm of both the deviation from the target reference SWC (SWC_{ref}) and the water usage (weighted by the design parameter c) along the prediction horizon N and is defined as follows:

$$J(SWC_1^k, SWC_2^k, \mathbf{IA}, \mathbf{P}, \mathbf{ET}_o, \mathbf{SWC}_{ref}) = \sum_{j=1}^N \left\| SWC_{ref}^{k+j} - SWC_1^{k+j} \right\|_{\infty} + c \left\| I^{k+j-1} \right\|_{\infty} \quad \text{Eq. 8.15}$$

where:

$$\mathbf{IA} = [IA^k, IA^{k+1}, \dots, IA^{k+N-1}]$$

$$\mathbf{P} = [P^k, P^{k+1}, \dots, P^{k+N-1}]$$

$$\mathbf{ET}_o = [ET_o^k, ET_o^{k+1}, \dots, ET_o^{k+N-1}]$$

$$\mathbf{SWC}_{ref} = [SWC_{ref}^{k+1}, SWC_{ref}^{k+2}, \dots, SWC_{ref}^{k+N}]$$

The irrigation is subject to the following constraint:

$$0 \leq IA^{k+j} \leq IA_{max} \forall j \in [0, N-1]$$

where IA_{max} is the maximum irrigation allowed by the user in one day.

Note that in order to evaluate J given an initial state and future input trajectory (which is the decision variable), a prediction of the precipitation and ET_o must also be provided. In general, these predictions can be obtained from weather models (i.e. from Internet, using the automatic irrigation controller –AIC- functionalities as described in

Chapter 6). Another issue is that the SWC reference must also be known. In general, defining these predictions is a hard problem and may define the performance of the control scheme. In this thesis we propose to use the deficit irrigation strategies studied in the previous chapters to define these values.

Given this information at a particular time step k , the controller solves the following optimization problem, which defines the proposed MPC scheme:

$$\min_I J(\text{SWC}_1^k, \text{SWC}_2^k, \mathbf{IA}, \mathbf{P}, \mathbf{ET}_o, \text{SWC}_{\text{ref}}) \quad \text{Eq. 8.16}$$

Subject to:

$$[\text{SWC}_1^{k+1}, \text{SWC}_2^{k+1}] = f_{PWA}(\text{SWC}_1^k, \text{SWC}_2^k, \text{IA}^k, P^k, \text{ET}_o^k, \text{LAI}^k, p^k)$$

$$0 \leq \text{IA}^{k+j} \leq \text{IA}_{\text{max}} \forall j \in [0, N-1]$$

Where LAI^0 and p^0 are the constant values of LAI and p along the whole prediction horizon.

This is a MILP problem which can be solved using well known algorithms for which there are a plethora of commercial solutions. In this thesis we use the Hybrid Toolbox for Matlab and the HYSDEL modelling language. Each day, given the future trajectories for \mathbf{P} and \mathbf{ET}_o , the model is recalculated; then a new optimization problem is reformulated; and finally the problem is solved to find the optimal irrigation (\mathbf{IA}^*). We tested the proposed MPC controller in computer simulations with the identified and validated model defined in sections 8.2.2-8.2.4. The implementation algorithm is the following:

1. Get measurements from SWC sensors (SWC_1 and SWC_2).
2. Estimate future values of ET_o and P from predictions of a weather forecast website (www.eltiempo.es).
3. Generate the model for optimal control.
4. Reformulate the optimization problem.
5. Solve the optimization problem (i.e. find the optimal irrigation future trajectory, \mathbf{IA}^*).

6. Apply IA^{k*}.
7. Wait for a new day and go to step 1.

Due to the restrictions imposed by the Hybrid toolbox and the HYSDEL model, we were forced to slightly modify the problem defined by Eqs 8.1-8.12 in order to carry out the simulations of this thesis. In particular, ET_o appears multiplying the states variables SWC_1 and SWC_2 (th1 and th2 in HYSDEL) in some of the equations of the HYSDEL code (appendix 8.A2). This would transform our problem in a non-linear hybrid system, which cannot be modelled using HYSDEL in order to obtain a controller. To avoid this inconvenience, we considered ET_o as a constant value along the receding horizon (i.e. $ET_o^{k+j} = ET_o^k \forall j \in [0, N]$) for the prediction model of the MPC controller. It should be noticed that this is not a limitation of MPC in general, but of the Hybrid toolbox and that, in the simulations, the model used to update the state of the system includes the appropriate ET_o .

In addition, the Hybrid Toolbox does not accept a direct inclusion of these predictions, but they can be indirectly treated as ‘virtual’ states of the prediction model used to define the MPC controller following a standard procedure. For this purpose, we implemented an N step model in HYSDEL, by augmenting the hybrid prediction model with additional states to include the predictions for P and SWC_{ref} . Thus the dynamic of these states was implemented as follows:

$$P^0 = P^1, P^1 = P^2, \dots, P^{l-1} = P^l, P^l = P^l$$

$$SWC_{ref}^0 = SWC_{ref}^1, SWC_{ref}^1 = SWC_{ref}^2, \dots, SWC_{ref}^{m-1} = SWC_{ref}^m, SWC_{ref}^m = SWC_{ref}^m$$

where l and m are the prediction horizons for P and SWC_{ref} . The HYSDEL model used to define the MPC controller, which takes into account these issues (both the ET_o and the predictions of P and SWC_{ref} .) is reported in the appendix 8.A3.

It is important to remark that the MPC control scheme proposed in this thesis takes into account explicitly predictions of both, the disturbances and the set point in the definition of the optimization problem. This information is used when finding the

solution that minimizes the function cost, and hence the performance of the controller is improved when compared with input/output schemes such as PID controllers, which cannot profit from this information. The simulations carried out show this positive property of MPC.

8.3. Results

8.3.1. Cropsyst validation results

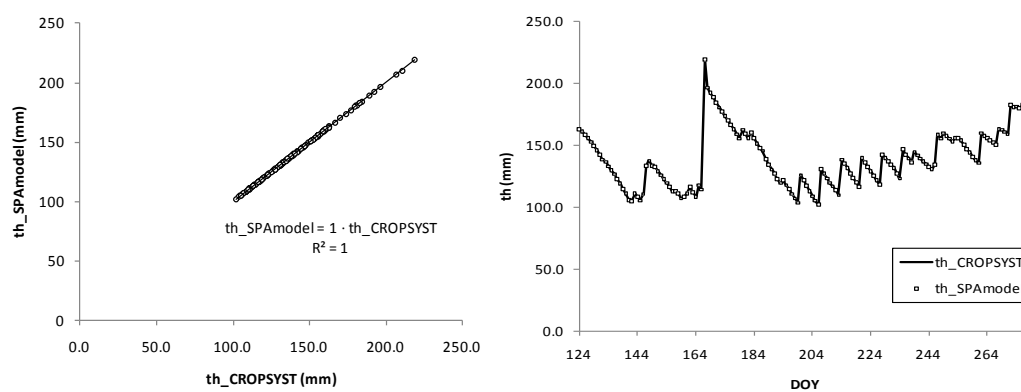
The time length for the simulation was 155 days. Two soil layers were considered for this test: a 0.5 m. depth soil layer that represent root growth zone; and a deeper layer (0.5 to 1.5 m.) to capture drainage losses. Other parameters defining the system were fixed for simulation purpose from heuristic knowledge and field measurements to represent a reference crop, as listed in Table 8.2. We performed simulations with CROPSYST and the proposed SPA model using these parameters and historical data as inputs for P , ET_o and IA . The results (Fig. 8.6 right) show that the proposed model provides a good approximation to the simulations obtained using CROPSYST. Both the linear correlation coefficient and the corresponding coefficient of determination (R^2) between the data provided by both model were 1 (Fig. 8.6 left).

8.3.2. Identified values of the parameters

As proposed in section 8.2.4, we fixed part of the parameters from previous knowledge, and the rest were identified and validated with real data from the almond orchard experiment described in Section 6.2. Considering that we were interested in modelling the irrigation season of adult almonds, we assumed that root depth and LAI were constant during the experiment. Thus, RG_{root} and RG_{LAI} were set to zero, and p_{max} and LAI_{max} were not relevant for our crop. The root distribution study carried out in Section 6.3 demonstrated that most of the roots were concentrated in first 0.5 m ($p = 500$ mm). For this reason, and assuming homogeneous properties of our soil, we defined the first layer, from surface to 0.5 m. depth ($L_1 = 500$ mm) to represent the root zone; and the second layer, from 0.5 to 1.5 m depth ($L_2 = 1000$ mm) to register drainage events. The crop covered more than 50% of the ground, thus K_r was equal to 1. Initials SWC1 (165

Table 8.2. Variables and parameters of the SPA model.

Initial state		
Name	Value	unit
SWC1 _o	163	mm
SWC2 _o	332	mm
LAI _o	6	m ² leaf (m ² soil) ⁻¹
p _o	500	mm
Parameters		
Name	Value	unit
K _{LAI}	0.5	dimensionless
FC _{rat}	0.4	mm mm ⁻¹
WP _{rat}	0.1	mm mm ⁻¹
K _c	0.8	mm mm ⁻¹
L ₁	500	mm
L ₂	1000	mm
K _r	1	mm mm ⁻¹
P _{max}	500	mm
LAI _{max}	6	m ² leaf (m ² soil) ⁻¹
tr	0.3	mm mm ⁻¹
RG _{root}	0	dimensionless
RG _{LAI}	0	dimensionless
SWC _{ini, rat}	0.3319	mm mm ⁻¹

**Fig. 8.6.** Dynamics of the soil water content (SWC) simulated with CROPSYST and the proposed SPA model.

mm) and SWC2 (330 mm) were obtained from SWC field measurements at the beginning of the experiment. We set $tr=0.3$ which means that we consider that transpiration is reduced when water is depleted below 30% of the water holding capacity (FC-WP).

Data provided by the experiment during season 2010 was divided in no-irrigation and irrigation periods (Fig. 8.5). During the no-irrigation period (DOY 26-117 and 224-270) precipitation was the only water input. During the irrigation period (DOY 118-223) water was applied by the AIC to supply the IN of the plants. Furthermore, in each of the periods we divide the data in two sets, for identification and validation purposes (Fig. 8.5). For the no-irrigation period, the validation data set starts in DOY 77 and ends in DOY 97 and for irrigation period, it starts in DOY 157 and ends in DOY 177. The rest of the data was used for identification. Validation data was chosen in the middle of the identification data sets, and the number of days (40) was enough to capture representative variations of SWC and input conditions (ET_o , P_e and I).

Table 8.3 shows the identified values of the parameters in the irrigation and in the no irrigation periods for the four models of K_c considered (annual K_c , monthly constant K_c , monthly averaged K_c and generalized curve) obtained by solving the nonlinear optimization problem (MATLAB `fmincon` function) which minimized the mean square error defined by Eq. 8.13 (see details in section 8.2.4).

We used the validation data set (Fig. 8.5) to simulate the model with the parameters identified as described in the previous section. We compared the mean quadratic errors of the simulated SWC with the four models for K_c . First we run 1-step validations, in which the model estimates SWC from the actual SWC of the previous day. Then we run N-step validations, in which the model estimates SWC for the whole season from the actual SWC in the first day of the validation period.

Figs. 8.7-8.8 show the actual and modeled SWC for the no irrigation and irrigation validation periods, for 1-step and N-step simulations and for the four K_c model with N equal to the simulation length (20 days). Table 8.4 summarizes maximum ($e_{r_{MAX}}$) and averaged relative errors (\bar{e}_r) for all these tests. These errors were evaluated as follows:

Table 8.3. Identified values the four models of the crop coefficient (K_c).

Annual K_c			Monthly K_c		
<i>Parameter</i>	<i>No Irrig.</i>	<i>Irrigation</i>	<i>Parameter</i>	<i>No irrig.</i>	<i>Irrigation</i>
K_{LAI}	0.5	0.5	K_{LAI}	0.5	0.5
d_{bulb}	0.6594	0.8595	d_{bulb}	0.6168	0.7392
K_{rain}	0.3133	0.3133	K_{rain}	0.3785	0.3785
FC_{rat}	0.4	0.4	FC_{rat}	0.4	0.4
WP_{rat}	0.1	0.1	WP_{rat}	0.1	0.1
LAI	6	6	LAI	6	6
K_c	0.5004	0.5004	K_{c1}	0.8681	0.8681
			K_{c2}	1.8854	1.8854
			K_{c3}	0.9679	0.9679
			K_{c4}	0.5013	0.1
			K_{c5}	0.52	0.6216
			K_{c6}	0.61	0.8691
			K_{c7}	0.61	0.978
			K_{c8}	0.6072	0.6072
			K_{c9}	0.1088	0.1088

Monthly averaged K_c			Generalized curve		
<i>Parameter</i>	<i>No irrig.</i>	<i>Irrigation</i>	<i>Parameter</i>	<i>No Irrig.</i>	<i>Irrigation</i>
K_{LAI}	0.5	0.5	K_{LAI}	0.4996	0.4996
d_{bulb}	0.5061	0.7654	d_{bulb}	0.6451	0.8217
K_{rain}	0.367	0.367	K_{rain}	0.3651	0.3651
FC_{rat}	0.4	0.4	FC_{rat}	0.4	0.4
WP_{rat}	0.1	0.1	WP_{rat}	0.1	0.1
LAI	6	6	LAI	5.9999	5.9999
K_{c1}	0.1	0.1	$K_{c,ini}$	1.4322	1.4322
K_{c2}	1.9	1.9	$K_{c,med}$	0.5334	0.5894
K_{c3}	0.84	0.84	$K_{c,fin}$	0.1	0.1
K_{c4}	0.1779	0.1	t_{ini}	49.4736	49.4736
K_{c5}	1.9	0.4735	t_{med1}	115	115
K_{c6}	0.61	0.8672	t_{med2}	223.0192	223.0192
K_{c7}	1.9	0.8841	t_{fin}	287.5671	287.5671
K_{c8}	0.6438	0.6438			
K_{c9}	0.1	0.1			

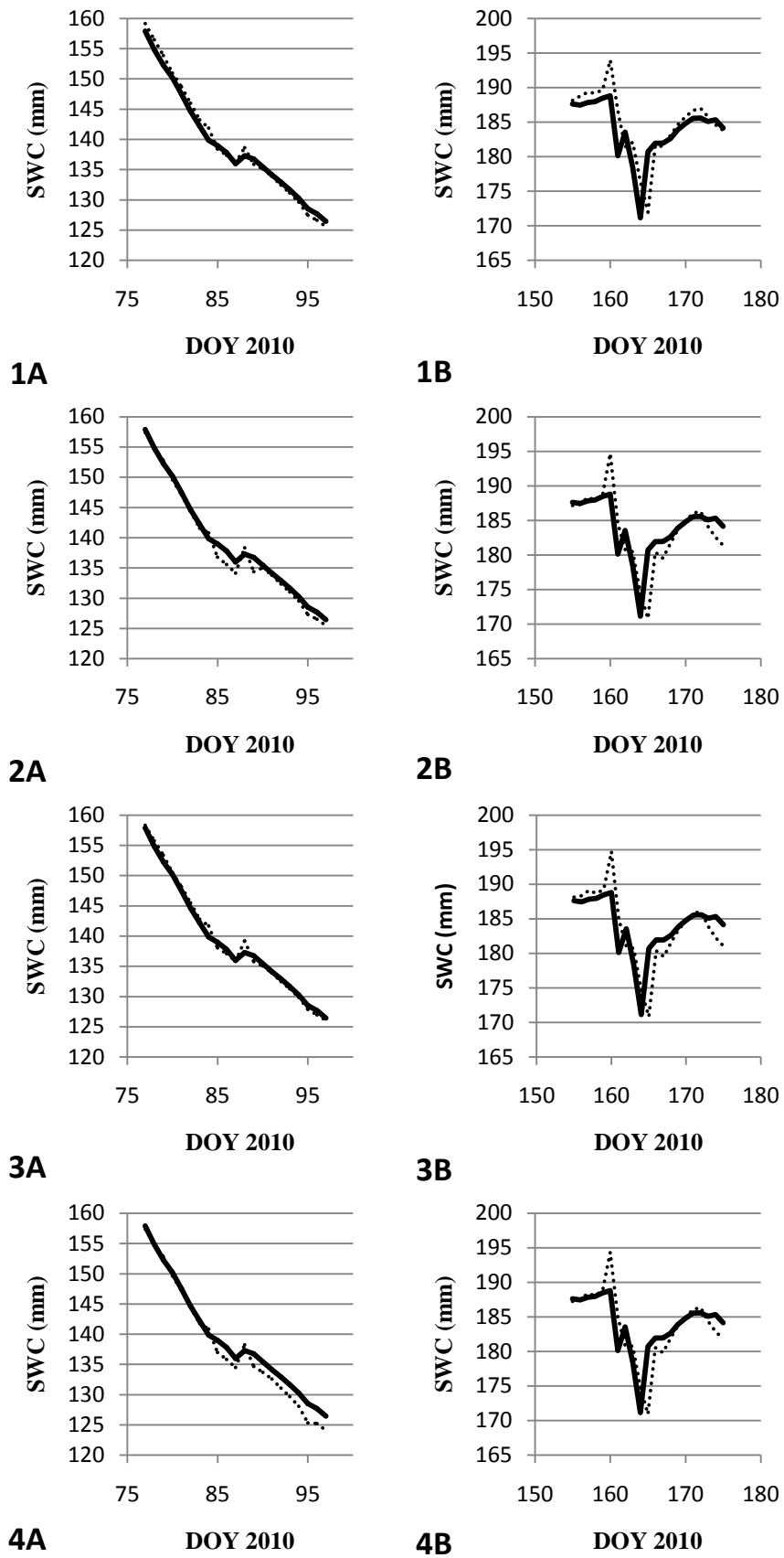


Fig. 8.7. Trajectories for the actual (dotted line) and the simulated (solid line) soil water content (SWC). One-step validation results. DOY = day of year.

*Annual K_c (1), monthly K_c (2), monthly averaged K_c (3) and generalized curve (4) models for the no irrigation (A) and irrigation (B) periods

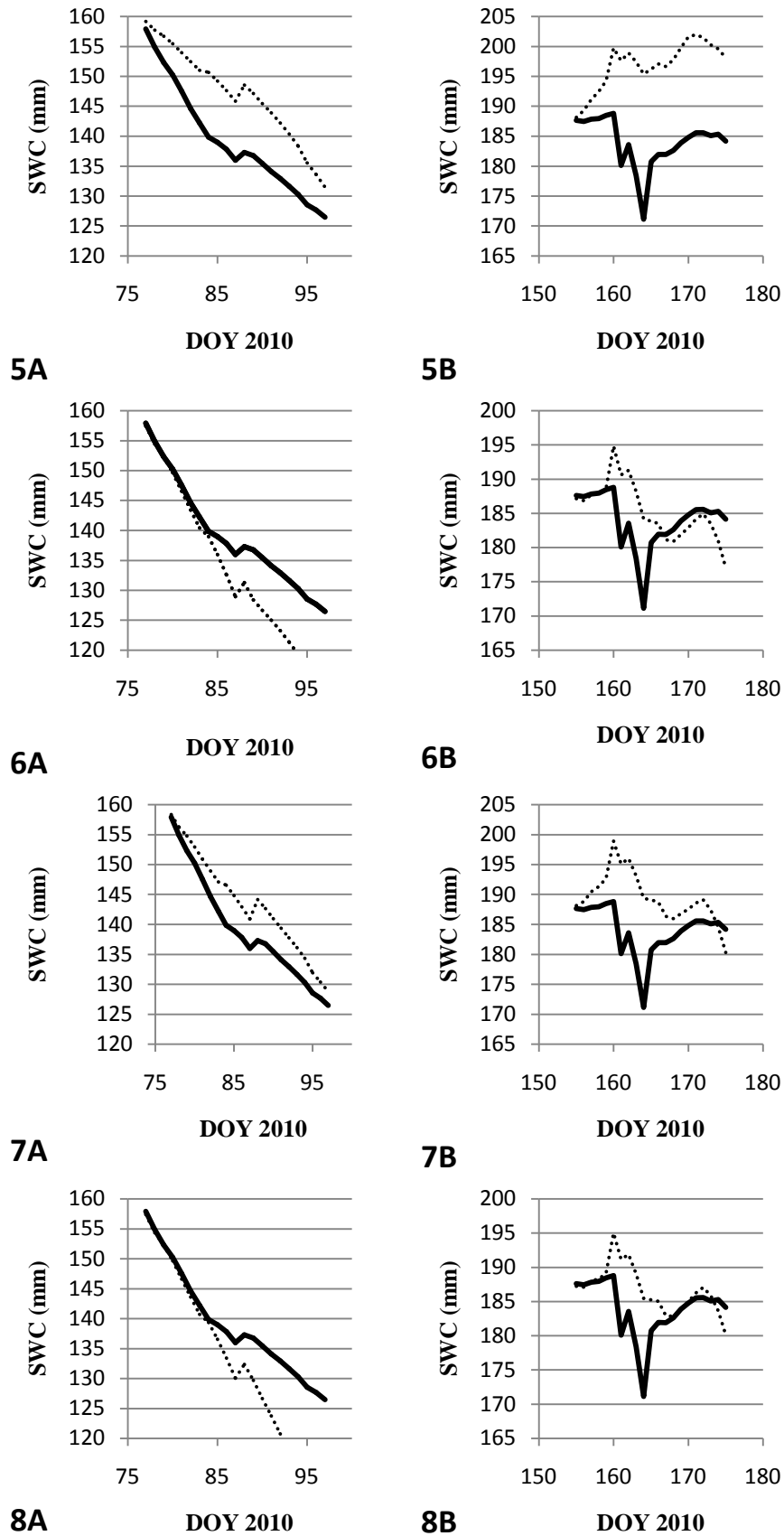


Fig. 8.8. Trajectories for the actual (dotted line) and the simulated (solid line) soil water content (SWC). N-step validation results. DOY = day of year.

*Annual K_c (1), monthly K_c (2), monthly averaged K_c (3) and generalized curve (4) models for the no irrigation (A) and irrigation (B) periods

Table 8.4. Maximum and averaged relative errors for 1-step and N-step validation

Maximum relative errors (%)							
1-Step			N-Step				
		Model				Model	
		<i>No Irrig.</i>	<i>Irrigation</i>			<i>No Irrig.</i>	<i>Irrigation</i>
K_c model	Annual	1.44	4.86	K_c model	Annual	8.18	14.17
	Monthly	1.74	5.49		Monthly	11.34	7.63
	Monthly averaged	1.39	5.46		Monthly averaged	4.99	10.65
	Generalized curve	2.49	5.42		Generalized curve	19.26	8.36
Averaged relative errors (%)							
1-Step			N-Step				
		Model				Model	
		<i>No Irrig.</i>	<i>Irrigation</i>			<i>No Irrig.</i>	<i>Irrigation</i>
K_c model	Annual	0.66	1.17	K_c model	Annual	5.65	7.09
	Monthly	0.68	1.11		Monthly	4.48	1.97
	Monthly averaged	0.51	1.23		Monthly averaged	3.03	3.27
	Generalized curve	1.04	1.09		Generalized curve	5.72	1.86

$$e_{r_{MAX}}(\%) = \max_{i=1 \dots N} \left(100 \cdot \left| \frac{SWC_{mod}^i - SWC_{act}^i}{SWC_{act}^i} \right| \right) \quad \text{Eq. 8.17}$$

$$\bar{e}_r(\%) = \frac{1}{N} \sum_{i=1}^N \left(100 \cdot \left| \frac{SWC_{mod}^i - SWC_{act}^i}{SWC_{act}^i} \right| \right) \quad \text{Eq. 8.18}$$

where, for the i time step, SWC_{mod}^i and SWC_{act}^i are the modeled and actual SWC.

The maximum errors for the 1-step predictions were 2% and 5% for the no irrigation and irrigation periods. For the N-steps predictions, the maximum errors grow up to 10-20%. These errors are low enough to use this model in a MPC setting because

although the prediction errors grow with the horizon, the controller is implemented with a receding horizon strategy, so the most relevant error is given by the first step. From the results we can conclude that the most suitable identified parameter set is the monthly average K_c model, which provides the lowest average N-steps prediction errors together with the lowest maximum error of the 1-step predictions in the irrigation period, which is the most relevant for precision irrigation purposes.

8.3.3. Controllers simulations

We used the model described in Section 8.2.2 with the parameters of the reference crop (Table 8.2) to test several irrigation control strategies through simulation using Simulink and Matlab. The time length for the simulations was set to 100 days. We considered two soil layers: the first 0.5 m. depth representing the root zone and the next 0.55 m. depth to represent drainage losses. To simulate the controllers in this section we set $WP = 10\%$ (50 mm), $FC = 50\%$ (250 mm) and $tr = 0.3$ (23%, 110 mm). We assume no precipitation events during the simulation period unless noted.

8.3.3.1. No irrigation

We first simulated a period with no irrigation (Fig. 8.9). The SWC trajectories show two different periods. After 26 days soil water content decreased below the water stress level defined by tr since evaporation and transpiration deplete soil water. The SWC decreases at a lower rate from that day on. These trajectories show clearly the hybrid nature of the SPA model.

8.3.3.2. Feedforward ET_c

Next we applied daily IAs calculated as 100% of the ET_c measured in the previous day. Fig. 8.10 shows how SWC remains close to its initial value, since we are just restoring the plant and atmosphere water use. As expected, this method is not able to achieve or follow a set point because the SWC just stays close to its initial value.

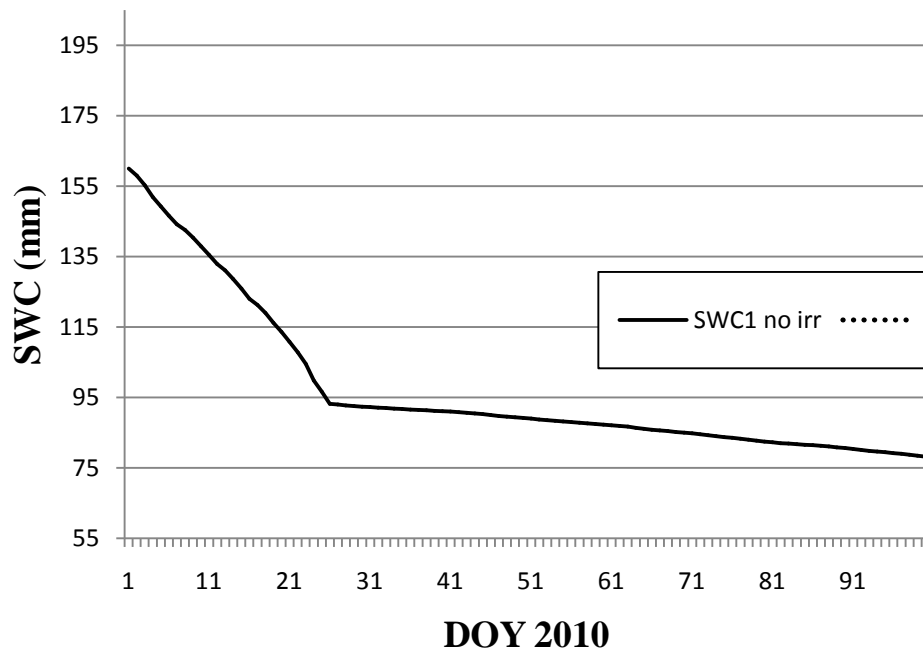


Fig. 8.9. Temporal evolution of the soil water content (SWC) when no irrigation was applied. DOY = day of year.

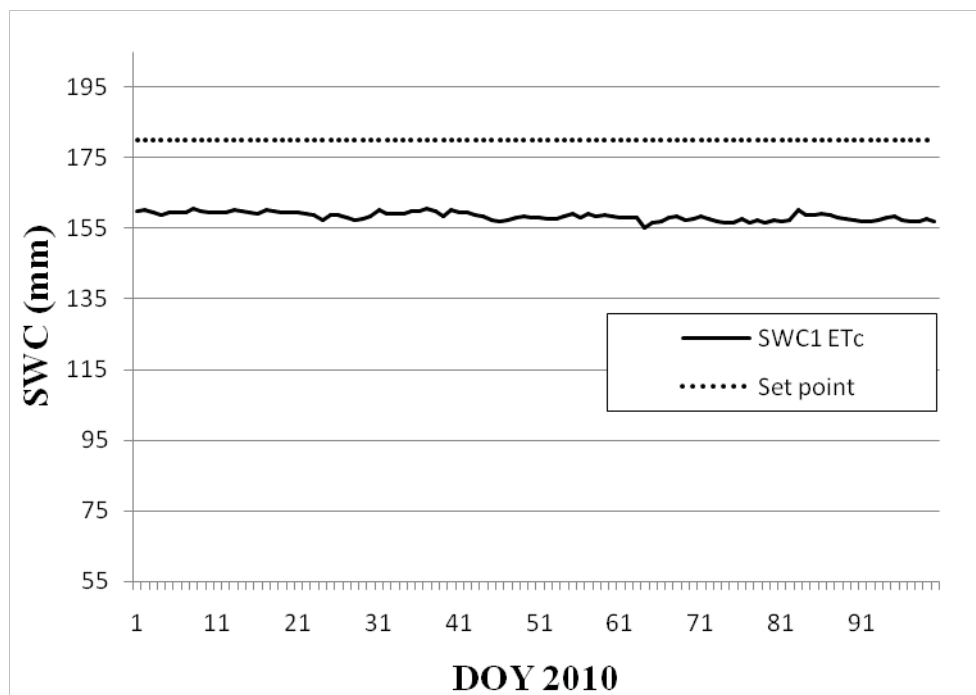


Fig. 8.10. Temporal evolution of the soil water content (SWC) when irrigation amounts are calculated as 100% of the crop evapotranspiration (ET_c) in the previous day. DOY = day of year.

8.3.3.3. PID

We also tested a PID to control irrigation. Fig. 8.11 shows the Simulink scheme of this controller. The set point for the SWC was 200 mm. The parameters of the PID were first tuned with a heuristic method, formally known as Ziegler-Nichols method (Ziegler and Nichols, 1942) and then manually tuned to obtain better performance (proportional gain $K_P = 0.8$, integral $K_I = 0.1$, derivative $K_D = 0$). The main advantage of this method is that the ET_o values are not necessary, although SWC must be measured to provide feedback to the controller. This feedback is crucial to guarantee the robustness of this controller. Set point is reached in nine days. Afterwards, soil water content remains inside $\pm 2.3\%$ set point bounds (Fig. 8.12). The trajectories show that the closed-loop system is sensible to variations on the ET_o , which the controller takes some time to compensate, which leads to some oscillations.

8.3.3.4. PID + Feedforward ET_c

Next we tested both control strategies together (Fig. 8.13); that is, feedforward ET_c was added to the PID output. PID performance is improved when ET_c feedforward is included. Set point is reached in five days, then the controller causes over-irrigation during seven days and finally, after twelve days, soil water content remains inside $\pm 1.7\%$ set point bounds (Fig. 8.14).

8.3.3.5. MPC

We tested the MPC implemented using the hybrid toolbox as described in the previous section. We compared the MPC vs. PID to control SWC assuming two scenarios: assuming no precipitation (Fig. 8.15) and simulating precipitation events (Fig. 8.16).

To do these simulations, the MPC controller used, as a prediction of the ET_o , the value of the previous day; that is, the precision forecast was used, and in general, although the ET_c varies slowly, these prediction introduced several errors which can be seen in the trajectories.

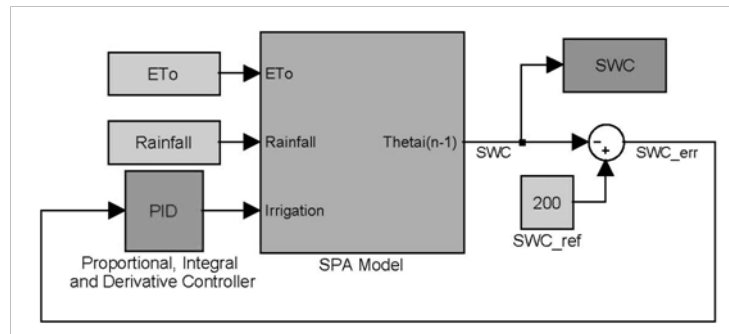


Fig. 8.11. PID control scheme.

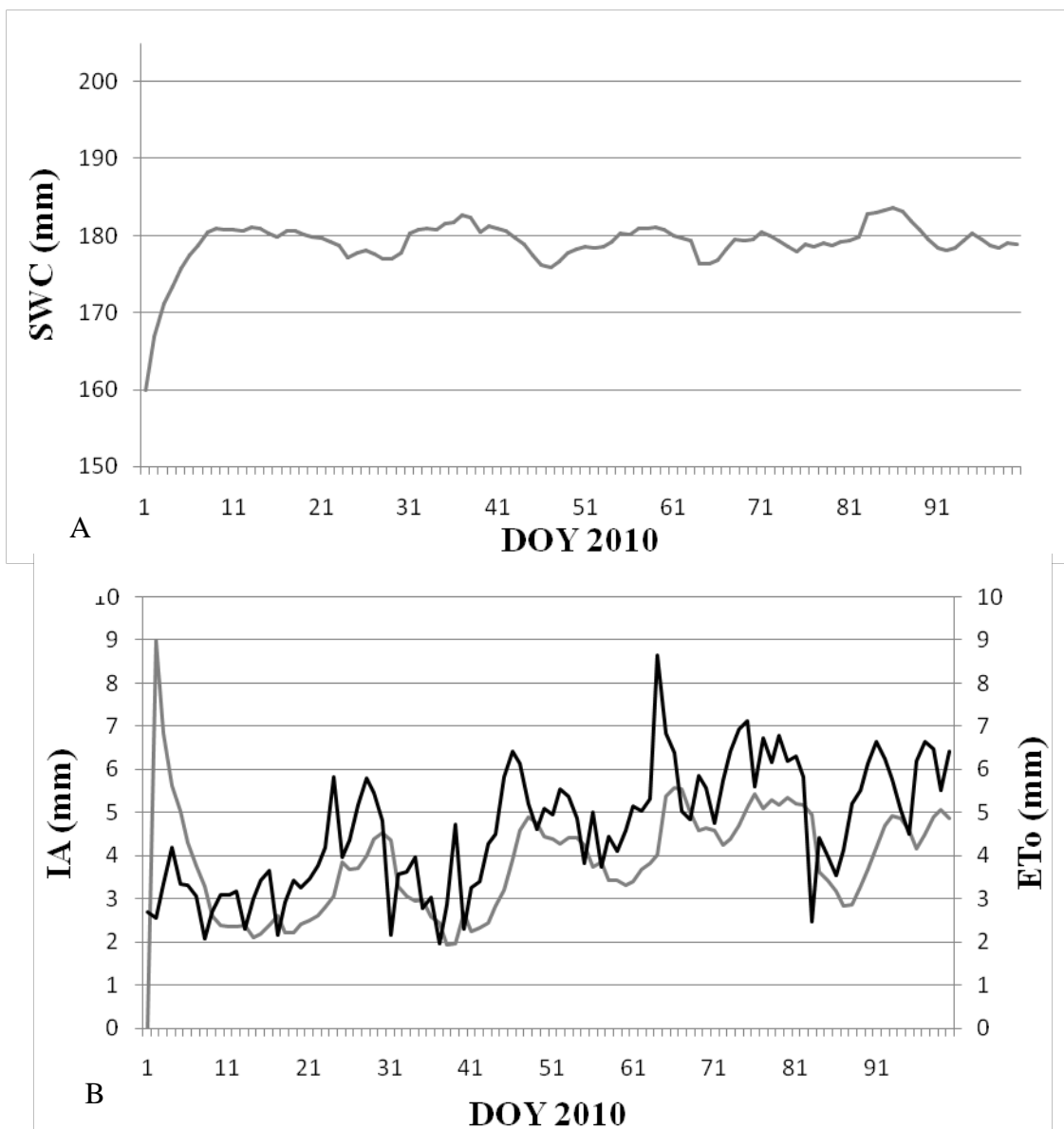


Fig. 8.12. Temporal evolution of A: the soil water content (SWC, A) and B: the irrigation amounts (IA) and potential evapotranspiration (ET_o) when PID irrigation controller is applied.

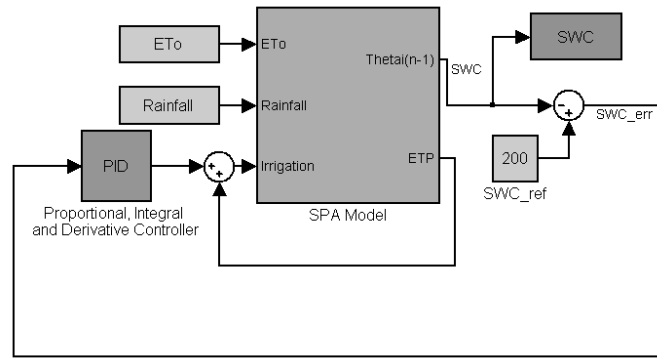


Fig. 8.13. Simulink model for the simulation of the proportional, integral and derivative (PID) + feedforward ETc irrigation controller.

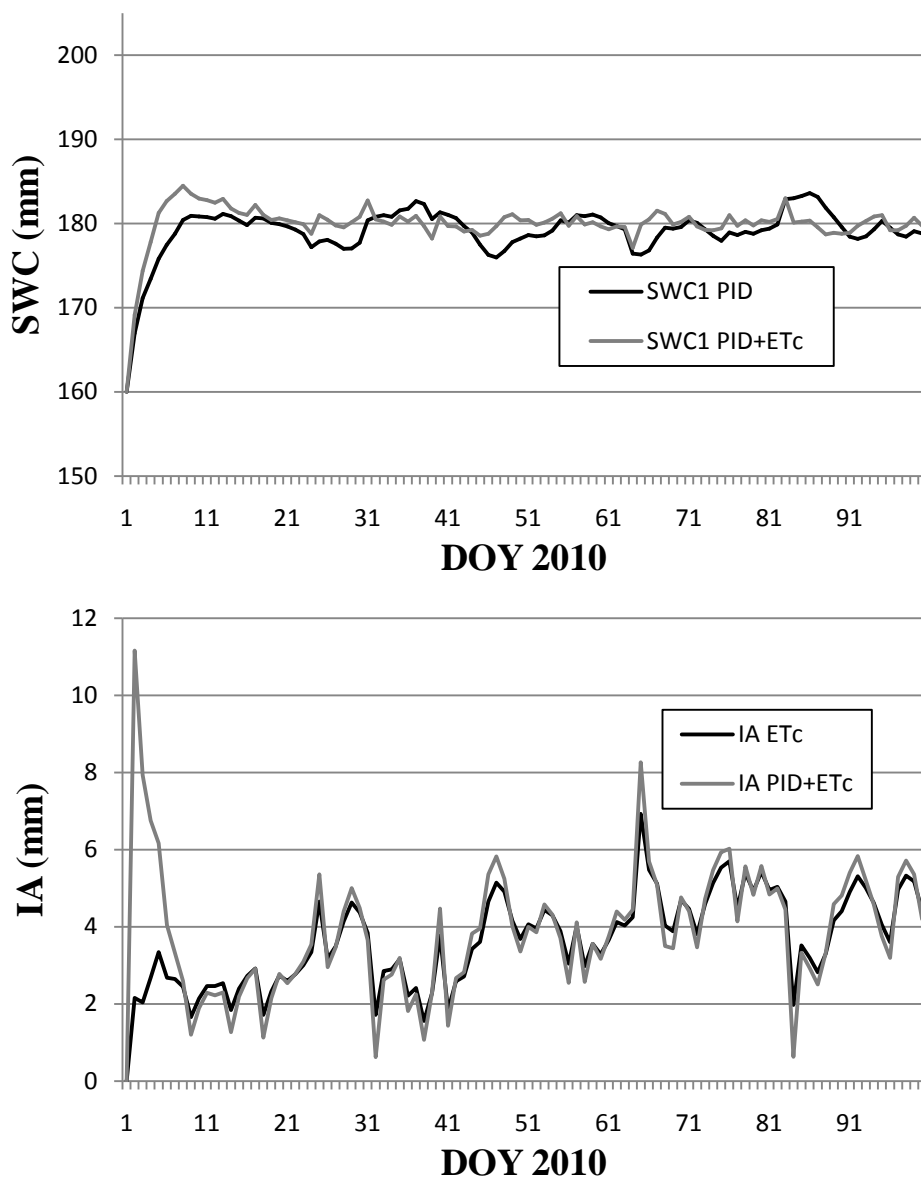


Fig. 8.14. Comparison of the trajectories of the soil water content (SWC) when applying PID and when applying PID with feedforward ETc. IA = irrigation amount. DOY = day of year.

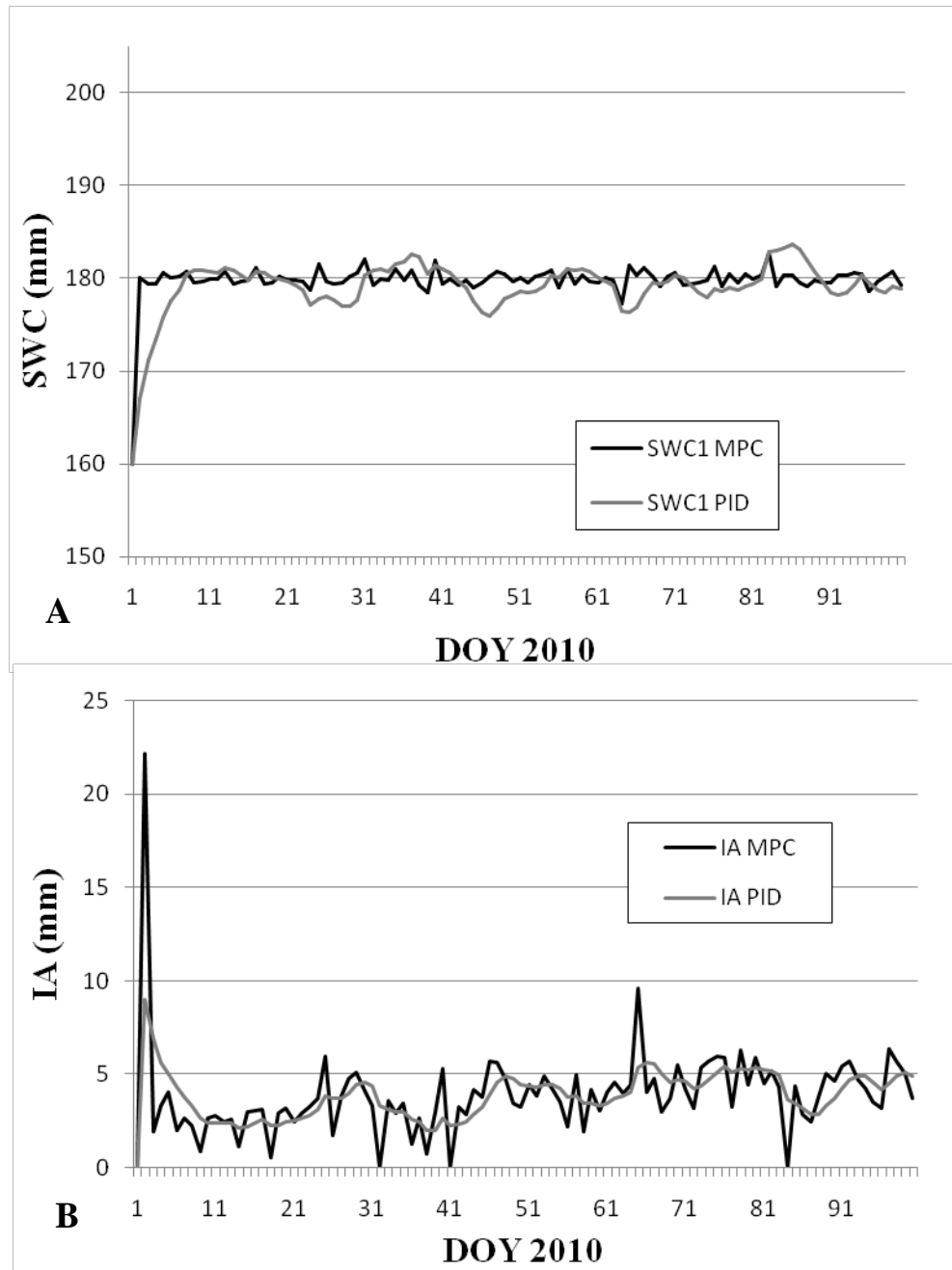


Fig. 8.15. Comparing soil water content trajectories (A) and irrigation amounts (B) of the MPC and PID controllers assuming no precipitations. DOY = day of year.

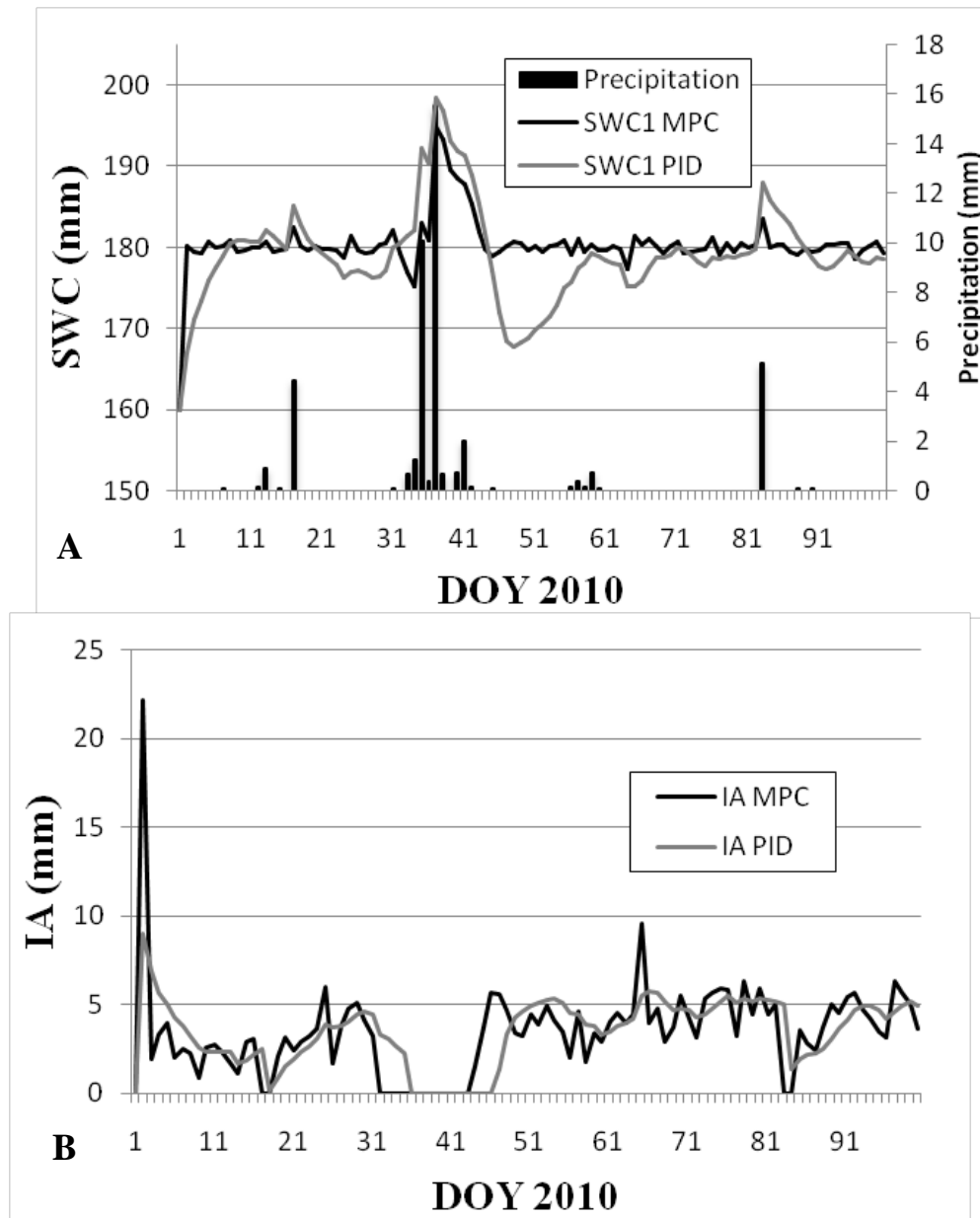


Fig. 8.16. Comparing soil water content trajectories (A) and irrigation amounts (B) of the MPC and PID controllers assuming precipitation events. DOY = day of year.

Fig. 8.15A shows the trajectories of the SWC in the root zone (SWC_1) and the references (set point) for the MPC and the PID simulations in the no-precipitation scenario. MPC reached the reference in the first day of simulation and remained closer to the reference for the rest of the test. From the analysis of the irrigation trajectories (Fig. 8.15B) is also clear that the MPC change more often and react to the errors introduced by the variable weather changes (ET_o).

In Fig. 8.16, MPC and PID are compared in the presence of precipitation events which can be predicted. Fig. 8.16A shows the corresponding SWC trajectories along with the daily precipitation values. In this scenario, MPC advantages are even more evident and again MPC was able to improve the control respect to the PID. Set point was achieved faster with the MPC, and SWC remained closer to the reference. The differences were especially significant in the beginning of the simulation and after the precipitation events. This was because the controller was able to adapt the irrigation needs in advance with the precipitation predictions. Note from the irrigation trajectories graph (Fig. 8.16B) that the MPC reduced irrigation from DOY 31, four days before the high precipitations occur (DOY 35), taking into account that there would be an excess of water inflow in the incoming days. On the contrary, PID controller reacted later, reducing irrigation from DOY 36. MPC was also able to increase irrigation (from DOY 44) three days before the PID controller did, predicting the future water inflow deficit after the precipitations period.

In Fig. 8.17A we plot the trajectories of the SWC in the root zone when we included the changes in the reference as known information for the controller, by using the modelling method mentioned in the previous section. This controller (MPCp) was compared with a simpler MPC, which not incorporated the information on the changes of references (MPCnp). This information improved the performance of the MPC, which was especially notable when the set point changed from 180 to 150 mm (DOY 159). The improved MPC was able to achieve the setpoint four days earlier, thanks to the inclusion in the controller of the setpoint prediction. The IA's applied by both MPC

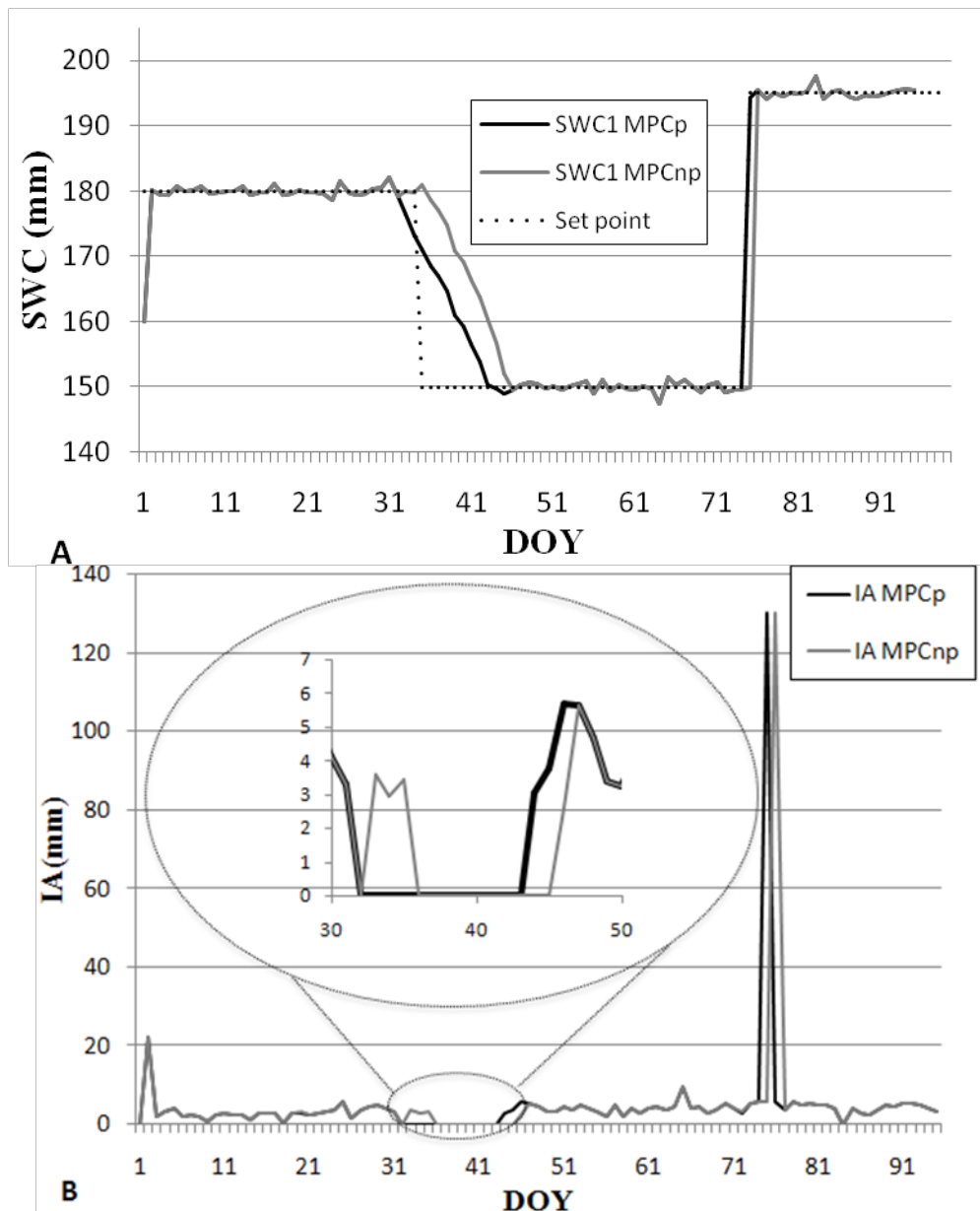


Fig. 8.17. Soil water content (SWC) trajectories (A) and irrigation amounts (IAs) applied (B) by the MPC with (MPCp) and without (MPCnp) the predictions of changes in the set point.

were quite similar (Fig. 8.17B). The main differences appeared after the change in the setpoint, during the days after DOY 159.

An important limitation of the PID technique is that when the actual SWC is above the setpoint, a negative control signal would be required. But, since irrigation cannot be negative, the only way to reduce SWC is just to wait for the plants and atmosphere to consume the exceed water in the rootzone. This limitation of the control signal leads to a problem with PID controllers known, in theory of control, as windup. Windup can occur in loops where the process has saturations and the controller has integral action. When the process saturates the feedback loop is broken. If there is an

error the integral may reach large values and the control signal may be saturated for a long time resulting in large overshoots and undesirable transients. Fig. 8.16 shows the effect of windup in an irrigation controller. After a precipitation period, the PID controller needs some time to start irrigating to account for water losses. Thus, windup should be taken in account in precise irrigation when applying a PID to control SWC. An important advantage of MPC is that it naturally incorporates the constraints of the system and thus, the windup problem is solved. Fig. 8.16 shows that the MPC controller regulates the SWC correctly even after a high precipitation period.

8.3.3.6. Irrigation controller comparative

Table 8.5 shows the IAs applied and the mean square error (MSE) for each irrigation controller for the same simulation conditions. The MSE was evaluated as follows:

$$\text{MSE} = \frac{1}{M} \sum_{i=1}^M \left| \frac{\text{SWC}_{\text{sim}}^i - \text{SWC}_{\text{ref}}^i}{\text{SWC}_{\text{ref}}^i} \right| \quad \text{Eq. 8.19}$$

where, for each time step i , $\text{SWC}_{\text{sim}}^i$ and $\text{SWC}_{\text{ref}}^i$ are the simulated and reference SWC respectively and M is the simulation time frame.

The lowest IA was achieved by feedforward ET_c , but this controller is only able to maintain SWC, but not to achieve a given set point. Thus, this strategy showed the highest MSE. The rest controllers applied similar IAs (386.5 ± 0.5 mm). The addition of the feedforward ET_c improved the PID performance. The lowest MSE was achieved with the MPC controller.

8.3.4. Application to real field of the PID controller

A PID irrigation controller was implemented in the almond orchard. PID parameters were set as in the simulations ($\text{KP} = 0.4$, $\text{KI} = 0.05$, $\text{KD} = 0$). We tested the PID performance in two different periods (13 and 12 days) during July-August 2010 (Fig. 8.18 and 8.19). After only 1 day, set point is achieved and remains in $\pm 5\%$ set point

Table 8.5. Irrigation amount (IA) and mean squared error (MSE) for the tested irrigation controllers.

<i>Irrigation controller</i>	IA (mm)	MSE (mm ²)
Feedforward ET _c	364.18	465.63
PID	385.99	5.92
PID+Feedforward ET _c	386.89	3.19
MPC	386.45	0.61

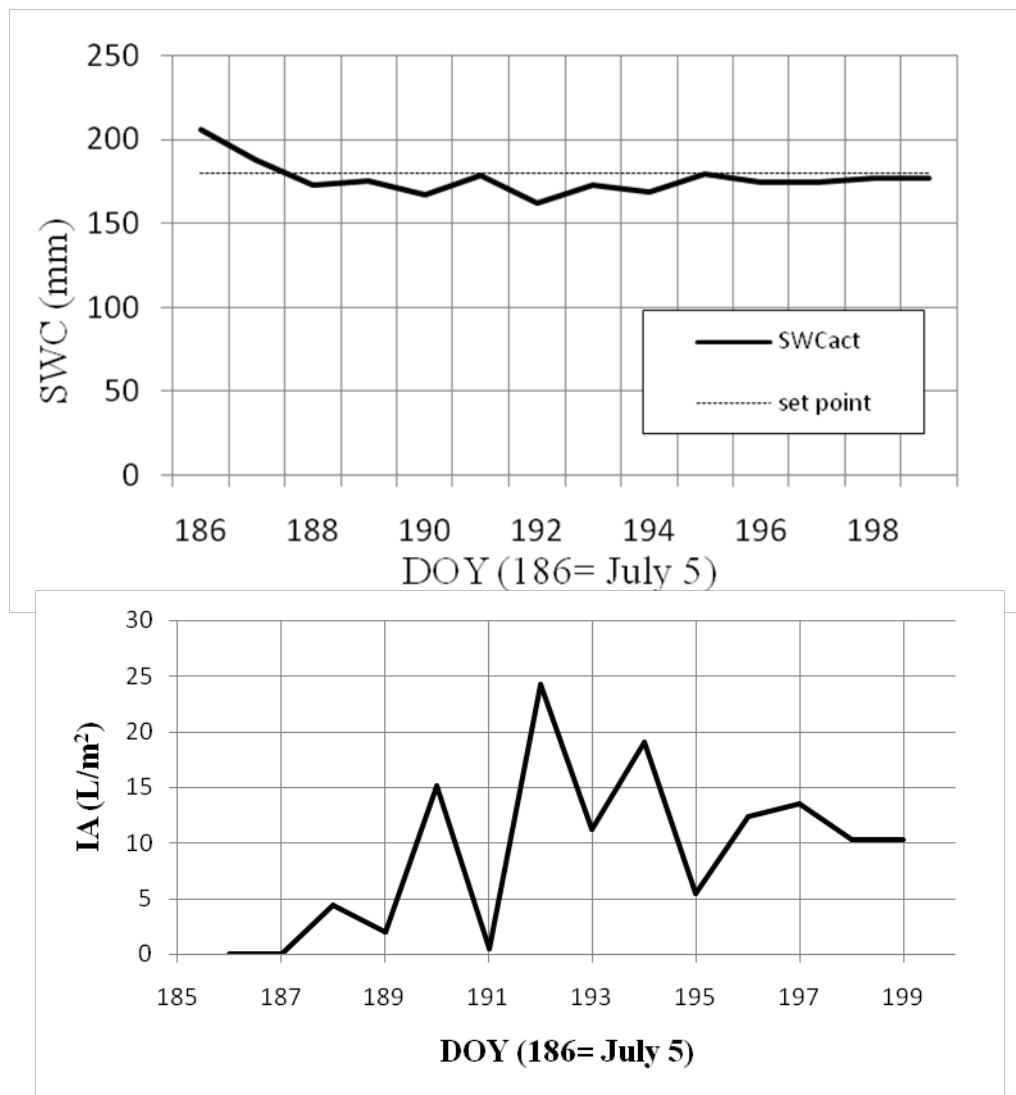


Fig. 8.18. Soil water content (SWC, A) and irrigation amounts (IA, B) when PID was applied in a real field experiments, from DOY 186 to 199. Setpoint was set to 180 mm.

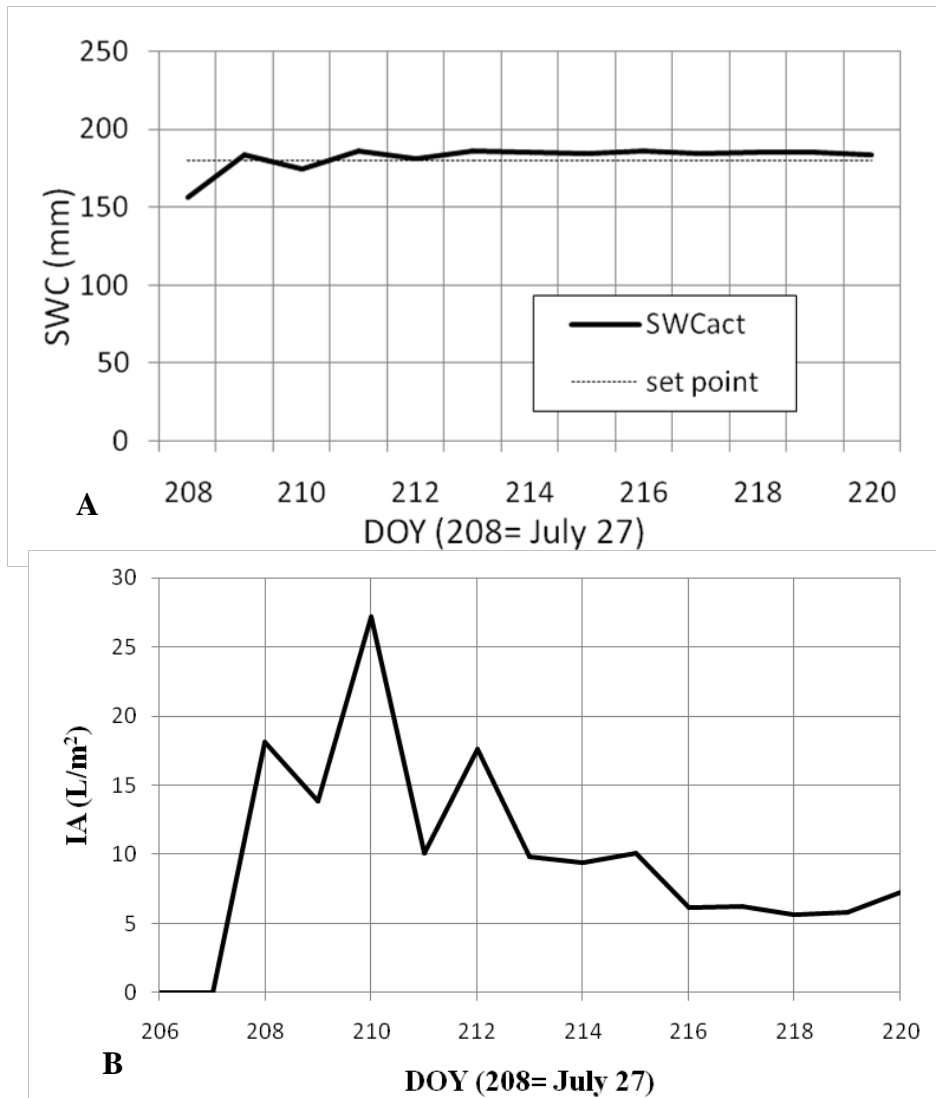


Fig. 8.19. Soil water content (SWC, A) and irrigation amounts (IA, B) when PID was applied in a real field experiments, from DOY 208 to 220. Setpoint was set to 180 mm.

bounds. During these periods of time, the irrigation controller operated in a fully autonomous manner, compensating weather conditions without any external information or forecast.

8.4. Discussion

The validation with Cropsyst confirms that our model correctly represents the SWC dynamic of a representative SPA system. Several authors have applied Cropsyst for different crops and environments (Donatelli *et al.*, 1997; Tubiello *et al.*, 2000; Peralta and Stöckle, 2002; Benli *et al.*, 2007; Singh *et al.*, 2008). Also, Bonfante *et al.* (2010) compared SWAP, Cropsyst and MACRO models. They concluded that the three models gave very satisfactory results. In the overall comparison SWAP shown slightly better

performance than Cropsyst, and this shown better results than MACRO. But as far as the coefficient of residual mass (CRM) index was concerned, Cropsyst was the best choice, since showed little differences in performances between calibration and validation years. Confalonieri et al. (2010) compared the performance of Cropsyst and CERES-Wheat models to simulate SWC for winter wheat systems. Cropsyst presented the highest accuracy.

The identification and validation processes that we proposed showed that our model acceptably represents the SWC dynamic in our almond orchard. However, it should be noticed that the complexity and variability of these systems inevitably reduce the accuracy of the predictions of the model. Similar conclusions have been pointed out by Calvet *et al.* (1998) and Tuzet *et al.* (2003).

The simulation of a no irrigation period revealed that soil-water storage is depleted below the fixed threshold point after 26 days since the evaporation and transpiration processes are taking out water from soil and there is not replenishment. The time length for soil-water depletion mainly depends on the climatic condition and the value of the soil and crop parameters used in the model. The wilting point threshold is also highly variable and species dependent. Fereres *et al.* (1979) studied the recovery of two orchards of Valencia orange trees, which had not been irrigated for 3 and 6 months. They showed that the trees were capable of recovery from high levels of water stress despite being in extremely dry soil with average soil matrix potential of -2.6 MPa before irrigation. Moriana *et al.* (2003) estimated that rain fed olive trees with leaf water potentials around -8 MPa extracted an additional 40 mm from below the conventional permanent wilting point of -1.5 MPa in a 240-cm deep profile.

When an ETc Feedforward strategy was modelled, SWC exceeded field capacity after 90 days. This indicates that ETc was not correctly calculated (crop water consumption was overestimated). This is mainly because of difference between TR and TP and ER and EP. ETc (that is the usual value to calculate irrigation) do not consider the reductions in transpiration and evaporation induced when SWC is bellow threshold values (*WP* or *tr*). ETc compensation is a typical method used successfully by farmers and it does not require SWC values to be measured. This is an advantage for farmers, because they can be advised for using suitable ETo, Kc and Kr values to estimate irrigation without investing in sensors. As disadvantages, Kc values are indentified in few experimental sites with specific climate conditions that usually differ of those

where the K_c values are applied. Hence, the differences between the local peculiarities of the plot, weather and crops might introduce many errors in the K_c estimation. Furthermore, stomatal control by plants or limited transpiration or evaporation (caused by dry soil conditions), can lead to over irrigation as shown in the simulation. ET_c Feedforward strategy has been widely tested in the literature. In particular, this is the typical strategy for the irrigation of the control treatment in DI research (Ruiz-Sánchez *et al.*, 2010; Fereres and Soriano, 2007; Fernandez *et al.*, 2008a, b). It should be notice that, although this strategy might be acceptable when studying periods with not irrigation, special care must be taken when rainfall events occurs during the experimental period. In the last case, the IN (ET_c -P) should be replenished instead of ET_c to avoid over-irrigation.

With the PID strategy, the setpoint for SWC (200 mm) was reached and followed accurately after 5 days of simulation. As mentioned, PID parameters were first tuned by using Ziegler–Nichols method and then readjusted to get optimal results. The main advantage of PID is that it can achieve an accurate performance with no information of ET or the model of the SPA. It only needs SWC feedback to outputs next corrective action. The advantages of PID for the control of environment in greenhouses have been reported in the past (Hashimoto, 1979 and Magliulo *et al.*, 2003). Hashimoto (1979) showed that PID and computer aided plantation are a useful control system for sunflower plants in greenhouses. Magliulo *et al.*, (2003) successfully applied a PID strategy to control the concentration of CO_2 in tomato plants. The plants growing in CO_2 enriched air improved both yield performance and water savings.

When both strategies (PID and ET_c feedforward) were applied at once setpoint takes more time to be reached than in the previous tests (25 days). Errors between setpoint and SWC were also increased. PID performance was not improved by including ET_c compensation. On the contrary, the accuracy was reduced because of the errors induced by the overestimations of the ET_c . MPC on the other hand is not only able to include the daily ET_c compensation, but also the future predictions of the weather conditions and reference changes. Fig. 8.15 shows how the MPC controller anticipates with respect to PID when one of these conditions change.

MPC simulations suggest that this might be the best strategy when a precise model of the system and acceptable predictions for ET_o and P_e are available. Given

these requisites, MPC should be able to calculate the optimum present and future IA's. At our knowledge, no application of MPC to precise irrigation of fruit orchards has been reported. However, several authors have shown the promising advantages of these controllers in other fields such as environmental control of greenhouses. Rodriguez *et al.* (2008) demonstrated the applicability of an adaptive hierarchical control to an industrial greenhouse, in which heating was controlled by means of an MPC algorithm. They obtained good tracking performance while diminishing fuel consumption associated costs. In Piñón *et al.* (2005), the authors simulated the application of an MPC for temperature control of a greenhouse. They concluded that an MPC with feedback linearization strategy seems to be attractive for a class of feedback linearizable systems due to its relative computational efficiency. El Ghoumari *et al.* (2005) compared an MPC and a PID controller for temperature regulation of a greenhouse. Their results showed the two main disadvantages of PID controllers: constraints are not considered, and only single input single output (SISO) loops are implemented, resulting in poor performance. They implemented an MPC algorithm in real time to solve the problems found for the PID controllers application.

8.5. Conclusions

We developed a discrete time mathematical model to obtain an approximate solution of the behaviour of a given SPA system. The model can be used for doing predictions and design precision irrigation strategies and controllers. The proposed model was first successfully checked with CROPSYST, and then it was identified and validated for a specific almond orchard using data from a whole irrigation season. Finally different control strategies (PID, ET_c feed forward, MPC) were tested and evaluated with the model in simulations.

The PID strategy proved to be robust and accurate controlling SWC. Better SWC evolution was achieved with PID than with feedforward ET_c method due to SWC measurement feedback. We also applied this PID controller in field during July-August 2010 with excellent results. After only 1 day, set point was achieved remaining in $\pm 5\%$ set point bounds during the experimental period. We conclude that PID is a robust and efficient strategy that provides precision irrigation when a reference for soil water

content (SWC, mm) is known. PID achieves better performance than ET_c compensation thanks to the SWC measurement feedback.

Extra information (e.g. ET_c and rainfall forecasts, and changes in SWC reference) can be incorporated in advance in the MPC controller to optimize the control of the SWC. Furthermore, in MPC the contribution of the weighting coefficients to the signal control can be pondered. These allow the farmer to find a mid-way solution between optimal soil water content and saving water. Our MPC controller showed promising results when simulated with the SPA model. Nevertheless, field experiments are required to confirm these results.

8.6. References

- Alimardani R, Javadikia P, Tabatabaeefar A, Omid M, Fathi M. 2009. Implementation of On/Off Controller for Automation of Greenhouse Using LabVIEW. *Artificial Intelligence and Computational Intelligence, Proceedings* 5855:251-259.
- Allen RG, Pereira LS, Raes D, Smith M. 1998. Crop evapotranspiration-Guidelines for computing crop water requirements-FAO Irrigation and drainage paper 56. FAO, Rome 300:6541.
- Bastiaanssen WGM, Allen RG, Droogers P, D'Urso G, Steduto P. 2007. Twenty-five years modeling irrigated and drained soils: State of the art. *Agric Water Manage* 92(3):111-125.
- Beeson RC. 2011. Weighing lysimeter systems for quantifying water use and studies of controlled water stress for crops grown in low bulk density substrates. *Agric Water Manage* 98(6):967-976.
- Bemporad A. 2004. Hybrid Toolbox - User's Guide. Available at <http://www.ing.unitn.it/~bemporad/hybrid/toolbox> (verified 8 Sept. 2011)
- Bemporad A, Borrelli F, Morari M. Piecewise linear optimal controllers for hybrid systems; 2000. IEEE. p 1190-1194 vol. 1192.
- Bemporad A, Morari M. 1999. Control of systems integrating logic, dynamics, and constraints. *Automatica* 35(3):407-428.

- Bengough AG, Castrignano A, L. P, Van Noordwijk M. 2000. Sampling Strategies, Scaling, and Statistics. In: Smit AL, Bengough AG, Engels C, Van Noordwijk M, Pellerin S, Van de Geijn SC, editors. *Root Methods A Handbook* Springer-Verlag Berlin Heidelberg New York. p 147-170.
- Benli B, Pala M, Stockle C, Oweis T. 2007. Assessment of winter wheat production under early sowing with supplemental irrigation in a cold highland environment using CropSyst simulation model. *Agric Water Manage* 93(1-2):45-53.
- Blasco X, Martínez M, Herrero JM, Ramos C, Sanchis J. 2007. Model-based predictive control of greenhouse climate for reducing energy and water consumption. *Comput Electron Agric* 55(1):49-70.
- Bonfante A, Basile A, Acutis M, De Mascellis R, Manna P, Perego A, Terribile F. 2010. SWAP, CropSyst and MACRO comparison in two contrasting soils cropped with maize in Northern Italy. *Agric Water Manage* 97(7):1051-1062.
- Breda NJJ. 2003. Ground based measurements of leaf area index: a review of methods, instruments and current controversies. *Journal of Experimental Botany* 54(392):2403.
- Brisson N, Seguin B, Bertuzzi P. 1992. Agrometeorological soil water balance for crop simulation models. *Agricultural and Forest Meteorology* 59(3-4):267-287.
- Calvet JC, Noilhan J, Roujean JL, Bessemoulin P, Cabelguenne M, Olioso A, Wigneron JP. 1998. An interactive vegetation SVAT model tested against data from six contrasting sites. *Agricultural and Forest Meteorology* 92(2):73-95.
- Camacho EF, Bordons C. 2004. *Model predictive control*: Springer Verlag. 405 p.
- Confalonieri R, Bregaglio S, Bocchi S, Acutis M. 2010. An integrated procedure to evaluate hydrological models. *Hydrological Processes* 24(19):2762-2770.
- Cutler CR, Ramaker BL. 1980. Dynamic matrix control - a computer control algorithm. *Joint Automatic Control Conference*, volume 1. San Francisco, California.
- Donatelli M, Stockle C, Ceotto E, Rinaldi M. 1997. Evaluation of CropSyst for cropping systems at two locations of northern and southern Italy. *European Journal of Agronomy* 6(1-2):35-45.

-
- El Ghoumari MY, Tantau HJ, Serrano JS. 2005. Non-linear constrained MPC: Real-time implementation of greenhouse air temperature control. *Comput Electron Agric* 49(3):345-356.
- Evelt SR, Heng LK, Moutonnet P, Nguyen ML. 2008. Field estimation of soil water content: A practical guide to methods, instrumentation, and sensor technology. IAEA-TCS-30. International Atomic Energy Agency, Vienna, Austria. Available at http://www-pub.iaea.org/MTCD/publications/PDF/TCS-30_web.pdf (verified 8 Sept. 2011).
- FAO. 1963. Carta bioclimática de la zona mediterránea. UNESCO-FAO.
- Farmer D, Sivapalan M, Jothityangkoon C. 2003. Climate, soil, and vegetation controls upon the variability of water balance in temperate and semiarid landscapes: Downward approach to water balance analysis. *Water Resources Research* 39(2):1035-1056.
- Feddes RA, de Rooij GH, van Dam JC. 2004. *Unsaturated-zone Modeling: Progress, Challenges and Applications*. Springer. p 95-141.
- Fereres E, Castel JR. 1981. Drip Irrigation Management. Division of Agricultural Sciences. University of California. Leaflet N° 21259. 2,11-24.
- Fereres E, Cruzromero G, Hoffman GJ, Rawlins SL. 1979. Recovery of orange trees following severe water-stress. *Journal of Applied Ecology* 16(3):833-842.
- Fereres E, Soriano MA. 2007. Deficit irrigation for reducing agricultural water use. *Journal of Experimental Botany* 58(2):147-159.
- Fernández JE, Green SR, Caspari HW, Díaz-Espejo A, Cuevas MV. 2008. The use of sap flow measurements for scheduling irrigation in olive, apple and Asian pear trees and in grapevines. *Plant and Soil* 305(1-2):91-104.
- Fernández JE, Romero R, Montano JC, Díaz-Espejo A, Muriel JL, Cuevas MV, Moreno F, Girón IF, Palomo MJ. 2008. Design and testing of an automatic irrigation controller for fruit tree orchards, based on sap flow measurements. *Aust J Agric Res* 59(7):589-598.

- Green SR. 2001. Pesticide and nitrate movement through Waikato and Franklin soils. Interim Progress Report, HortRes, 2002/007, Palmerston North, NZ.
- Hashimoto Y. 1979. Computer control of short term plant growth by monitoring leaf temperature. *Acta Hort (ISHS)* 106:139-146.
- Jonckheere I, Fleck S, Nackaerts K, Muys B, Coppin P, Weiss M, Baret F. 2004. Review of methods for in situ leaf area index determination: Part I. Theories, sensors and hemispherical photography. *Agricultural and Forest Meteorology* 121(1-2):19-35.
- Jothityangkoon C, Sivapalan M, Farmer DL. 2001. Process controls of water balance variability in a large semi-arid catchment: downward approach to hydrological model development. *Journal of Hydrology* 254(1-4):174-198.
- Love J. 2007. *Process Automation Handbook: a guide to theory and practice*. Springer-Verlag, p 155-171.
- Magliulo V, Bindi M, Rana G. 2003. Water use of irrigated potato (*Solanum tuberosum* L.) grown under free air carbon dioxide enrichment in central Italy. *Agric Ecosyst Environ* 97(1-3):65-80.
- Moriana A, Orgaz F, Pastor M, Fereres E. 2003. Yield responses of a mature olive orchard to water deficits. *Journal of the American Society for Horticultural Science* 128(3):425-431.
- Muñoz-Carpena R, Dukes MD, Li Y, Klassen W. 2008. Design and Field Evaluation of a New Controller for Soil-Water Based Irrigation. *Applied Engineering in Agriculture* 24(2):183.
- Nogueira LC, Dukes MD, Haman DZ, Scholberg JM, Cornejo C. 2003. Data Acquisition System and Irrigation Controller Based on CRI OX Datalogger and TDR Sensor. *Proceedings*, Volume 62:38-46.
- O'Shaughnessy SA, Evett SR. 2010. Canopy temperature based system effectively schedules and controls center pivot irrigation of cotton. *Agric Water Manage* 97(9):1310-1316.

-
- Peralta JM, Stockle CO. 2002. Dynamics of nitrate leaching under irrigated potato rotation in Washington State: a long-term simulation study. *Agriculture, ecosystems & environment* 88(1):23-34.
- Peters RT, Evett SR. 2008. Automation of a center pivot using the temperature-time-threshold method of irrigation scheduling. *Journal of Irrigation and Drainage Engineering* 134:286-291.
- Piñón S, Camacho EF, Kuchen B, Pena M. 2005. Constrained predictive control of a greenhouse. *Comput Electron Agric* 49(3):317-329.
- Qin SJ, Badgwell TA. 1997. An overview of industrial model predictive control technology. *Chemical Process Control - V*, volume 93, no 316: AIChE Symposium Series - American Institute of Chemical Engineers. p 232-256.
- Richalet J, Rault A, Testud JL, Papon J. 1978. Model predictive heuristic control:: Applications to industrial processes. *Automatica* 14(5):413-428.
- Rodriguez F, Guzman JL, Berenguel M, Arahal MR. 2008. Adaptive hierarchical control of greenhouse crop production. *Int J Adapt Control Signal Process* 22(2):180-197.
- Ruiz Sánchez MC, Domingo Miguel R, Castel Sánchez JR. 2010. Review. Deficit irrigation in fruit trees and vines in Spain. *Plant Soil* 120:299-302.
- Shock CC, Feibert EBG, Saunders LD, Eldredge EP. Automation of subsurface drip irrigation for crop research; 2002. p 809-816.
- Singh AK, Tripathy R, Chopra UK. 2008. Evaluation of CERES-Wheat and CropSyst models for water-nitrogen interactions in wheat crop. *Agric Water Manage* 95(7):776-786.
- Torrissi FD, Bemporad A. 2004. HYSDEL-a tool for generating computational hybrid models for analysis and synthesis problems. *Control Systems Technology, IEEE Transactions on* 12(2):235-249.
- Tubiello FN, Donatelli M, Rosenzweig C, Stockle CO. 2000. Effects of climate change and elevated CO₂ on cropping systems: model predictions at two Italian locations. *European Journal of Agronomy* 13(2-3):179-189.

Tuzet A, Perrier A, Leuning R. 2003. A coupled model of stomatal conductance, photosynthesis and transpiration. *Plant Cell and Environment* 26(7):1097-1116.

van Dam JC, Groenendijk P, Hendriks RFA, Kroes JG. 2008. Advances of modeling water flow in variably saturated soils with SWAP. *Vadose Zone Journal* 7(2):640-653.

Weiss M, Baret F, Smith GJ, Jonckheere I, Coppin P. 2004. Review of methods for in situ leaf area index (LAI) determination:: Part II. Estimation of LAI, errors and sampling. *Agricultural and Forest Meteorology* 121(1-2):37-53.

Ziegler JG, Nichols NB. 1942. Optimum settings for automatic controllers. *Trans ASME* 64(8):759-768.

Appendix 8

8.A1. C code of the PID implementation

```
float PID (float r0, float y0)
(
  e0 = r0-y0;
  D = qd * (e0-e1);
  I = I+ qi * (r0-y0);
  u = Kp * e0+ D+ I;
  e1 = e0;
)
```

8.A2. Hysdel code for simulating SPA system

```

/* SPA model
   July 2010 by R. Romero & D. Muñoz*/
SYSTEM SPAmodel {
INTERFACE {
  STATE { REAL th1 [0,1000];
          REAL th2 [0,1000];}
  INPUT { REAL I [0,1000];
          REAL R [0,1000];}
  OUTPUT { REAL y1;
           REAL y2;}
  PARAMETER { REAL Ts,WP1,WP2,FC,ETo;
              REAL k,kc,LAI,L1,L2,tr;}
}
IMPLEMENTATION {
  AUX { REAL D1,D2,ER2,ER3,TR1_2,TR1_3,TR2_2,TR2_3;
        BOOL D1mode, D2mode;
        BOOL ERmode2,ERmode2b, ERmode3;
        BOOL TR1mode2,TR1mode2b, TR1mode3;
        BOOL TR2mode2,TR2mode2b, TR2mode3;}
  AD { D1mode = th1+I+R-FC*L1>=0;
        D2mode = th2-FC*L2>=0;
        ERmode2 = th1>=WP1/3;
        ERmode2b = th1<=WP1;
        ERmode3 = th1>=WP1;
        TR1mode2 = (th1-WP1)/(FC*L1-WP1)>=WP1;
        TR1mode2b = (th1-WP1)/(FC*L1-WP1)<=tr;
        TR1mode3 = (th1-WP1)/(FC*L1-WP1)>=tr;
        TR2mode2 = (th2-WP2)/(FC*L2-WP2)>=WP2;
        TR2mode2b = (th2-WP2)/(FC*L2-WP2)<=tr;
        TR2mode3 = (th2-WP2)/(FC*L2-WP2)>=tr;}
  DA { D1 = {IF D1mode THEN th1+I+R-FC*L1 ELSE 0};
        D2 = {IF D2mode THEN th2-FC*L2 ELSE 0};
        ER2 = {IF ERmode2 & ERmode2b THEN ETo*kc*exp(-
k*LAI)*(th1-WP1/3)/(WP1-WP1/3) ELSE 0};
        ER3 = {IF ERmode3 THEN ETo*kc*exp(-k*LAI) ELSE 0};
        TR1_2 = {IF TR1mode2 & TR1mode2b THEN (th1-
WP1)*ETo*kc*(1-exp(-k*LAI))/(FC*L1-WP1) ELSE 0};
        TR1_3 = {IF TR1mode3 THEN ETo*kc*(1-exp(-k*LAI)) ELSE
0};
        TR2_2 = {IF TR2mode2 & TR2mode2b THEN (th2-
WP2)*ETo*kc*(1-exp(-k*LAI))/(FC*L2-WP2) ELSE 0};
        TR2_3 = {IF TR2mode3 THEN ETo*kc*(1-exp(-k*LAI)) ELSE
0};}
  CONTINUOUS { th1 = Ts*(th1+R+I-ER2-ER3-D1-TR1_2-TR1_3);
               th2 = Ts*(th2+D1-D2-TR2_2-TR2_3);}
  OUTPUT { y1 = th1;
           y2 = th2;}
}
}

```

8.A3. Hysdel code for generating the MPC controller

```

/* SPA model
   July 2010 by R. Romero */
SYSTEM SPAmode1 {
INTERFACE {
    STATE { REAL th1 [0,1000];
            REAL th2 [0,1000];
            REAL p0 [0,1000];
            REAL p1 [0,1000];
            REAL p2 [0,1000];
            REAL p3 [0,1000];
            REAL p4 [0,1000];
            REAL p5 [0,1000];
            REAL p6 [0,1000];
            REAL p7 [0,1000];
            REAL p8 [0,1000];
            REAL rth0 [0,1000];
            REAL rth1 [0,1000];
            REAL rth2 [0,1000];
            REAL rth3 [0,1000];
            REAL rth4 [0,1000];
            REAL rth5 [0,1000];};
    INPUT { REAL I [0,1000];}
    OUTPUT { REAL y1;}
    PARAMETER { REAL Ts,WP1,WP2,FC,ETo;
                REAL k,kc,LAI,L1,L2,tr;}
}
IMPLEMENTATION {
    AUX { REAL D1,D2,ER2,ER3,TR1_2,TR1_3,TR2_2,TR2_3;
          BOOL D1mode, D2mode;
          BOOL ERmode2,ERmode2b, ERmode3;
          BOOL TR1mode2,TR1mode2b, TR1mode3;
          BOOL TR2mode2,TR2mode2b, TR2mode3;}
    AD { D1mode = th1+I+p0-FC*L1>=0;
          D2mode = th2-FC*L2>=0;
          ERmode2 = th1>=WP1/3;
          ERmode2b = th1<=WP1;
          ERmode3 = th1>=WP1;
          TR1mode2 = (th1-WP1)/(FC*L1-WP1)>=WP1;
          TR1mode2b = (th1-WP1)/(FC*L1-WP1)<=tr;
          TR1mode3 = (th1-WP1)/(FC*L1-WP1)>=tr;
          TR2mode2 = (th2-WP2)/(FC*L2-WP2)>=WP2;
          TR2mode2b = (th2-WP2)/(FC*L2-WP2)<=tr;
          TR2mode3 = (th2-WP2)/(FC*L2-WP2)>=tr;}
    DA { D1 = {IF D1mode THEN th1+I+p0-FC*L1 ELSE 0};
          D2 = {IF D2mode THEN th2-FC*L2 ELSE 0};
          ER2 = {IF ERmode2 & ERmode2b THEN ETo*kc*exp(-
k*LAI)*(th1-WP1/3)/(WP1-WP1/3) ELSE 0};
          ER3 = {IF ERmode3 THEN ETo*kc*exp(-k*LAI) ELSE 0};
          TR1_2 = {IF TR1mode2 & TR1mode2b THEN (th1-
WP1)*ETo*kc*(1-exp(-k*LAI))/(FC*L1-WP1) ELSE 0};
          TR1_3 = {IF TR1mode3 THEN ETo*kc*(1-exp(-k*LAI)) ELSE
0};
          TR2_2 = {IF TR2mode2 & TR2mode2b THEN (th2-
WP2)*ETo*kc*(1-exp(-k*LAI))/(FC*L2-WP2) ELSE 0};
          TR2_3 = {IF TR2mode3 THEN ETo*kc*(1-exp(-k*LAI)) ELSE
0};}
}

```

```
CONTINUOUS { th1 = Ts*(th1+I-ER2-ER3-D1-TR1_2-TR1_3+p0);
              th2 = Ts*(th2+D1-D2-TR2_2-TR2_3);
              p0= p1;
              p1= p2;
              p2= p3;
              p3= p4;
              p4= p5;
              p5= p6;
              p6= p7;
              p7= p8;
              p8= p8;
              rth0 = rth1;
              rth1 = rth2;
              rth2 = rth3;
              rth3 = rth4;
              rth4 = rth5;
              rth5 = rth5;}
OUTPUT { y1 = th1-rth0;}
}
```


Chapter 9

Concluding remarks

9.1. Deficit irrigation

We carried out three experiments in commercial orange orchards to study deficit irrigation strategies in orange orchards located in the Guadalquivir River Valley, SW Spain.

First we compared three SDI treatments with different levels of water reduction (77%, 67% and 53% of IN) in a 12-year-old orange orchard (*Citrus Sinensis* L. Osbeck, cv. Salustiana). The results showed that irrigation water savings of up to 55% of IN had no significant impact on tree yield, but affected key quality factors (TSS and TA). The greatest increase in WP was detected in the SDI53 treatment. However, the low values of Ψ_{stem} detected in this treatment suggest stresses levels that could result in reductions of yield in the future. A longer experiment is required to evaluate this aspect. The SDI67 and SDI77 treatments, however, did not cause significant Ψ_{stem} reductions as compared to the fully-irrigated, control treatment.

We also implemented four RDI strategies in 11-year-old orange trees (*Citrus sinensis* L. Osb. cv. Navelina). Although WP increased in all tested RDI treatments, our results show that RDI-776 (37% IN) was the best strategy. This treatment allowed 1200 m³ ha⁻¹ yr⁻¹ water savings, with no significant effect in yield. It also improved fruit quality parameters as TSS and TA. The rest of the tested RDI treatments involved a greater reduction of irrigation water at flowering (44% of control). All of them reduced fruit number. Furthermore, maintaining this reduction during the fruit growth period caused a significant loss in fruit weight and some changes in fruit quality parameters, such as an increase of TSS and TA. Our results show that the differences on water

distribution along the irrigation season caused by the irrigation strategy, had a greater effect on the response of orange trees than the annual IA applied in each treatment.

In another set of experiments, a LFDI treatment was applied to 11-year-old orange trees *Citrus sinensis* L. Osbeck, cv. Navelina) and compared with a fully irrigated control treatment (110% of the crop IN) and a SDI treatment in which total water supplies amounted to 58% of the crop IN. Water savings amounted to 41% for the LFDI treatment, as compared to the control. The reduction in yield was 18% only, and the quality parameters TSS, TA and MI improved. In the SDI treatment, water savings were slightly higher than in the LFDI treatment (48%), but the yield reduction was substantially greater (40% reduction).

The described results suggest that, although SDI treatments potentially improve WP and fruit quality respect to a full-irrigation treatment, RDI strategies might be more suitable. Thus, knowledge on the sensitivity of the crop to water stress depending on the phenological stage avoids severe water restrictions at critical stages and, therefore, negative effects of DI strategies on yield and long-term crop performance. Results from the LFDI treatment suggest that a quick recovery after a DI period also contributes to mitigate yield reductions. We suggest a new strategy that exploits the advantage of both RDI and LFDI strategies. It is based on a RDI strategy but alternating DI periods and quick recoveries in each phenological stage. We encourage new research on this approach to further refine the most appropriate irrigation strategy for orange orchards in the area. Our results also show the usefulness of S_{Ψ} and S_{RI} as reliable water stress indices, although their usefulness for precise irrigation is limited by their low temporal resolution. This problem is avoided by the use of the MDS and MXSD indices derived from TDV records. Because of their capability for continuous and automatic data recording and data transfer, they are an advantageous alternative to Ψ_{stem} for the assessment of tree water stress in the orchard.

9.2. Automatic irrigation controllers

One of the main objectives of this thesis was the development of AICs. The CRP, in which IAs are calculated from sap flow readings in the trunk of trees, was tested in an olive orchard close to Seville (Spain). The CRP proved to be a robust device able to calculate and supply daily IA to the orchard, in accordance with the specified irrigation

protocol. In our experiment the daily values of the E_{pNI}/E_{pOI} ratio had not enough resolution for the desired irrigation approach, intended to replace the daily crop water consumption. This was due to the experimental trees being old trees with large rhizospheres growing in a soil of medium to high water holding capacity. The CRP, however, was able to react to a sudden increase in the tree's water stress caused by the soil water content falling below the threshold for soil water deficit. This suggests that the device could be suitable for applying DI in olive orchards with similar characteristics as our experimental orchard. The resolution of the E_{pNI}/E_{pOI} ratio could be greater when irrigating species with a lower capacity to take up water from drying soils, especially if the trees are small and grow in a soil of low water-holding capacity.

The AIC that we tested in an almond orchard calculated the IAs based on the crop coefficient approach and SWC measurements. The prototype we developed and evaluated proved to be robust and reliable enough for the automatic control of high-frequency irrigation in the orchard. The device seems to be useful to minimize ponding conditions and water losses by drainage and evaporation from the soil surface, and it can be used for irrigating orchards in remote areas, through the Internet. Our results show that IAs can be precisely controlled by combining soil water measurements with the crop coefficient approach, which takes into account the response of the crop to the atmospheric demand. Widely recommended K_c values for almond orchards resulted too high for our orchard conditions.

9.3. New sap flow methods

Our experiments with DI strategies and AICs proved the usefulness of plant-based measurements to estimate the IN of the crop and to identify water stress thresholds. One of the most promising variables for this objective is sap flow. We proposed and evaluated two new methods for extending the measurement range of current heat-pulse methods to measure sap flow. These new methods successfully captured the dynamic pattern of daily sap flow, as compared to simulations with a big-leaf model for a single branch and measurements with conventional CHP and T-max methods. These comparisons showed strong linear relationships for wide ranges of sap flux densities. In theory, these new methods are also well suited to low and even reverse flows. Although

more experiments should be carried out to check and calibrate our two new methods, the preliminary results presented here are promising.

9.4. Modeling and control of SPA systems

Finally, we developed a discrete time mathematical model to obtain an approximate solution of the behaviour of a given SPA system. The model can be used for doing predictions and for designing precision irrigation strategies and AICs. The model was first successfully checked with CROPSYST. Then we used two different set of data from a whole irrigation season to identify and validate the model for a specific almond orchard. Finally different control strategies (PID, feedforward ET_c , MPC) were tested and evaluated with the model in simulation exercises.

The PID strategy proved to be robust and accurate for controlling SWC. Better SWC evolution was achieved with PID than with the feedforward ET_c method, due to the use of SWC measurement as a feedback signal. We also applied this PID controller in field during July-August 2010 with excellent results. After only 1 day, the set point was achieved, remaining in $\pm 5\%$ set point bounds during the experimental period. We concluded that PID is a robust and efficient strategy that allows precision irrigation when a reference for SWC is known. PID achieves better performance than feedforward ET_c thanks to the SWC measurement feedback.

Extra information (e.g. ET_c and rainfall forecasts, and changes in SWC reference) can be incorporated in advance in the MPC controller to optimize the control of the SWC. Furthermore, in MPC the contribution of the weighting coefficients to the signal control can be pondered. These allow the farmer to find a mid-way solution between optimal SWC and saving water. Our MPC controller showed promising results when simulated with the SPA model. Nevertheless, field experiments are required to confirm these results.